NUWC-NPT Technical Report 11,150
26 July 1999

Detection Performance of Or-ing Device with Pre- and Post-Averaging: Part I – Random Signal

Albert H. Nuttall
Surface Undersea Warfare Department

Naval Undersea Warfare Center Division
Newport, Rhode Island

PREFACE

The work described in this report was sponsored by the Independent Research Program of the Naval Undersea Warfare Center (NUWC) Division, Newport, RI, Project No. B102369, "Performance Analysis of Or-ing with Arbitrary Amounts of Pre-Averaging and Post-Averaging," principal investigator Albert H. Nuttall (Code 3102). The Independent Research Program is funded by the Office of Naval Research; NUWC Division Newport program manager Richard B. Philips (Code 102). This report was also partially funded by Project No. A196009, "Passive Advanced Processing Build," principal investigator David Pistacchio (Code 2123). The sponsoring activity is the Program Executive Office, Undersea Warfare, Advanced Systems and Technology Office (ASTO-D1), program manager Robert Zarnich.

The technical reviewer for this report was Erik B. Siborg (Code 2111).

Reviewed and Approved: 26 July 1999

Patricia J. Dean

Patricia J. Dean
Director, Surface Undersea Warfare

REPORT DOCUMENTATION PAGE

Form Approved
OMB No. 0704-0188

1. AGENCY USE ONLY (Leave Blank)	2. REPORT DATE	3. REPORT TYPE AND DATES COVERED
	26 July 1999	Final

4. TITLE AND SUBTITLE

Detection Performance of Or-ing Device with Pre- and Post-Averaging: Part I—Random Signal

5. FUNDING NUMBERS

PR B102369
PR A196009

6. AUTHOR(S)

Albert H. Nuttall

7. PERFORMING ORGANIZATION NAME(S) AND ADDRESS(ES)

Naval Undersea Warfare Center Division
1176 Howell Street
Newport, RI 02841-1708

8. PERFORMING ORGANIZATION REPORT NUMBER

TR 11,150

9. SPONSORING/MONITORING AGENCY NAME(S) AND ADDRESS(ES)

Office of Naval Research
800 North Quincy Street
Arlington, VA 22217-5160

Program Executive Office
for Undersea Warfare (ASTO D1)
2531 Jefferson Davis Highway
Arlington, VA 22242-5160

10. SPONSORING/MONITORING AGENCY REPORT NUMBER

11. SUPPLEMENTARY NOTES

12a. DISTRIBUTION/AVAILABILITY STATEMENT

Approved for public release; distribution is unlimited.

12b. DISTRIBUTION CODE

13. ABSTRACT (Maximum 200 words)

The detection performance of an or-ing device with pre-averaging and post-averaging has been determined in the form of numerous receiver operating characteristics covering a wide range of input signal-to-noise ratios. Numerical evaluation of the false alarm probability P_f and detection probability P_d has been conducted for the case of a random Gaussian signal in the presence of additive Gaussian noise, for a wide range of values of K, the amount of pre-averaging before or-ing; N, the number of channels or-ed; and M, the amount of post-averaging after or-ing. Also, a MATLAB program is listed that can be used to extend these results to parameter values outside the range studied here.

The tradeoffs associated with switching from post-averaging to pre-averaging, or vice-versa, have been thoroughly investigated and tabulated for a standard operating point P_f = 1E-3, P_d = 0.5, and for a high-quality operating point P_f = 1E-6, P_d = 0.9. The losses associated with doing too little pre-averaging can be severe, especially for large numbers, N, of or-ed channels.

14. SUBJECT TERMS

Signal Processing
Or-ing
Random Signals

15. NUMBER OF PAGES
154

16. PRICE CODE

17. SECURITY CLASSIFICATION OF REPORT	18. SECURITY CLASSIFICATION OF THIS PAGE	19. SECURITY CLASSIFICATION OF ABSTRACT	20. LIMITATION OF ABSTRACT
Unclassified	Unclassified	Unclassified	SAR

TABLE OF CONTENTS

TABLE OF CONTENTS (Cont'd)

LIST OF ILLUSTRATIONS

LIST OF ILLUSTRATIONS (Cont'd)

LIST OF ILLUSTRATIONS (Cont'd)

LIST OF ILLUSTRATIONS (Cont'd)

LIST OF TABLES

LIST OF ABBREVIATIONS, ACRONYMS, AND SYMBOLS

a	Auxiliary parameter $1/(1+\rho)$, equation (68)
a_k, b_k	Gaussian signal components, equation (7)
APP	A posteriori probability
CDF	Cumulative distribution function
CF	Characteristic function
$\{c_j\}$	Convolution weights, equation (5)
c_v	Cumulative distribution function of v(t), (31)
c_0, c_1	Cumulative distribution functions of $y_n(t)$, (31)
d	Additive constant, equations (27), (28)
$\underline{d}$	Scaled constant, equation (38)
dB	Decibels
EDF	Exceedance distribution function
$\{e_k\}$	Exponential random variables, equation (10)
$e_n(x)$	Auxiliary function, equation (50)
e_w	Exceedance distribution function of w(t), (36)
FFT	Fast Fourier transform
f_v	Characteristic function of v(t)
f_w	Characteristic function of w(t)
f_x	Characteristic function of $x_n(t)$
$\{g_k\}$	Pre-averager weights, equation (5)
$\{g_k\}$	Gaussian random variables, equation (7)
$\{h_k\}$	Gaussian random variables, equation (7)
$\{h_m\}$	Post-averager weights, equation (5)
HOP	High-quality operating point, P_f = 1E-6, P_d = 0.9
H_0, H_1	Signal-absent, signal-present hypotheses

LIST OF ABBREVIATIONS, ACRONYMS, AND SYMBOLS (Cont'd)

J	Skip factor, equation (2)
K	Amount of pre-averaging, figure 1
M	Amount of post-averaging, figure 1
n	Channel number
N	Total number of channels or-ed, figure 1
or-ing	Pass only the largest of N inputs
p_0, p_1	Probability density functions of $y_n(t)$, (32)
p,PDF	Probability density function
P_d	Detection probability
P_f	False alarm probability
p_v	Probability density function of v(t), (31), (32)
p_w	Probability density function of w(t), (48)
Q_K	Q-function of order K, equation (54)
ROC	Receiver operating characteristic
RV	Random variable
SNR	Signal-to-noise ratio
SOP	Standard operating point, P_f = 1E-3, P_d = 0.5
t	Time instant
T	Time-bandwidth product, equation (3)
v(t)	Or-ing output, figure 1
w(t)	System output, figure 1
w( )	Error function of complex argument, equation (46)
$x_n(t)$	Input data in n-th channel, figure 1
$y_n(t)$	Pre-averager output in n-th channel, figure 1
$(z)_n$	Pochhammer's symbol, equation (72)

LIST OF ABBREVIATIONS, ACRONYMS, AND SYMBOLS (Cont'd)

Δ_ξ	Sampling increment in ξ
Δ_u	Sampling increment in u
θ_k	Random phase, equation (16)
ϕ	Gaussian probability density function, equation (38)
Φ	Gaussian cumulative distribution function, (38)
ρ	Common input power signal-to-noise ratio, (11)
$\underline{\rho}$	Scaled input signal-to-noise ratio, equation (50)
ρ_k	Input power signal-to-noise ratio at time k, (8)
ξ	Argument of characteristic functions
μ_v	Mean of v(t), equation (58)
χ_v	Cumulant of v(t), equation (75)

boldface	Random variable
overbar	Ensemble average

DETECTION PERFORMANCE OF OR-ING DEVICE WITH PRE- AND POST-AVERAGING: PART I - RANDOM SIGNAL

INTRODUCTION

The need to process and condense large amounts of data is encountered frequently in modern Navy systems that employ multiple beams, frequency bins, range cells, et cetera. One way of accomplishing this goal is by or-ing a number of inputs into a single output; that is, allow only the largest of a set of quantities to pass on for further processing and completely reject the remainder. However, since this or-ing operation is highly nonlinear, destroys information, and tends to cause small-signal suppression, some pre-averaging of the inputs to the or-ing device is often employed in an effort to build up the signal-to-noise ratio (SNR) prior to the maximum comparison. Additionally, at the or-ing output, some additional post-averaging is frequently employed, once again in an effort to build up the SNR, this time before a threshold comparison is made for purposes of declaring a signal present versus absent. The pertinent block diagram is displayed in figure 1.

There are N channels of real input data available for processing, namely, $\{x_n(t)\}$ for $1 \leq n \leq N$, where time has been normalized so that time sampling instant t is integer. Under hypothesis H_0, there is Gaussian noise only in all the inputs, whereas under hypothesis H_1, a signal is also present in one

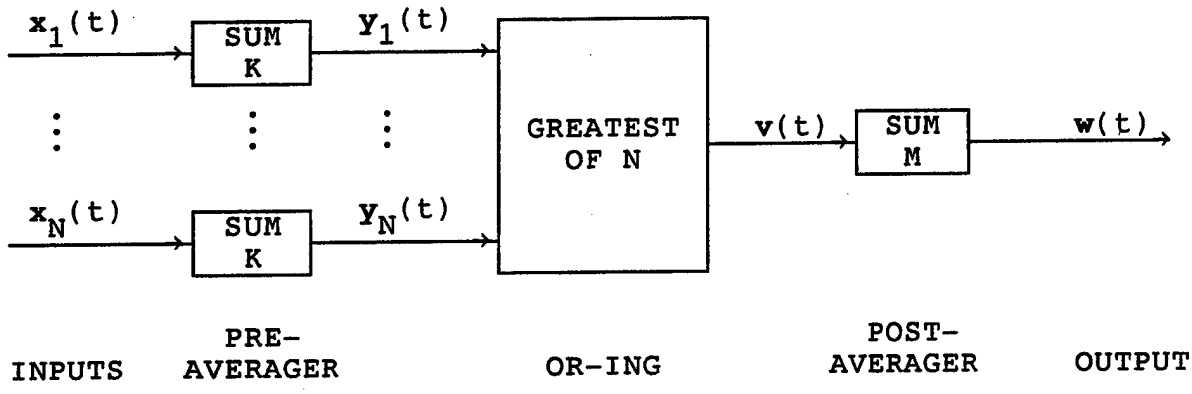

Figure 1. Or-ing with Pre- and Post-Averaging

(unknown) channel. The goal of the processor in figure 1 is to determine signal presence with a high detection probability while realizing a specified acceptable low false alarm probability. Each pre-averager accumulates K statistically independent consecutive samples of its corresponding input $x_n(t)$, yielding output $y_n(t)$, which is then subjected to or-ing amongst N competitors. The or-ing output is

$$v(t) = \max\{y_1(t),\cdots,y_N(t)\} \ . \qquad (1)$$

Finally, the post-averager accumulates M samples of its input v(t), and compares its output w(t) with a fixed threshold.

There is an additional complication of the post-averaging procedure, which is not indicated explicitly in figure 1. In particular, the or-ing output v(t) is sampled every J-th time instant and summed over M samples to give processor output

$$w(t) = \sum_{m=0}^{M-1} v(t-mJ) = v(t) + v(t-J) + \cdots + v(t-J(M-1))$$

$$= \max\{y_1(t) ,..., y_N(t)\} + \max\{y_1(t-J) ,..., y_N(t-J)\} + \cdots$$

$$+ \max\{y_1(t-J(M-1)) ,..., y_N(t-J(M-1))\} , \qquad (2)$$

where J is the skip factor. If skip factor J = K, then system output w(t) is the sum of M nonoverlapping adjacent blocks of pre-averaged data, each of length K, covering a total of KM time instants.

More generally, for arbitrary J, since the pre-averager spans a time interval of length K-1, and the post-averager spans time interval J(M-1), the total observation time is composed of

$$T = J(M-1) + K \qquad (3)$$

samples. Alternatively, the last term in equation (2) involves the quantities $\{x_n(t-J(M-1)-K+1)\}$, whereas the first term in equation (2) involves $\{x_n(t)\}$, for a total of T time instants.

More accurately, T can be interpreted as the time-bandwidth product of the input data utilized by the processor in figure 1. Hypothesis H_1 presumes that a signal is present in the same (unknown) channel for time instants t, t-1,..., t-J(M-1)-(K-1), for a total of T samples. If J = K, then equation (3) reduces to time-bandwidth product T = KM, as above; this special case is called block processing and is the major focus of this study.

The reason for allowing $1 \leq J \leq K$ is that the possibility exists that some information may be lost unless intermediate values of or-ing output v(t) are observed, at least more frequently than every K samples; see equation (2). However, this general case causes statistically dependent non-Gaussian random variables (RVs) to be accumulated in the post-averager, which in turn leads to an intractable analysis problem. Therefore, the study of the detectability performance for this particular feature, namely, skip factor $J < K$, must be accomplished by simulation. Even if every $x_n(t)$ is statistically independent of every $x_m(u)$ if $n \neq m$ or $t \neq u$, the system output w(t) is a sum of statistically dependent RVs with non-Gaussian statistics, when $J < K$. Finally, the case of $J > K$ is not considered at all, because that leads to discarding relevant new information in or-ing output v(t) and a definite degradation in performance.

SCALING PROPERTY

Consider a set of scaled inputs $\{\underline{x}_n(t)\}$ such that

$$x_n(t) = a\ \underline{x}_n(t) + b\ , \quad a > 0\ , \quad 1 \leq n \leq N\ . \tag{4}$$

It can then be easily shown that the corresponding pre-averager outputs $y_n(t) = a\ \underline{y}_n(t) + bK$, and that the or-ing outputs satisfy $v(t) = a\ \underline{v}(t) + bK$, leading to output relationship $w(t) = a\ \underline{w}(t) + KM$. Thus, w(t) is a scaled version of $\underline{w}(t)$, along with an additive constant. Since the transformation between the two

processor outputs w(t) and $\underline{w}(t)$ is monotonic, the receiver operating characteristics (ROCs) of the two or-ing processors, one operating on $\{x_n(t)\}$ and the other operating on $\{\underline{x}_n(t)\}$, are identical, regardless of the values of scaling parameters a and b in equation (4). Then, without loss of generality, the scalings can be chosen, for example, so that input $x_n(t)$ has zero mean and unit variance under H_0, if desired. That still allows $x_n(t)$ to have arbitrary mean and variance under H_1. Alternatively, if $x_n(t)$ is always a positive RV, the choice of b = 0 with unit variance of $x_n(t)$ under H_0 is a possibility. This still leaves the variance of $x_n(t)$ under H_1 arbitrary. The point is to choose the two free parameters a and b in equation (4) so that the statistics of $\{x_n(t)\}$ under H_0 are as simple as possible; this feature will be utilized without comment in the future developments.

STANDARD OF COMPARISON

The standard of comparison against which to measure system performance losses is N = 1, no or-ing. Then, for arbitrary pre-averager weights $\{g_k\}$ and arbitrary post-averager weights $\{h_m\}$, the various processor waveforms for N = 1 in figure 1 are

$$y_1(t) = \sum_k g_k \, x_1(t-k) \ , \qquad v(t) = y_1(t) \ ,$$

$$w(t) = \sum_m h_m \, v(t-m) = \sum_j c_j \, x_1(t-j) \ , \tag{5}$$

where weights $\{c_j\}$ are the convolution of the pre-averager weights $\{g_k\}$ and the post-averager weights $\{h_m\}$ (including skip factor J). For statistically independent time inputs $\{x_1(t)\}$, the characteristic function (CF) of processor output w(t) is given, for N = 1, no or-ing, by ensemble average

$$f_w(\xi) = \overline{\exp(i\xi w(t))} = \prod_j f_x(c_j \xi) \ , \qquad (6)$$

using equation (5), where f_x is the CF of $x_1(t)$ under the appropriate hypothesis, either H_0 or H_1. This particular processor output CF (for N = 1) can be accomplished analytically and then Fourier transformed numerically to get accurate ROCs for any K, M, and sets of weights $\{g_k\}$ and $\{h_m\}$.

OUTLINE

For skip factor J = K, namely, block processing in figure 1, expressions will be derived that allow for accurate evaluation of the false alarm probability P_f and the detection probability P_d for the decision variable w(t). Furthermore, this will be accomplished for arbitrary amounts of pre-averaging K, arbitrary amounts of or-ing N, arbitrary amounts of post-averaging M, and arbitrary input SNRs. No approximations are involved, the analysis is not limited to mean and variance calculations, and no appeal is made to the central limit theorem. Rather, the approach employs a judicious combination of analysis with computer-aided numerical calculations. The accuracy of the end

result is limited only by the computer accuracy. An entire ROC can be generated in minutes.

There are three different input signal models in additive Gaussian noise that are of interest here; they are:

(I) Random (Gaussian) signal,

(II) Phase-incoherent signal, and

(III) Coherent (deterministic) signal.

This report will address all three signal models, but will concentrate numerically on part I, the random Gaussian signal, and will present numerous ROCs that completely characterize the performance of the or-ing system in figure 1. Some related past work on or-ing is listed in references 1 through 9.

For all three signal models, the optimum processor can also be determined and its ROCs calculated. Then, the exact losses that the or-ing procedure causes can be accurately quantified. That chore will be completed here in part I for the random signal; parts II and III are reserved for follow-on work.

The analytical approach utilized here can be extended to include quantizers on the inputs $\{x_n(t)\}$ in figure 1 and still obtain accurate ROCs for decision variable w(t). In fact, not only can there be arbitrary amounts of quantization (L levels), but the input probability density functions (PDFs) can be completely arbitrary. Documentation of this work is reserved for the future.

Some or-ing processors perform quantization on the output v(t) of the Greatest-Of device in figure 1, prior to post-averaging. The PDFs at the output of this quantizer are then collections of impulses, whose areas are governed by the cumulative distribution functions of v(t) under hypotheses H_0 and H_1. If the quantizer levels are equally spaced, then the impulse locations are also equally spaced, and a complete analytic approach is possible, all the way to processor output w(t) in figure 1. See references 3 and 4, for example.

INPUT DATA MODELS

In the following, g_k and h_k are independent zero-mean unit-variance Gaussian RVs, and e_k is an exponential RV with unit mean, that is, with PDF exp(-u) for u > 0.

RANDOM GAUSSIAN SIGNAL IN GAUSSIAN NOISE

In the signal channel, the system input to figure 1, at time t_k under hypothesis H_1, is an envelope-squared variate

$$x_k \equiv x_n(t_k) = \frac{1}{2}\left[(a_k + g_k)^2 + (b_k + h_k)^2\right] , \qquad (7)$$

where signal components a_k and b_k are independent zero-mean Gaussian RVs with common variance ρ_k, and g_k and h_k are additive Gaussian noise components. The input mean is then

$$\overline{x_k} = 1 + \rho_k \qquad (8)$$

for signal present. Since x_k is an envelope-squared quantity, ρ_k is an input (per sample) power SNR measure.

The CF of x_k under H_1 is, from equations (7) and (8),

$$f_k(\xi) = \overline{\exp(i\xi x_k)} = \frac{1}{1 - i\xi(1 + \rho_k)} . \qquad (9)$$

Since this CF corresponds to an exponential RV with mean $1 + \rho_k$, it is possible to use, instead of form (7), input data value

$$x_k = (1 + \rho_k)\, e_k \ , \tag{10}$$

both for analysis as well as simulation purposes under H_1. For the noise channels, $\rho_k = 0$ and $x_k = e_k$ under H_0.

When $\rho_k = \rho$ for all k, that is, constant signal powers with time, the pre-averager output for the signal channel under H_1 is

$$y = \sum_{k=1}^{K} x_k = (1 + \rho) \sum_{k=1}^{K} e_k = (1 + \rho)\, y^o \ , \tag{11}$$

where y^o is the corresponding noise-only pre-averager output. This property can be used advantageously for both analysis as well as simulation purposes. The ROCs can be parameterized by input power SNR ρ; this is the mathematical setup for part I.

ALTERNATIVE ADDITION OF ENVELOPES FOR RANDOM GAUSSIAN SIGNAL

If the input data value in figure 1 is an envelope instead, denote it by $\underline{x}_k = (x_k)^{1/2}$ in terms of the RV in equation (7). This means that $\underline{x}_k$ can be generated alternatively according to

$$\underline{x}_k = (1 + \rho_k)^{1/2}\, e_k^{1/2} \ . \tag{12}$$

The mean-square value of envelope $\underline{x}_k$ is then

$$\overline{\underline{x}_k^2} = 1 + \rho_k \ , \tag{13}$$

where ρ_k is an input power SNR measure.

For the noise channels, $\rho_k = 0$, thereby yielding envelope

$$\underline{x}_k = \left(\frac{1}{2}(g_k^2 + h_k^2)\right)^{\frac{1}{2}} = e_k^{\frac{1}{2}} , \qquad (14)$$

where e_k is a unit-mean exponential RV.

When $\rho_k = \rho$ for all k, the pre-averager output for the signal channel under H_1 is

$$\underline{y} = \sum_{k=1}^{K} \underline{x}_k = (1 + \rho)^{\frac{1}{2}} \sum_{k=1}^{K} e_k^{\frac{1}{2}} = (1 + \rho)^{\frac{1}{2}} \underline{y}^{o} , \qquad (15)$$

where $\underline{y}^{o}$ is the corresponding noise-only pre-averager output. The ROCs can be parameterized in terms of input power SNR measure ρ. The investigation in this report on the random signal, part I, will <u>not</u> address the sum of envelopes, as given by equation (15), but will concentrate on the sum of envelopes squared, as given by equation (11), with constant powers $\rho_k = \rho$.

PHASE-INCOHERENT SIGNAL IN GAUSSIAN NOISE

In the signal channel, the input for this signal model, part II, at time t_k under H_1 is an envelope-squared variate

$$x_k = \frac{1}{2}\left[(g_k + A_k \cos\theta_k)^2 + (h_k + A_k \sin\theta_k)^2\right] , \qquad (16)$$

where signal amplitude A_k is nonrandom, and phase θ_k is a RV with arbitrary PDF, that is, incoherent phase. The input mean is

$$\overline{x_k} = 1 + \frac{1}{2} A_k^2 \equiv 1 + \rho_k \ , \tag{17}$$

regardless of the value of θ_k. Since x_k is an envelope-squared quantity, $\rho_k = A_k^2/2$ is an input (per sample) power SNR measure.

The CF of x_k under H_1, conditioned on a particular value of RV θ_k, is, by use of equation (16),

$$f_k(\xi|\theta_k) = \overline{\exp(i\xi x_k)} = \frac{1}{1 - i\xi} \exp\left(\rho_k \frac{i\xi}{1 - i\xi}\right) \ . \tag{18}$$

But, since the right-hand side of CF (18) is independent of θ_k, it is possible to use the data value

$$x_k = \frac{1}{2}\left[(g_k + A_k)^2 + h_k^2\right] \tag{19}$$

for the signal channel input under H_1. On the other hand, for the noise channels, $A_k = 0$ and CF (18) reduces to $(1 - i\xi)^{-1}$, which corresponds to a unit-mean exponential RV. Therefore, for the noise channel inputs, use the quantity

$$x_k = e_k \ . \tag{20}$$

When $A_k = A$ for all k, constant signal amplitudes with time, the pre-averager output for the signal channel can be expressed

$$y = \sum_{k=1}^{K} x_k = \frac{1}{2} \sum_{k=1}^{K} (g_k^2 + h_k^2) + A \sum_{k=1}^{K} g_k + K \frac{A}{2}^2$$

$$= y^o + A \sum_{k=1}^{K} g_k + K \frac{A}{2}^2 \ , \tag{21}$$

under H_1, where y^o is the corresponding noise-only pre-averager output. (However, the k-th term in the sum for y cannot be replaced by $e_k + A\, g_k + A^2/2$, where e_k is an independent exponential RV, because the CF of this latter combination is

$$\frac{1}{1 - i\xi} \exp[\rho\, i\xi(1 + i\xi)] \ , \quad \rho \equiv \frac{A^2}{2} \ , \tag{22}$$

which is not identical in form to equation (18). The two CFs do, however, have the same mean and variance.) The ROCs for figure 1 using pre-averager (21) can be parameterized by input amplitude SNR measure A or by input power SNR measure ρ.

Because of the way parameters $\{\rho_k\}$ appear in equation (18), the CF of the pre-averager output can be found in the closed form

$$f_y(\xi) = (1-i\xi)^{-K} \exp\left(\rho_K \frac{i\xi}{1-i\xi}\right) \ , \quad \rho_K = \sum_{k=1}^{K} \rho_k \ .$$

Therefore, all the following results pertaining to the phase-incoherent signal with equal SNRs ρ and sums of squared-envelopes actually hold for arbitrary SNRs $\{\rho_k\}$, if ρ is replaced by ρ_K/K. However, this observation is of limited utility unless all of the M sums of $\{\rho_k\}$, one for each post-averaging interval, are identical.

ALTERNATIVE ADDITION OF ENVELOPES FOR PHASE-INCOHERENT SIGNAL

If the input data value in figure 1 is an envelope instead, denote it by $\underline{x}_k = (x_k)^{\frac{1}{2}}$ in terms of the RV in equation (16).

Since the conditional CF of x_k is independent of θ_k, according to equation (18), the conditional PDF of x_k is independent of θ_k. Therefore, any nonlinear transformation of x_k, such as $\underline{x}_k$, will also have a conditional PDF independent of θ_k. This means that $\underline{x}_k$ can be generated alternatively according to

$$\underline{x}_k = \left(\frac{1}{2}\left[(g_k + A_k)^2 + h_k^2\right]\right)^{\frac{1}{2}} \tag{23}$$

under H_1. The mean-square value of envelope $\underline{x}_k$ is then

$$\overline{\underline{x}_k^2} = 1 + \frac{1}{2} A_k^2 \equiv 1 + \rho_k \ , \tag{24}$$

where ρ_k is an input power SNR measure.

For the noise channels, $A_k = 0$, thereby yielding envelope

$$\underline{x}_k = \left(\frac{1}{2}(g_k^2 + h_k^2)\right)^{\frac{1}{2}} = e_k^{\frac{1}{2}} \ , \tag{25}$$

where e_k is a unit-mean exponential RV.

When $A_k = A$ for all k, the pre-averager output for the signal channel under H_1 is

$$\underline{Y} = \sum_{k=1}^{K} \underline{x}_k = \sum_{k=1}^{K} \left(\frac{1}{2}(g_k^2 + h_k^2) + A\, g_k + \frac{A^2}{2}\right)^{\frac{1}{2}} \ , \tag{26}$$

which cannot be simplified or expressed in terms of alternative RVs. The ROCs can be parameterized in terms of input amplitude SNR measure A or in terms of input power SNR measure $\rho \equiv A^2/2$.

COHERENT (DETERMINISTIC) SIGNAL IN GAUSSIAN NOISE

In the signal channel, the input for this signal model, part III, at time t_k under H_1 is <u>amplitude</u> variate

$$x_k = g_k + d_k \ , \tag{27}$$

where d_k is nonrandom. The input mean is $\overline{x_k} = d_k$, while the input variance is $\mathrm{var}(x_k) = 1$. Thus, d_k is an input <u>amplitude</u> SNR measure, while d_k^2 (or $d_k^2/2$) is an input power SNR measure.

For the noise channels, $x_k = g_k$, with zero mean and unit variance. Thus, d_k can be interpreted as a per-sample difference in mean inputs, divided by the common input standard deviation.

When $d_k = d$ for all k, constant signal amplitudes with time, the pre-averager output under H_1 for the signal channel is

$$y = \sum_{k=1}^{K} x_k = \sum_{k=1}^{K} g_k + K\,d = y^o + K\,d \ , \tag{28}$$

where y^o is the corresponding noise-only pre-averager output. The ROCs can be parameterized by input amplitude SNR measure d or input power SNR measure d^2 (or $d^2/2$). More generally, the single parameter value $d_T = \Sigma_k\, d_k$ characterizes the performance of the processor when the amplitude SNRs $\{d_k\}$ are unequal and arbitrary. However, this observation is of limited utility unless all of the M sums of $\{d_k\}$, one for each post-averaging interval, are identical.

OPTIMUM PROCESSING OF AVAILABLE DATA

The optimum processors for all three signal models are derived in appendix A for the case where channel occupancy identification is required, as well as the alternative case where channel identification is irrelevant. For all situations, the optimum processor is essentially given by threshold comparison

$$\max_{1 \le n \le N} \left\{ \sum_{t=1}^{T} x_n(t) \right\} \gtrless v \ ; \tag{29}$$

see equations (A-13), (A-19), and (A-26). This operation is equivalent to doing <u>all</u> pre-averaging and <u>no</u> post-averaging in figure 1, that is, take K = T and M = 1. Doing so defers the nonlinearity (or-ing) until after all possible linear combining (pre-averaging) has been accomplished. This case will be thoroughly numerically evaluated and will serve as the basis of comparison for the various combinations of pre-averaging and post-averaging, that is, M > 1 or K < T.

PERFORMANCE ANALYSIS FOR BLOCK PROCESSING

Due to the pre-averaging, each RV $y_n(t)$ in figure 1 is a sum of K independent RVs with identical statistics. Also, all N channel inputs are statistically independent of each other. In order for or-ing to be present, $N \geq 2$ is required in the following considerations. (The special case of N = 1, no or-ing, has already been addressed in equations (5) and (6).)

For a noise-only channel, let p_0 be the PDF of pre-averager output $y_n(t)$, and let c_0 be the corresponding cumulative distribution function (CDF). For signal present in channel 1, let p_1 and c_1 be the PDF and CDF of $y_1(t)$, respectively.

The or-ing output v(t) in figure 1 is

$$v(t) = \max\{y_1(t),\ldots,y_N(t)\} \ . \tag{30}$$

Its CDF for signal present, that is, hypothesis H_1, is

$$c_{v1}(u) = c_1(u)\ [c_0(u)]^{N-1} \ , \tag{31}$$

which leads to the corresponding PDF of v(t) under H_1 as

$$\begin{aligned} p_{v1}(u) = c'_{v1}(u) &= p_1(u)\ [c_0(u)]^{N-1} + c_1(u)\ (N-1)\ [c_0(u)]^{N-2}\ p_0(u) \\ &= [c_0(u)]^{N-2}\ [p_1(u)\ c_0(u) + (N-1)\ p_0(u)\ c_1(u)] \ . \end{aligned} \tag{32}$$

The signal-absent PDF of v(t) under H_0 follows immediately as

$$p_{v0}(u) = N\, p_0(u)\, [c_0(u)]^{N-1} \quad . \tag{33}$$

The CF of or-ing output v(t) is given by Fourier transform

$$f_v(\xi) = \overline{\exp(i\xi v(t))} = \int du\, \exp(i\xi u)\, p_v(u) \quad , \tag{34}$$

where either relevant form, p_{v0} or p_{v1} above, is to be used. Finally, for block processing, J = K, there is no overlap of the data used in the post-averager, meaning that processor output w(t) is the sum of M <u>independent</u>, identically distributed RVs. Therefore, the CF of the decision variable w(t) is simply

$$f_w(\xi) = [f_v(\xi)]^M \quad . \tag{35}$$

One final Fourier transform is required to manipulate CF $f_w(\xi)$ into the desired exceedance distribution function (EDF) of processor output w(t); see reference 9. This EDF will be the false alarm probability P_f or the detection probability P_d, depending on whether PDF p_{v0} or p_{v1} is used, respectively.

The fundamental Fourier transform in equation (34) will generally have to be accomplished numerically by means of a fast Fourier transform (FFT). If pre-averager output statistics p_0 and c_0 can be found in closed form or readily computed form, this cascaded FFT approach will lead to exact false alarm probability results for the or-ing processor in figure 1. If pre-averager output probability functions p_1 and c_1 can also be readily evaluated, accurate detection probability results can be

calculated as well. Some important numerical considerations for this cascaded FFT approach are presented in appendix B.

For the special case of M = 1, no post-averaging, output RV w(t) = v(t), and the corresponding EDFs follow, for any K, N, as

$$e_{w1}(u) = 1 - c_1(u)\,[c_0(u)]^{N-1} \quad , \tag{36}$$

$$e_{w0}(u) = 1 - [c_0(u)]^{N} \quad . \tag{37}$$

Now, return to arbitrary values of K, N, and M, and specialize the general results above to the three signal models of interest. J is set equal to K, that is, block processing.

COHERENT (DETERMINISTIC) SIGNAL

Define $\underline{d} = \sqrt{K}\, d$ and auxiliary Gaussian functions

$$\phi(x) = (2\pi)^{-\frac{1}{2}} \exp(-x^2/2) \quad , \quad \Phi(x) = \int_{-\infty}^{x} du\ \phi(u) \quad . \tag{38}$$

Then, for constant signal amplitudes, the requisite probability functions for pre-averager outputs $\{y_n(t)\}$ for any K, all u, are

$$p_0(u) = \frac{1}{(2\pi K)^{\frac{1}{2}}} \exp\left(-\frac{u^2}{2K}\right) = \frac{1}{\sqrt{K}}\,\phi\left(\frac{u}{\sqrt{K}}\right) \quad , \tag{39}$$

$$p_1(u) = \frac{1}{(2\pi K)^{\frac{1}{2}}} \exp\left(-\frac{(u - Kd)^2}{2K}\right) = \frac{1}{\sqrt{K}}\,\phi\left(\frac{u}{\sqrt{K}} - \underline{d}\right) \quad , \tag{40}$$

$$c_0(u) = \Phi\left(\frac{u}{\sqrt{K}}\right) , \qquad c_1(u) = \Phi\left(\frac{u}{\sqrt{K}} - \underline{d}\right) . \tag{41}$$

Using equations (33) and (32), the PDFs for or-ing output v(t) for any K and N, under H_0 and H_1, are, respectively,

$$p_{v0}(u) = \frac{N}{\sqrt{K}} \phi\left(\frac{u}{\sqrt{K}}\right) \Phi\left(\frac{u}{\sqrt{K}}\right)^{N-1} , \tag{42}$$

$$p_{v1}(u) = \frac{1}{\sqrt{K}} \Phi\left(\frac{u}{\sqrt{K}}\right)^{N-2} \left[\phi\left(\frac{u}{\sqrt{K}} - \underline{d}\right) \Phi\left(\frac{u}{\sqrt{K}}\right) + (N-1) \phi\left(\frac{u}{\sqrt{K}}\right) \Phi\left(\frac{u}{\sqrt{K}} - \underline{d}\right)\right] . \tag{43}$$

The corresponding CFs are

$$f_{v0}(\xi) = N \int dx \exp(i\xi K^{\frac{1}{2}} x) \phi(x) \Phi(x)^{N-1} , \tag{44}$$

$$f_{v1}(\xi) = \int dx \exp(i\xi K^{\frac{1}{2}} x) \Phi(x)^{N-2} [\phi(x-\underline{d}) \Phi(x) + (N-1) \phi(x) \Phi(x-\underline{d})]. \tag{45}$$

When M = 1, the EDFs in equations (36) and (37) can be combined with the results in equation (41) to immediately yield closed form expressions for P_f and P_d for any K, N, and SNR ρ.

For the special case of N = 2, these integrals can be evaluated in terms of the error function of complex argument, w( ); see reference 10, chapter 7. There follows

$$f_{v0}(\xi) = \exp(-\gamma^2) w(\gamma) , \tag{46}$$

and

$$f_{v1}(\xi) = \frac{1}{2} \exp(-\gamma^2-\nu^2+i2\gamma\nu) [w(\gamma+i\nu) + w(\gamma-i\nu)] , \tag{47}$$

where $\gamma = K^{\frac{1}{2}}\xi/2$, $\nu = K^{\frac{1}{2}}d/2$. The amount K of pre-averaging is arbitrary. The CFs of decision variable w(t) are given by the M-th powers of the above two results under H_0 and H_1, respectively, when N = 2.

For N = 1, no or-ing, and K and M arbitrary, these results simplify to system output PDF

$$p_{w1}(u) = \frac{1}{(2\pi T)^{\frac{1}{2}}} \exp\left(-\frac{(u - Td)^2}{2T}\right) , \quad T = K M , \tag{48}$$

and output EDF

$$P_d(v) = \int_v^\infty du\ p_{w1}(u) = \Phi\left(qd - \frac{v}{q}\right) , \quad q = T^{\frac{1}{2}} = (KM)^{\frac{1}{2}} . \tag{49}$$

Obviously, for N = 1, only the product KM matters, at least for unity weights in both the pre- and post-averagers.

PHASE-INCOHERENT SIGNAL

Some of the following was presented in reference 3, pages 52 and 53. Define $\underline{\rho} = K\ \rho$ with (reference 10, equation 6.5.11)

$$e_n(x) = \sum_{k=0}^{n} \frac{x^k}{k!} . \tag{50}$$

Then, for constant signal amplitudes and u > 0, the pertinent PDFs and CDFs of $\{y_n(t)\}$ are

$$p_0(u) = \frac{u^{K-1}\exp(-u)}{(K-1)!}\ , \quad c_0(u) = 1 - \exp(-u)\ e_{K-1}(u)\ , \tag{51}$$

$$p_1(u) = \left(\frac{u}{\underline{\rho}}\right)^{\frac{K-1}{2}} \exp(-u-\underline{\rho})\ I_{K-1}\left(2(\underline{\rho}u)^{\frac{1}{2}}\right)\ , \tag{52}$$

$$f_1(\xi) = (1 - i\xi)^{-K} \exp\left(\underline{\rho}\ \frac{i\xi}{1 - i\xi}\right)\ , \tag{53}$$

$$c_1(u) = 1 - Q_K\left((2\underline{\rho})^{\frac{1}{2}},(2u)^{\frac{1}{2}}\right)\ . \tag{54}$$

The PDFs for or-ing output v(t) for u > 0 are then

$$p_{v0}(u) = N\ \frac{u^{K-1}\exp(-u)}{(K-1)!}\ [1 - \exp(-u)\ e_{K-1}(u)]^{N-1}\ , \tag{55}$$

$$p_{v1}(u) = [1 - \exp(-u)\ e_{K-1}(u)]^{N-2} \left[\left(\frac{u}{\underline{\rho}}\right)^{\frac{K-1}{2}} \exp(-u-\underline{\rho})\ I_{K-1}\left(2(\underline{\rho}u)^{\frac{1}{2}}\right)\right.$$

$$\left. \times\ [1 - \exp(-u)\ e_{K-1}(u)] + (N-1)\frac{u^{K-1}\exp(-u)}{(K-1)!}\left(1-Q_K\left((2\underline{\rho})^{\frac{1}{2}},(2u)^{\frac{1}{2}}\right)\right)\right]\ . \tag{56}$$

In the special case of K = 1, that is, no pre-averaging, the CF of v(t) with or-ing and signal present is available in closed form by Fourier transforming $p_{v1}(u)$ to obtain, using reference 11, equation 6.631 4, and reference 12, equation (24),

$$f_{v1}(\xi) = i\xi \sum_{k=0}^{N-1} \binom{N-1}{k} \frac{(-1)^{k+1}}{(k - i\xi)(k + 1 - i\xi)} \exp\left(-\rho\ \frac{k - i\xi}{k + 1 - i\xi}\right) \tag{57}$$

for any N ≥ 1. The mean of v(t) with signal present follows as

$$\mu_{v1} = 1 + \rho + \sum_{k=1}^{N-1} \binom{N-1}{k} \frac{(-1)^{k-1}}{k(k+1)} \exp\left(-\rho \frac{k}{k+1}\right) . \qquad (58)$$

Finally, when $\rho = 0$, equation (57) reduces to the more useful form for the CF as

$$f_{v0}(\xi) = \left[\prod_{n=1}^{N}\left(1 - \frac{i\xi}{n}\right)\right]^{-1}, \quad \mu_{v0} = \sum_{n=1}^{N} \frac{1}{n} ; \qquad (59)$$

this alternative CF form will be derived in the next subsection.

For the special case of $K = 2$ and no signal present, the CF of $v(t)$ is available by Fourier transforming PDF $p_{v0}(u)$ to get

$$f_{v0}(\xi) = N! \sum_{n=0}^{N-1} \frac{(-1)^n}{(N-1-n)!} \sum_{k=0}^{n} \frac{k+1}{(n-k)!\ (n+1-i\xi)^{k+2}} . \qquad (60)$$

This result holds for arbitrary amounts of or-ing, $N \geq 1$.

For $N = 2$, the CF of $v(t)$ under H_1 is available (after considerable labor) by Fourier transforming PDF $p_{v1}(u)$ to get

$$f_{v1}(\xi) = \frac{1}{z_1\, z_2^{2K-1}} \exp\left(-\underline{\rho}\, \frac{z_1}{z_2}\right) \sum_{k=0}^{K-1} \binom{2K-1}{K+k} z_1^{-k}\, e_k\left(\underline{\rho}\, \frac{z_1}{z_2}\right)$$

$$+ \frac{1}{z_1^K} \exp\left(\underline{\rho}\, \frac{i\xi}{z_1}\right) - \frac{1}{z_2^{2K-1}} \exp\left(-\underline{\rho}\, \frac{z_1}{z_2}\right) \sum_{k=0}^{K-1} \binom{2K-1}{K+k} z_1^{k}\, e_k\left(\frac{\underline{\rho}}{z_1 z_2}\right) \qquad (61)$$

for any $K \geq 1$, where $z_1 = 1 - i\xi$, $z_2 = 2 - i\xi$. For $K = 2$, the mean follows as $\mu_{v1} = 2(1 + \rho) + \exp(-\rho)\,(6 + \rho)/8$, using $\underline{\rho} = 2\rho$.

For N = 2 and signal absent, the Fourier transform of PDF $p_{v0}(u)$ yields CF

$$f_{v0}(\xi) = \frac{2}{(1 - i\xi)^K} - 2 \sum_{k=0}^{K-1} \binom{K - 1 + k}{k} \frac{1}{(2 - i\xi)^{K+k}} , \qquad (62)$$

with mean

$$\mu_{v0} = 2K \left(1 - \sum_{k=0}^{K-1} \binom{K + k}{k} \frac{1}{2^{K+k+1}}\right) . \qquad (63)$$

This form for CF $f_{v0}(\xi)$ in equation (62) is not obtained by setting $\underline{\rho} = 0$ in equation (61); however, numerical investigation of both forms reveals they are equal. For K = 2, the CF in equation (62) further specializes to

$$f_{v0}(\xi) = \frac{2}{(1 - i\xi)^2} - \frac{2}{(2 - i\xi)^2} - \frac{4}{(2 - i\xi)^3} . \qquad (64)$$

The CF of decision variable w(t) for signal present is given by

$$f_{w1}(\xi) = [f_{v1}(\xi)]^M . \qquad (65)$$

When CF $f_{w1}(\xi)$ is available, a Fourier transform will yield the detection (and false alarm) probabilities for any K, N, and M. When M = 1, the EDFs in equations (36) and (37) can be combined with results (51) and (54) to immediately yield closed form expressions for P_f and P_d for any K, N, and SNR ρ.

When N = 1, no or-ing and K and M are arbitrary, the results simplify, respectively, to PDF and EDF

$$p_{w1}(u) = \left(\frac{u}{B}\right)^{\frac{T-1}{2}} \exp(-u-B)\ I_{T-1}\left(2(Bu)^{\frac{1}{2}}\right) \quad \text{for } u > 0\ , \tag{66}$$

$$P_d(v) = \int_v^\infty du\ p_{w1}(u) = Q_T\left((2B)^{\frac{1}{2}},(2v)^{\frac{1}{2}}\right) \quad \text{for } v > 0\ , \tag{67}$$

where $T = KM$, $B = T\rho = KM\rho$. Obviously, for N = 1 here, only the product KM matters; this presumes unity weights in both the pre- and post-averagers.

RANDOM GAUSSIAN SIGNAL

Some of this material appeared in reference 3, pages 51 and 52. Define $a = 1/(1 + \rho)$. Then, for constant signal powers and $u > 0$, the pertinent PDFs are

$$p_0(u) = \frac{u^{K-1}\ \exp(-u)}{(K-1)!}\ , \quad c_0(u) = 1 - \exp(-u)\ e_{K-1}(u)\ , \tag{68}$$

$$p_1(u) = \frac{a^K\ u^{K-1}\ \exp(-au)}{(K-1)!}\ , \quad c_1(u) = 1 - \exp(-au)\ e_{K-1}(au)\ . \tag{69}$$

The PDFs for or-ing output v(t) are, under hypotheses H_0 and H_1, respectively,

$$p_{v0}(u) = N\ \frac{u^{K-1}\ \exp(-u)}{(K-1)!}\ [1 - \exp(-u)\ e_{K-1}(u)]^{N-1}\ , \tag{70}$$

which behaves as u^{KN-1} as $u \to 0+$, and

$$p_{v1}(u) = [1 - \exp(-u)\ e_{K-1}(u)]^{N-2}\ \frac{u^{K-1}}{(K-1)!}\ \Big(a^K \exp(-au)$$

$$\times\ [1 - \exp(-u)\ e_{K-1}(u)] + (N-1)\ \exp(-u)\ [1 - \exp(-au)\ e_{K-1}(au)]\Big). \tag{71}$$

In the special case of K = 1, that is, no pre-averaging, the CF of v(t) with or-ing and signal present is available in closed form by Fourier transforming PDF p_{v1} to get (reference 11, equations 3.191 3 and 8.384 1)

$$f_{v1}(\xi) = (1)_{N-1}\ \left(\frac{i\xi}{(a-i\xi)_N} + \frac{1}{(1-i\xi)_{N-1}}\right)\ , \tag{72}$$

for any $N \geq 1$. Here, $(z)_n = z(z+1) \cdots (z+n-1)$ is Pochhammer's symbol; see reference 10, equation 6.1.22. When $\rho = 0$, then $a = 1$ and this CF reduces to

$$f_{v0}(\xi) = \frac{(1)_N}{(1-i\xi)_N} = \left[\prod_{n=1}^{N}\left(1 - \frac{i\xi}{n}\right)\right]^{-1}\ . \tag{73}$$

The CF of decision variable w(t) for signal present is given by closed form

$$f_{w1}(\xi) = [f_{v1}(\xi)]^M \tag{74}$$

in this special case of K = 1, where CF f_{v1} is given by equation (72). Then, one single Fourier transform will yield the detection and false alarm probabilities (P_d and P_f) for any N and M, that is, arbitrary amounts of or-ing and post-averaging.

When M = 1, the EDFs in equations (36) and (37) can be combined with results (68) and (69) to immediately yield closed form expressions for P_f and P_d for any K, N, and SNR ρ.

The cumulants $\{\chi_v(k)\}$ of v(t), for signal present, are rather involved, even for K = 1. The mean and variance are presented below, while the moments and cumulants of general order k are derived in appendix C. For K = 1,

$$\chi_v(1) = \sum_{n=1}^{N-1} \frac{1}{n} + r \ , \quad \text{with} \quad r = \frac{(1)_{N-1}}{(a)_N} \ , \tag{75}$$

$$\chi_v(2) = \sum_{n=1}^{N} \frac{1}{n^2} - \left(r - \frac{1}{N}\right)^2 - 2(a-1)r \sum_{n=1}^{N} \frac{1}{n(n+a-1)} \ . \tag{76}$$

For signal strength $\rho = 0$, a = 1 and the k-th cumulant of v(t) is, for K = 1,

$$\chi_v(k) = (k-1)! \sum_{n=1}^{N} \frac{1}{n^k} \quad \text{for } k \geq 1 \ . \tag{77}$$

These results allow for arbitrary amounts of or-ing, that is, $N \geq 1$.

For the special case of K = 2 and no signal present, the CF of or-ing output v(t) is available in closed form by Fourier transforming PDF $p_{v0}(u)$ to get

$$f_{v0}(\xi) = N! \sum_{n=0}^{N-1} \frac{(-1)^n}{(N-1-n)!} \sum_{k=0}^{n} \frac{k+1}{(n-k)! \ (n+1-i\xi)^{k+2}} \ . \tag{78}$$

This result holds for arbitrary amounts of or-ing. CF $f_{v1}(\xi)$ for K = 2 can also be found in closed form, although it is more complicated than the result above. Larger values of K yield progressively more complicated closed forms for $f_{v0}(\xi)$ and $f_{v1}(\xi)$. For example, $p_{v1}(u)$ for K = 2 and N = 2 can be Fourier transformed to yield CF

$$f_{v1}(\xi) = \frac{1}{(1 - i\xi)^2} + \frac{a^2}{(a - i\xi)^2} + \frac{(1+a^2)i\xi - (1+a)^3}{(1 + a - i\xi)^3} , \qquad (79)$$

with mean

$$\mu_{v1} = 2\,\frac{1 + 3a + 3a^2 + 3a^3 + a^4}{a\,(1 + a)^3} = 2\,\frac{11 + 22\rho + 18\rho^2 + 7\rho^3 + \rho^4}{(2 + \rho)^3} . \qquad (80)$$

When N = 1, no or-ing and K and M are arbitrary, these results simplify to processor output PDF

$$p_{w1}(u) = \frac{a^T\, u^{T-1}\, \exp(-au)}{(T-1)!} \quad \text{for } u > 0 , \qquad (81)$$

and EDF

$$P_d(v) = \int_v^\infty du\; p_{w1}(u) = \exp(-av)\; e_{T-1}(av) \quad \text{for } v > 0 , \qquad (82)$$

where T = KM. For N = 1, only the product KM matters; the above results presume unity weights in both the pre- and post-averagers.

QUANTITATIVE PERFORMANCE RESULTS

This section gives specific quantitative detectability results for or-ing with various amounts of pre-averaging K and post-averaging M. In particular, numerous ROCs are presented in appendices D, E, F, and G for the cases of KM = 4, 16, 64, and 256, respectively. The particular cases run are indicated in table 1; a total of 124 ROCs are represented. For N = 1, since only the product KM matters, only one ROC need be presented (the first curve in each appendix) under the title labeled M = 1.

Table 1. Cases Run

K	M	N	
4	1	1,2,4,8,16,32	Appendix D
2	2		1 + 15 ROCs
1	4		
16	1	1,2,4,8,16,32	Appendix E
8	2		1 + 25 ROCs
4	4		
2	8		
1	16		
64	1	1,2,4,8,16,32	Appendix F
32	2		1 + 35 ROCs
16	4		
8	8		
4	16		
2	32		
1	64		
256	1	1,2,4,8,16,32	Appendix G
128	2		1 + 45 ROCs
64	4		
32	8		
16	16		
8	32		
4	64		
2	128		
1	256		

NUMERICAL APPROACH

Whenever the CF of or-ing output v(t) can be derived in closed form, such as in equations (72), (73), (78), or (79), it is used directly in equation (35) to find the CF of decision variable w(t). However, when this is not possible, the closed-form results for the or-ing output PDFs given in equations (32) and (33) are used, instead, in the cascaded FFT procedure outlined in equations (34) and (35). In the former case, the fundamental sampling increment is Δ_ξ, starting in the CF domain, whereas in the latter case, the fundamental sampling increment is Δ_u, starting in the PDF domain. The pertinent numerical parameter values used for each case investigated are indicated on the appropriate ROCs in appendices D through G.

REQUIRED INPUT SIGNAL-TO-NOISE RATIOS

The numerous ROCs in appendices D through G enable a user to easily investigate and determine the amount of system input SNR required for the or-ing device to achieve a specified level of detectability performance, in terms of a desired false alarm probability P_f and detection probability P_d, over a wide range of parameter values. In an effort to partially condense this voluminous information, a standard operating point (SOP) is defined here as P_f = 1E-3, P_d = 0.5, and a high-quality operating point (HOP) is defined as P_f = 1E-6, P_d = 0.9. The corresponding required values of input SNR $\rho(dB) = 10 \log(\rho) = 10 \log(\sigma_s^2/\sigma_n^2)$,

as determined from the ROCs in appendices D through G, are listed in tables 2 through 9. (These accurate values were interpolated from the ROCs while the false alarm and detection probability numbers, P_f and P_d, were still resident in the computer; eyeball interpolation from the plotted ROCs cannot be done this accurately.)

These input SNR requirements are plotted in figures 2 through 9. As expected, the required input SNR ρ increases monotonically with the number N of channels or-ed if K and M are held fixed. Also, the required input SNR ρ increases monotonically with the amount M of post-averaging employed, if N and KM are held fixed; alternatively, the required input SNR ρ decreases with the amount K of pre-averaging employed, if N and KM are held fixed. The exact rates can be determined from figures 2 through 9.

Table 2. Required Input SNR ρ(dB) for P_f = 1E-3, P_d = 0.5, KM = 4, Gaussian Signal

K	M	N = 1	N = 2	N = 4	N = 8	N = 16	N = 32
4	1	4.08	4.46	4.81	5.13	5.42	5.70
2	2	4.08	4.66	5.17	5.62	6.02	6.38
1	4	4.08	4.82	5.47	6.05	6.55	7.00

Table 3. Required Input SNR ρ(dB) for P_f = 1E-6, P_d = 0.9, KM = 4, Gaussian Signal

K	M	N = 1	N = 2	N = 4	N = 8	N = 16	N = 32
4	1	10.50	10.67	10.84	11.00	11.16	11.31
2	2	10.50	10.81	11.10	11.37	11.59	11.83
1	4	10.50	10.96	11.37	11.73	12.08	12.39

Table 4. Required Input SNR ρ(dB) for P_f = 1E-3, P_d = 0.5, KM = 16, Gaussian Signal

K	M	N = 1	N = 2	N = 4	N = 8	N = 16	N = 32
16	1	-0.03	0.31	0.61	0.89	1.14	1.38
8	2	-0.03	0.53	1.00	1.42	1.79	2.12
4	4	-0.03	0.73	1.39	1.95	2.43	2.86
2	8	-0.03	0.91	1.72	2.42	3.02	3.54
1	16	-0.03	1.03	1.98	2.81	3.51	4.12

Table 5. Required Input SNR ρ(dB) for P_f = 1E-6, P_d = 0.9, KM = 16, Gaussian Signal

K	M	N = 1	N = 2	N = 4	N = 8	N = 16	N = 32
16	1	4.51	4.65	4.79	4.92	5.05	5.17
8	2	4.51	4.78	5.03	5.26	5.47	5.67
4	4	4.51	4.95	5.34	5.69	6.01	6.29
2	8	4.51	5.13	5.67	6.15	6.57	6.94
1	16	4.51	5.27	5.95	6.55	7.08	7.54

Table 6. Required Input SNR ρ(dB) for P_f = 1E-3, P_d = 0.5, KM = 64, Gaussian Signal

K	M	N = 1	N = 2	N = 4	N = 8	N = 16	N = 32
64	1	-3.58	-3.28	-3.00	-2.74	-2.52	-2.31
32	2	-3.58	-3.06	-2.61	-2.22	-1.89	-1.58
16	4	-3.58	-2.83	-2.19	-1.66	-1.20	-0.81
8	8	-3.58	-2.61	-1.80	-1.11	-0.53	-0.04
4	16	-3.58	-2.44	-1.45	-0.61	0.09	0.68
2	32	-3.58	-2.33	-1.18	-0.21	0.61	1.32
1	64	-3.58	-2.26	-1.03	0.07	1.01	1.83

Table 7. Required Input SNR ρ(dB) for P_f = 1E-6, P_d = 0.9, KM = 64, Gaussian Signal

K	M	N = 1	N = 2	N = 4	N = 8	N = 16	N = 32
64	1	0.12	0.24	0.36	0.47	0.57	0.68
32	2	0.12	0.36	0.57	0.77	0.96	1.13
16	4	0.12	0.52	0.88	1.19	1.48	1.74
8	8	0.12	0.72	1.24	1.69	2.08	2.43
4	16	0.12	0.92	1.60	2.19	2.70	3.14
2	32	0.12	1.08	1.91	2.64	3.27	3.80
1	64	0.12	1.18	2.15	3.00	3.73	4.37

Table 8. Required Input SNR ρ(dB) for P_f = 1E-3, P_d = 0.5, KM = 256, Gaussian Signal

K	M	N = 1	N = 2	N = 4	N = 8	N = 16	N = 32
256	1	-6.87	-6.57	-6.32	-6.07	-5.87	-5.65
128	2	-6.87	-6.37	-5.94	-5.57	-5.24	-4.96
64	4	-6.87	-6.12	-5.51	-5.00	-4.56	-4.18
32	8	-6.87	-5.89	-5.08	-4.42	-3.87	-3.39
16	16	-6.87	-5.67	-4.69	-3.86	-3.18	-2.60
8	32	-6.87	-5.52	-4.35	-3.36	-2.55	-1.86
4	64	-6.87	-5.42	-4.10	-2.97	-2.01	-1.21
2	128	-6.87	-5.36	-3.96	-2.69	-1.60	-0.68
1	256	-6.87	-5.36	-3.90	-2.53	-1.33	-0.30

Table 9. Required Input SNR ρ(dB) for P_f = 1E-6, P_d = 0.9, KM = 256, Gaussian Signal

K	M	N = 1	N = 2	N = 4	N = 8	N = 16	N = 32
256	1	-3.57	-3.46	-3.36	-3.25	-3.15	-3.06
128	2	-3.57	-3.36	-3.15	-2.98	-2.81	-2.64
64	4	-3.57	-3.18	-2.86	-2.57	-2.31	-2.07
32	8	-3.57	-2.99	-2.49	-2.07	-1.70	-1.39
16	16	-3.57	-2.77	-2.10	-1.54	-1.06	-0.65
8	32	-3.57	-2.57	-1.72	-1.01	-0.41	0.10
4	64	-3.57	-2.42	-1.40	-0.54	0.19	0.80
2	128	-3.57	-2.30	-1.16	-0.16	0.69	1.41
1	256	-3.57	-2.25	-1.01	0.10	1.07	1.90

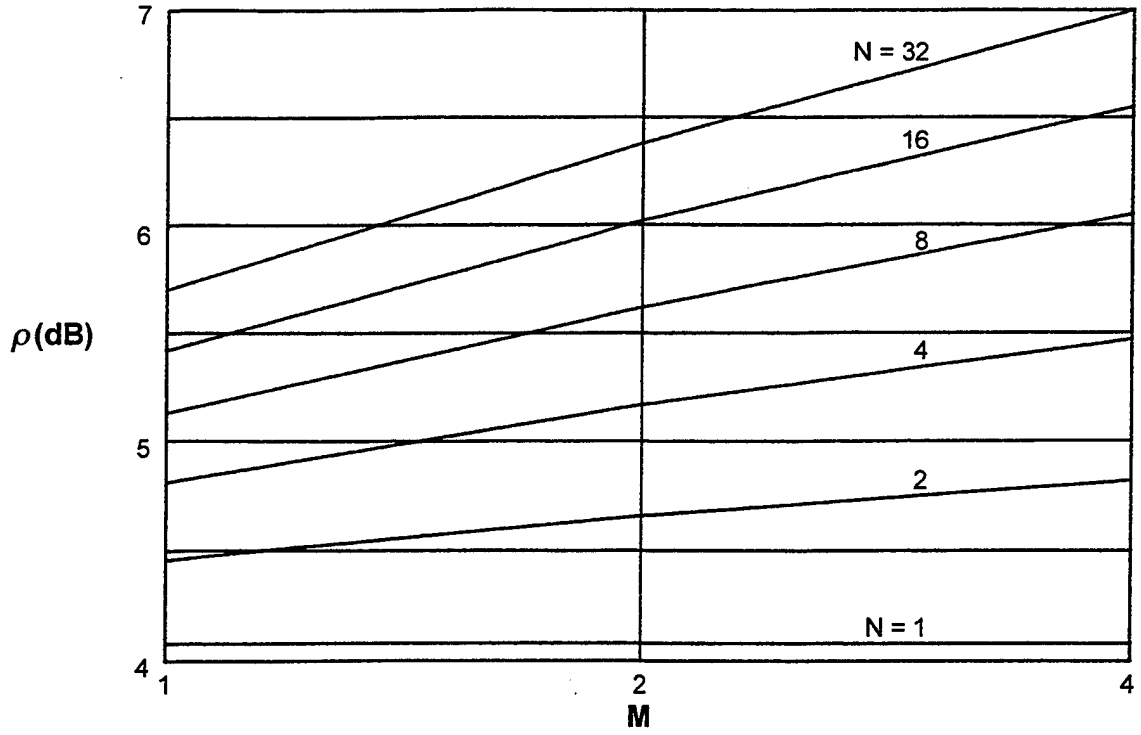

Figure 2. Required Input SNR for P_f = 1E - 3, P_d = 0.5, KM = 4, Gaussian Signal

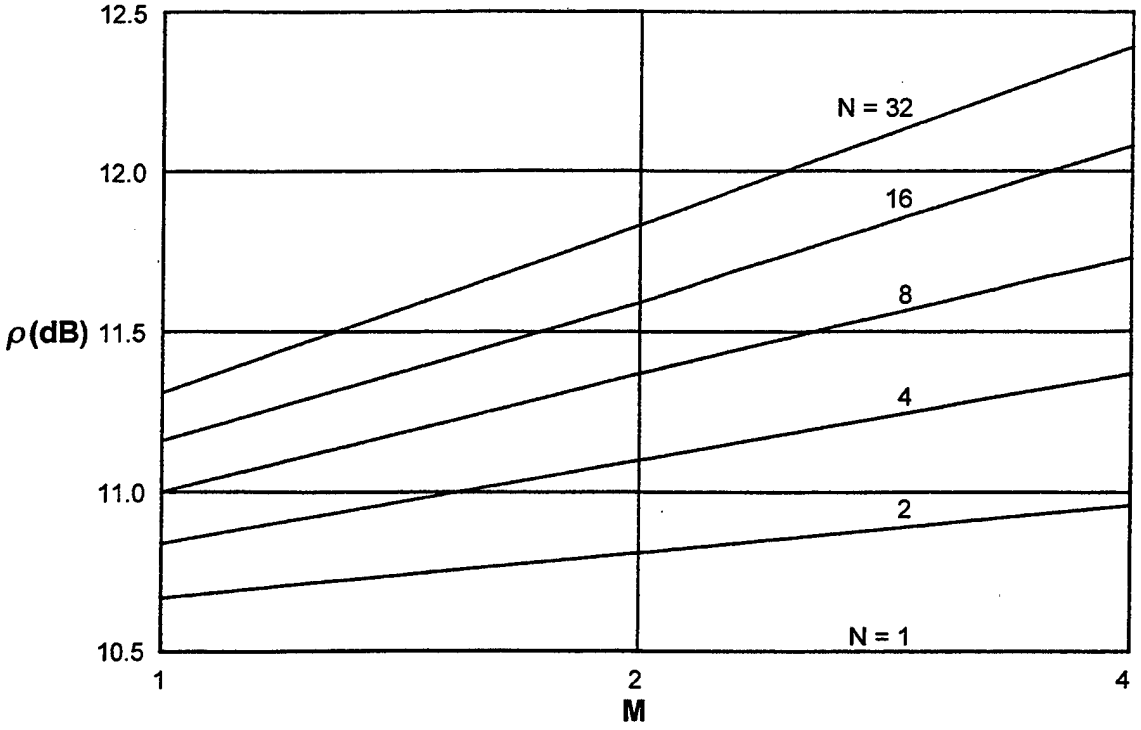

Figure 3. Required Input SNR for P_f = 1E - 6, P_d = 0.9, KM = 4, Gaussian Signal

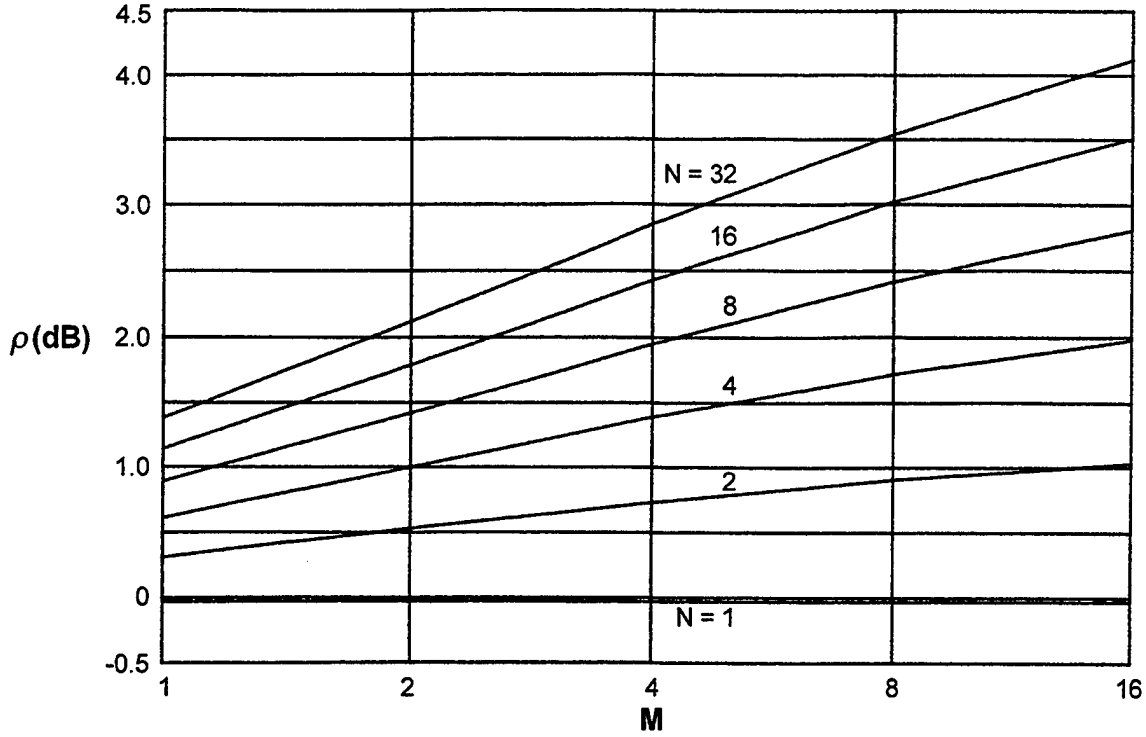

Figure 4. Required Input SNR for P_f = 1E - 3, P_d = 0.5, KM = 16, Gaussian Signal

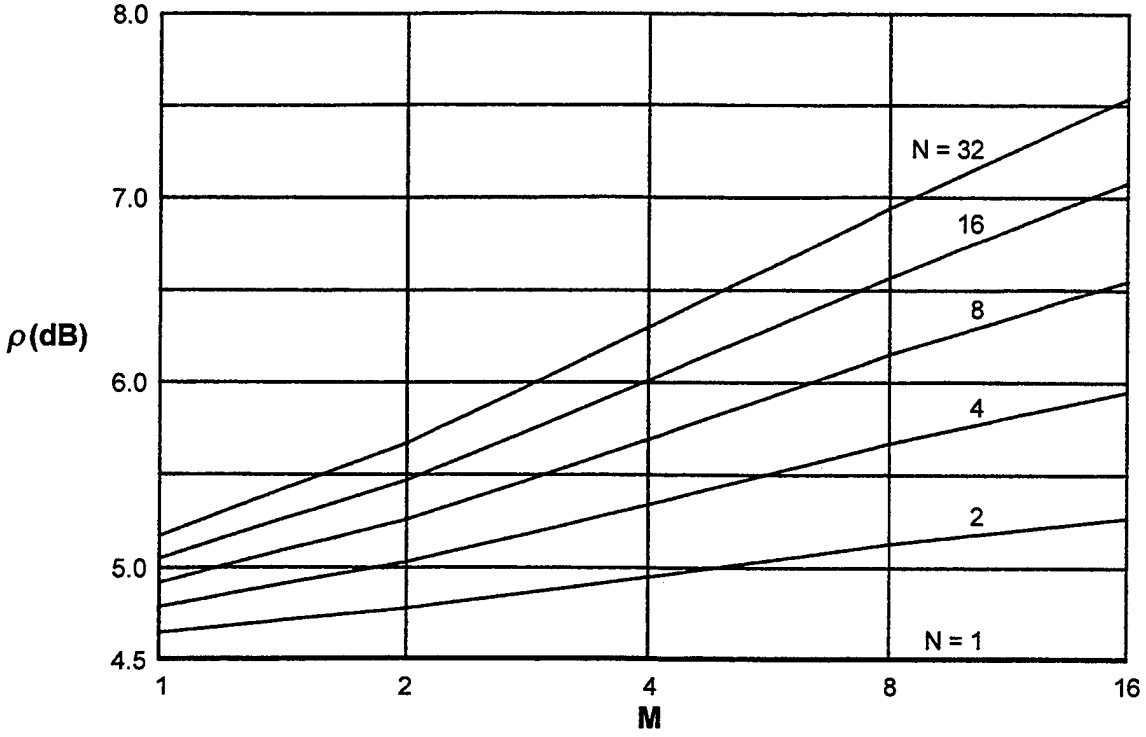

Figure 5. Required Input SNR for P_f = 1E - 6, P_d = 0.9, KM = 16, Gaussian Signal

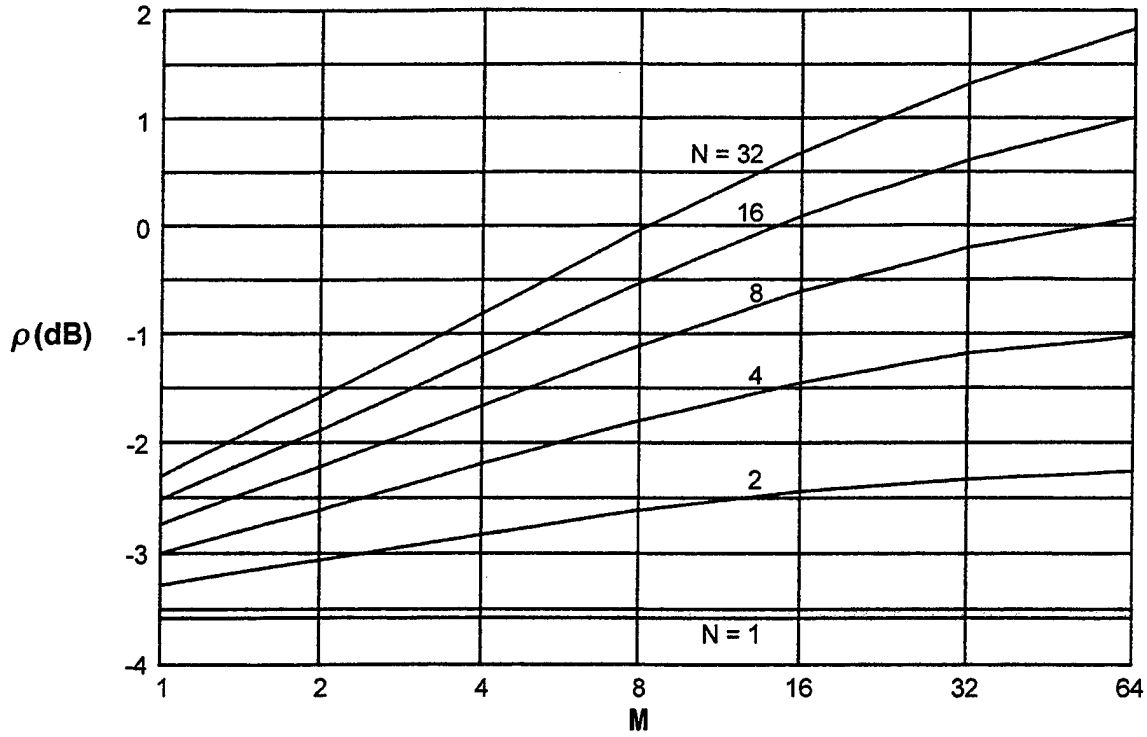

Figure 6. Required Input SNR for P_f = 1E - 3, P_d = 0.5, KM = 64, Gaussian Signal

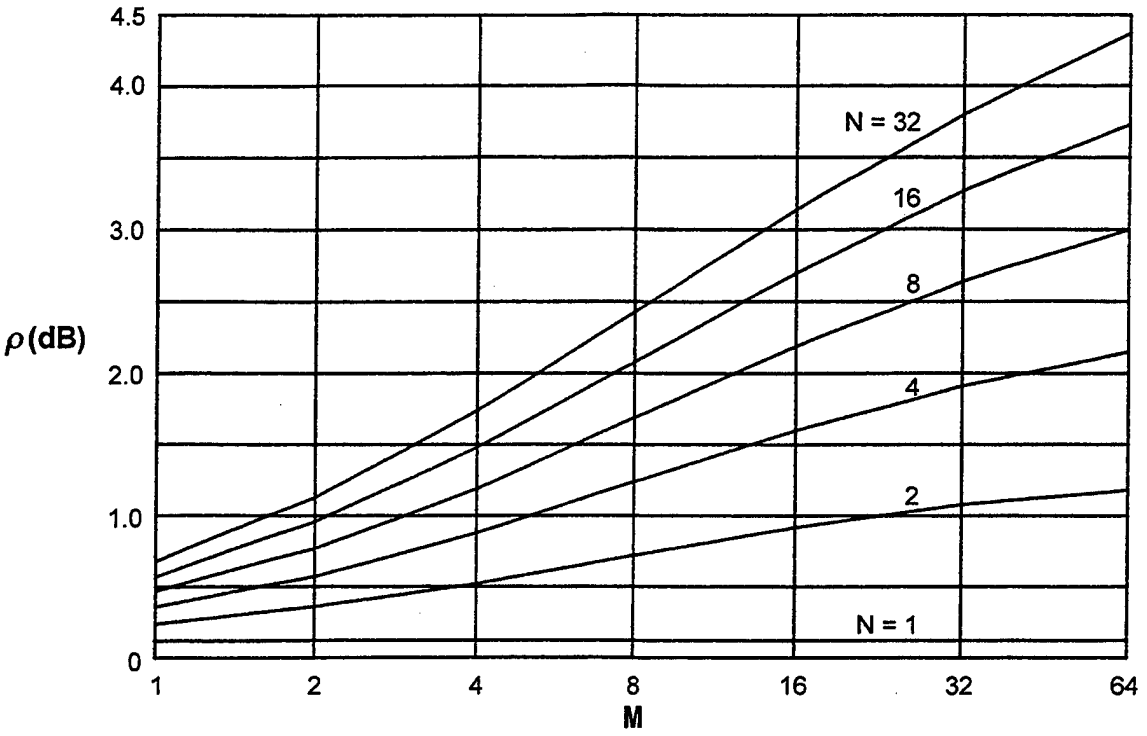

Figure 7. Required Input SNR for P_f = 1E - 6, P_d = 0.9, KM = 64, Gaussian Signal

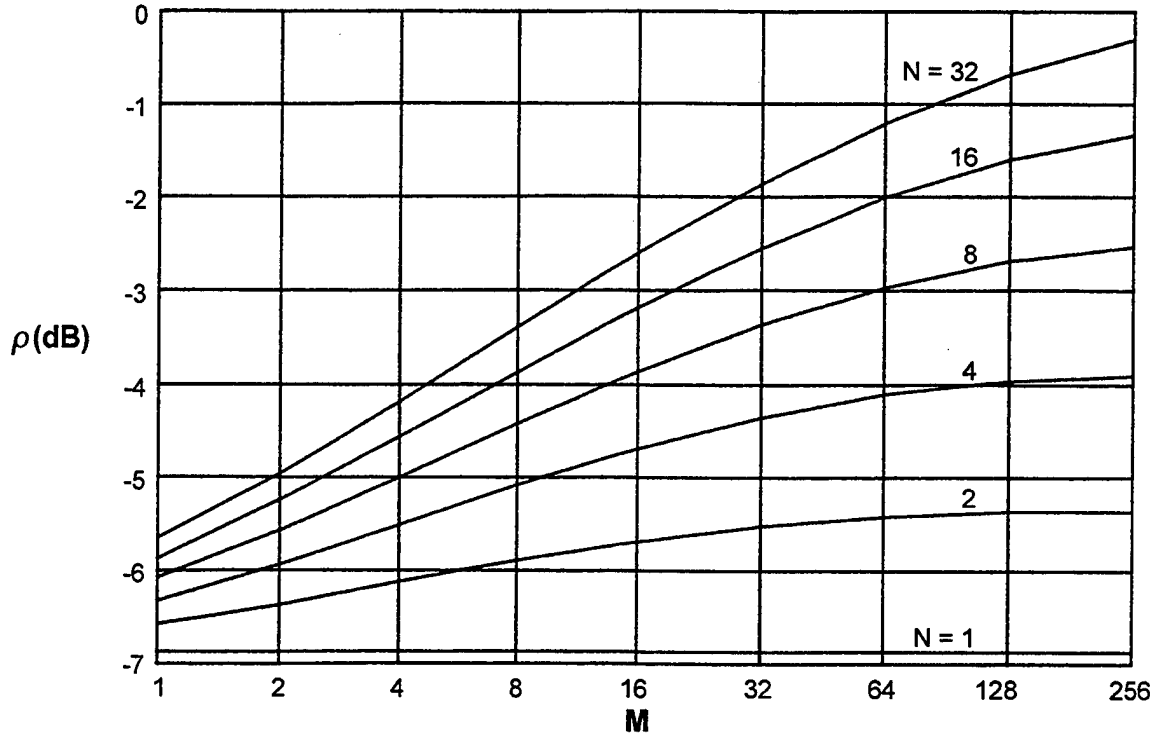

Figure 8. Required Input SNR for P_f = 1E - 3, P_d = 0.5, KM = 256, Gaussian Signal

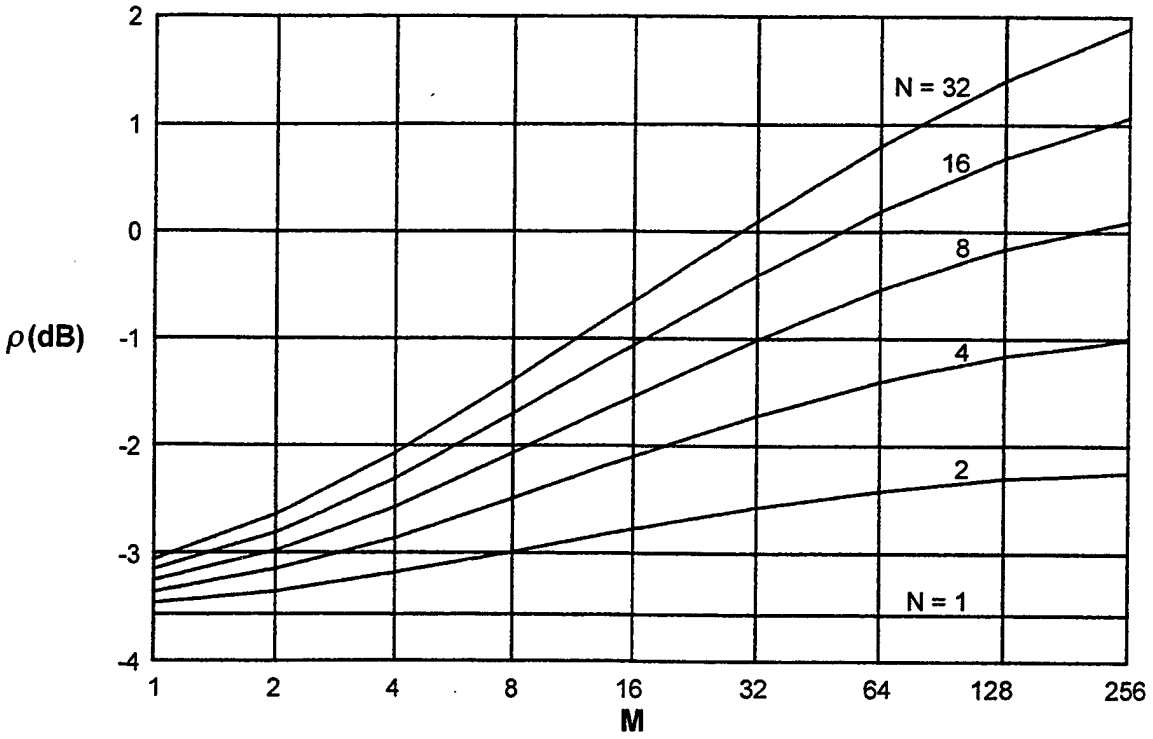

Figure 9. Required Input SNR for P_f = 1E - 6, P_d = 0.9, KM = 256, Gaussian Signal

TRADEOFF BETWEEN PRE- AND POST-AVERAGING

For a fixed amount of total time-bandwidth product, that is, KM constant, it is possible to shift some of the pre-averaging to post-averaging, or vice-versa. For example, if KM = 16, this could be accomplished by taking K = 16, M = 1, which corresponds to no post-averaging, and switching to K = 1, M = 16, which corresponds to no pre-averaging. Alternatively, intermediate values such as K = 4, M = 4, could be used, still keeping KM = 16.

In all cases, increasing M at the sake of K requires larger input SNRs to maintain the same operating point; see figures 2 through 9. This is related to the fact that the optimum processor corresponds to conducting all pre-averaging before any nonlinear operations; see appendix A. For example, if KM = 16, in order to maintain the SOP, table 4 indicates that increases of 0.72 dB, 1.37 dB, 1.92 dB, 2.37 dB, 2.74 dB are required for N = 2, 4, 8, 16, 32, respectively, if the switch is made from all pre-averaging to all post-averaging. Alternatively, for the HOP, the corresponding differences in table 5 are smaller (0.62 dB, 1.16 dB, 1.63 dB, 2.03 dB, 2.37 dB for N = 2, 4, 8, 16, 32, respectively).

For a HOP like P_f = 1E-6, P_d = 0.9, larger input SNRs are naturally required to achieve this level of performance. At these larger input SNRs, the or-ing process is more frequently

dominated by the signal-bearing channel. Therefore, as the number N of channels or-ed increases, the required increases in SNR are less severe with increasing N than for a lower-quality operating point, such as P_f = 1E-3, P_d = 0.5. For example, for K = 16, M = 1, increasing N from 2 to 32 requires a 1.07-dB SNR increase to maintain the SOP, whereas only an additional 0.52 dB is needed at the HOP.

A related observation is that, for a given configuration (fixed K and M), the increase in SNR required to maintain the SOP, as the amount of or-ing increases, is more severe for the larger M values. Thus, for KM = 16, as N increases from 2 to 32, a 1.07-dB SNR increase (1.38 - 0.31) suffices to maintain the SOP for M = 1, whereas a 3.09-dB increase (4.12 - 1.03) is required for M = 16. The corresponding increases at the HOP are 0.52 dB (5.17 - 4.65) for M = 1 versus 2.27 dB (7.54 - 5.27) for M = 16, as N increases from 2 to 32. The behaviors are similar for the other values of KM, although the required input SNR ρ values are smaller as KM increases, due to the additional observation times allowed.

EFFECT OF OVERLAPPING DATA AVERAGES

Each pre-averager output is the result of an accumulation of the past K data values at its input. Therefore, each adjacent pair of pre-averager time outputs is rather highly correlated, especially for large K. However, the or-ing output is the result of a comparison of N independent pre-averager outputs, with only the largest surviving. For large N, this competition decreases the correlation of successive or-ing time outputs, because a different channel may dominate the or-ing decision each time sample (see appendix H). This decrease in correlation suggests that the or-ing output should be sampled more often than once every K samples, which corresponds to block averaging of non-overlapping adjacent blocks of data, that is, skip factor $J = K$.

However, there are two conflicting factors that tend to favor sampling only once every K samples. The first one is that, for signal present with a fairly reasonable input SNR, the same or-ing channel input will tend to dominate the decision, thereby tending to keep the or-ing output correlation at larger values, which would obviate the need for more frequent sampling.

The second factor is that when the sampling interval at the or-ing output is $J = K$, the effective weighting of the input data is uniform over the total observation time T. This uniform effective weighting would be optimum for detection purposes if there were no or-ing, $N = 1$, since none of the input time samples

are preferred over any other time samples (see appendix A). At the other extreme of sampling every successive or-ing time output, the effective weighting has a trapezoidal shape, peaking in the interior of the observation interval. This effective weighting discounts the edge samples in the observation interval in terms of their effect on the decision variable.

Determining which effect dominates the processor performance can be ascertained only by conducting simulations to evaluate the ROCs for a variety of parameter values, including the amount M of post-averaging. Each of the three results in tables 10, 11, and 12 (for a Gaussian signal) has been obtained under the simultaneous conditions of keeping the pre-averaging time K fixed, keeping the post-averaging time (M-1)J fixed, and, therefore, keeping the total observation time T = K + (M-1)J fixed. The three cases considered correspond, respectively, to a small total observation time T = 24, an intermediate value T = 64, and a large value T = 256. The amount of or-ing is varied from N = 1 to N = 32.

In tables 10, 11, and 12, the required SNR values ρ(dB) that are not enclosed in parentheses correspond to the SOP, whereas the values in parentheses are for the HOP. The latter sets are given only for J = K or N = 1, both of which special cases can be evaluated accurately analytically. The remaining SNR values in tables 10, 11, and 12 were obtained by simulations using one million trials; therefore, estimation of the required input SNR

to achieve P_f = 1E-6 is not possible with this few trials. (The HOP values for the top row, N = 1, of table 12 are -3.57, -3.53, -3.50, -3.48, -3.47 dB, respectively.)

Tables 10, 11, and 12 are plotted in figures 10, 11, and 12. Perusal of these results reveals that the losses associated with increased or-ing, N, are not significantly ameliorated by using J < K, when the amounts of pre- and post-averaging are kept constant. For example, from table 10, with a Gaussian signal, K = 8, N = 32, (M-1)J = 16, the improvement in switching from J = 8 to J = 1 is virtually nil. In fact, it is better to use J = 4 for this particular example with N = 32, that is, 50% overlap, for which the improvement is approximately 0.1 dB (1.44 - 1.31) relative to J = 8. The reason for this behavior is the effective trapezoidal weighting. In fact, for slight or-ing, that is, small N, the effective trapezoidal weighting for small J actually leads to losses in performance relative to J = K.

In the second Gaussian-signal example, table 11, with K = 4, N = 32, (M-1)J = 60, the gain at the SOP, in switching from J = K to J = 1, is only 0.3 dB (0.68 - 0.36). Smaller N values achieve even smaller gains. Finally, the long observation time T = 256, shown in table 12, confirms the trends anticipated earlier. In summary, for moderate amounts of or-ing, overlapped averaging is not worthwhile. On the other hand, for a significant amount of or-ing, N >> 1, the gains would be more substantial, and the use of J < K, say 50% overlap, might be worth re-considering.

Table 10. Required Input SNR ρ(dB) for P_f = 1E-3, P_d = 0.5, K = 8, (M-1)J = 16, T = 24, Gaussian Signal

N	M=3, J=8	M=5, J=4	M=9, J=2	M=17, J=1
1	-1.10 (3.12)	-0.86 (3.43)	-0.68 (3.66)	-0.56 (3.80)
2	-0.43 (3.47)	-0.32	-0.18	-0.08
4	0.14 (3.79)	0.14	0.25	0.33
8	0.63 (4.08)	0.57	0.64	0.71
16	1.06 (4.34)	0.97	1.01	1.07
32	1.44 (4.58)	1.31	1.34	1.38

Table 11. Required Input SNR ρ(dB) for P_f = 1E-3, P_d = 0.5, K = 4, (M-1)J = 60, T = 64, Gaussian Signal

N	M=16, J=4	M=31, J=2	M=61, J=1
1	-3.58 (0.12)	-3.54 (0.17)	-3.51 (0.20)
2	-2.44 (0.92)	-2.50	-2.51
4	-1.45 (1.60)	-1.60	-1.61
8	-0.61 (2.19)	-0.82	-0.86
16	0.09 (2.70)	-0.13	-0.19
32	0.68 (3.14)	0.41	0.36

Table 12. Required Input SNR ρ(dB) for P_f = 1E-3, P_d = 0.5, K = 16, (M-1)J = 240, T = 256, Gaussian Signal

N	M=16,J=16	M=31,J=8	M=61,J=4	M=121,J=2	M=241,J=1
1	-6.87 (-3.57)	-6.83	-6.80	-6.79	-6.78
2	-5.67 (-2.77)	-5.77	-5.78	-5.77	-5.77
4	-4.69 (-2.10)	-4.89	-4.92	-4.91	-4.92
8	-3.86 (-1.54)	-4.10	-4.16	-4.18	-4.17
16	-3.18 (-1.06)	-3.47	-3.53	-3.55	-3.55
32	-2.60 (-0.65)	-2.93	-3.01	-3.03	-3.04

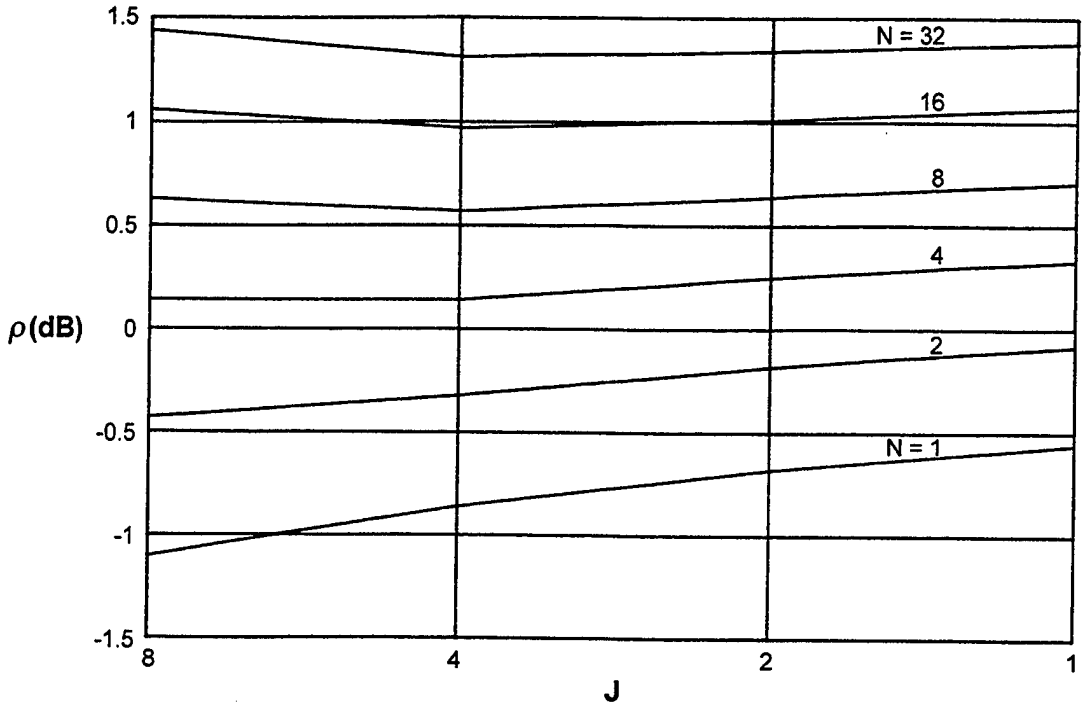

Figure 10. Required Input SNR for P_f = 1E - 3, P_d = 0.5, K = 8, (M - 1)J = 16, T = 24, Gaussian Signal

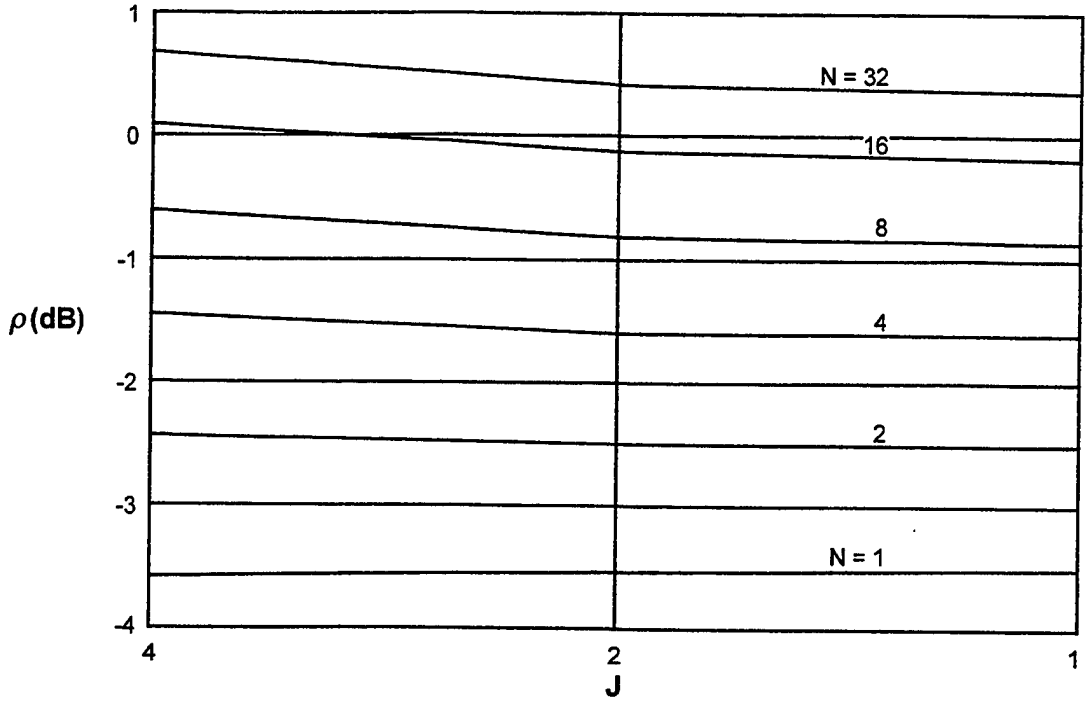

Figure 11. Required Input SNR for P_f = 1E - 3, P_d = 0.5, K = 4, (M - 1)J = 60, T = 64, Gaussian Signal

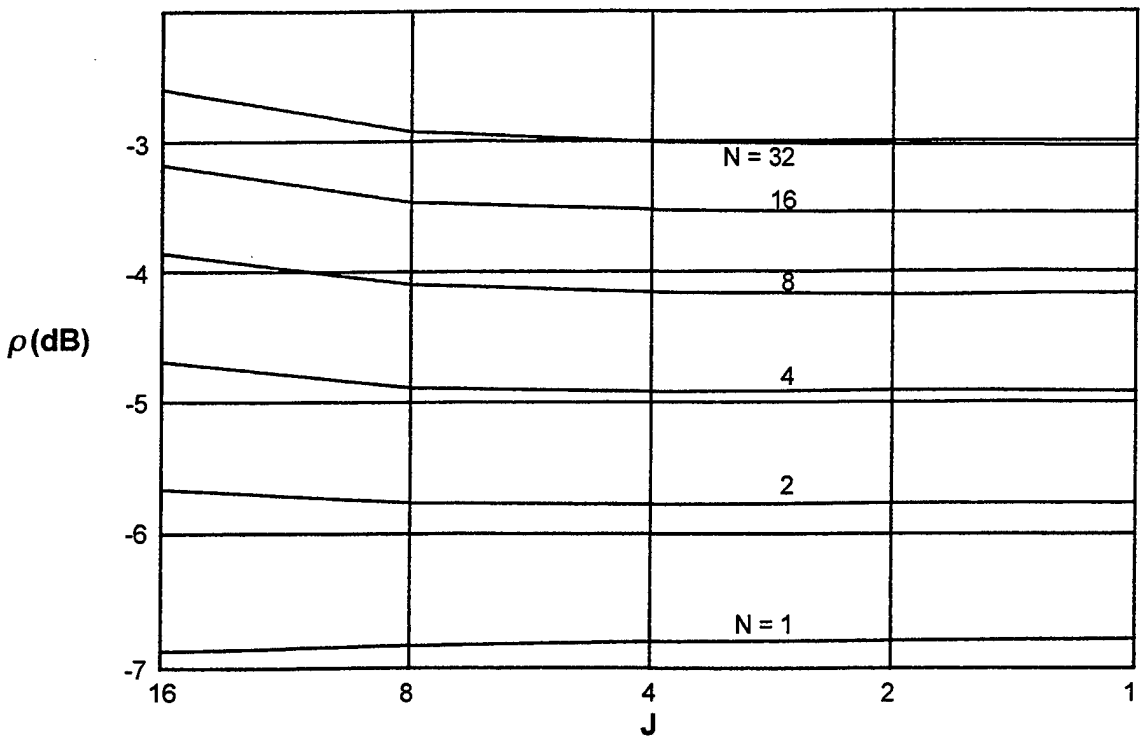

Figure 12. Required Input SNR for P_f = 1E - 3, P_d = 0.5, K = 16, (M - 1)J = 240, T = 256, Gaussian Signal

SUMMARY

For three different signal models in Gaussian noise, closed forms have been derived for the PDFs at the output of a pre-averager followed by an or-ing operation. In the case of a random Gaussian signal, these forms have been numerically transformed to yield accurate results for the EDFs at the output of a post-averager, under both hypotheses H_0 and H_1, for numerous values of the parameters of the complete processor. These results enable investigation of the or-ing processor for false alarm probabilities P_f in the range of 1E-6 and smaller; there is no need to resort to lengthy simulations.

Numerous ROCs have been generated, which enable a user or system designer to quickly assess the losses to be expected from employing or-ing in a processor. Also, quantitative evaluation of the tradeoffs between pre-averaging versus post-averaging has been conducted. Finally, since the enclosed tabulations will undoubtedly not cover all cases of practical interest, a MATLAB program for evaluation of the ROCs is presented in appendix I for additional evaluation and tabulation.

The possibility of employing overlapping data in the post-averager has been investigated by simulation and found to be insignificant, at least for moderate values of N, the number of channels or-ed. For very large values of N, this conclusion may require reconsideration.

Numerical results have been presented for KM = 4, 16, 64, and 256. For completeness, the special case of KM = 1 is presented here. The P_f is given by a combination of equations (37) and (68), while P_d is given by equations (36) and (69), with K = 1. For given values of P_f and N, the required threshold value u can be solved. Then, for a given P_d and the above solution for u, the required input SNR ρ can be found, using $a = 1/(1 + \rho)$, in the explicit form for a Gaussian signal as

$$\rho = \frac{\ln(1 - \alpha)}{\ln(1 - \alpha\beta)} - 1 \ , \quad \alpha = (1 - P_f)^{1/N} \ , \quad \beta = \frac{1 - P_d}{1 - P_f} \ . \qquad (83)$$

This relation is plotted in figure 13 as a function of the amount of or-ing N for both the SOP and the HOP.

The two alternative cases of a phase-incoherent signal and a deterministic signal in additive Gaussian noise are currently under investigation. Tabulation of the corresponding ROCs and tradeoffs between pre- and post-averaging will be conducted in a similar manner and for the same parameter values as accomplished here.

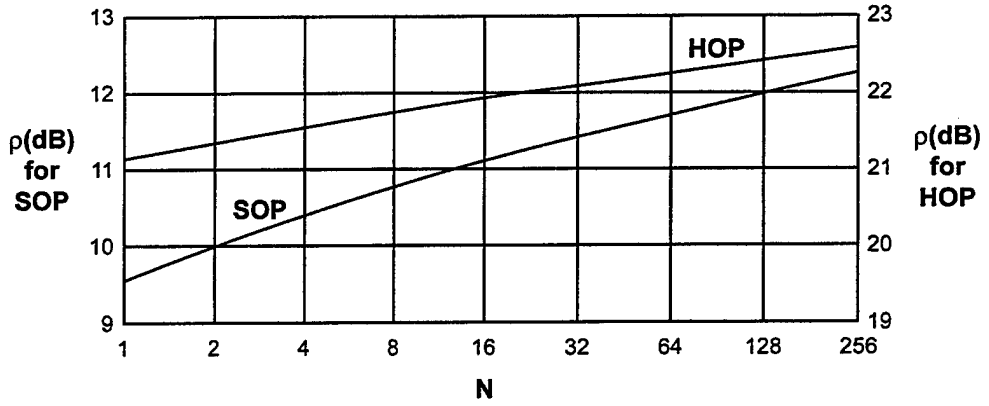

Figure 13. Required Input SNR for K = 1, M = 1

APPENDIX A — OPTIMUM PROCESSING OF TOTAL DATA SET

The observed data in the n-th channel are $x_n(t)$ for $1 \leq t \leq T$. There are N channels giving rise to the total data set

$$\{x_n(t)\} \equiv x_n(t) \quad \text{for } 1 \leq n \leq N \ , \ 1 \leq t \leq T \ . \tag{A-1}$$

All N T of these samples are statistically independent of each other. Some of the following analysis was presented earlier in reference 3, appendix E.

It is desired to determine the a posteriori probability (APP) that channel number j contains a signal, namely,

$$\Pr(j|\{x_n(t)\}) = \frac{\Pr(j)\ p_j(\{x_n(t)\})}{p_c(\{x_n(t)\})} \quad \text{for } 0 \leq j \leq N \ . \tag{A-2}$$

The case j = 0 corresponds to no signal present. For $j \geq 1$, Pr(j) is the a priori probability of the signal occupying channel j (during the entire observation interval T), and $p_j(\cdot)$ is the PDF of total observation $\{x_n(t)\}$ when the signal is in channel j. Denominator $p_c(\cdot)$ is the combined PDF of the total data, namely, the sum of the numerator terms from j = 0 to N.

Let p denote the PDF of individual sample $x_n(t)$ for signal absent, and let $\underline{p}$ denote the PDF of $x_n(t)$ for signal present. Then, the j = 0 PDF in the numerator of equation (A-2) is

$$p_0(\{x_n(t)\}) = \prod_{n=1}^{N} \prod_{t=1}^{T} p(x_n(t)) \ , \tag{A-3}$$

while the other terms are

$$p_j(\{x_n(t)\}) = \left\{\prod_{t=1}^{T} p(x_j(t))\right\} \prod_{\substack{n=1 \\ n\neq j}}^{N} \prod_{t=1}^{T} p(x_n(t))$$

$$= p_0(\{x_n(t)\}) \prod_{t=1}^{T} L(x_j(t)) \quad \text{for} \quad 1 \leq j \leq N \ , \tag{A-4}$$

where auxiliary function

$$L(u) \equiv \frac{p(u)}{p(u)} \ . \tag{A-5}$$

The APPs in equation (A-2) are

$$Pr(0|\cdot) = Pr(0)\ p_0(\cdot)/p_c(\cdot) \ ,$$

$$Pr(j|\cdot) = Pr(j)\ p_0(\cdot)/p_c(\cdot) \prod_{t=1}^{T} L(x_j(t)) \quad \text{for } 1 \leq j \leq N \ . \tag{A-6}$$

Optimum processing corresponds to selection of the channel with the largest APP. Upon canceling common factors, this rule leads to consideration of the maximum of N+1 quantities according to

$$\max\left\{Pr(0),\ Pr(1) \prod_{t=1}^{T} L(x_1(t)),\ \ldots\ ,\ Pr(N) \prod_{t=1}^{T} L(x_N(t))\right\} \ . \tag{A-7}$$

If the zeroth-order term is largest, a declaration is made that no signal is present. If the j-th term is largest, $j > 0$, a signal is declared present in channel j.

An alternative processing procedure is obtained when channel identification is not of interest; rather, only the presence or

absence of a signal is relevant. Then, for equal a priori probabilities, $Pr(j) = Pr(1)$ for $1 \leq j \leq N$, the APP of signal present somewhere is, upon use of equations (A-2) and (A-4),

$$\frac{Pr(1)}{p_c(\cdot)} \sum_{j=1}^{N} p_j(\cdot) = Pr(1) \frac{p_0(\cdot)}{p_c(\cdot)} \sum_{j=1}^{N} \prod_{t=1}^{T} L(x_j(t)) \ . \qquad \text{(A-8)}$$

The alternative APP of signal absent is

$$Pr(0) \frac{p_0(\cdot)}{p_c(\cdot)} \ . \qquad \text{(A-9)}$$

Picking the largest of these two quantities is tantamount to a threshold comparison according to

$$\sum_{n=1}^{N} \prod_{t=1}^{T} L(x_n(t)) \underset{<}{\overset{>}{}} v \ . \qquad \text{(A-10)}$$

The two alternative test statistics (A-7) and (A-10) will now be calculated for the three signal models of interest here.

COHERENT (DETERMINISTIC) SIGNAL

$$p(u) = (2\pi\sigma^2)^{-\frac{1}{2}} \exp\left(-\frac{u^2}{2\sigma^2}\right) \ , \quad \underline{p}(u) = (2\pi\sigma^2)^{-\frac{1}{2}} \exp\left(-\frac{(u-m)^2}{2\sigma^2}\right) \ ,$$

$$\underline{f}(\xi) = \exp(i\xi m - \xi^2\sigma^2/2) \ ,$$

$$L(u) = \exp\left(\frac{mu}{\sigma^2} - \frac{d^2}{2}\right) \ , \quad d \equiv \frac{m}{\sigma} \ . \qquad \text{(A-11)}$$

The CF corresponding to PDF $\underline{p}(u)$ is $\underline{f}(\xi)$. For $1 \leq n \leq N$, the

n-th data processing term in equation (A-7) is

$$\prod_{t=1}^{T} L(x_n(t)) = \exp(-Td^2/2) \exp\left(\frac{d}{\sigma} \sum_{t=1}^{T} x_n(t)\right) . \qquad \text{(A-12)}$$

Therefore, the optimum test statistic takes the form of threshold comparison

$$\max_{1 \le n \le N} \left\{ \sum_{t=1}^{T} x_n(t) \right\} \gtrless v . \qquad \text{(A-13)}$$

Physically, each channel output is summed over the entire observation interval T, and the largest channel sum is compared with a threshold for declaration of signal presence and channel number. If none exceed the threshold, signal is declared absent.

On the other hand, when channel identity is irrelevant, equations (A-10) and (A-12) yield test

$$\sum_{n=1}^{N} \exp\left(\frac{d}{\sigma} \sum_{t=1}^{T} x_n(t)\right) \gtrless v . \qquad \text{(A-14)}$$

Again, each channel is summed in time, but must now be scaled by d/σ, exponentiated, and summed over all channels prior to threshold comparison. For reasonable input SNRs d, the outer sum on n will be dominated by the exponential with the largest inner sum on t; in that case, test (A-14) substantially reduces to test (A-13). This is fortunate, because scaling d/σ will not likely be known in practice. Thus, test (A-13) is essentially the optimum processor for both cases of whether channel identification is desired or not.

PHASE-INCOHERENT SIGNAL

$$p(u) = \frac{1}{\sigma^2} \exp\left(\frac{-u}{\sigma^2}\right) , \qquad \underline{p}(u) = \frac{1}{\sigma^2} \exp\left(\frac{-u}{\sigma^2} - \rho\right) I_o\left(\frac{2(\rho u)^{\frac{1}{2}}}{\sigma}\right) ,$$

$$\underline{f}(\xi) = \frac{1}{1 - i\xi\sigma^2} \exp\left(\rho \frac{i\xi\sigma^2}{1 - i\xi\sigma^2}\right) , \qquad \overline{x_n(t)} = \sigma^2(1 + \rho) ,$$

$$L(u) = \exp(-\rho)\, I_o\left(\frac{2(\rho u)^{\frac{1}{2}}}{\sigma}\right) ; \qquad \rho = \frac{A^2/2}{\sigma^2} , \quad u > 0 . \tag{A-15}$$

For $1 \leq n \leq N$, the n-th data processing term in equation (A-7) is

$$\prod_{t=1}^{T} L(x_n(t)) = \exp(-T\rho) \prod_{t=1}^{T} I_o\left(\frac{2\rho^{\frac{1}{2}}}{\sigma} \{x_n(t)\}^{\frac{1}{2}}\right) . \tag{A-16}$$

It is important to notice that the arguments of the Bessel function I_o have not undergone any summations, either on t or n. (This is in contrast to test (A-14), where the arguments of exp are summed on t before exponentiation.) Therefore, these arguments in equation (A-16) are typically small, allowing the approximation $I_o(z) \simeq \exp(z^2/4)$ for small z, since

$$I_o(z) = 1 + \frac{z^2}{4} + \frac{(z^2/4)^2}{4} + \cdots ,$$

$$\exp(z^2/4) = 1 + \frac{z^2}{4} + \frac{(z^2/4)^2}{2} + \cdots . \tag{A-17}$$

This leads to an approximation for equation (A-16), namely,

$$\exp(-T\rho) \prod_{t=1}^{T} \exp\left(\frac{\rho}{\sigma^2} x_n(t)\right) = \exp(-T\rho) \exp\left(\frac{\rho}{\sigma^2} \sum_{t=1}^{T} x_n(t)\right) . \tag{A-18}$$

Therefore, the optimum test statistic takes the form of

threshold comparison

$$\max_{1\le n\le N}\left\{\sum_{t=1}^{T} x_n(t)\right\} \underset{<}{>} v \ . \qquad \text{(A-19)}$$

Although this approximate test has a form identical to equation (A-13), $x_n(t)$ here is a squared envelope, whereas it was an amplitude quantity previously; see equation (A-15) versus equation (A-11).

On the other hand, processor (A-10), with the help of equation (A-18), yields the alternative test

$$\sum_{n=1}^{N} \exp\left(\frac{\rho}{\sigma^2}\sum_{t=1}^{T} x_n(t)\right) \underset{<}{>} v \ . \qquad \text{(A-20)}$$

The N temporal sums are scaled by ρ/σ^2, exponentiated, and then summed over all channels. For reasonable input SNRs ρ, the n-sum is dominated by the exponential with the largest t-sum; thus, this test is essentially equivalent to test (A-19). Therefore, test (A-19) is virtually the optimum processor under both cases of channel identification.

ACCESSIBILITY TO IN-PHASE AND QUADRATURE COMPONENTS

The statistical model in equation (A-15) corresponds to sampling the squared envelope of the received data. If, instead, the in-phase and quadrature components are accessible, input data value $x_n(t)$ in the signal channel should be replaced by the two

RVs

$$I_n(t) = A(t)\cos\theta(t) + g_i(t) ,$$

$$Q_n(t) = A(t)\sin\theta(t) + g_q(t) , \qquad \text{(A-21)}$$

where amplitude A(t) is non-random, RV $\theta(t)$ is uniformly distributed over 2π, and $g_i(t)$ and $g_q(t)$ are independent, identically distributed Gaussian RVs with zero mean and variance σ^2. The joint CF of RVs $I_n(t)$ and $Q_n(t)$ is

$$\underline{f}(\xi,\eta) \equiv \overline{\exp[i\xi I_n(t)+i\eta Q_n(t)]} = J_o\left(A(t)(\xi^2+\eta^2)^{\frac{1}{2}}\right) \exp\left(-\frac{\sigma^2}{2}(\xi^2+\eta^2)\right). \qquad \text{(A-22)}$$

From this point on, it is presumed that amplitude A(t) is constant, that is, A(t) = A for all t in the observation interval. The joint PDF corresponding to equation (A-22) is then

$$\underline{p}(I,Q) = \frac{1}{2\pi\sigma^2} \exp\left(-\frac{I^2+Q^2+A^2}{2\sigma^2}\right) I_o\left(\frac{A(I^2+Q^2)^{\frac{1}{2}}}{\sigma^2}\right) . \qquad \text{(A-23)}$$

Since this expression doesn't factor in I and Q, the in-phase and quadrature components are statistically dependent on each other. However, equation (A-23) depends only on the combination $I^2 + Q^2$, and not on I or Q separately; any optimum processor derived using the joint PDF (A-23) must process the accessible data $I_n(t)$ and $Q_n(t)$ in the form $I_n^2(t) + Q_n^2(t)$. In fact, if one identifies original data $x_n(t) = [I_n^2(t) + Q_n^2(t)]/2$, the resulting PDF $\underline{p}(u)$ for $x_n(t)$, as obtained from equation (A-23), is precisely

equation (A-15), where $\rho = \frac{1}{2}A^2/\sigma^2$. The end result is that accessibility to in-phase and quadrature data values (A-21) would yield the same optimum processor as that required to use squared envelopes $\{x_n(t)\}$ directly.

RANDOM GAUSSIAN SIGNAL

$$p(u) = \frac{1}{\sigma^2}\exp\left(\frac{-u}{\sigma^2}\right) , \quad \underline{p}(u) = \frac{1}{\sigma^2 + \underline{\sigma}^2}\exp\left(\frac{-u}{\sigma^2 + \underline{\sigma}^2}\right) ,$$

$$\underline{f}(\xi) = \frac{1}{1 - i\xi\sigma^2(1 + \rho)} , \quad \overline{x_n(t)} = \sigma^2(1 + \rho) ,$$

$$L(u) = \frac{1}{1 + \rho}\exp\left(\frac{\rho}{1 + \rho}\frac{u}{\sigma^2}\right) ; \quad \rho = \underline{\sigma}^2/\sigma^2 , \quad u > 0 . \qquad \text{(A-24)}$$

The n-th data processing term for $1 \leq n \leq N$ in equation (A-7) is

$$\prod_{t=1}^{T} L(x_n(t)) = (1 + \rho)^{-T}\exp\left(\frac{\rho}{1 + \rho}\frac{1}{\sigma^2}\sum_{t=1}^{T} x_n(t)\right) . \qquad \text{(A-25)}$$

Therefore, the optimum test statistic takes the form of threshold comparison

$$\max_{1\leq n\leq N}\left\{\sum_{t=1}^{T} x_n(t)\right\} \begin{matrix} > \\ < \end{matrix} v . \qquad \text{(A-26)}$$

Although this test has a form identical to test (A-13), $x_n(t)$ is an envelope-squared quantity here, whereas it was an amplitude quantity previously; see equation (A-24) versus equation (A-11).

On the other hand, processor (A-10) yields the alternative test

$$\sum_{n=1}^{N} \exp\left(\frac{\rho}{1+\rho}\,\frac{1}{\sigma^2}\sum_{t=1}^{T} x_n(t)\right) \gtrless v \ . \qquad \text{(A-27)}$$

The N temporal sums are scaled, exponentiated, and then summed over all channels. For reasonable input SNRs ρ, the n-sum is dominated by the exponential with the largest t-sum, and this test is essentially equivalent to test (A-26). Thus, test (A-26) is virtually the optimum processor under both cases of channel identification.

ACCESSIBILITY TO IN-PHASE AND QUADRATURE COMPONENTS

The statistical model in equation (A-24) corresponds to sampling the squared envelope of the received data. If, instead, the in-phase and quadrature components are accessible, input data value $x_n(t)$ in the signal channel should be replaced by the two RVs

$$I_n(t) = a_i(t) + g_i(t) \ ,$$

$$Q_n(t) = a_q(t) + g_q(t) \ , \qquad \text{(A-28)}$$

where all the quantities are independent zero-mean Gaussian RVs, with signal samples a_i and a_q having variance $\underline{\sigma}^2$, while noise samples g_i and g_q have variance σ^2.

The joint PDF for the RVs in equation (A-28) is obviously

$$\underline{p}(I,Q) = \frac{1}{2\pi(\sigma^2+\underline{\sigma}^2)} \exp\left(-\frac{I^2+Q^2}{2(\sigma^2+\underline{\sigma}^2)}\right) . \qquad \text{(A-29)}$$

Thus, $I_n(t)$ and $Q_n(t)$ in equation (A-28) are independent RVs. More importantly, PDF (A-29) depends only on the combination $I^2 + Q^2$, and not on I or Q separately; any optimum processor derived using joint PDF (A-29) must process the accessible data $I_n(t)$ and $Q_n(t)$ in the form $I_n^2(t) + Q_n^2(t)$. In fact, if one identifies original data value $x_n(t) = [I_n^2(t) + Q_n^2(t)]/2$, the resulting PDF $\underline{p}(u)$ for $x_n(t)$, as obtained from equation (A-29), is precisely equation (A-24), where $\rho = \underline{\sigma}^2/\sigma^2$. The end result is that accessibility to in-phase and quadrature data values (A-28) would yield the same optimum processor as that required to use squared envelopes $\{x_n(t)\}$ directly.

APPENDIX B – ON THE USE OF CASCADED FAST FOURIER TRANSFORMS FOR DISTRIBUTION CALCULATION

The PDF of or-ing output v(t) is often available in closed form, albeit complicated, for signal present as well as signal absent; see equations (32) and (33). For independent inputs to the post-averager, that is, skip factor J = K, the CF of the post-averager output is the M-th power of its input CF. In order to find the post-averager output PDF and EDF, its input PDF must be Fourier transformed to find the corresponding input CF, then raised to the M-th power, followed by another Fourier transform back to the density or distribution domains. This cascaded FFT operation requires care in its evaluation in order to control aliasing errors.

Let p(u) be the post-averager input PDF of interest. If this function is sampled at increment Δ_u, and Fourier transformed, the result is an approximation to desired CF

$$f(\xi) = \int du \, \exp(i\xi u) \, p(u) \, , \tag{B-1}$$

namely, continuous function

$$\tilde{f}(\xi) \equiv \Delta_u \sum_n \exp(i\xi n\Delta_u) \, p(n\Delta_u) = \sum_m f\left(\xi - m \frac{2\pi}{\Delta_u}\right) . \tag{B-2}$$

This aliased CF $\tilde{f}(\xi)$ has period $2\pi/\Delta_u$ in ξ. In order to minimize the aliasing inherent in $\tilde{f}(\xi)$, sampling increment Δ_u must be taken small enough to separate the lobes in equation (B-2) and avoid significant overlap.

Now, the aliased CF $\tilde{f}(\xi)$ will be evaluated at special selected intervals, namely,

$$\tilde{f}\left(\frac{2\pi k}{N_1 \Delta_u}\right) = \Delta_u \sum_n \exp(i2\pi kn/N_1)\, p(n\Delta_u) \quad \text{for } 0 \le k \le N_1 - 1 \ , \quad \text{(B-3)}$$

which covers one period of $\tilde{f}(\xi)$. N_1 and k are integers.

The samples of p(u) must be taken far enough out in u that the two neglected tails yield insignificant truncation errors. If the number of u samples exceeds N_1, the sample at $u = n\Delta_u$ can simply be prealiased into bin (n MODULO N_1), since the factor $\exp(i2\pi kn/N_1)$ treats all p(u) samples separated by $N_1\Delta_u$ equally. Thus, the truncation error in u can be controlled to any desired degree by taking enough samples of PDF p(u) on its tails. Equation (B-3) can be accomplished numerically by an N_1-point FFT.

Proper selection of sampling increment Δ_u can be achieved by looking at a plot of the magnitude of equation (B-3); see figure B-1. The right skirt of the desired lobe centered at $\xi = 0$

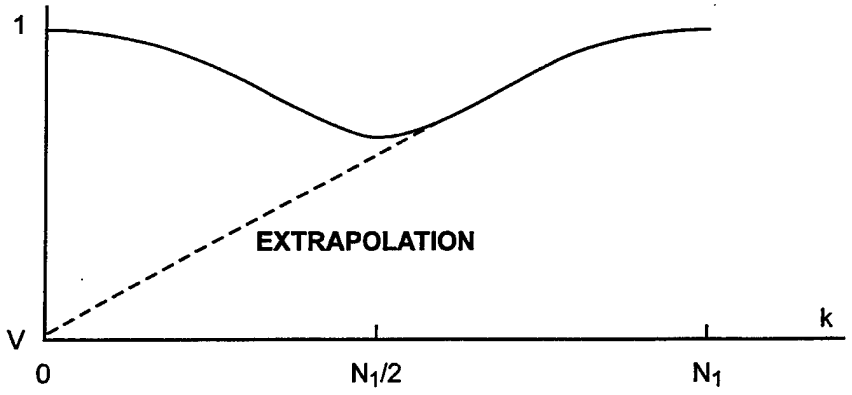

Figure B-1. Magnitude of Approximate CF $\tilde{f}$

(k = 0) will cross the left skirt of the aliasing lobe centered at $\xi=2\pi/\Delta_u$ ($k = N_1$) at $\xi = \pi/\Delta_u$ ($k = N_1/2$). However, it is <u>not</u> necessary that $|\tilde{f}(\xi)|$ be extremely small at this crossover at $k = N_1/2$. Rather, it is necessary that the <u>extrapolation</u> of the left skirt of the aliasing lobe be very small at $\xi = 0$ ($k = 0$); this result can be visually observed. If origin value V of the extrapolation (dashed curve) is not sufficiently small, then Δ_u must be decreased and the procedure repeated before going on.

The magnitude of the absolute error of equation (B-2), namely, $|\tilde{f}(\xi) - f(\xi)|$ for $0 < \xi < \pi/\Delta_u$, is typically (but not always) less than the error at $\xi = 0$. Thus, estimating and controlling this origin error (by means of Δ_u) is an essential step. This error can be measured quantitatively by printing out $\tilde{f}(0)$. Its discrepancy from the desired value $f(0) = 1$ can serve as an indicator whether to increase or decrease Δ_u <u>before</u> proceeding any further.

Notice that FFT size N_1 has <u>nothing</u> to do with the accuracy of approximation $\tilde{f}$ in equation (B-3). Rather, N_1 merely sets the increment

$$\Delta_\xi = \frac{2\pi}{N_1 \Delta_u} \qquad \text{(B-4)}$$

at which samples of $\tilde{f}(\xi)$ are taken in the ξ domain according to equation (B-3). However, N_1 will become a very relevant parameter in the remaining part of the cascade FFT procedure.

Once a satisfactory value of Δ_u has been ascertained (by trial and error) in order to realize a sufficiently small error in $\tilde{f}(0)$, the approximation to the post-averager output CF is computed at the same selected intervals according to

$$\underline{f}\left(\frac{2\pi k}{N_1 \Delta_u}\right) \equiv \left[\tilde{f}\left(\frac{2\pi k}{N_1 \Delta_u}\right)\right]^M \quad \text{for } 0 \leq k \leq N_1 - 1 \ . \tag{B-5}$$

(The values for $k > N_1/2$ correspond to negative ξ values.) Although the relative error of $\tilde{f}$ in the neighborhood of $k = N_1/2$ is 100%, these values are suppressed to insignificance by the M-th power. However, the small error in $\tilde{f}$ at $k = 0$ is <u>magnified</u> by a factor of approximately M, and shows up in approximation $\underline{f}$. Therefore, large values of M may require that Δ_u be decreased even further in anticipation of this inherent error magnification caused by the M-th power in equation (B-5).

The approximation to the post-averager output PDF is given by continuous function (inverse Fourier transform)

$$\underline{p}(u) \equiv \frac{1}{2\pi} \Delta_\xi \sum_{k=0}^{N_1-1} \exp(-iuk\Delta_\xi) \ \underline{f}(k\Delta_\xi) \ . \tag{B-6}$$

This function has period $2\pi/\Delta_\xi = N_1 \Delta_u$ in u. In order that the inherent aliasing lobes in $\underline{p}(u)$ not severely contaminate the approximation, period $N_1 \Delta_u$ must be made large enough that the aliasing lobes of $\underline{p}(u)$ do not overlap significantly. This can be ascertained by computing approximation $\underline{p}(u)$ at the selected points $u_j \equiv j \ \delta_u \equiv j \ 2\pi/(N_2 \Delta_\xi)$, getting

$$\underline{p}\left(\frac{2\pi j}{N_2 \Delta_\xi}\right) = \frac{1}{N_1 \Delta_u} \sum_{k=0}^{N_1-1} \exp(-i2\pi jk/N_2)\ \underline{f}\left(\frac{2\pi k}{N_1 \Delta_u}\right) \quad \text{for } 0 \le j \le N_2-1, \quad \text{(B-7)}$$

which covers one period of $\underline{p}(u)$. This can be done by an N_2-point FFT. If $N_2 < N_1$, simply prealias $\underline{f}(2\pi k/(N_1\Delta_u))$ into bin (k MODULO N_2), since the exponential factor $\exp(-i2\pi jk/N_2)$ treats all $\underline{f}$ samples separated by N_2 equally. The u-increment in equation (B-7) is

$$\delta_u = \frac{2\pi}{N_2 \Delta_\xi} = \frac{N_1}{N_2}\,\Delta_u \quad \text{(B-8)}$$

in terms of the original sampling increment Δ_u on input PDF $p(u)$. Integer N_2 can be taken larger or smaller than N_1, since it merely controls the increment δ_u at which approximation $\underline{p}$ is computed in equation (B-7).

In the special case $N_2 = N_1$, then $\delta_u = \Delta_u$, which is the same sampling increment used on input PDF $p(u)$. Since the post-averager output is the sum of M variables, the standard deviation is $M^{1/2}$ larger than at the summer input, making the output PDF spread over a larger range. If Δ_u was small enough to track $p(u)$, then $\delta_u = \Delta_u$ is probably fine enough to track $\underline{p}(u)$.

Integer N_2 has no effect on the accuracy of approximation $\underline{p}$. However, integer N_1 in FFT (B-3) now has a significant effect on the accuracy of the calculated PDF at the post-averager output, namely, equation (B-6). Period $N_1\Delta_u$ of $\underline{p}(u)$ must be larger than

the extent of the actual unknown output PDF. This aliasing effect in $\underline{p}(u)$ can be observed by plotting equation (B-7), which covers one period, and looking for overlap of the PDF tails before they have sufficiently decayed. Since the period of $\underline{p}(u)$ is $N_1\Delta_u$, it can be increased only by increasing N_1, because Δ_u has already been selected as large as possible without causing significant aliasing in $\tilde{f}(\xi)$.

A limitation could arise at this point. If Δ_u had to be chosen very small because input CF $f(\xi)$ was a very slowly decaying CF (see equation (B-2)), N_1 may have to be so large that sufficient storage is not available to conduct N_1-point FFT (B-3). (For example, PDFs (56) and (71) behave as u^{KN-1} as $u \to 0+$.) One possibility is then to break p(u) into the sum of two parts, the first being a simple analytic function that takes on the highest singularities of p(u) and has a known closed-form Fourier transform. The second part, which is smoother in u, will have a Fourier transform that decays faster and can profitably be numerically transformed via an FFT. The sum of the two Fourier transforms is the approximation to the desired CF $f(\xi)$.

For present purposes, where false alarm and detection probabilities are of interest, one does not actually compute PDF $\underline{p}$ in equations (B-6) or (B-7), but instead proceeds directly from CF $\underline{f}$ to the corresponding EDF. This accurate efficient procedure is given in reference 9. Nevertheless, the criterion above for choosing FFT size N_1 is still directly relevant.

APPENDIX C - MOMENTS OF CHARACTERISTIC FUNCTION (72)

The CF of or-ing RV v(t) for a random Gaussian signal and K = 1 is

$$f_{v1}(\xi) = (1)_{N-1}\left(\frac{i\xi}{(a-i\xi)_N} + \frac{1}{(1-i\xi)_{N-1}}\right), \quad a = 1/(1+\rho), \quad \text{(C-1)}$$

under H_1; see equation (72). In order to determine the moments of v(t), consider the following development:

$$(b-i\xi)_J = \prod_{j=1}^{J}(b-i\xi+j-1), \quad \text{(C-2)}$$

giving

$$\ln[(b-i\xi)_J] = \sum_{j=1}^{J} \ln(b+j-1-i\xi)$$

$$= \sum_{j=1}^{J} \ln(b+j-1) + \sum_{j=1}^{J} \ln\left(1 - \frac{i\xi}{b+j-1}\right)$$

$$= \ln[(b)_J] - \sum_{j=1}^{J}\sum_{k=1}^{\infty} \frac{1}{k}\left(\frac{i\xi}{b+j-1}\right)^k = \ln[(b)_J] - \sum_{k=1}^{\infty} \frac{(i\xi)^k}{k}\beta_k(J,b), \quad \text{(C-3)}$$

where

$$\beta_k(J,b) \equiv \sum_{j=1}^{J} \frac{1}{(b+j-1)^k} \quad \text{for } k \geq 1. \quad \text{(C-4)}$$

From equation (C-3), there follows

$$(b-i\xi)_J = (b)_J \exp\left(-\sum_{k=1}^{\infty} \frac{(i\xi)^k}{k}\beta_k(J,b)\right). \quad \text{(C-5)}$$

Now, identifying $J \to N$, $b \to a$ in equation (C-5), one has

$$(1)_{N-1} \frac{i\xi}{(a-i\xi)_N} = (1)_{N-1} \frac{i\xi}{(a)_N} \exp\left(\sum_{k=1}^{\infty} \frac{(i\xi)^k}{k} \beta_k(N,a)\right) . \quad \text{(C-6)}$$

On the other hand, identifying $J \to N-1$, $b \to 1$ in equation (C-5),

$$\frac{(1)_{N-1}}{(1-i\xi)_{N-1}} = \exp\left(\sum_{k=1}^{\infty} \frac{(i\xi)^k}{k} \beta_k(N-1,1)\right) . \quad \text{(C-7)}$$

Now, CF $f_{v1}(\xi)$ in equation (C-1) is given by the sum of equations (C-6) and (C-7).

To simplify the two relations in equations (C-6) and (C-7), the following expansion (reference 13, appendix A) is used:

$$\exp\left(\sum_{k=1}^{\infty} \frac{(i\xi)^k}{k} \beta_k(J,b)\right) = \sum_{k=0}^{\infty} (i\xi)^k \gamma_k(J,b) , \quad \text{(C-8)}$$

where coefficients

$$\gamma_o(J,b) = 1 , \gamma_k(J,b) = \frac{1}{k} \sum_{j=1}^{k} \beta_j(J,b) \gamma_{k-j}(J,b) \quad \text{for } k \geq 1. \quad \text{(C-9)}$$

Use of equation (C-8) on equations (C-6) and (C-7) gives CF (C-1) as

$$f_{v1}(\xi) = \frac{(1)_{N-1}}{(a)_N} \sum_{k=0}^{\infty} (i\xi)^{k+1} \gamma_k(N,a) + \sum_{k=0}^{\infty} (i\xi)^k \gamma_k(N-1,1). \quad \text{(C-10)}$$

The moments $\{\mu_v(k)\}$ of or-ing output $v(t)$ are then immediately available as

$$\frac{\mu_v(k)}{k!} = \frac{(1)_{N-1}}{(a)_N}\,\gamma_{k-1}(N,a) + \gamma_k(N-1,1) \quad \text{for } k \geq 1 \ . \qquad \text{(C-11)}$$

The cumulants, $\chi_v(k)$, of v(t) can be readily found by using the recursion in reference 13, equation (C-7):

$$\chi_v(k) = \mu_v(k) - \sum_{j=1}^{k-1} \binom{k-1}{j} \chi_v(k-j)\,\mu_v(j) \quad \text{for } k \geq 1 \ . \qquad \text{(C-12)}$$

Defining normalized statistics

$$\underline{\mu}_v(k) = \mu_v(k)/k! \ , \quad \underline{\chi}_v(k) = \chi_v(k)/(k-1)! \ , \qquad \text{(C-13)}$$

equation (C-12) becomes (also, see reference 13, equation (C-9))

$$\underline{\chi}_v(k) = k\,\underline{\mu}_v(k) - \sum_{j=1}^{k-1} \underline{\chi}_v(k-j)\,\underline{\mu}_v(j) \quad \text{for } k \geq 1 \ . \qquad \text{(C-14)}$$

In summary, if moments $\{\mu_v(k)\}$ and cumulants $\{\chi_v(k)\}$ of or-ing output v(t), with signal present and K = 1, for order k = 1 to J are of interest, the following calculations are required, with $a = 1/(1+\rho)$:

from equation (C-4), evaluate $\{\beta_k(N,a)\}$ up to k = J-1;

from equation (C-4), evaluate $\{\beta_k(N-1,1)\}$ up to k = J;

from equation (C-9), evaluate $\{\gamma_k(N,a)\}$ up to k = J-1;

from equation (C-9), evaluate $\{\gamma_k(N-1,1)\}$ up to k = J;

from equation (C-11), evaluate moments $\{\mu_v(k)\}$ up to k = J;

from equation (C-12), evaluate cumulants $\{\chi_v(k)\}$ up to k = J.

APPENDIX D - ROCS FOR KM = 4, RANDOM GAUSSIAN SIGNAL

This appendix contains the ROCs for or-ing with pre- and post-averaging, when the time-bandwidth product KM is fixed at 4; the possible combinations (from table 1) are repeated here:

K	M	N
4	1	1,2,4,8,16,32
2	2	
1	4	

For N = 1, only the product KM matters; the first plot in this appendix covers this special case, under the labeling K = 4, N = 1, M = 1. The other 5 values of N, along with the 3 possible combinations of K and M, yield 15 additional ROCs, for a total of 16 ROCs in this appendix.

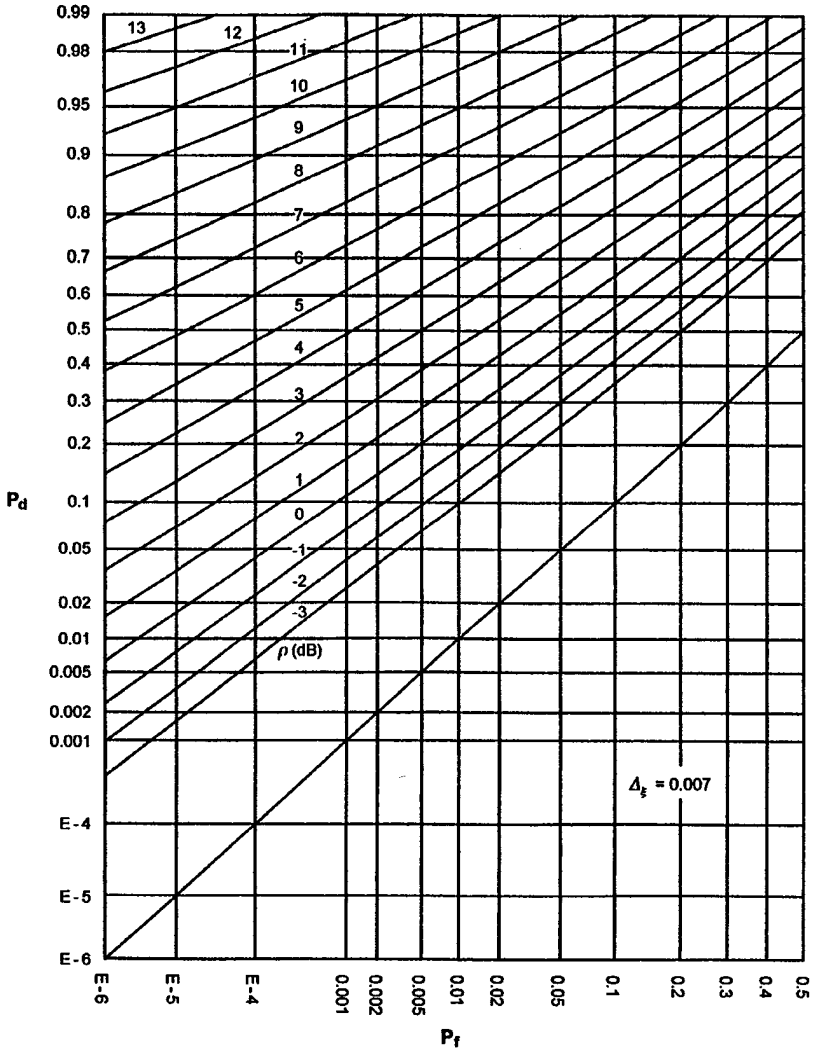

Figure D-1. ROCs for K = 4, N = 1, M = 1

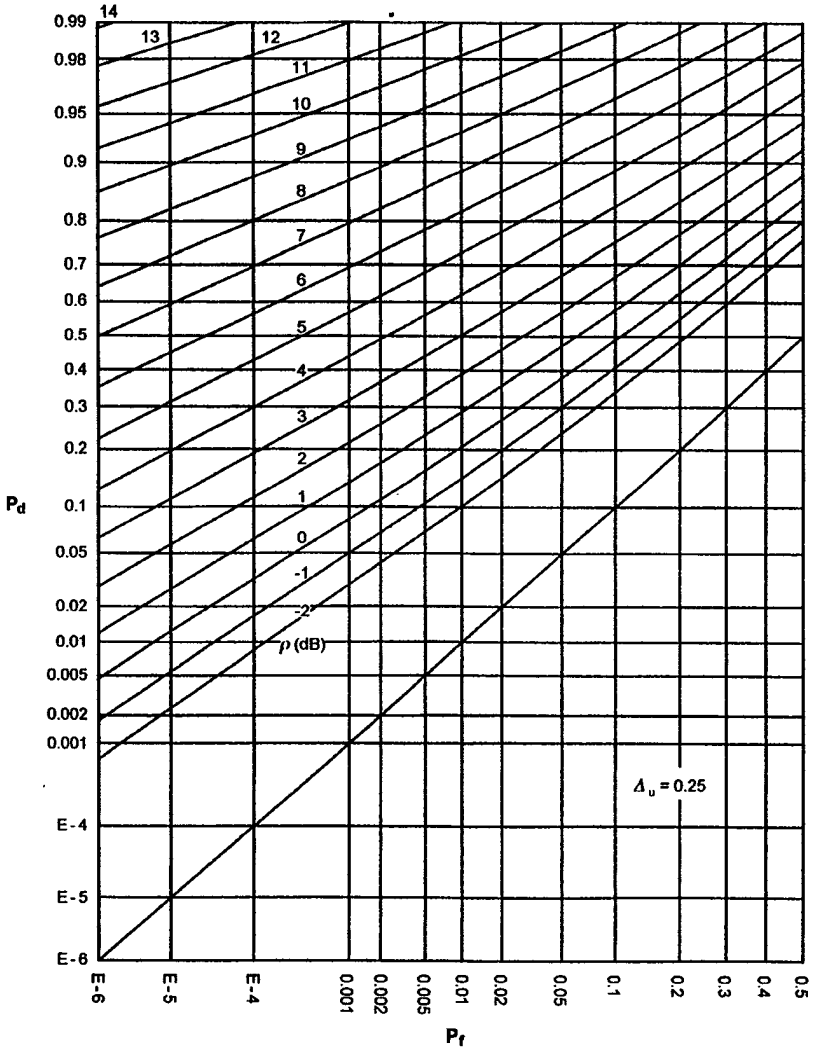

Figure D-2. ROCs for K = 4, N = 2, M = 1

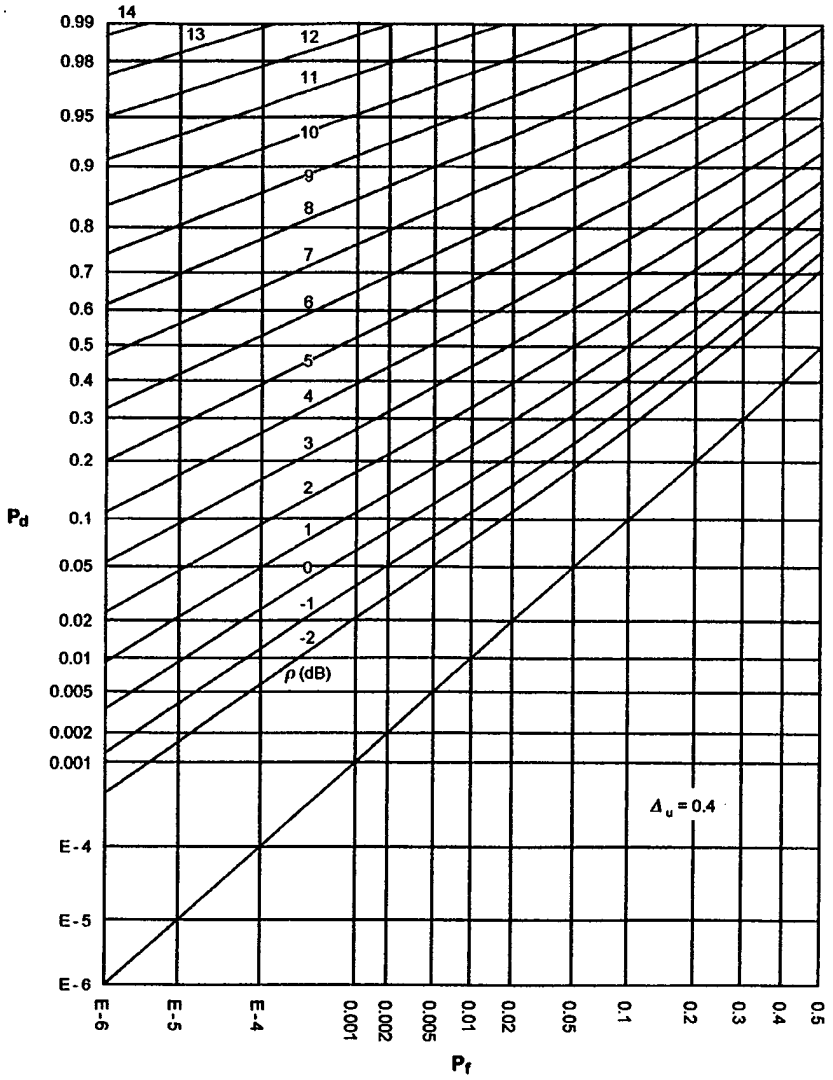

Figure D-3. ROCs for K = 4, N = 4, M = 1

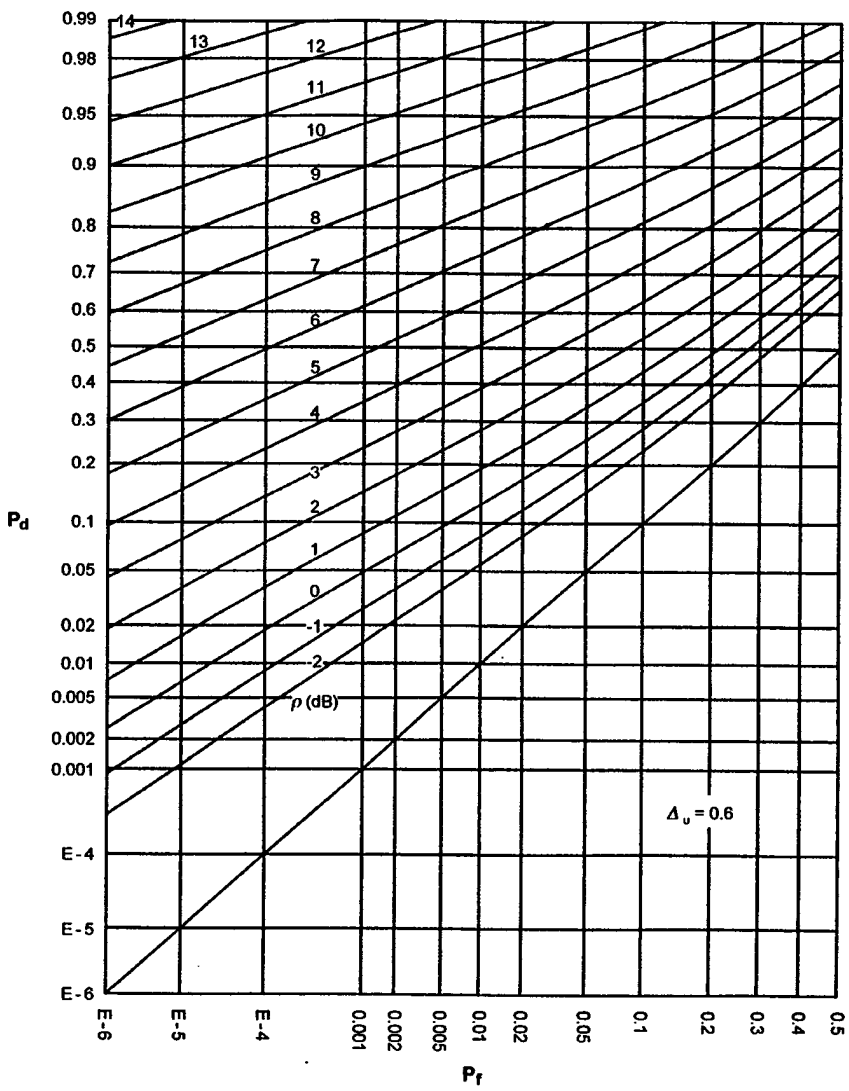

Figure D-4. ROCs for K = 4, N = 8, M = 1

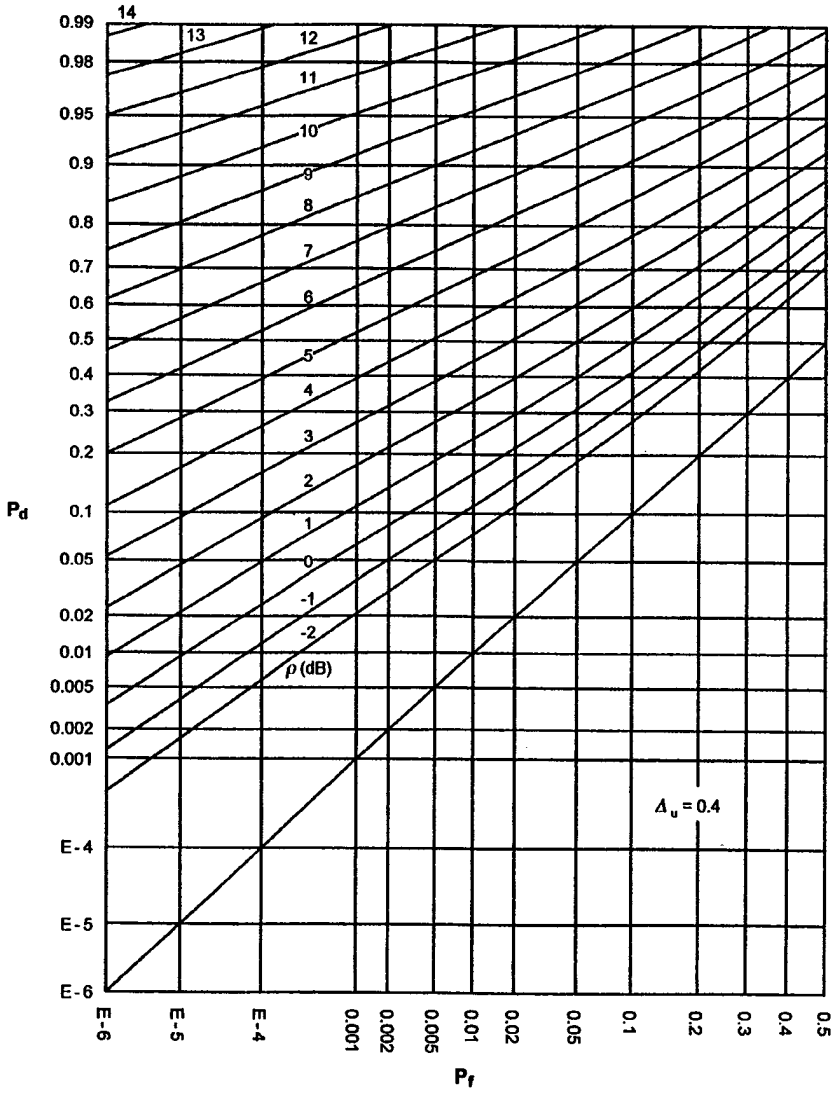

Figure D-5. ROCs for K = 4, N = 16, M = 1

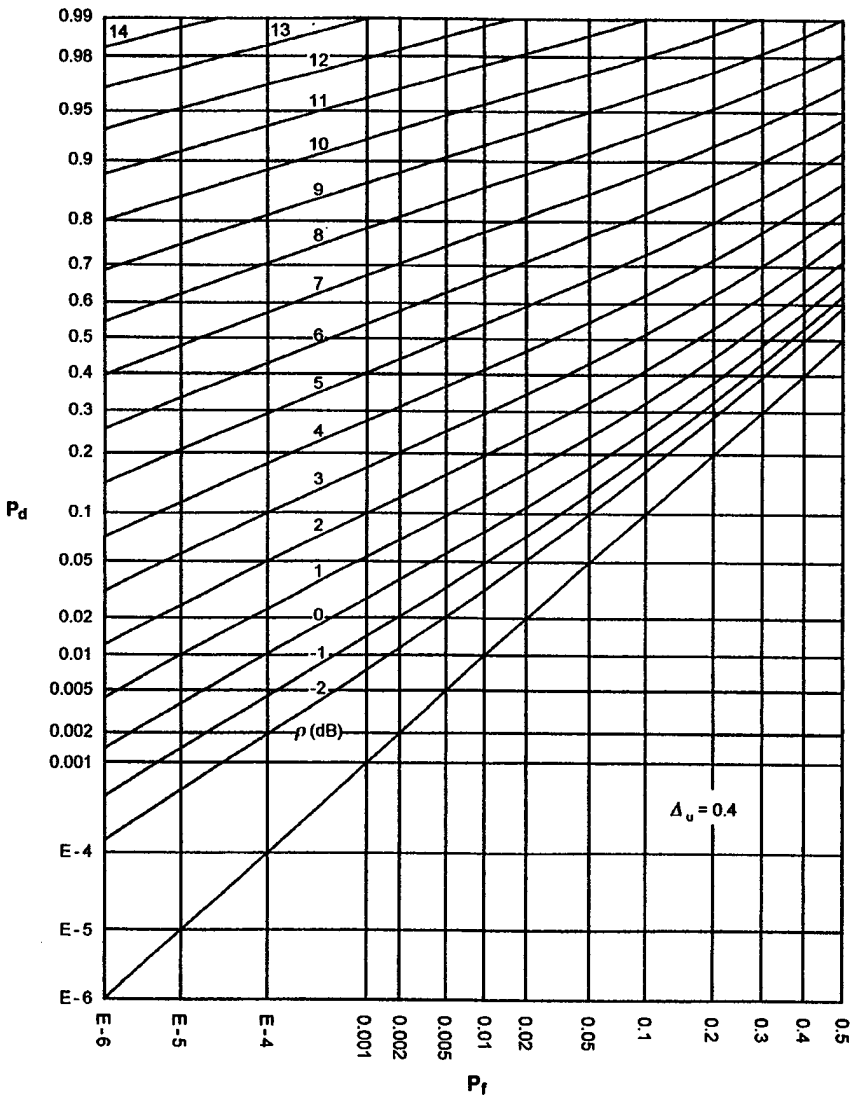

Figure D-6. ROCs for K = 4, N = 32, M = 1

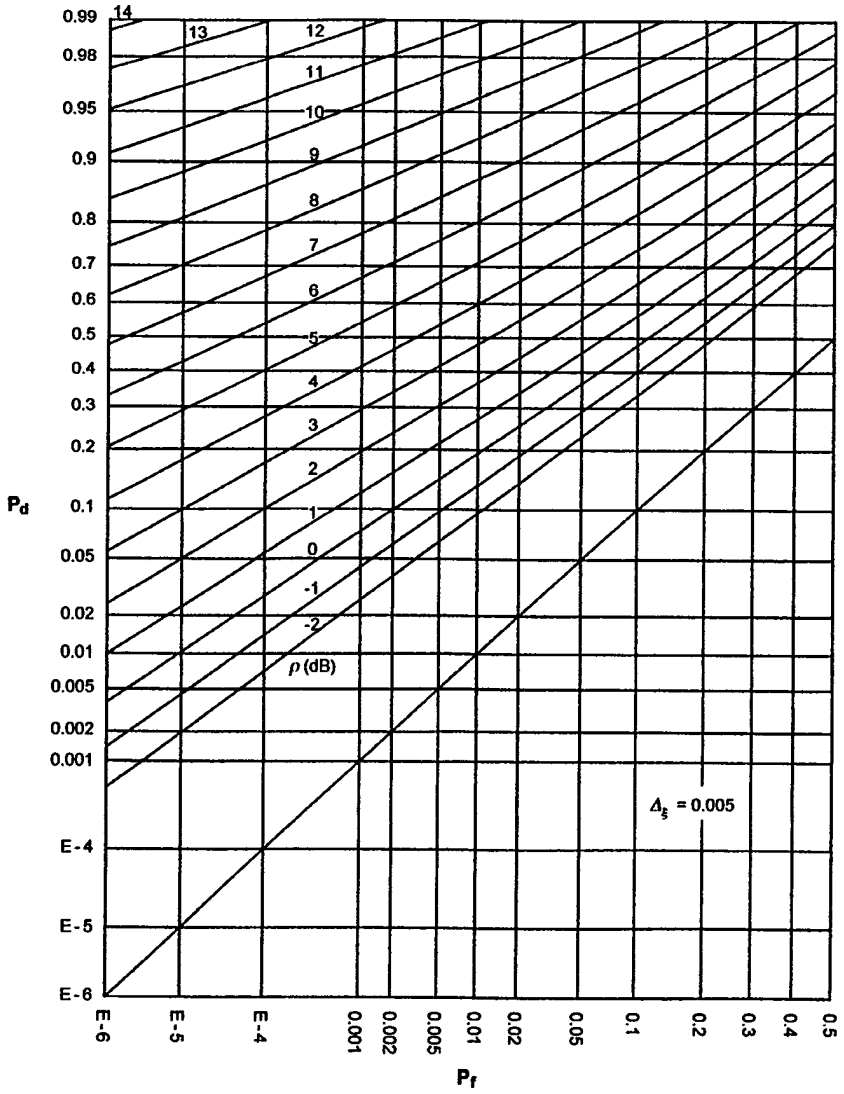

Figure D-7. ROCs for K = 2, N = 2, M = 2

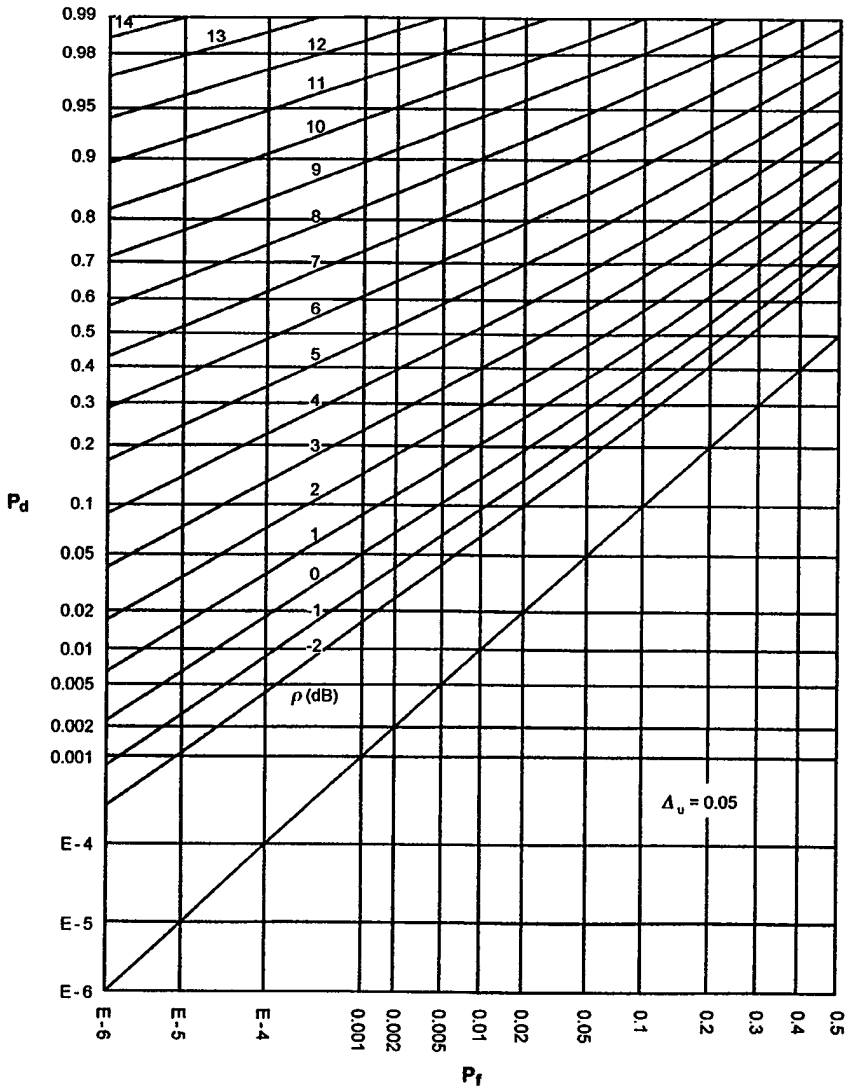

Figure D-8. ROCs for K = 2, N = 4, M = 2

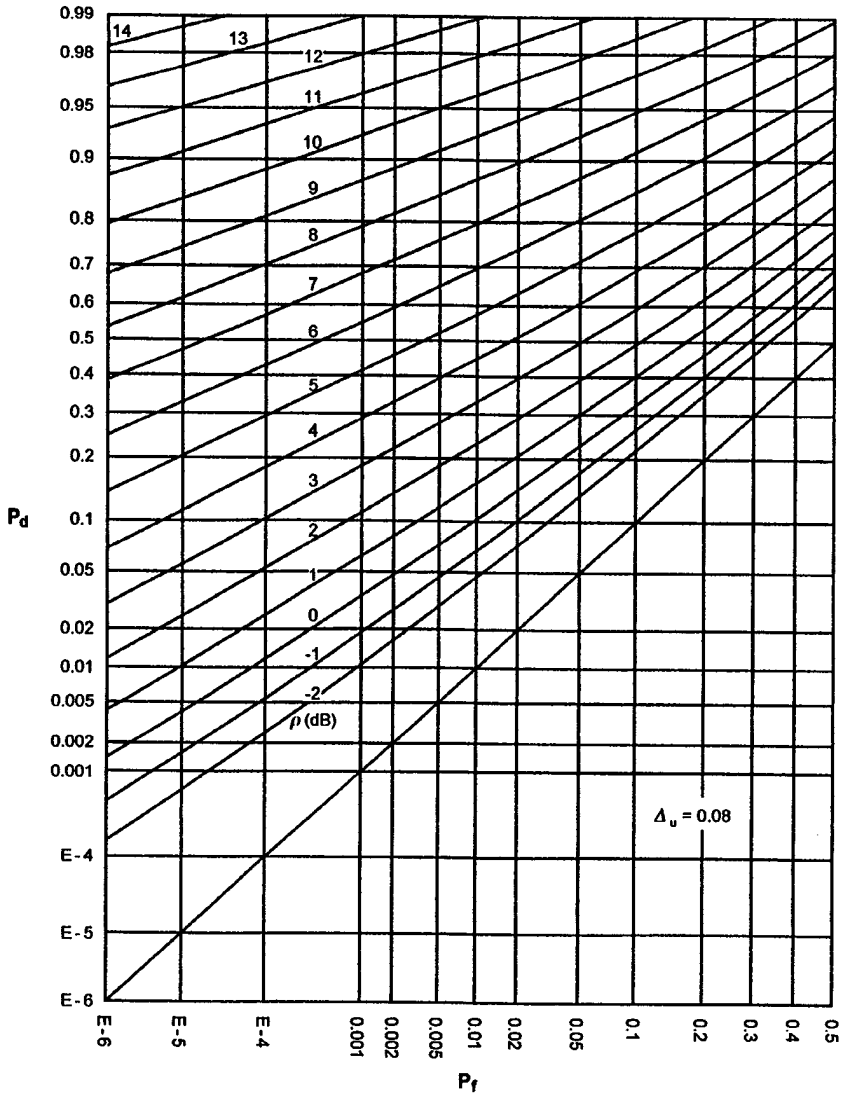

Figure D-9. ROCs for K = 2, N = 8, M = 2

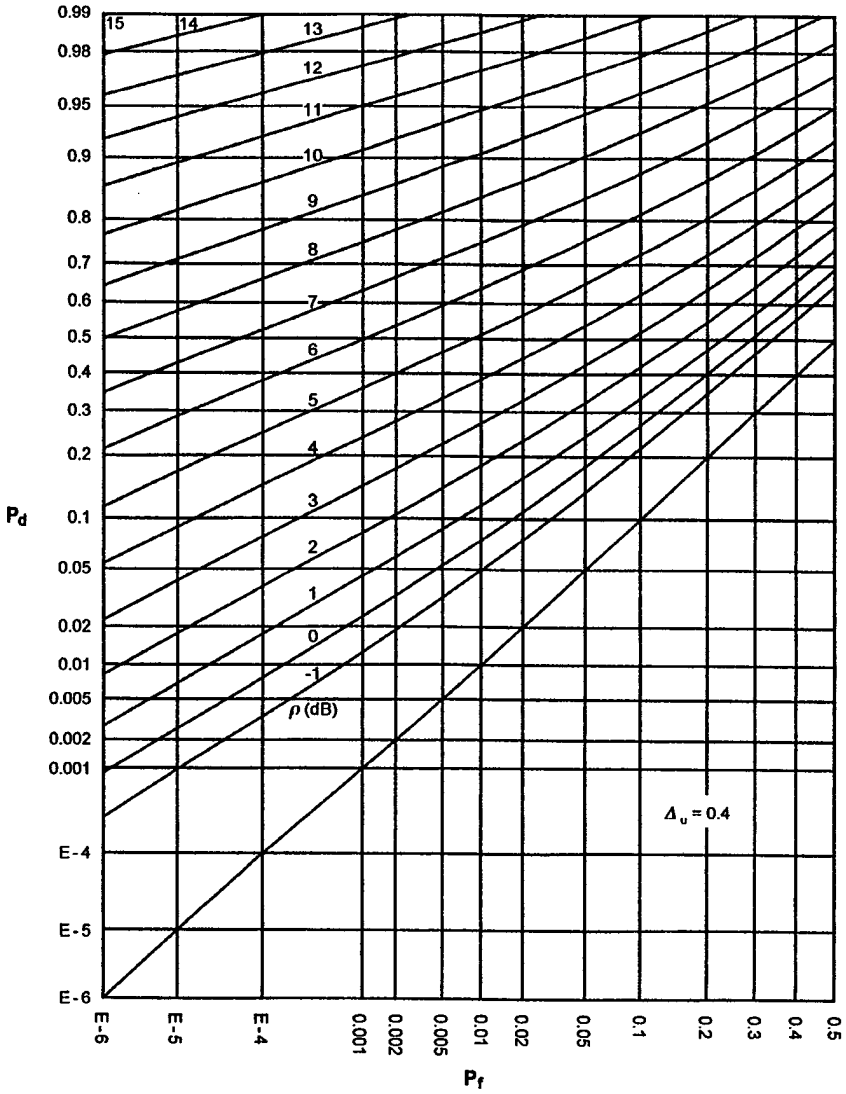

Figure D-10. ROCs for K = 2, N = 16, M = 2

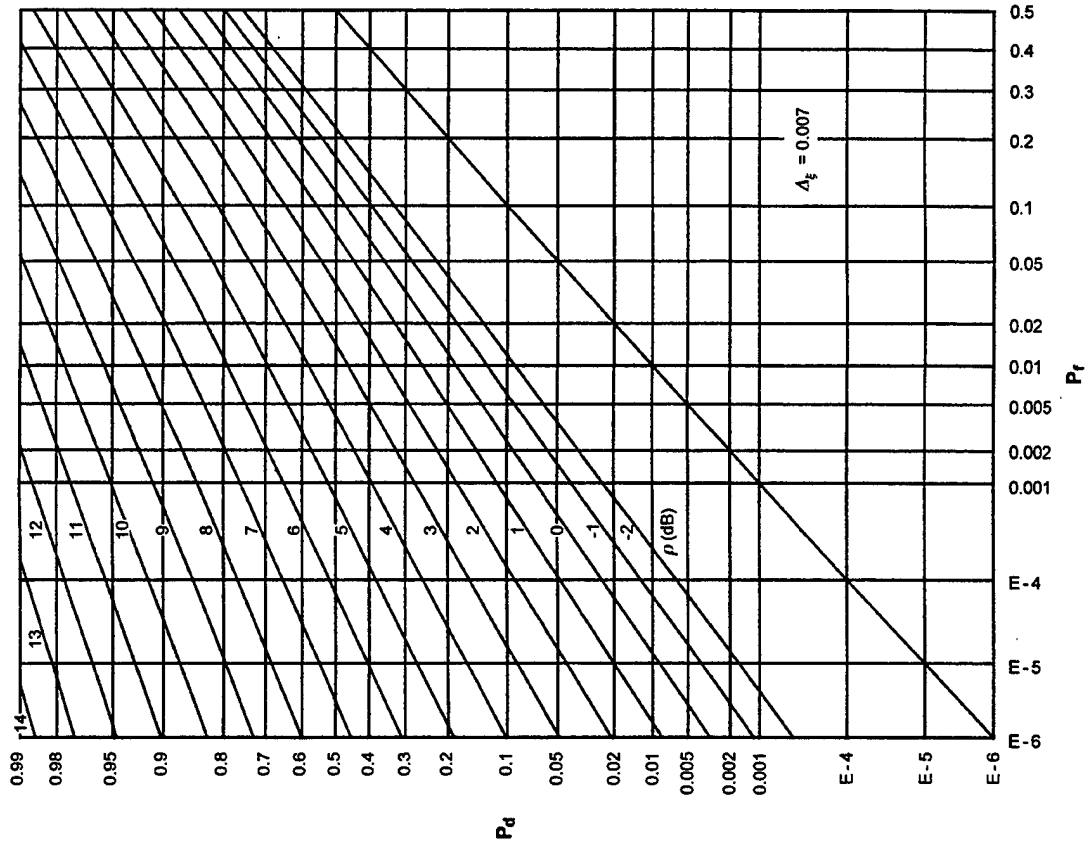

Figure D-12. ROCs for K = 1, N = 2, M = 4

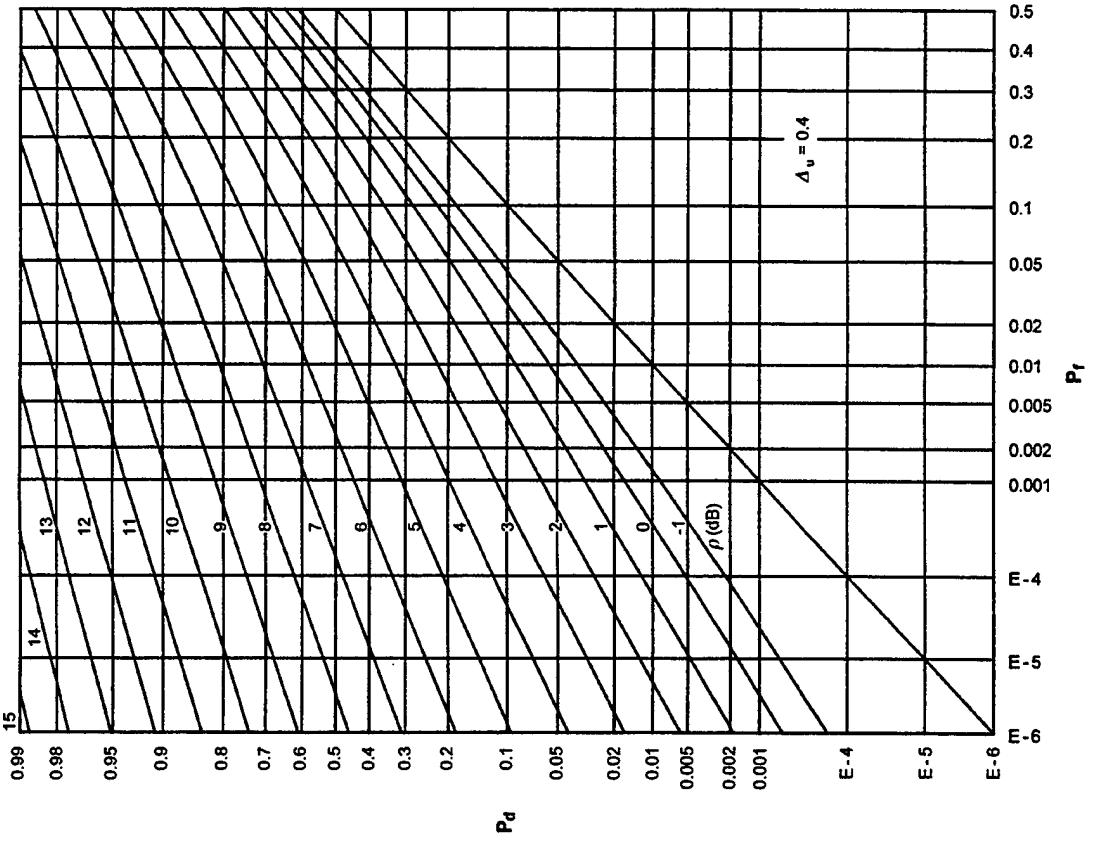

Figure D-11. ROCs for K = 2, N = 32, M = 2

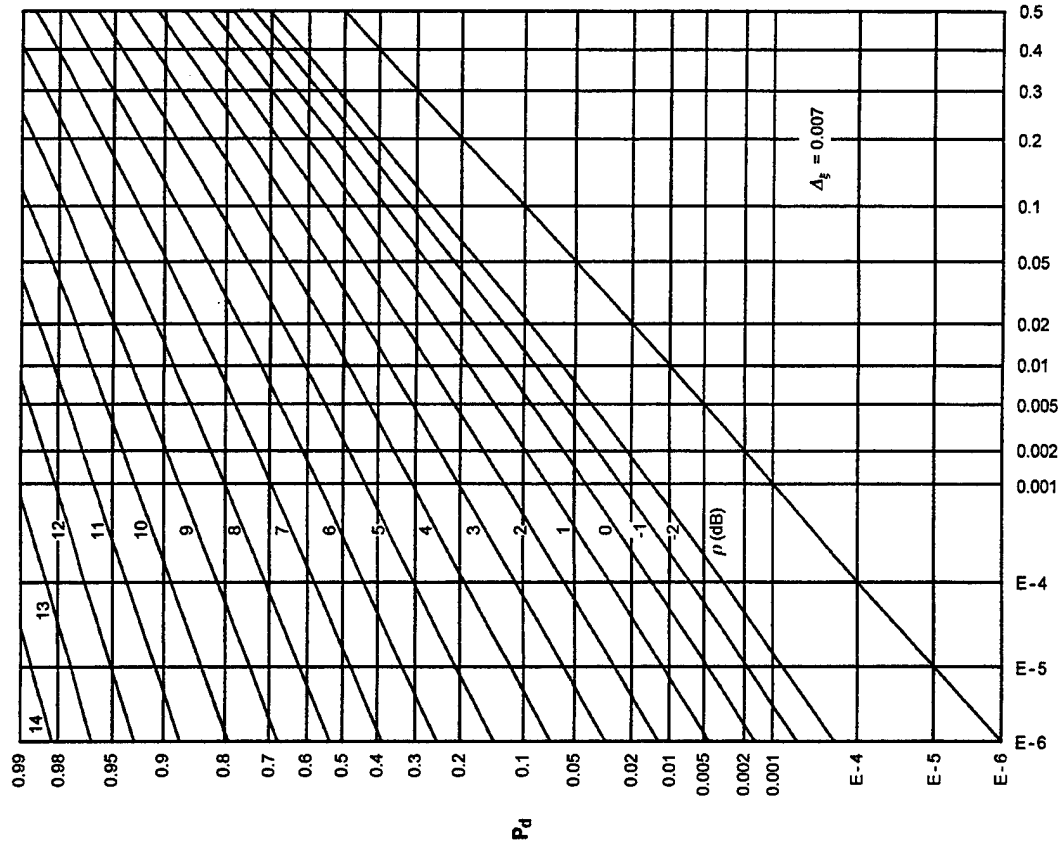

Figure D-14. ROCs for K = 1, N = 8, M = 4

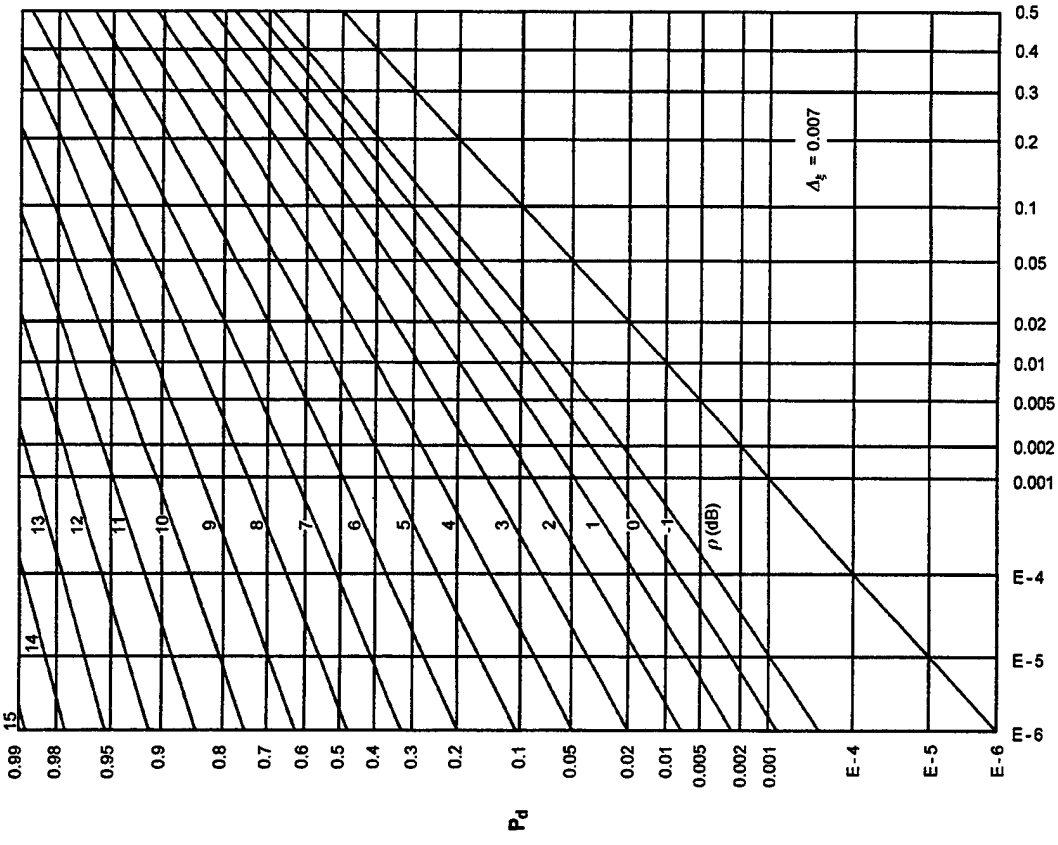

Figure D-13. ROCs for K = 1, N = 4, M = 4

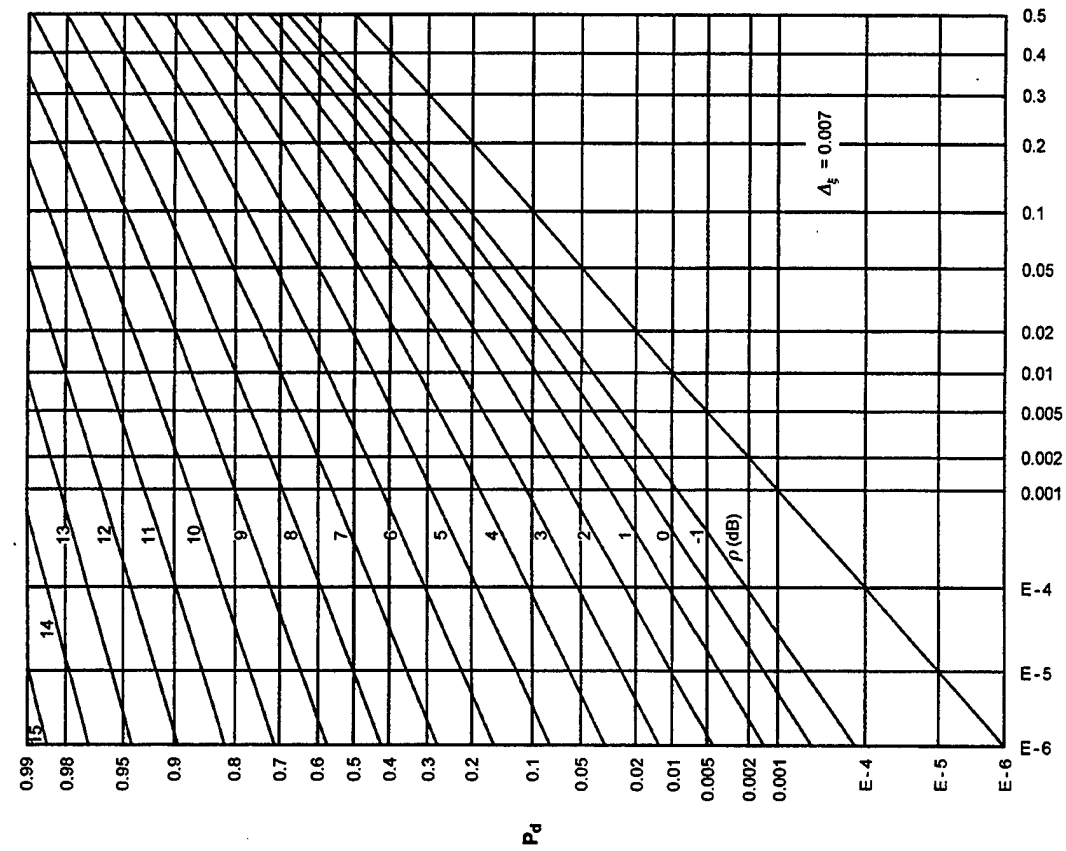

Figure D-16. ROCs for K = 1, N = 32, M = 4

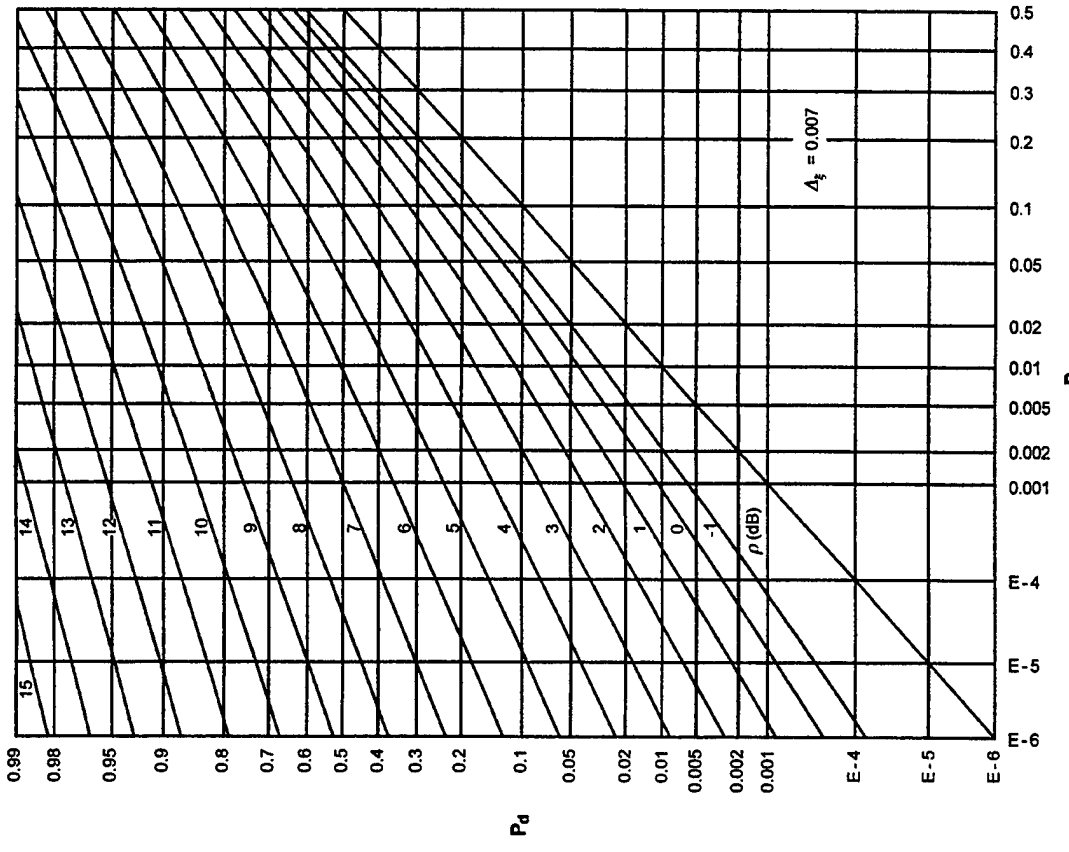

Figure D-15. ROCs for K = 1, N = 16, M = 4

APPENDIX E - ROCS FOR KM = 16, RANDOM GAUSSIAN SIGNAL

This appendix contains the ROCs for or-ing with pre- and post-averaging when the time-bandwidth product KM is fixed at 16; the possible combinations (from table 1) are repeated here:

K	M	N
16	1	1,2,4,8,16,32
8	2	
4	4	
2	8	
1	16	

For N = 1, only the product KM matters; the first plot in this appendix covers this special case, under the labeling K = 16, N = 1, M = 1. The other 5 values of N, along with the 5 possible combinations of K and M, yield 25 additional ROCs, for a total of 26 ROCs in this appendix.

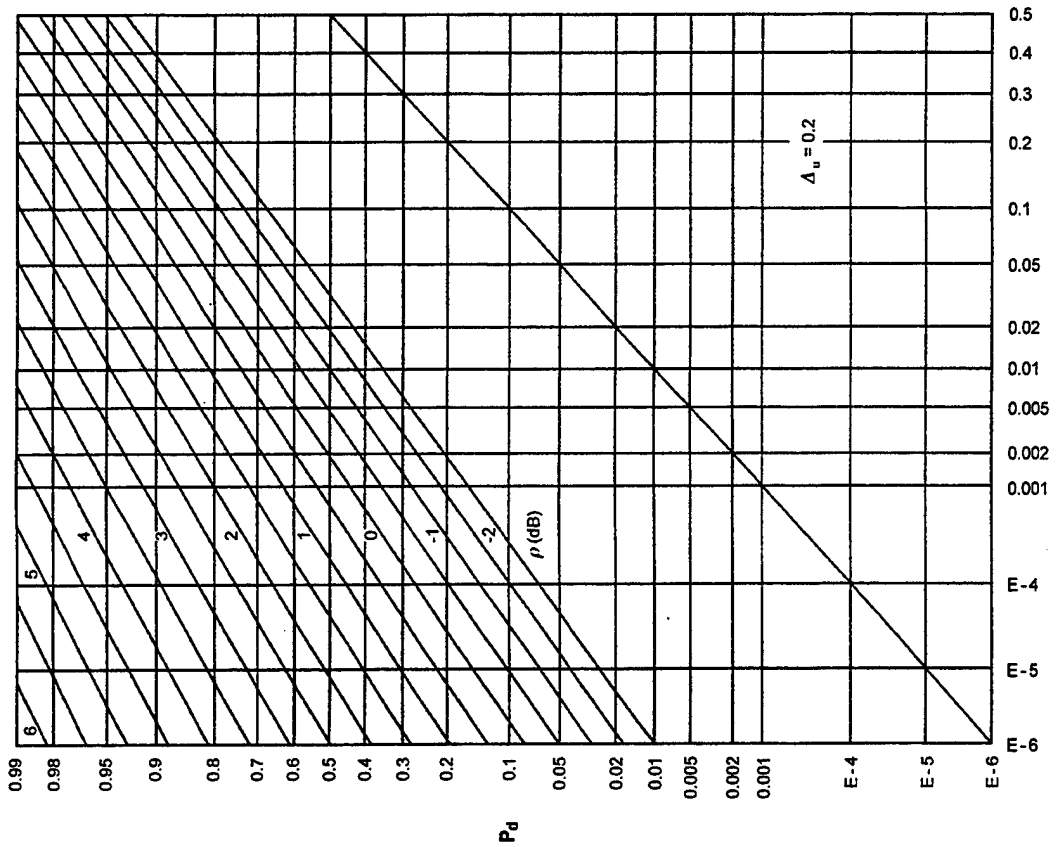

Figure E-2. ROCs for K = 16, N = 2, M = 1

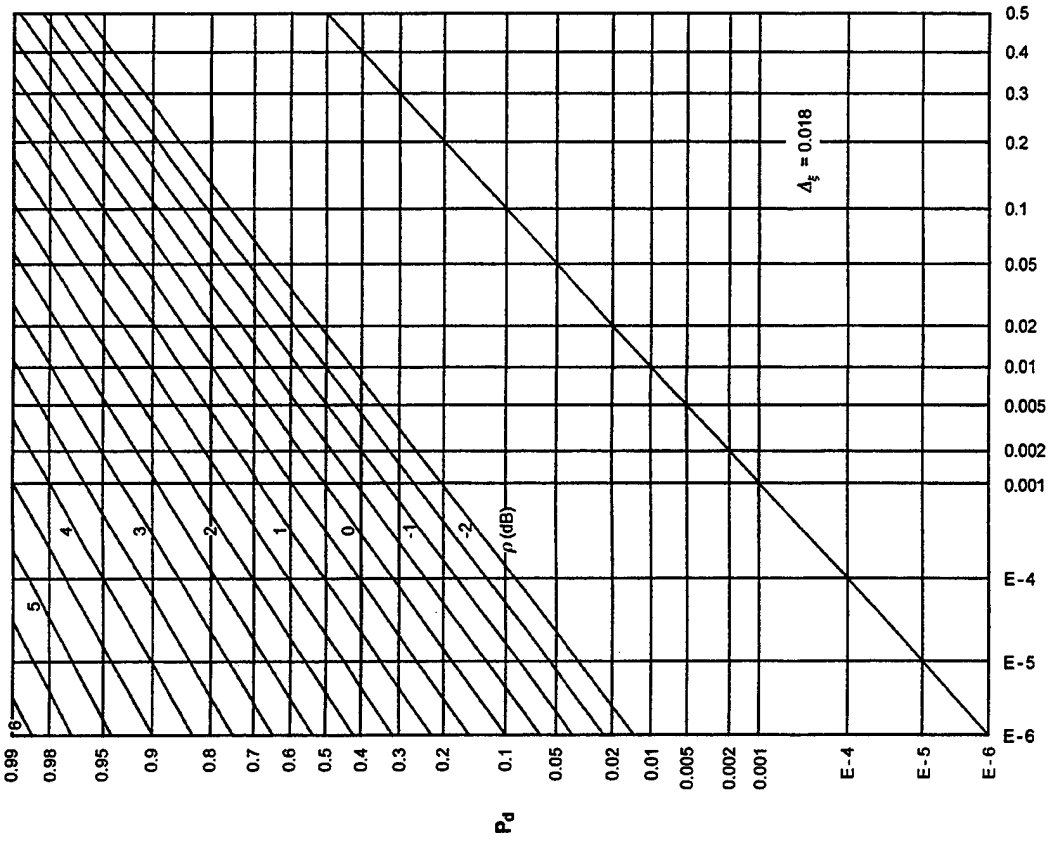

Figure E-1. ROCs for K = 16, N = 1, M = 1

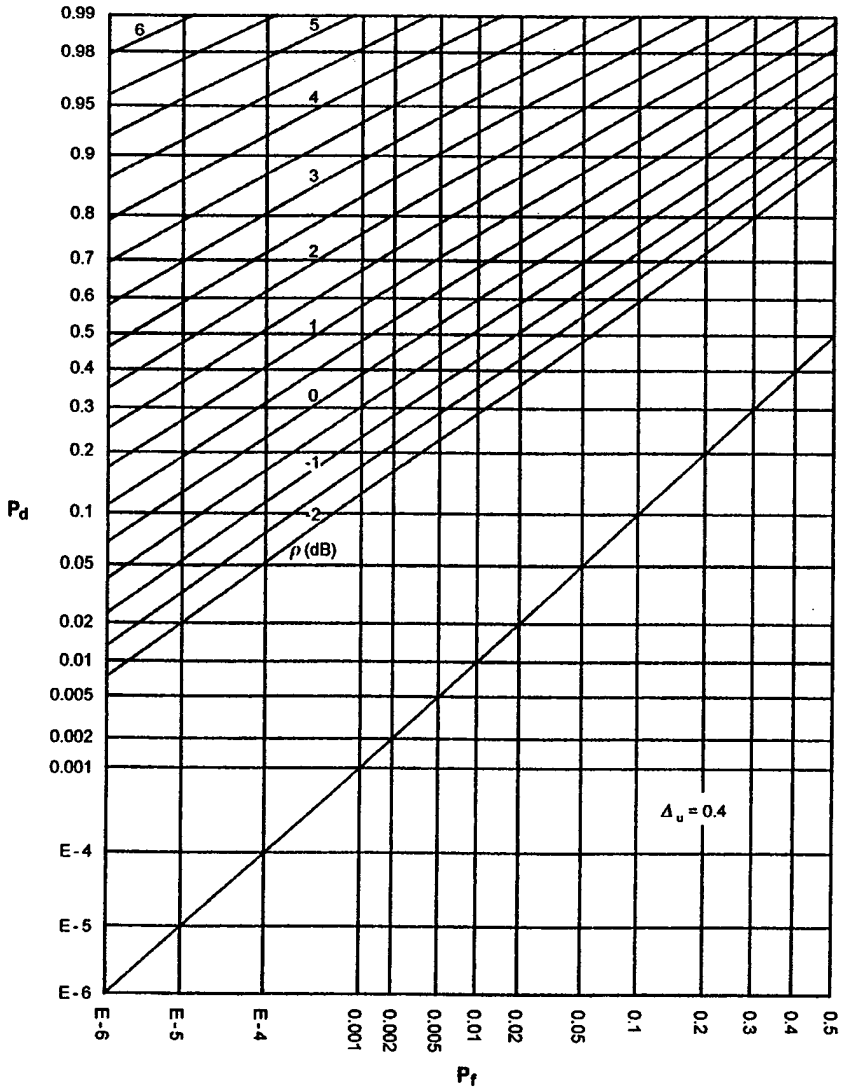

Figure E-3. ROCs for K = 16, N = 4, M = 1

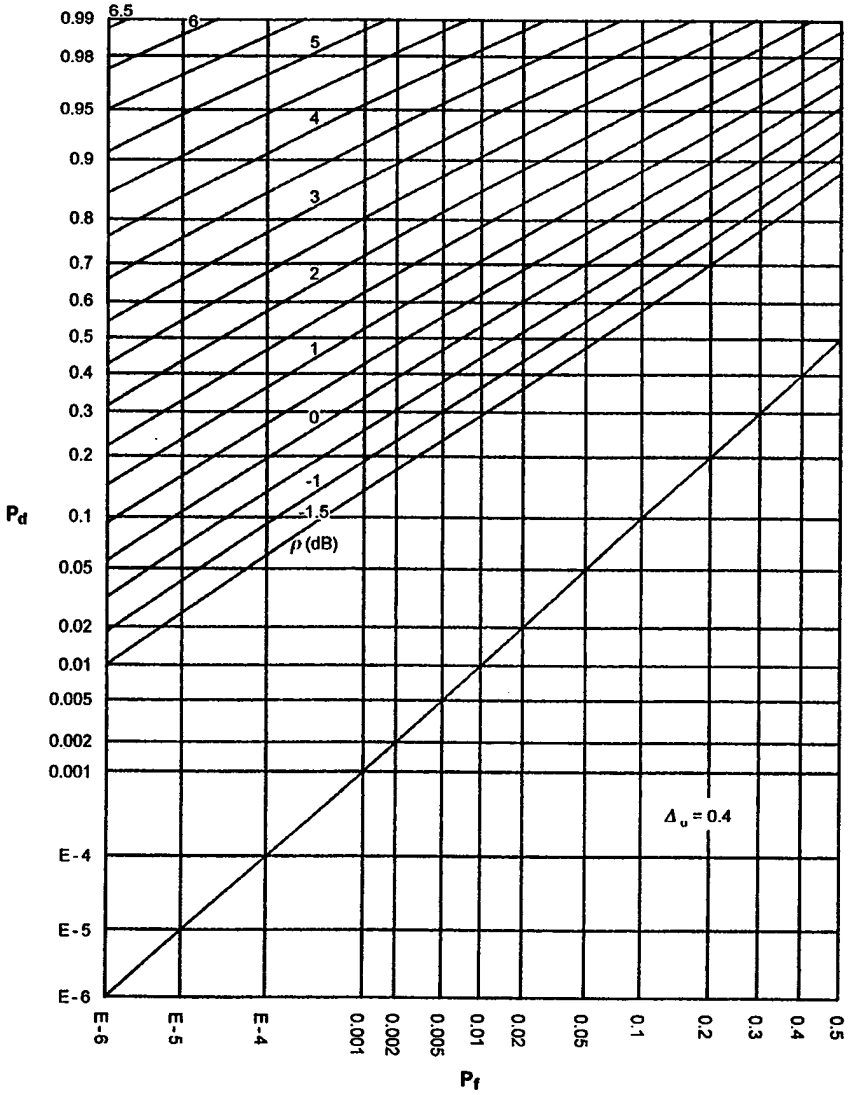

Figure E-4. ROCs for K = 16, N = 8, M = 1

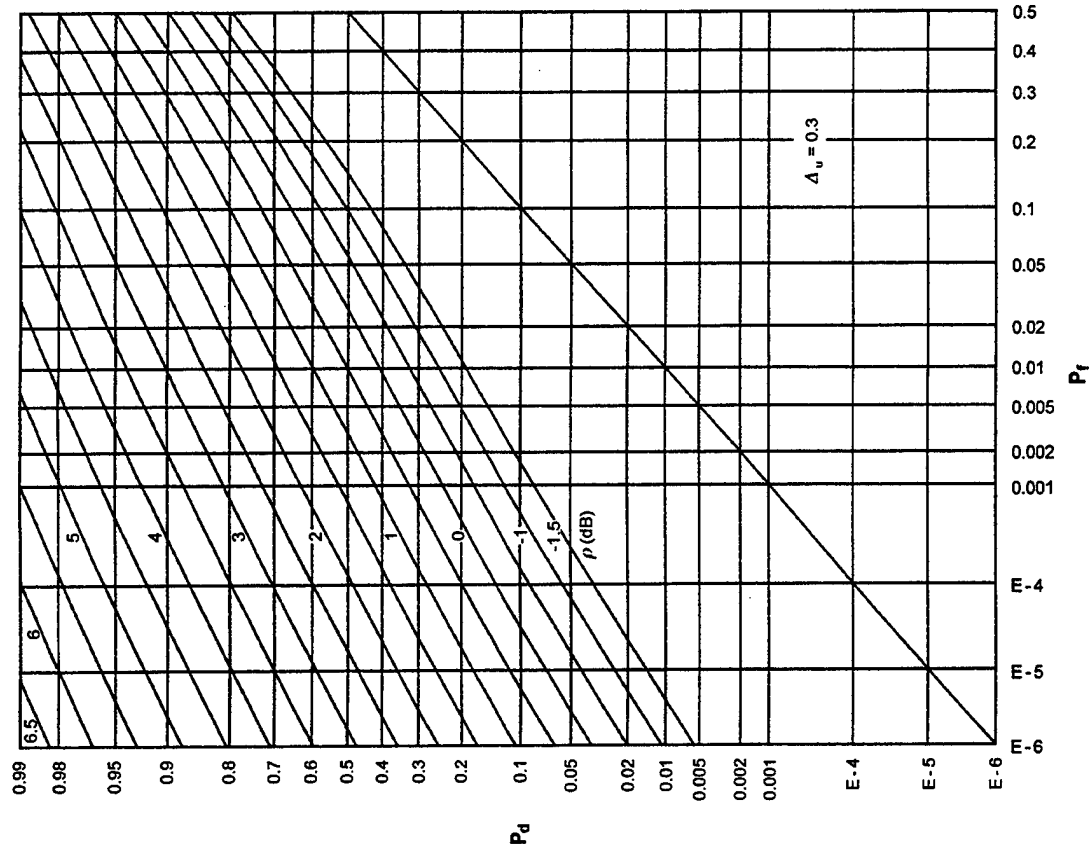

Figure E-6. ROCs for K = 16, N = 32, M = 1

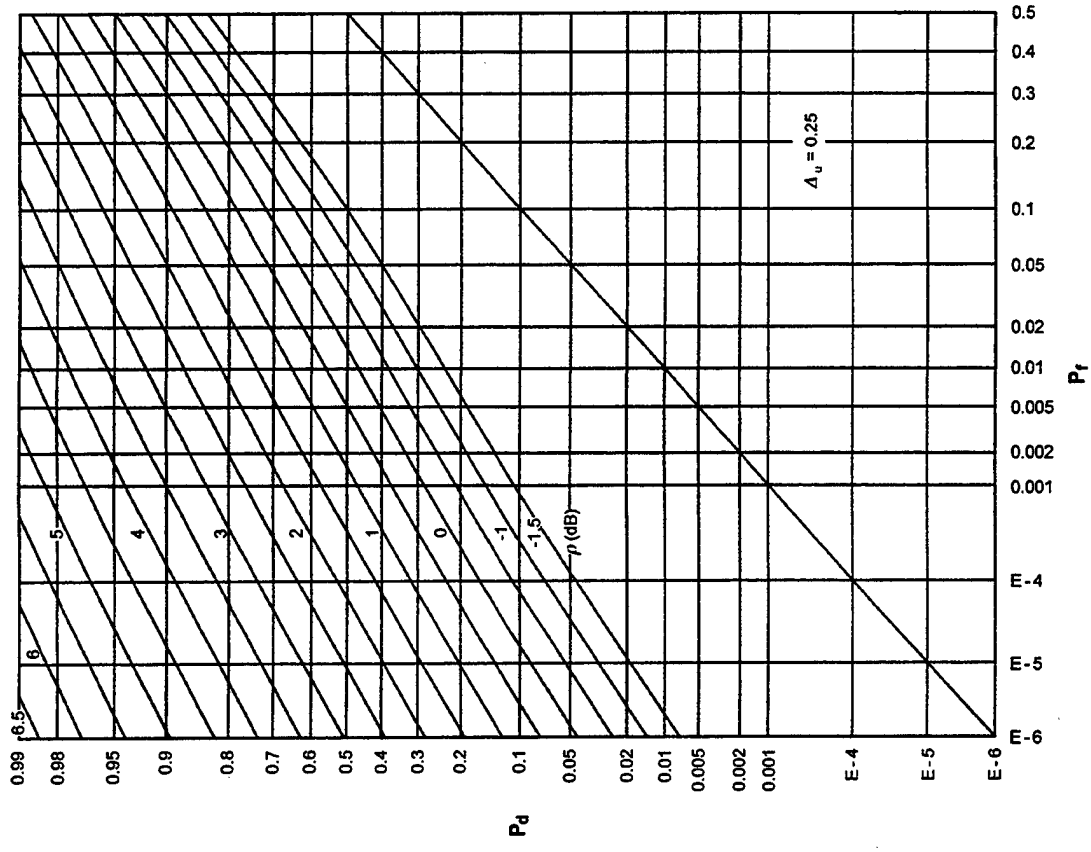

Figure E-5. ROCs for K = 16, N = 16, M = 1

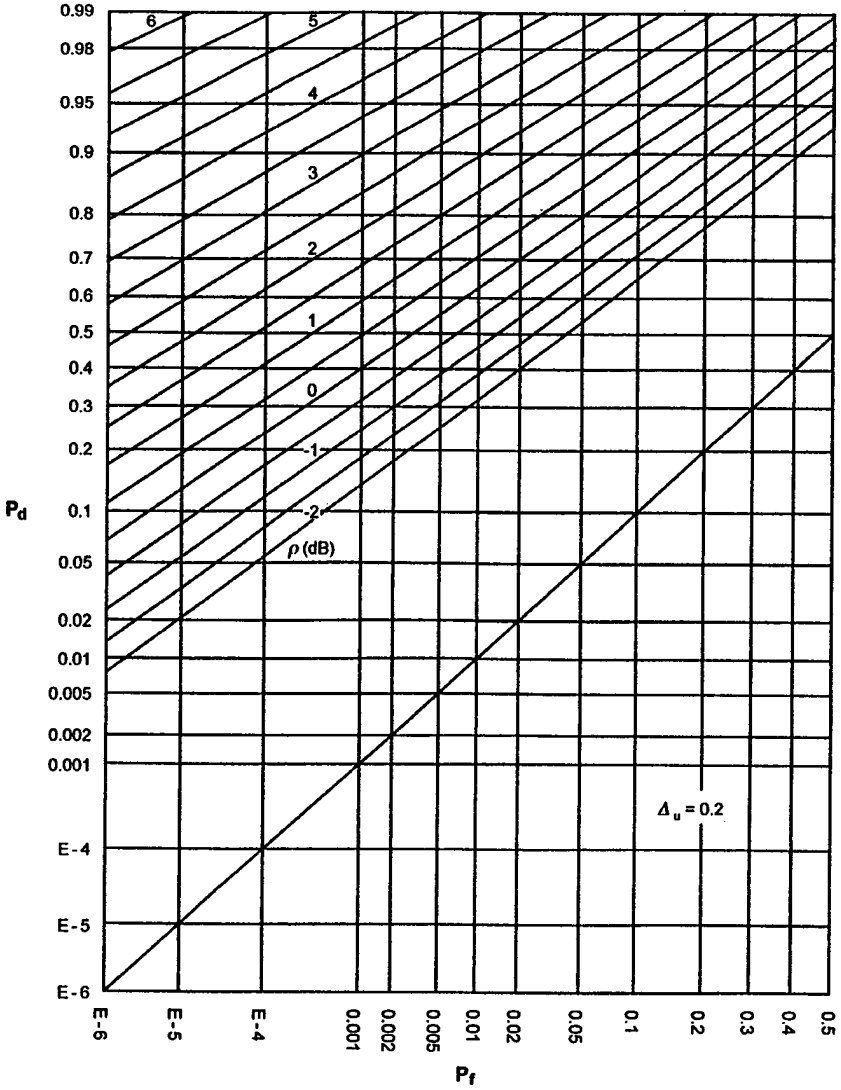

Figure E-7. ROCs for K = 8, N = 2, M = 2

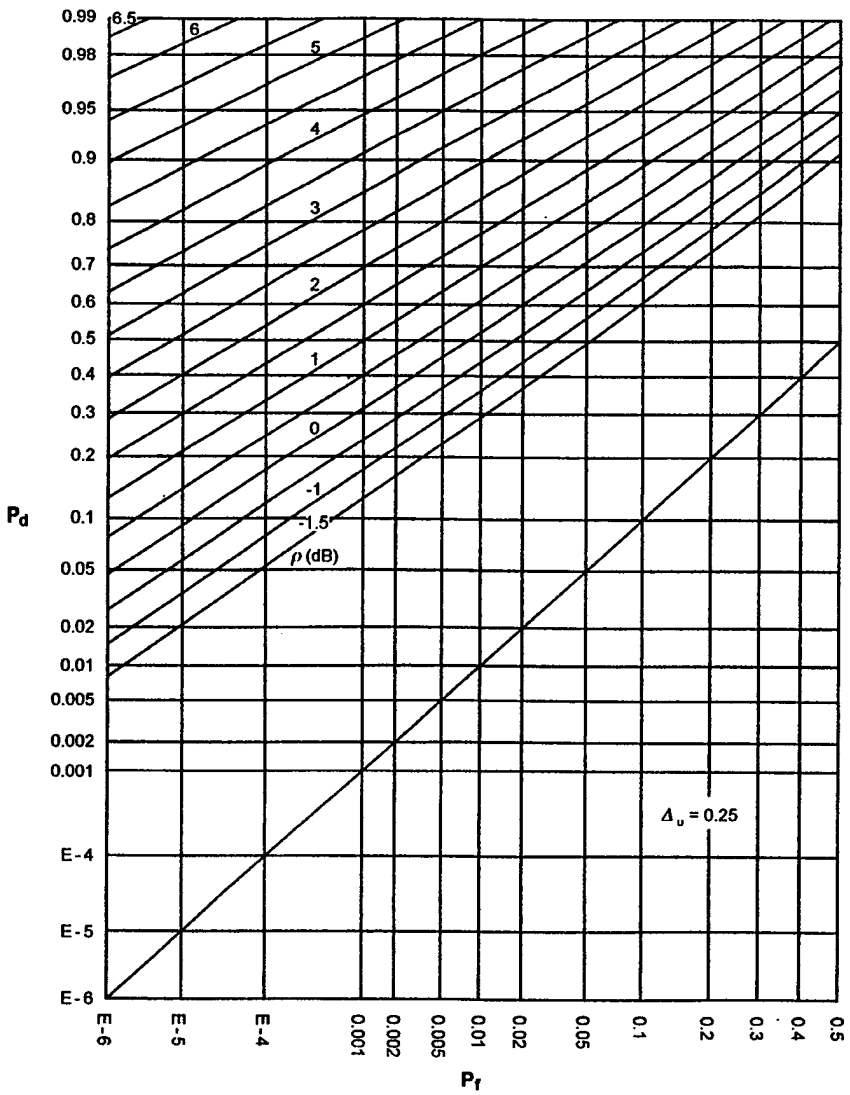

Figure E-8. ROCs for K = 8, N = 4, M = 2

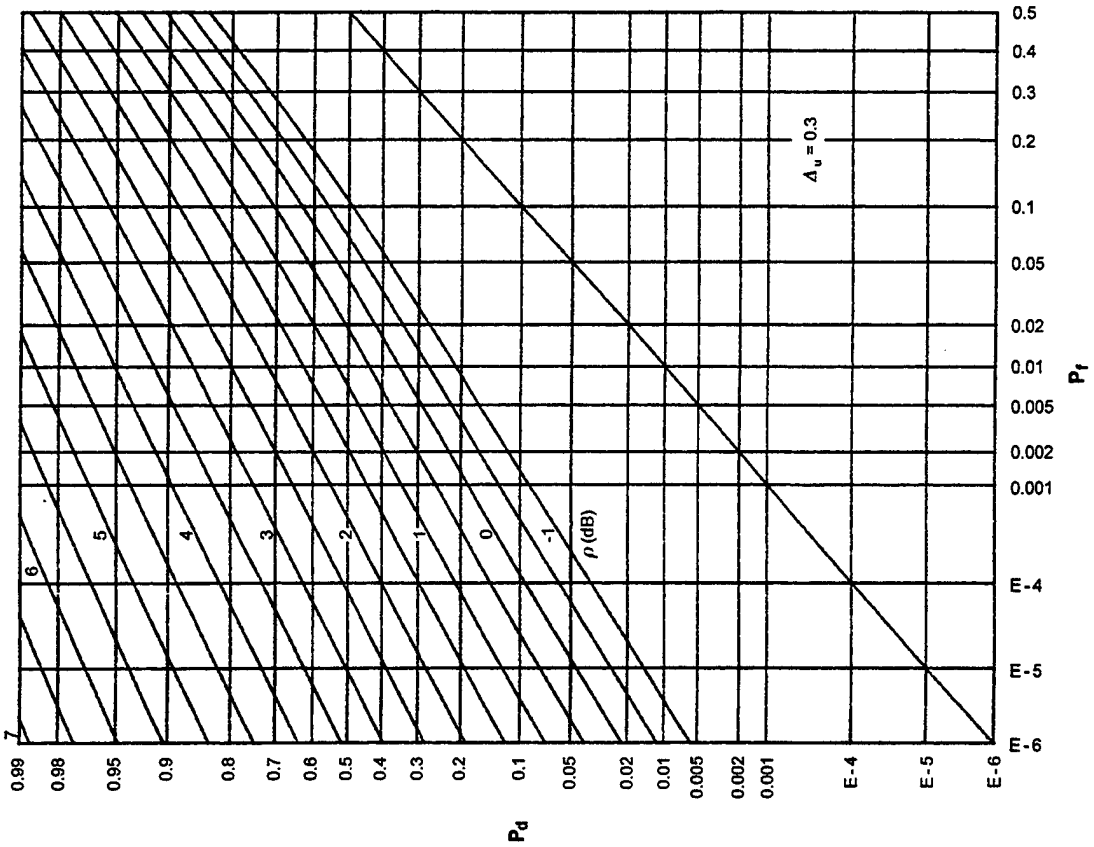

Figure E-10. ROCs for K = 8, N = 16, M = 2

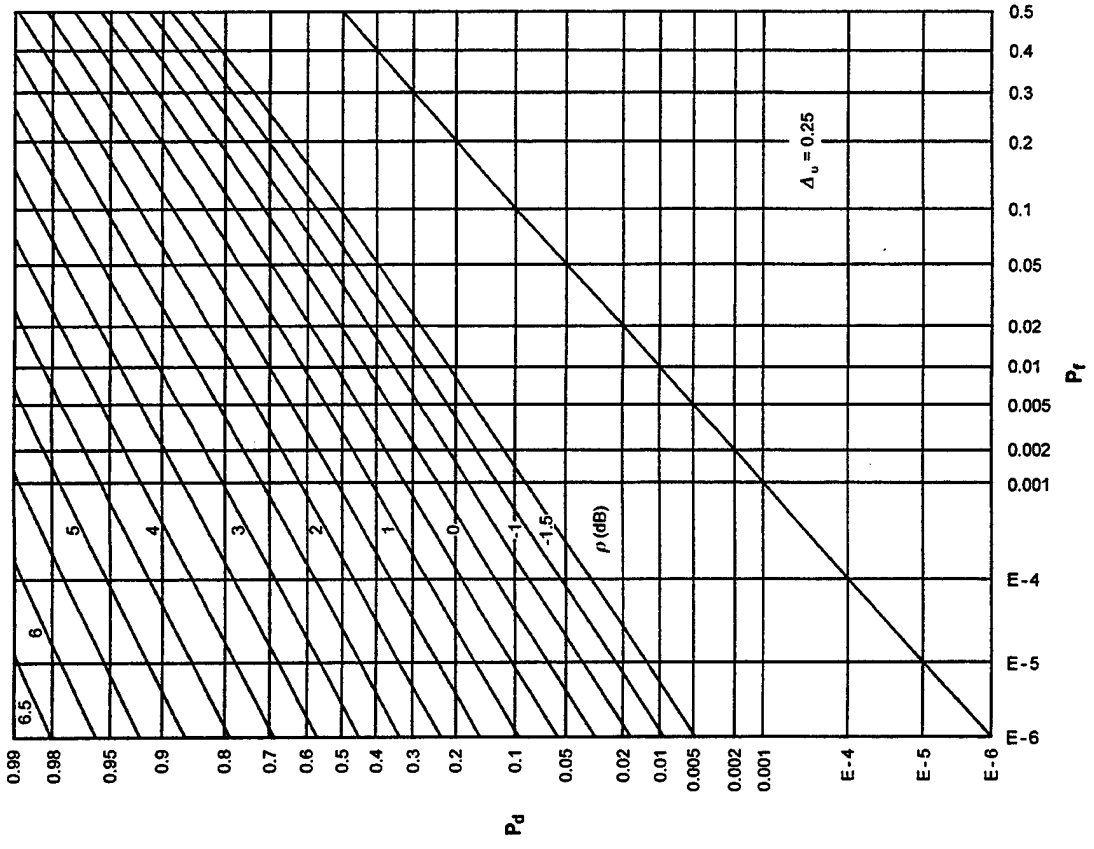

Figure E-9. ROCs for K = 8, N = 8, M = 2

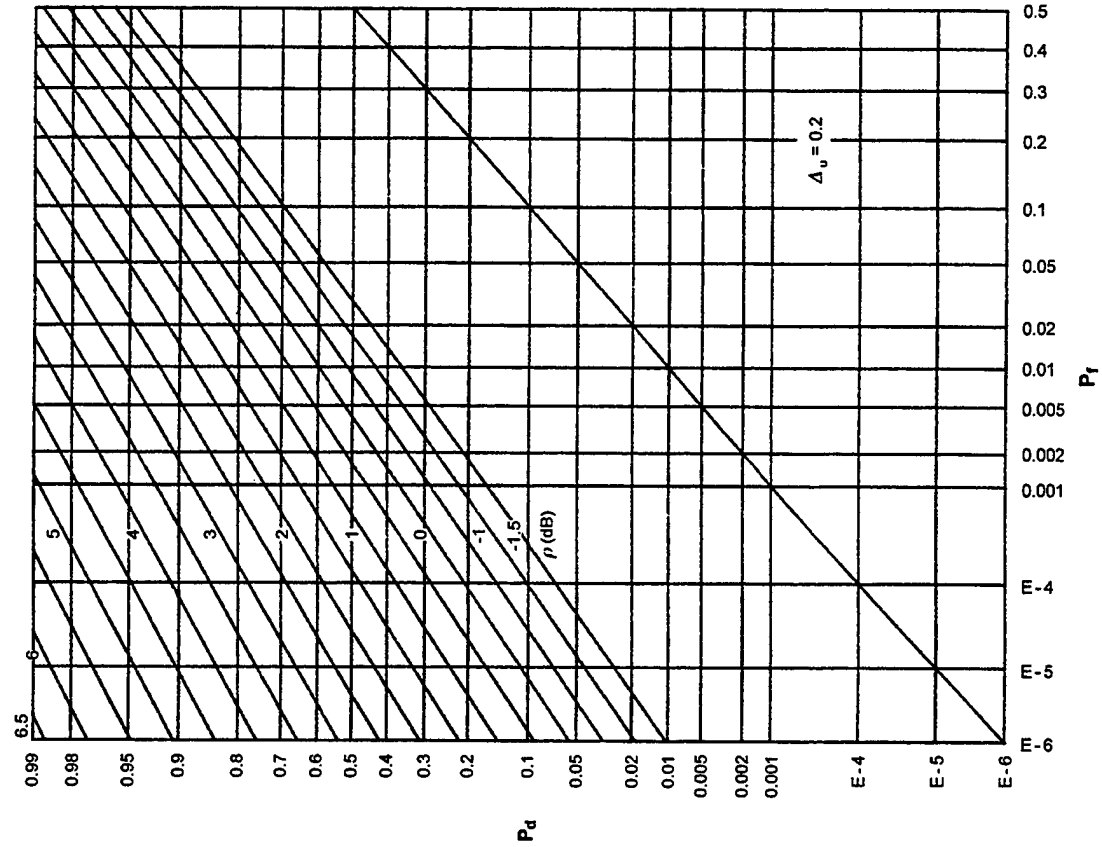

Figure E-12. ROCs for K = 4, N = 2, M = 4

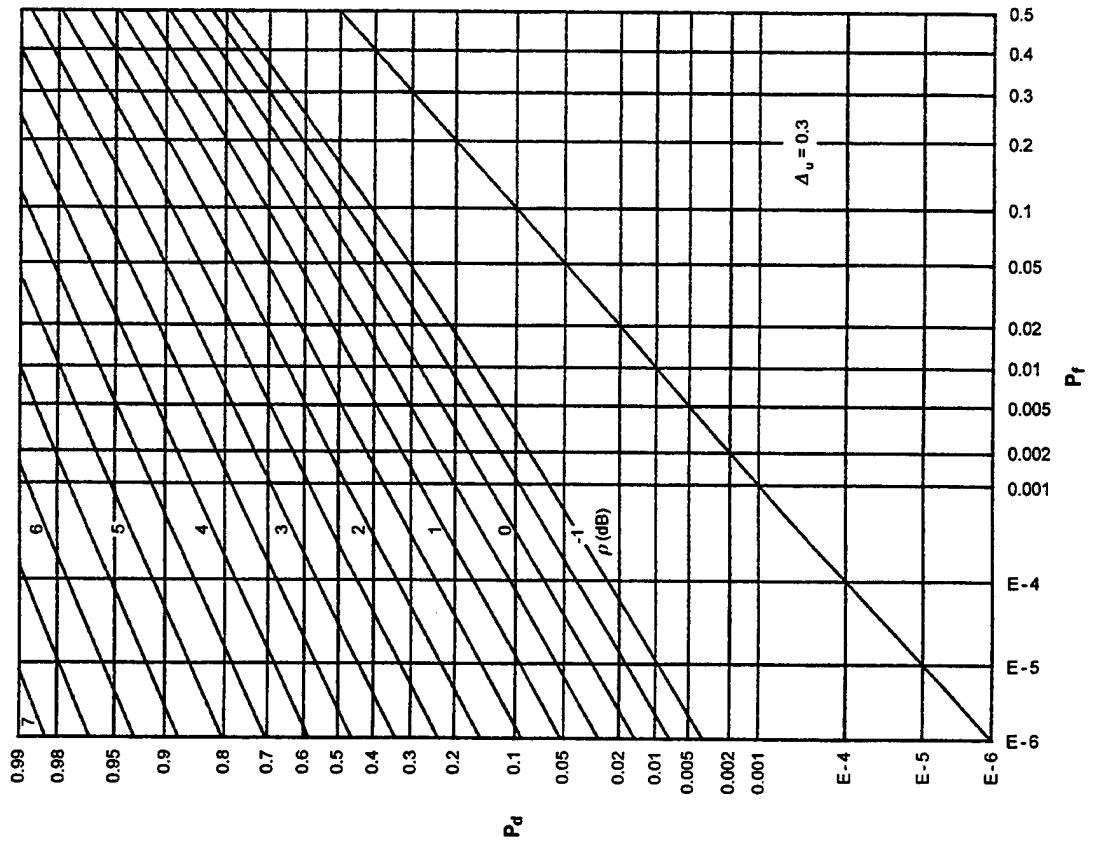

Figure E-11. ROCs for K = 8, N = 32, M = 2

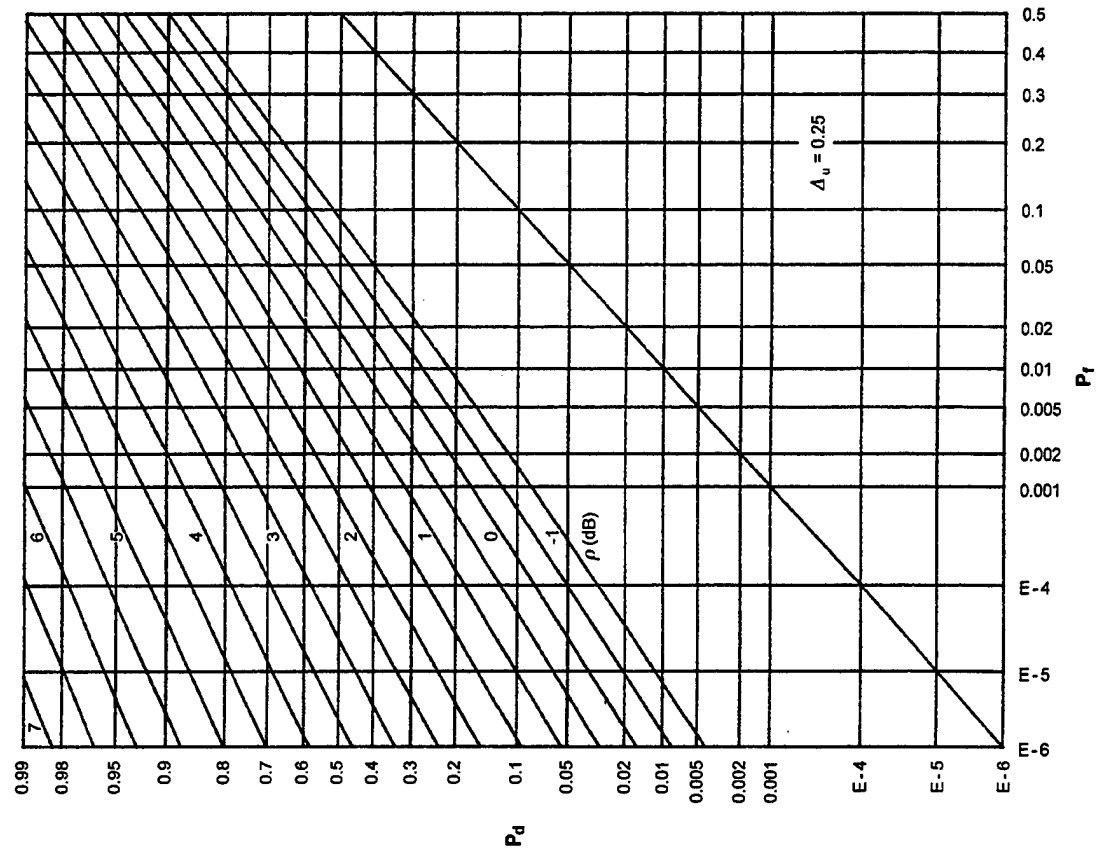

Figure E-14. ROCs for K = 4, N = 8, M = 4

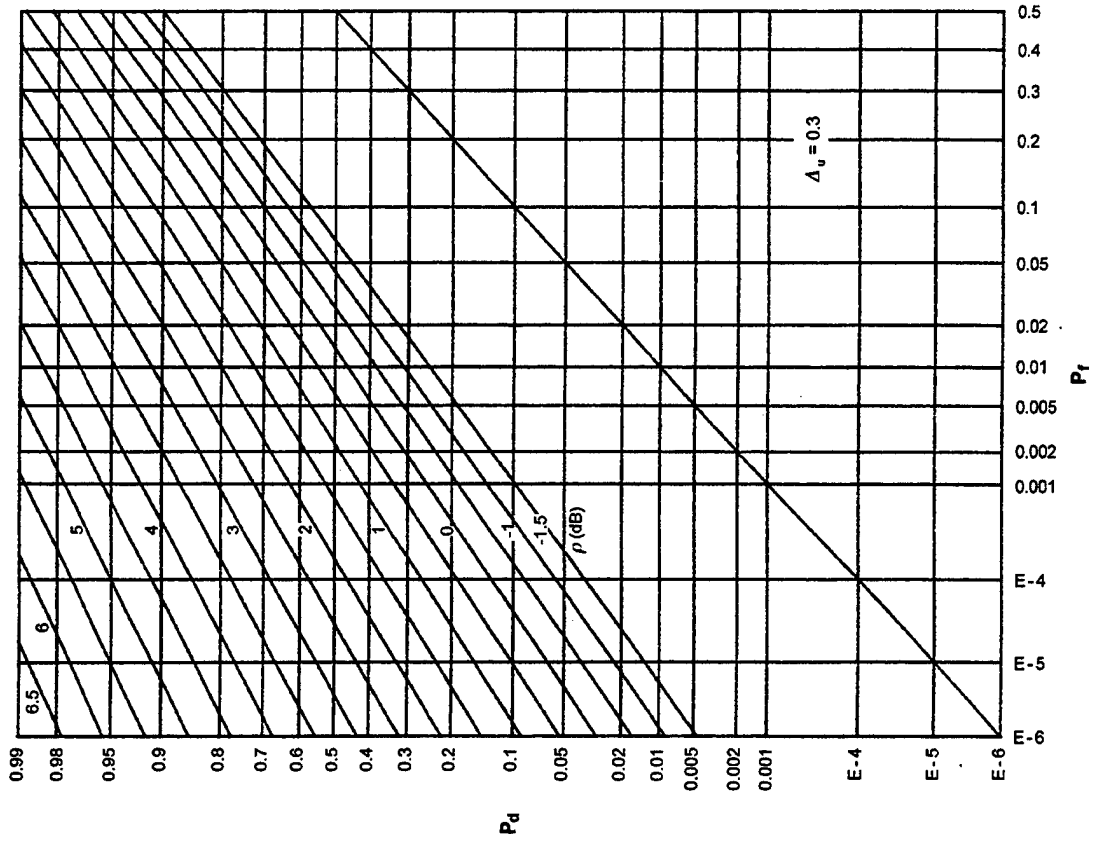

Figure E-13. ROCs for K = 4, N = 4, M = 4

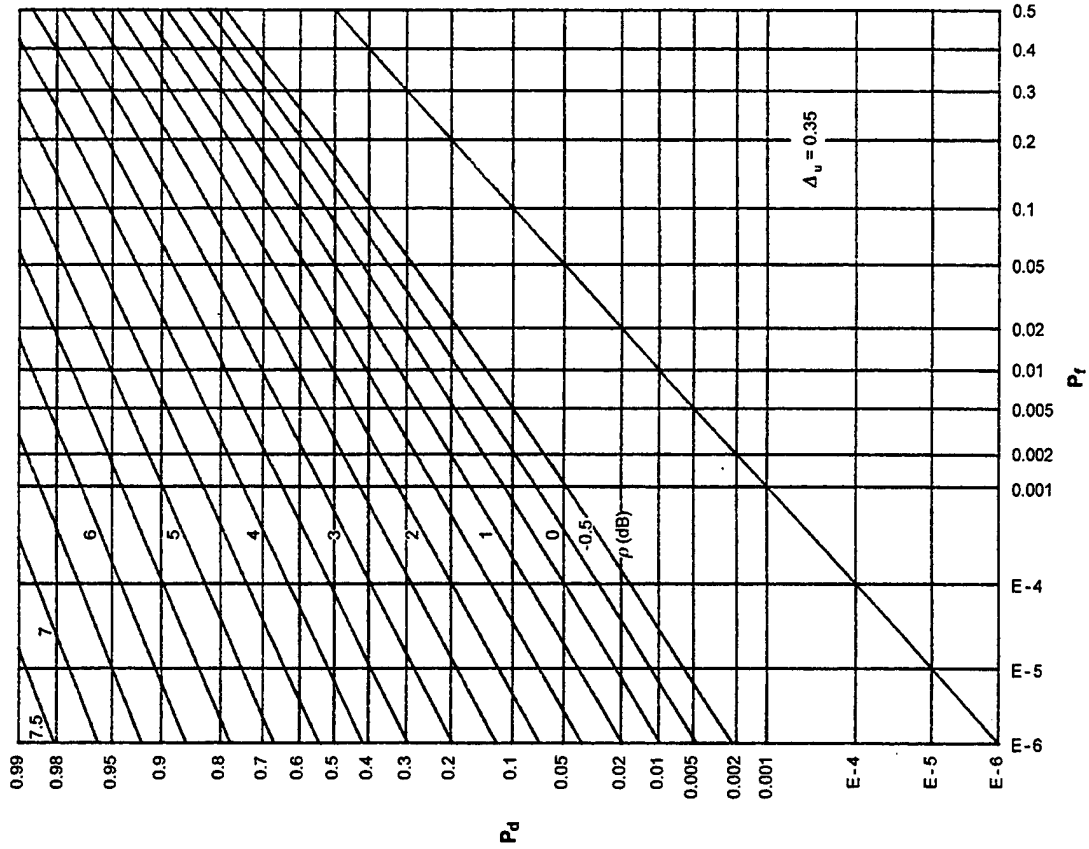

Figure E-16. ROCs for K = 4, N = 32, M = 4

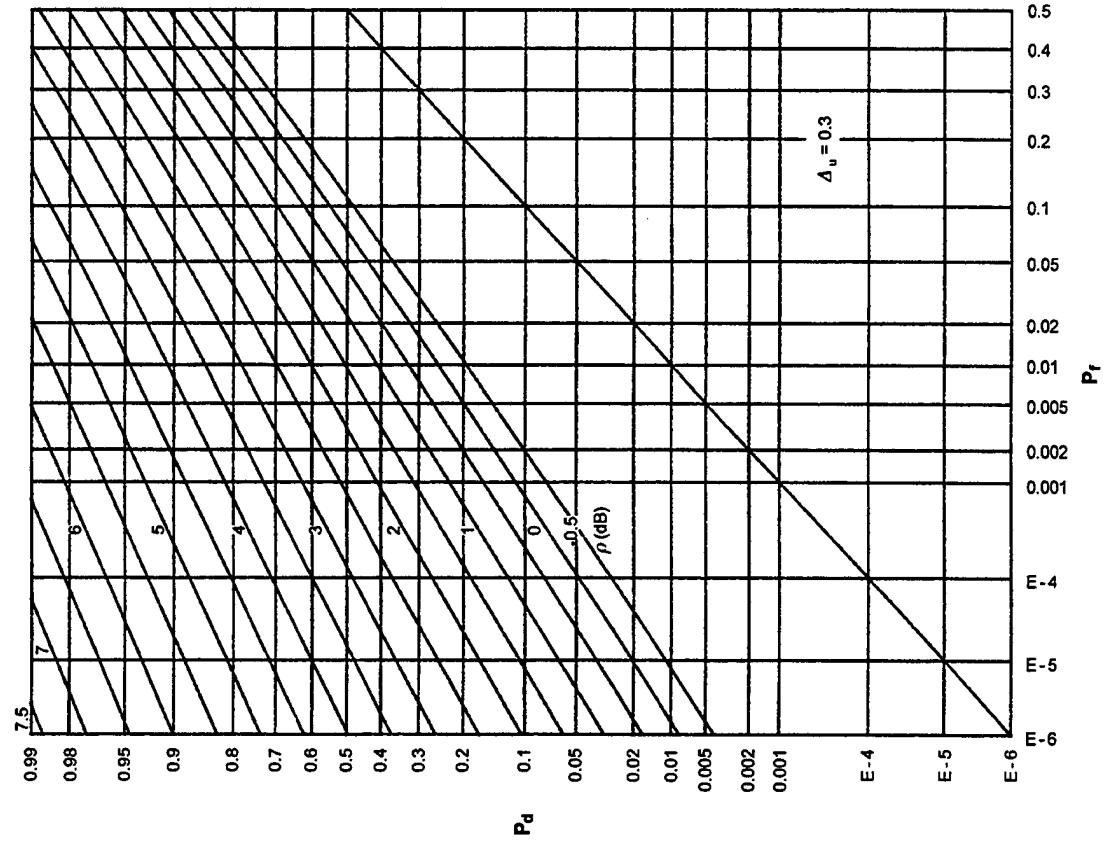

Figure E-15. ROCs for K = 4, N = 16, M = 4

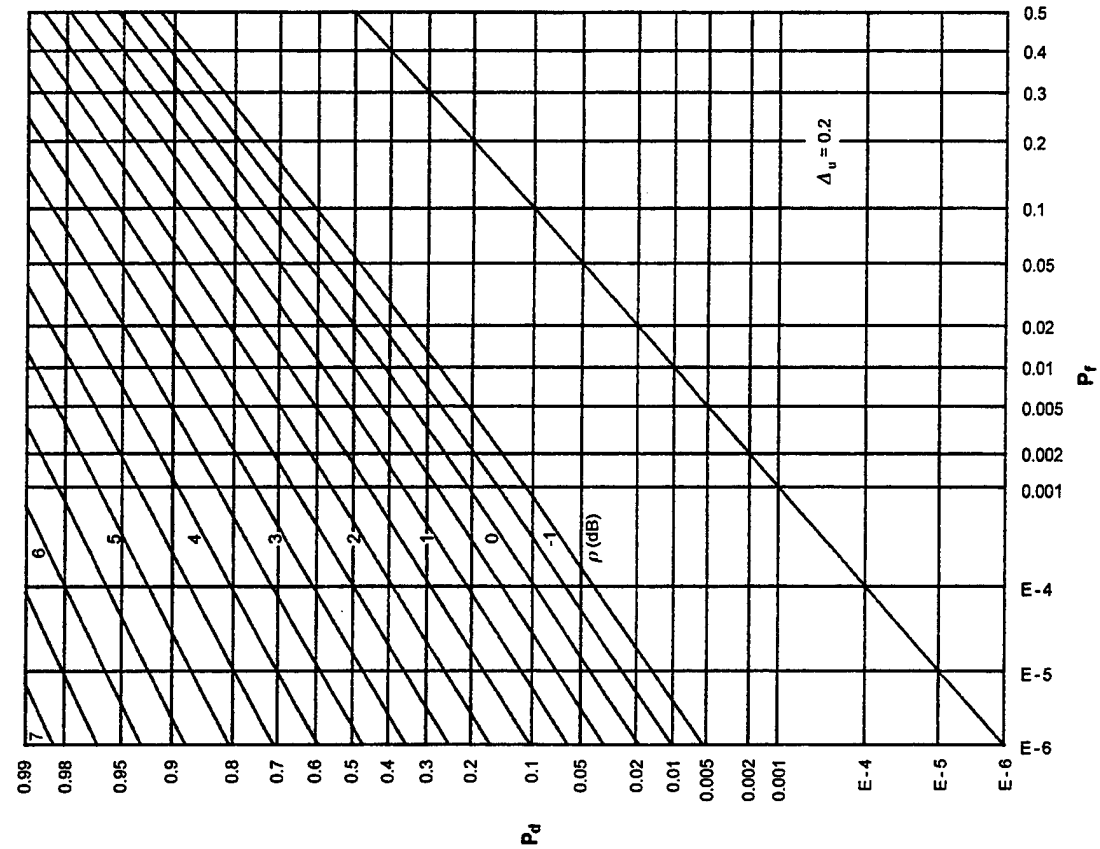

Figure E-18. ROCs for K = 2, N = 4, M = 8

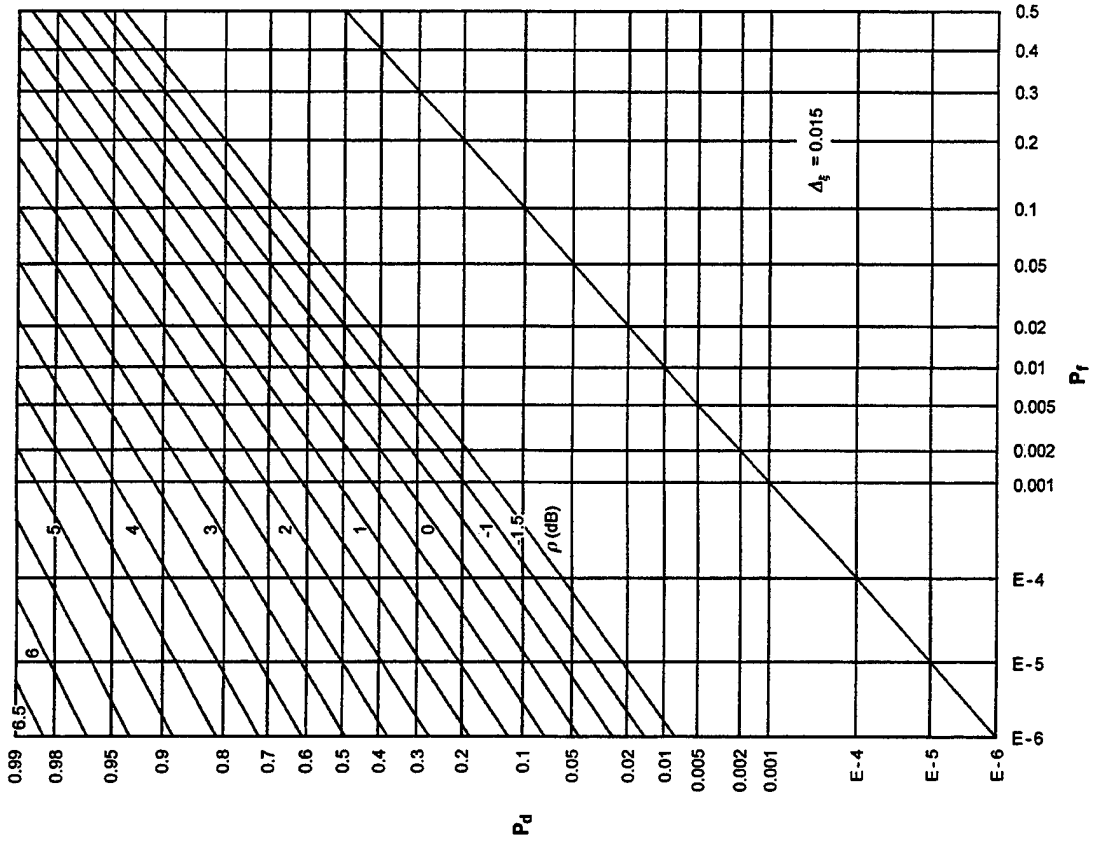

Figure E-17. ROCs for K = 2, N = 2, M = 8

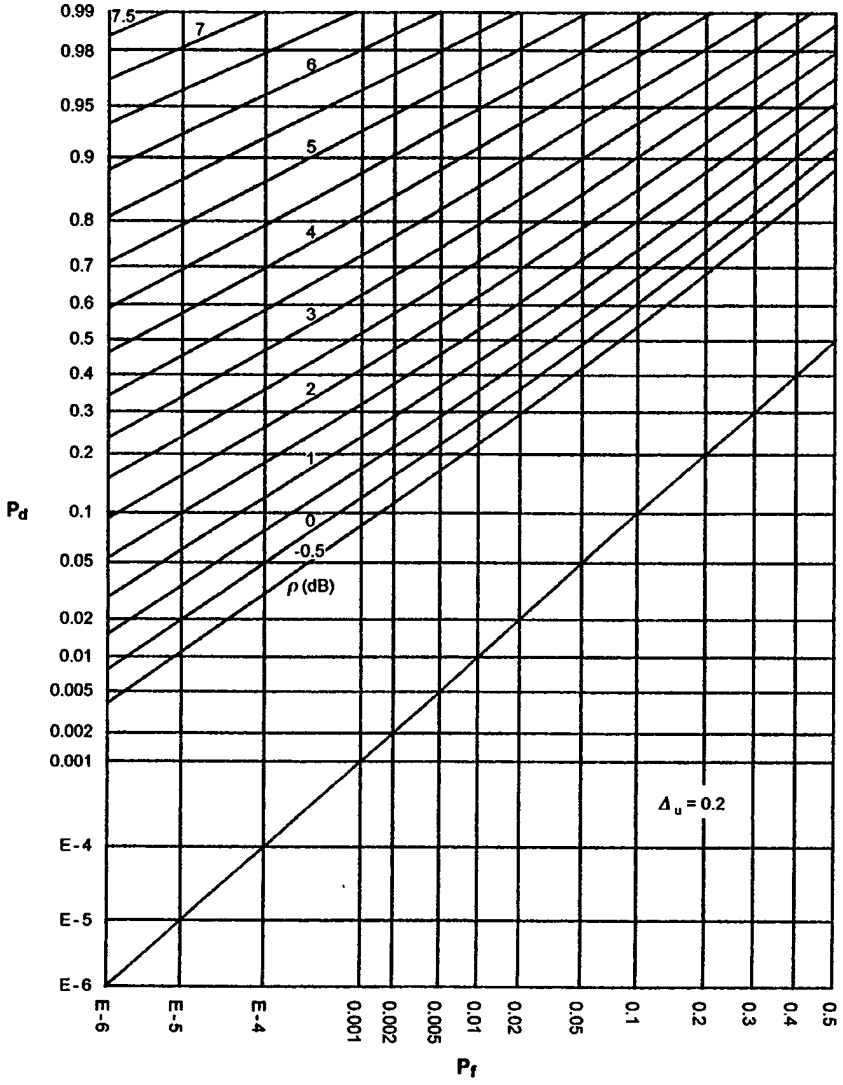

Figure E-19. ROCs for K = 2, N = 8, M = 8

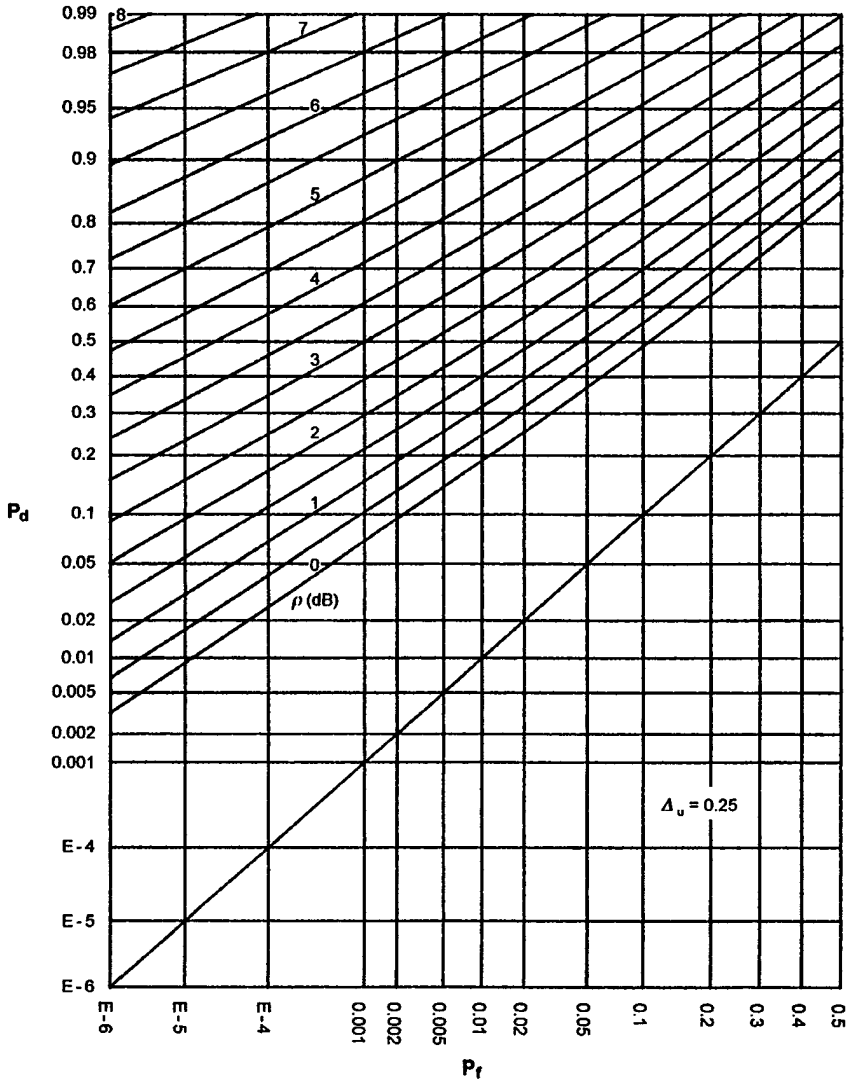

Figure E-20. ROCs for K = 2, N = 16, M = 8

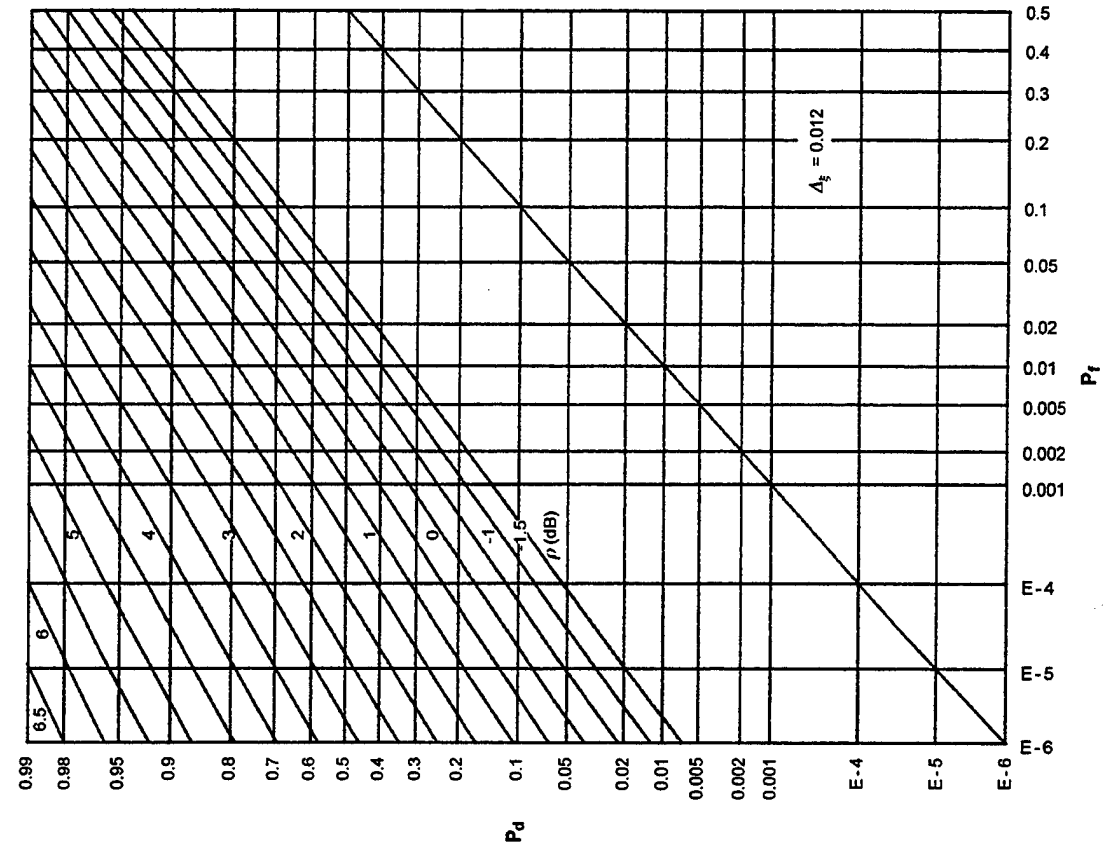

Figure E-22. ROCs for K = 1, N = 2, M = 16

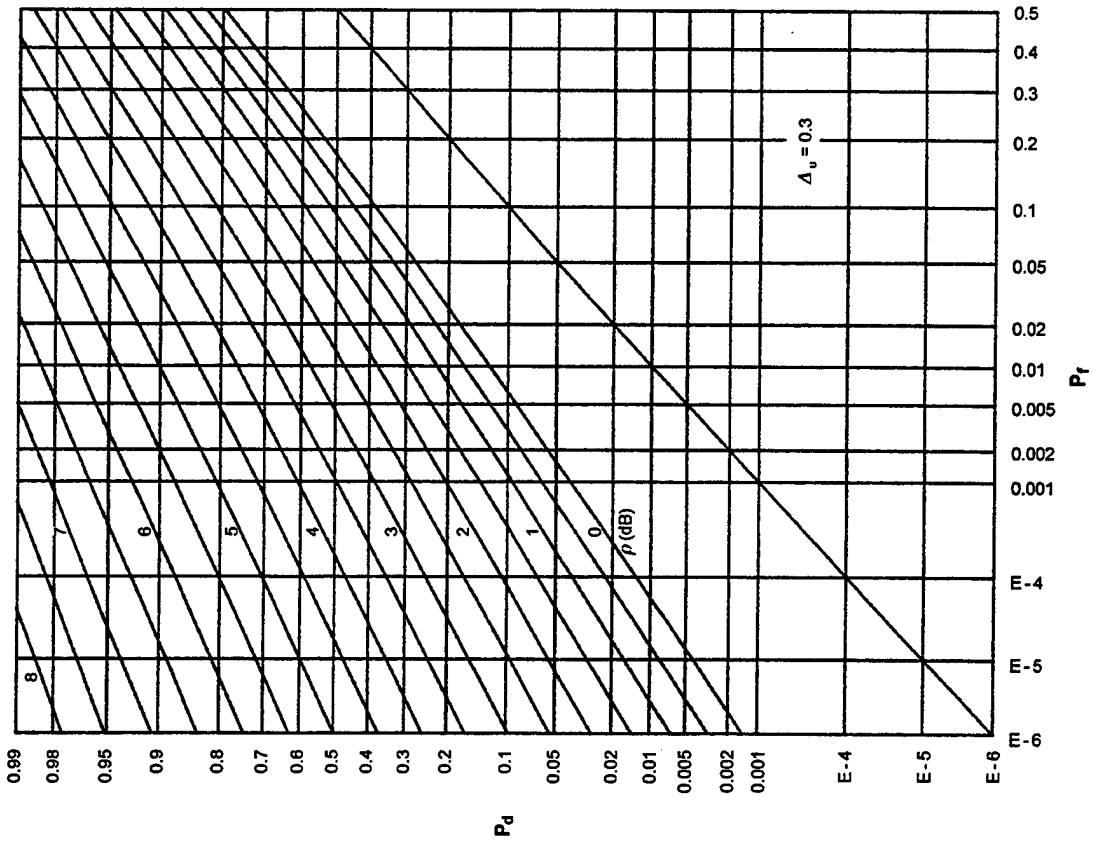

Figure E-21. ROCs for K = 2, N = 32, M = 8

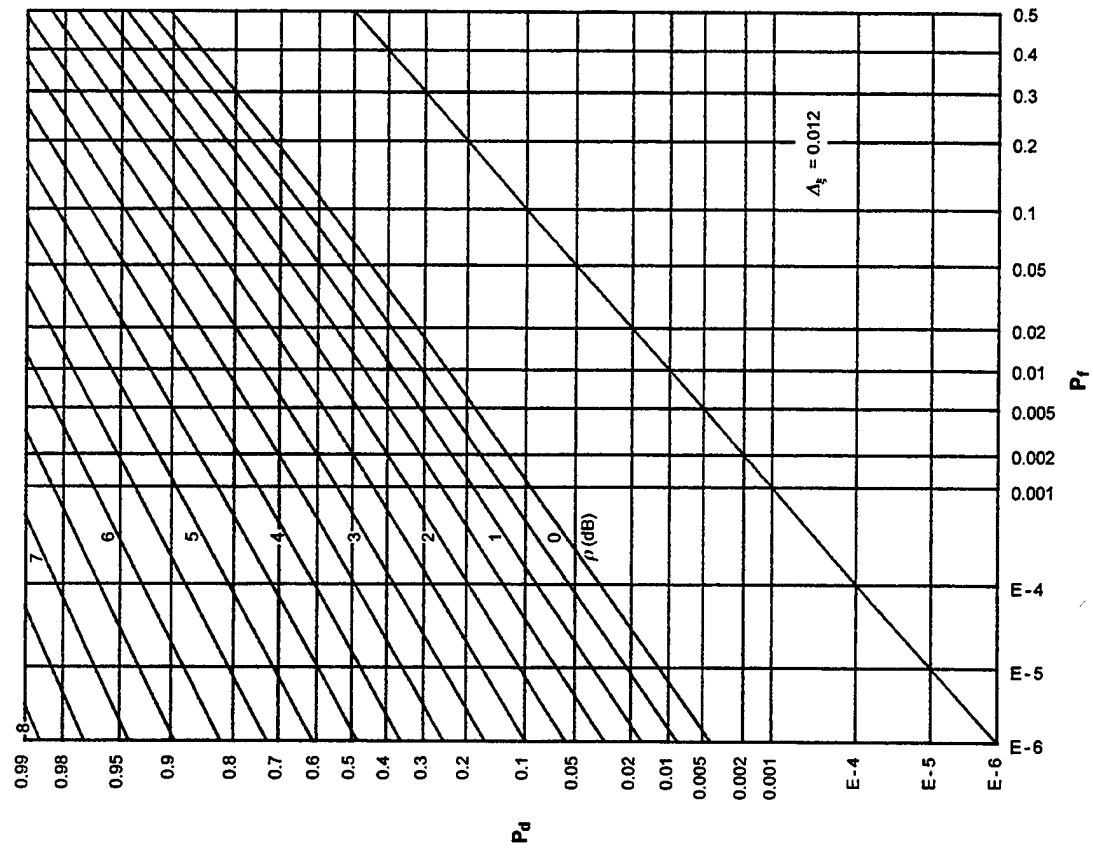

Figure E-24. ROCs for K = 1, N = 8, M = 16

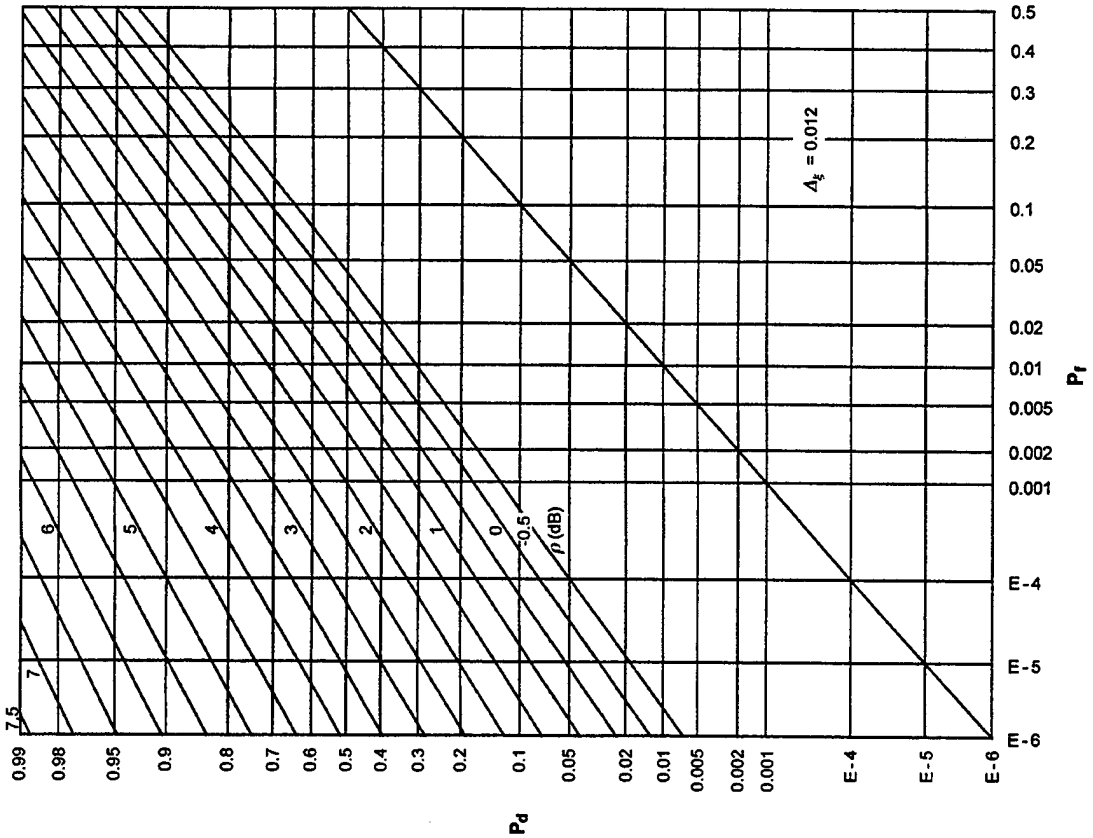

Figure E-23. ROCs for K = 1, N = 4, M = 16

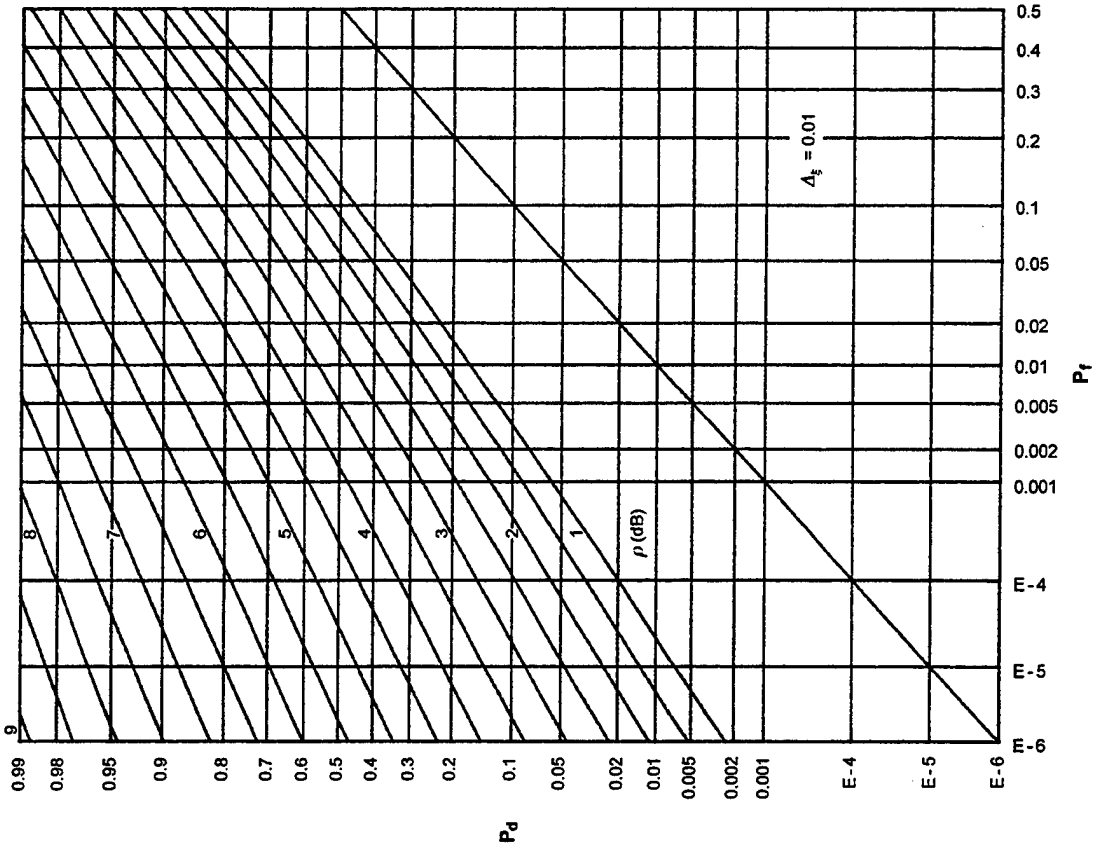

Figure E-26. ROCs for K = 1, N = 32, M = 16

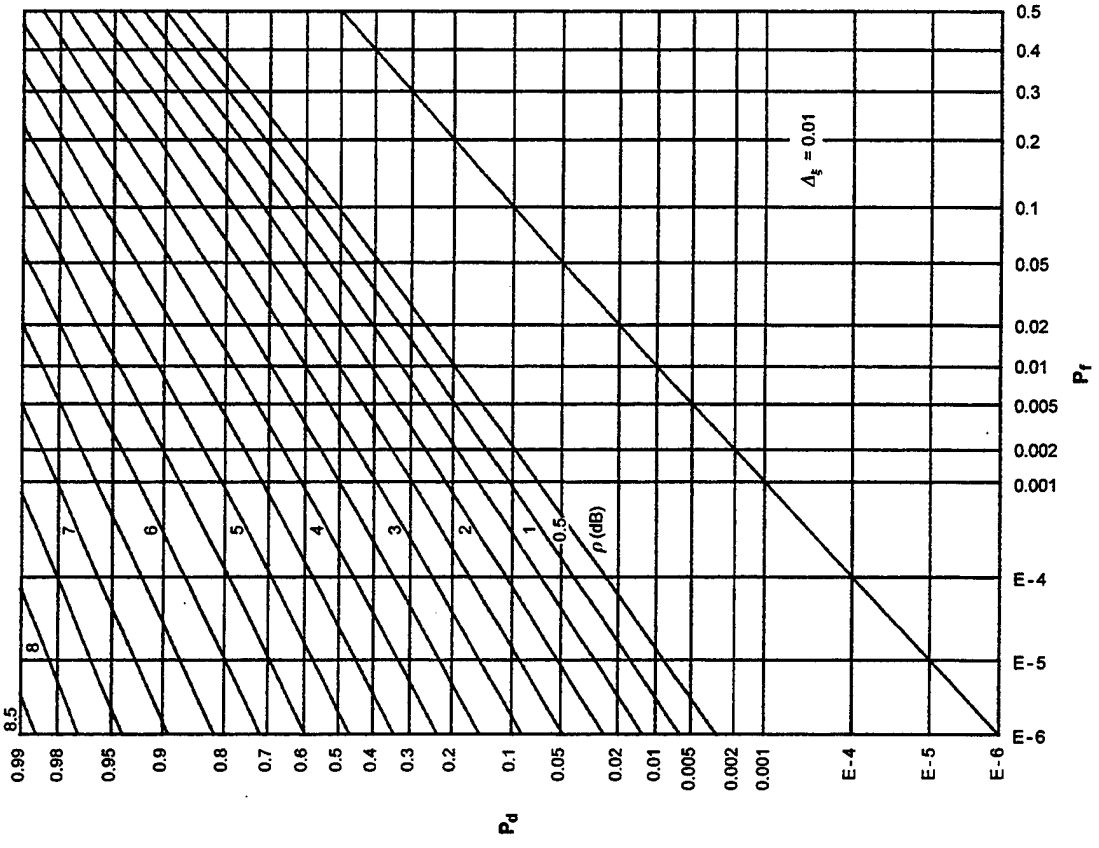

Figure E-25. ROCs for K = 1, N = 16, M = 16

APPENDIX F - ROCS FOR KM = 64, RANDOM GAUSSIAN SIGNAL

This appendix contains the ROCs for or-ing with pre- and post-averaging when the time-bandwidth product KM is fixed at 64; the possible combinations (from table 1) are repeated here:

K	M	N
64	1	1,2,4,8,16,32
32	2	
16	4	
8	8	
4	16	
2	32	
1	64	

For N = 1, only the product KM matters; the first plot in this appendix covers this special case, under the labeling K = 64, N = 1, M = 1. The other 5 values of N, along with the 7 possible combinations of K and M, yield 35 additional ROCs, for a total of 36 ROCs in this appendix.

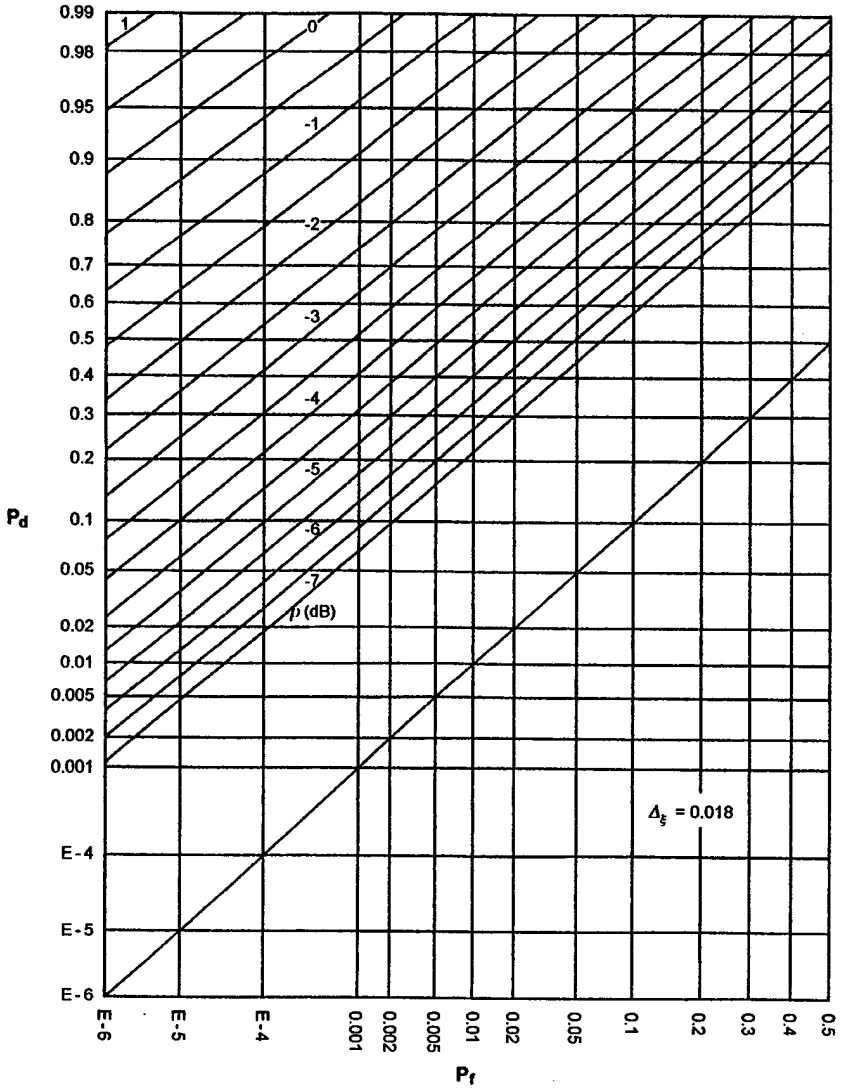

Figure F-1. ROCs for K = 64, N = 1, M = 1

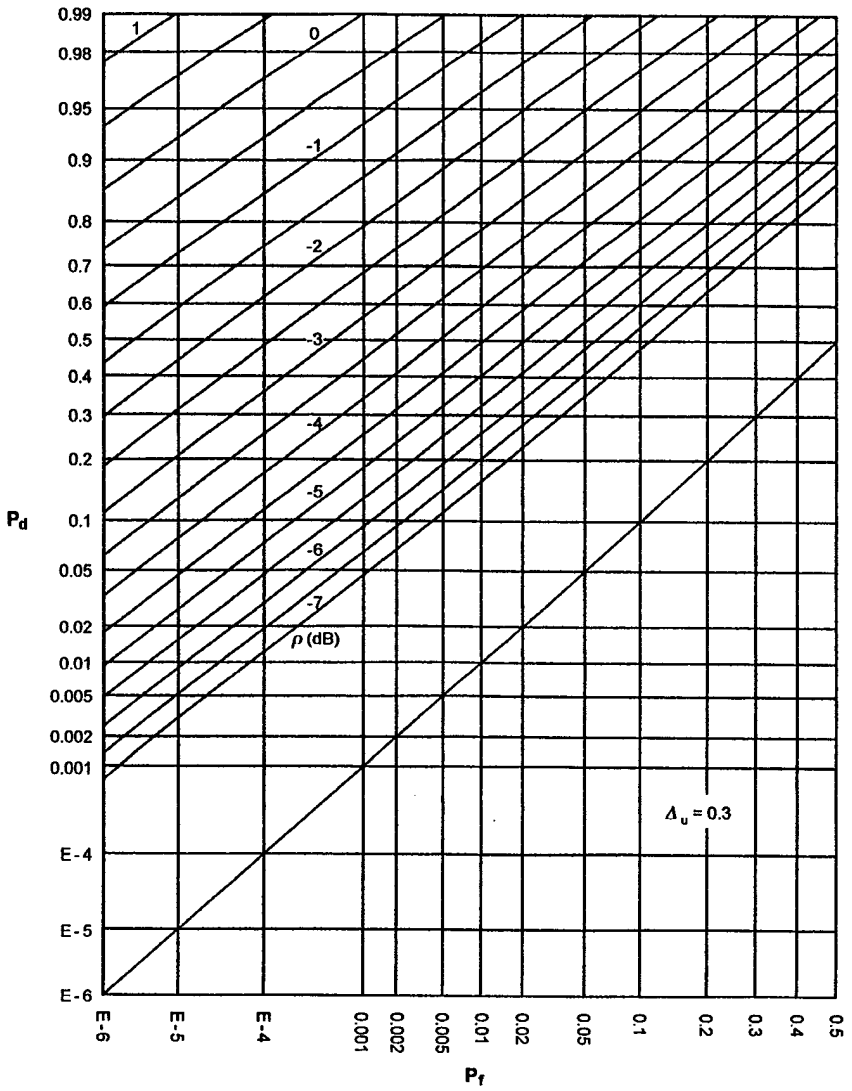

Figure F-2. ROCs for K = 64, N = 2, M = 1

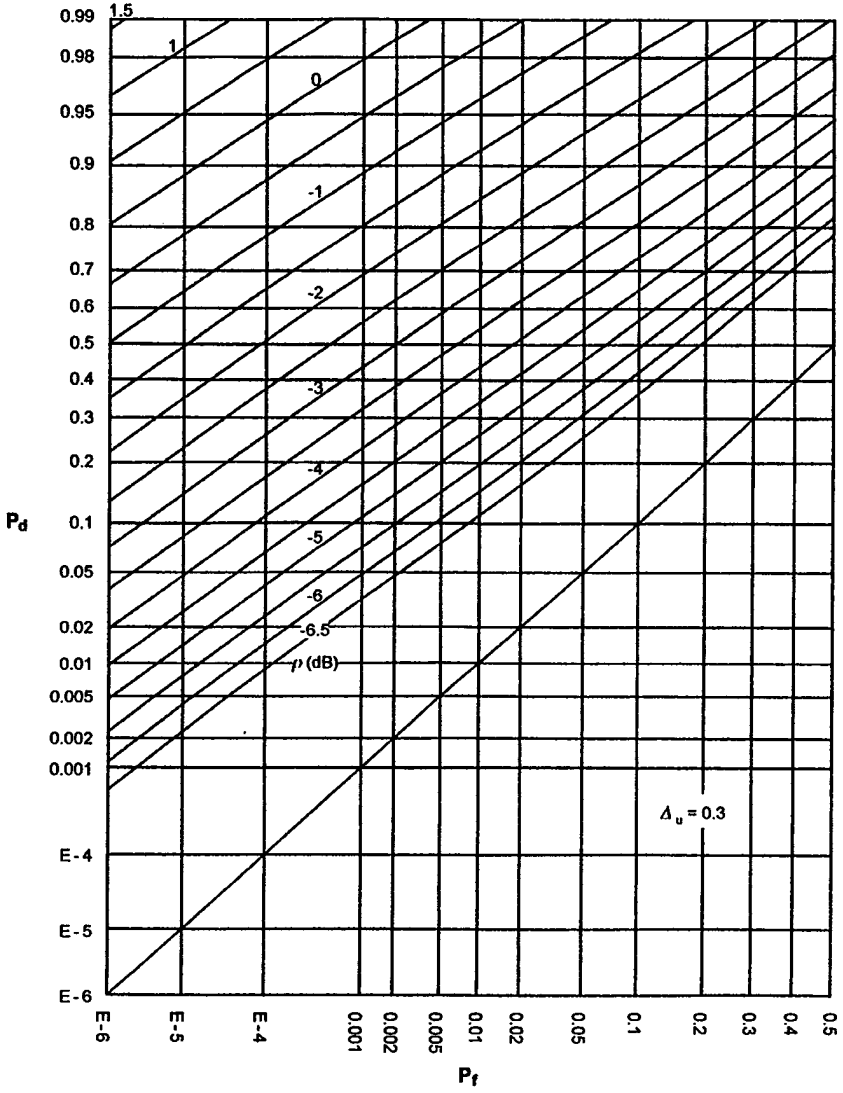

Figure F-3. ROCs for K = 64, N = 4, M = 1

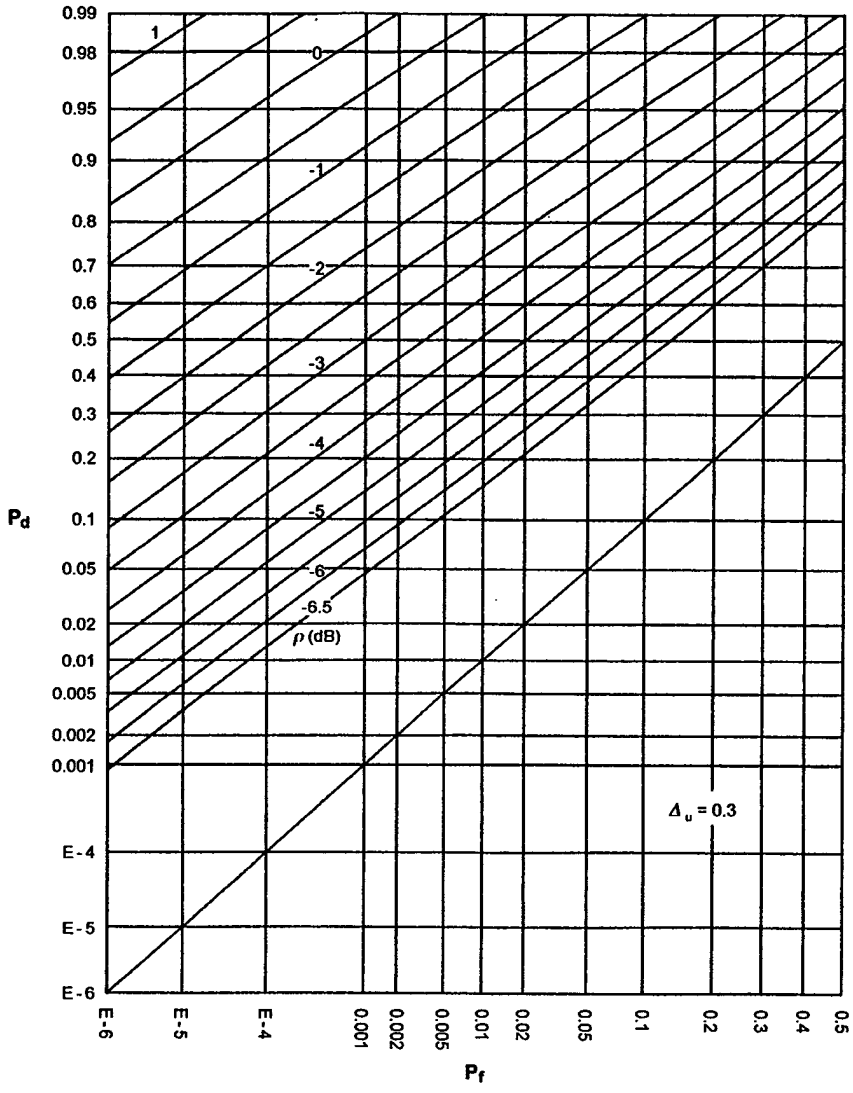

Figure F-4. ROCs for K = 64, N = 8, M = 1

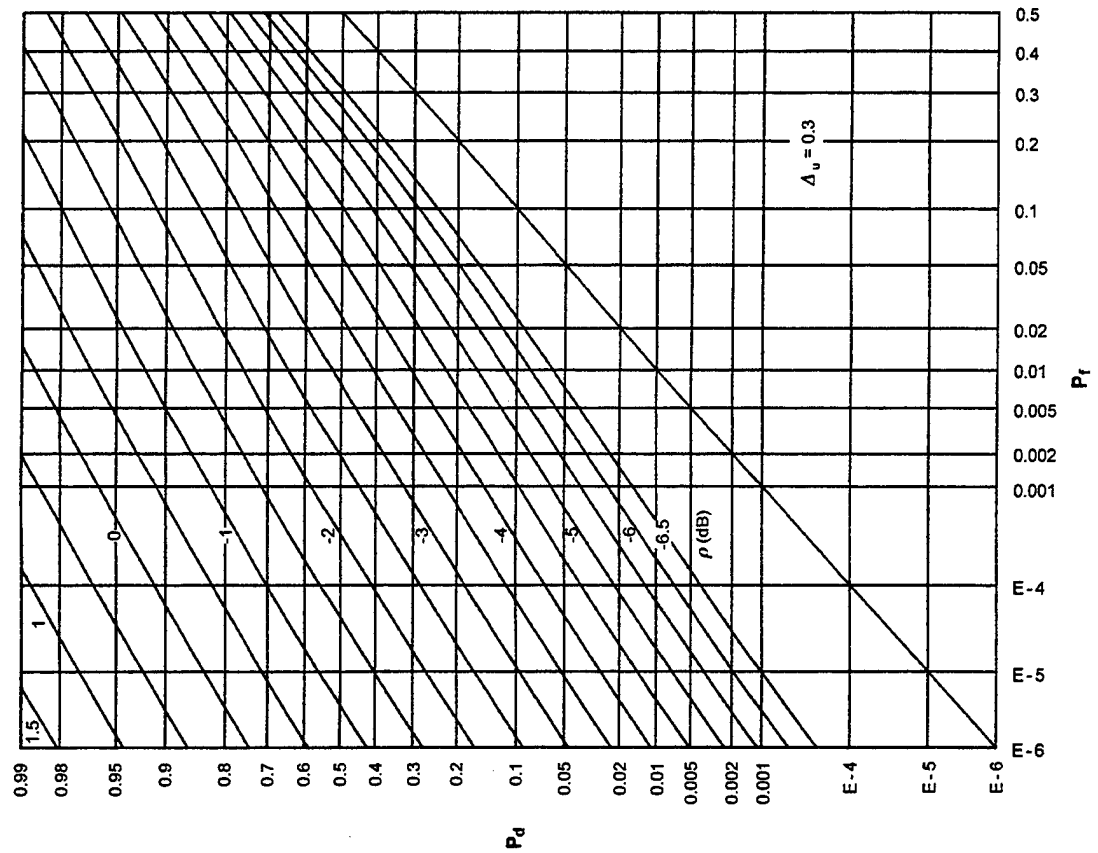

Figure F-6. ROCs for K = 64, N = 32, M = 1

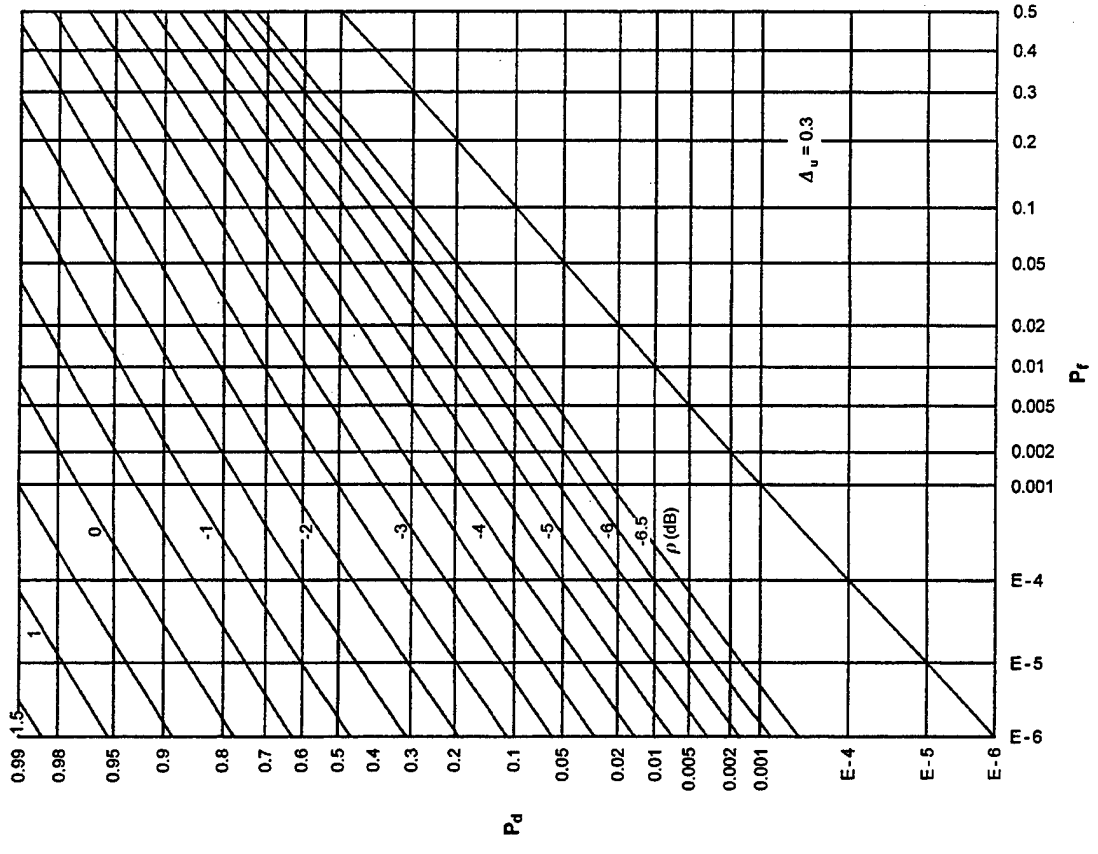

Figure F-5. ROCs for K = 64, N = 16, M = 1

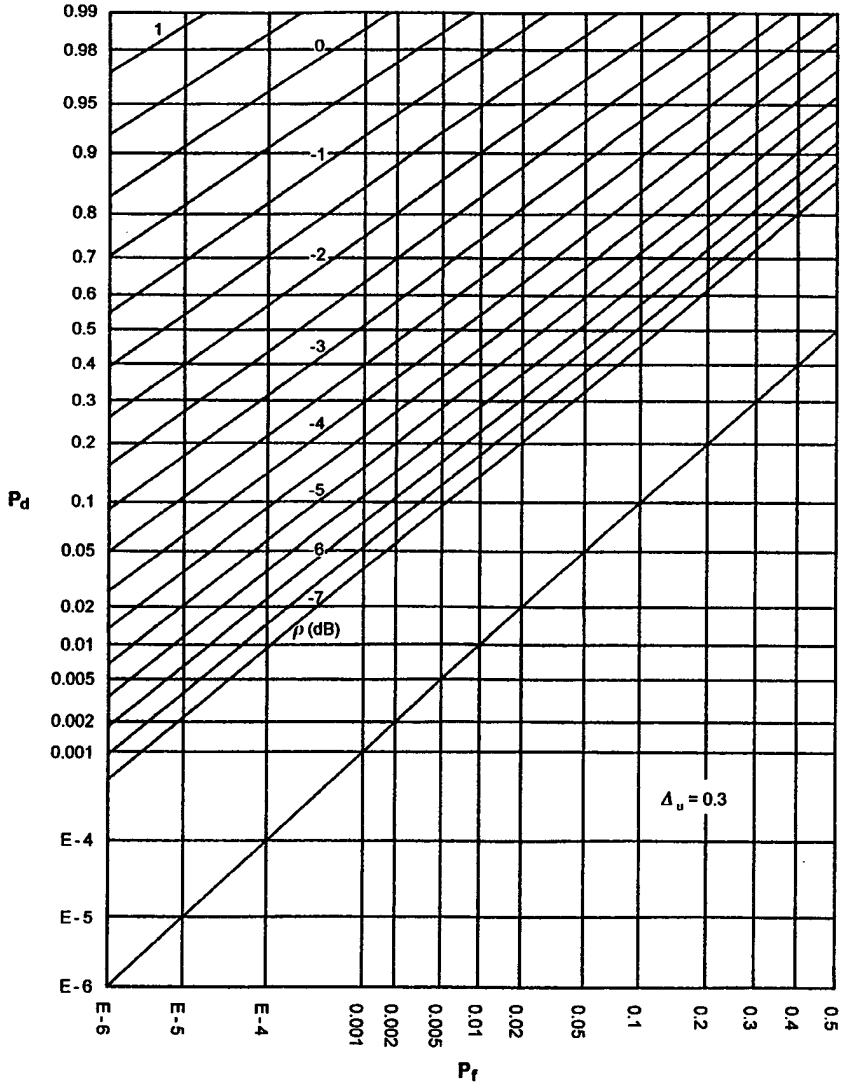

Figure F-7. ROCs for K = 32, N = 2, M = 2

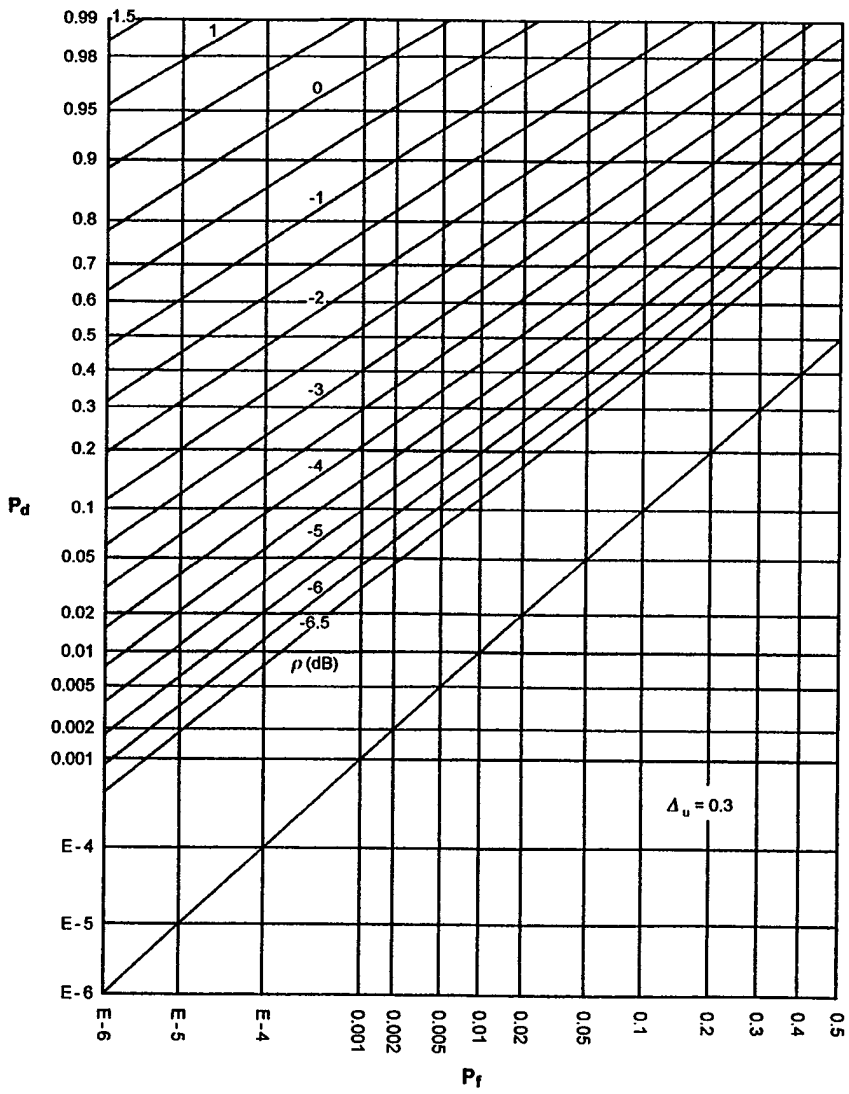

Figure F-8. ROCs for K = 32, N = 4, M = 2

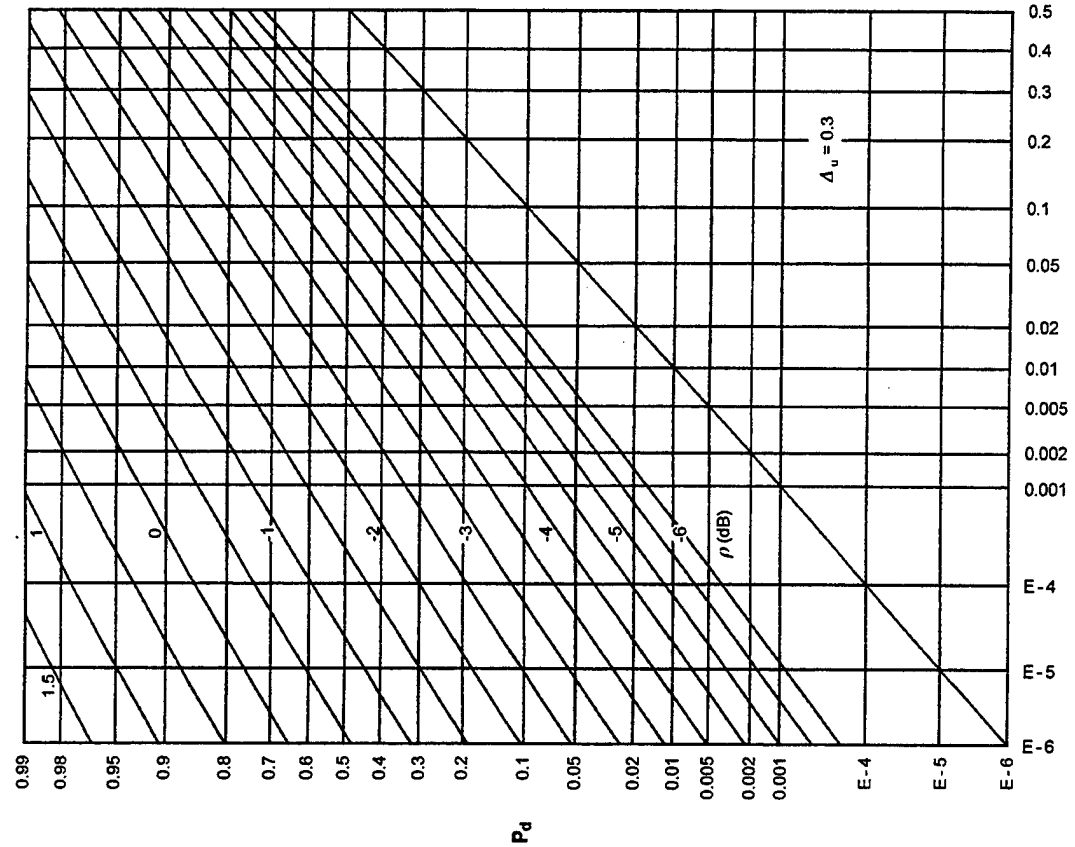

Figure F-10. ROCs for K = 32, N = 16, M = 2

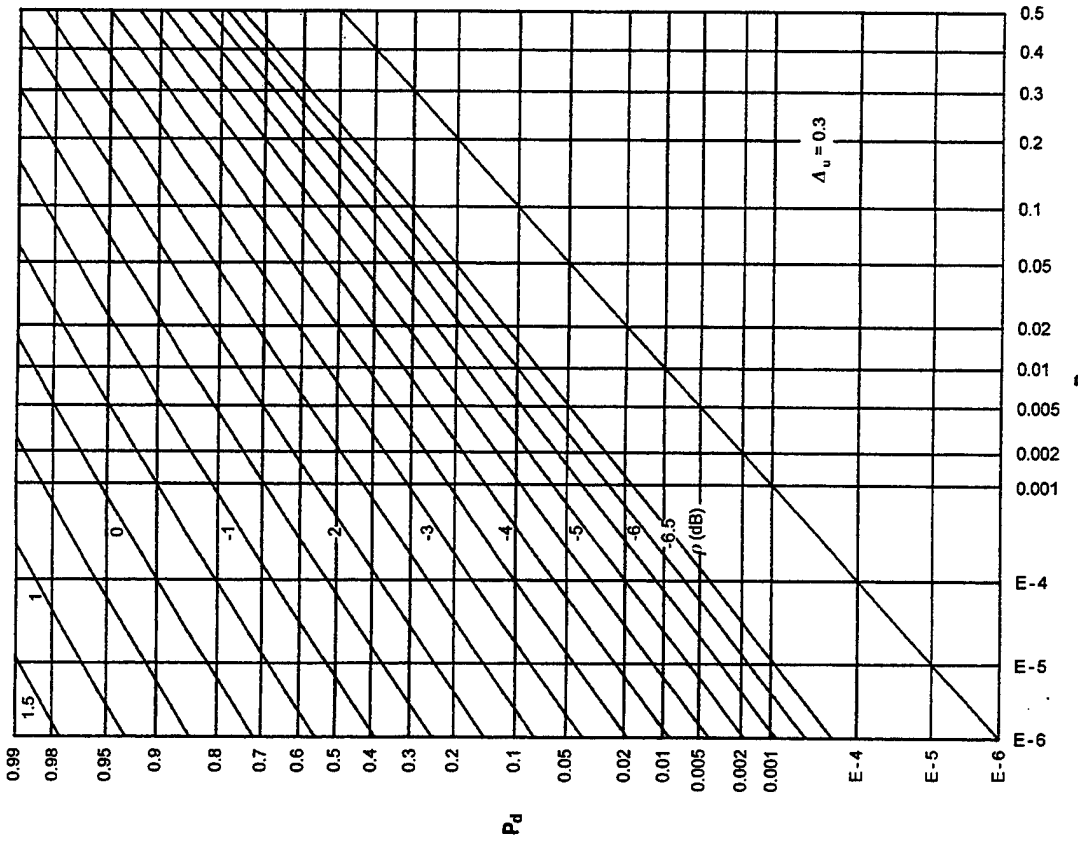

Figure F-9. ROCs for K = 32, N = 8, M = 2

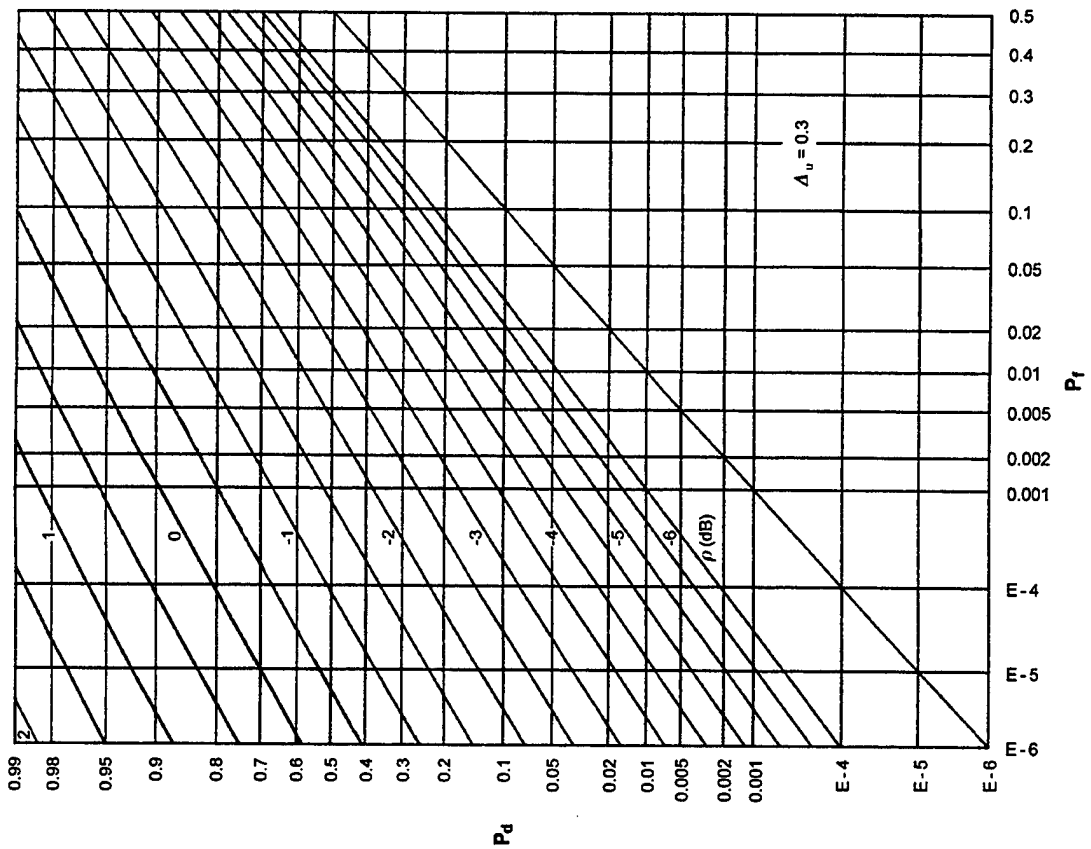

Figure F-12. ROCs for K = 16, N = 2, M = 4

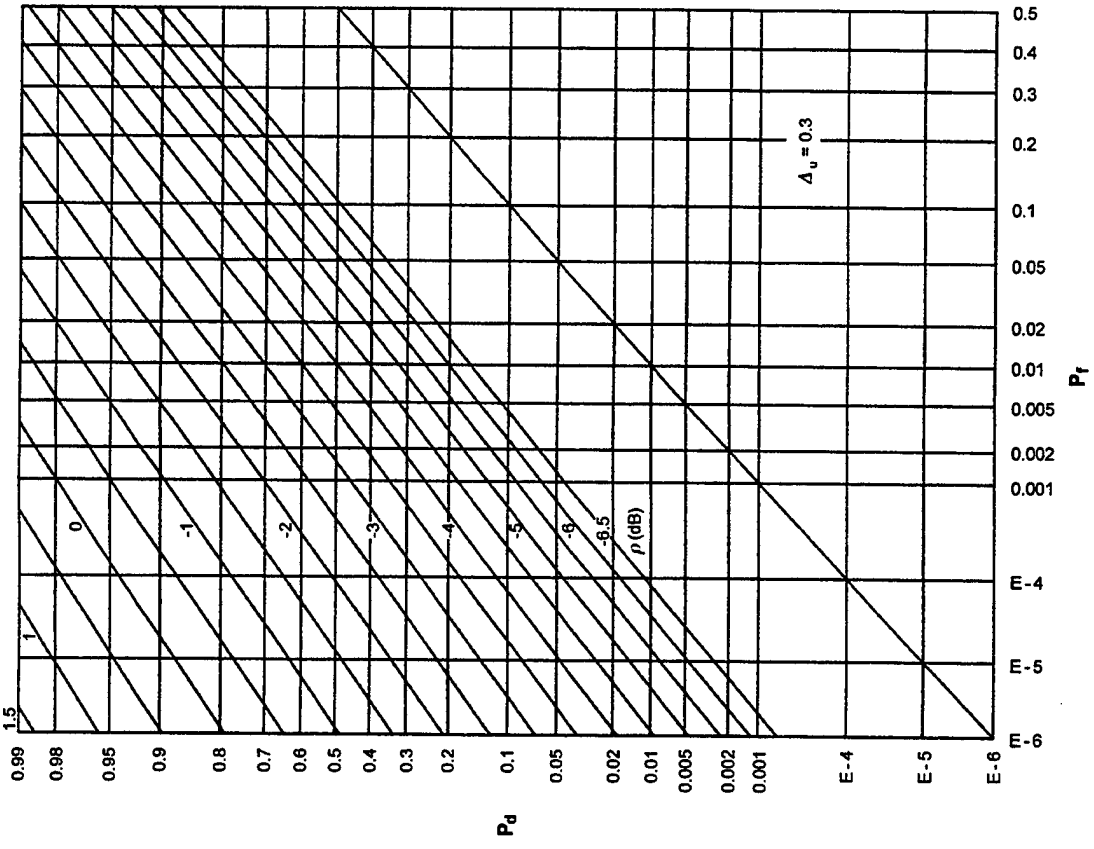

Figure F-11. ROCs for K = 32, N = 32, M = 2

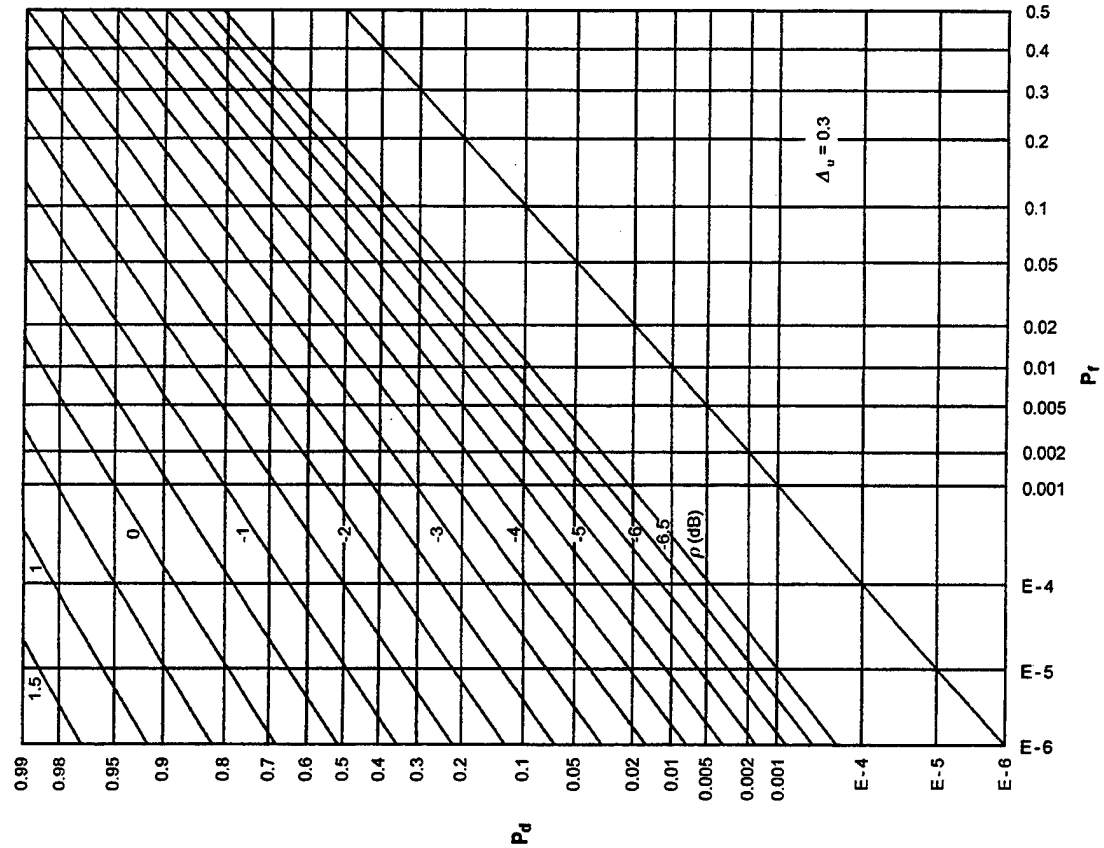

Figure F-14. ROCs for K = 16, N = 8, M = 4

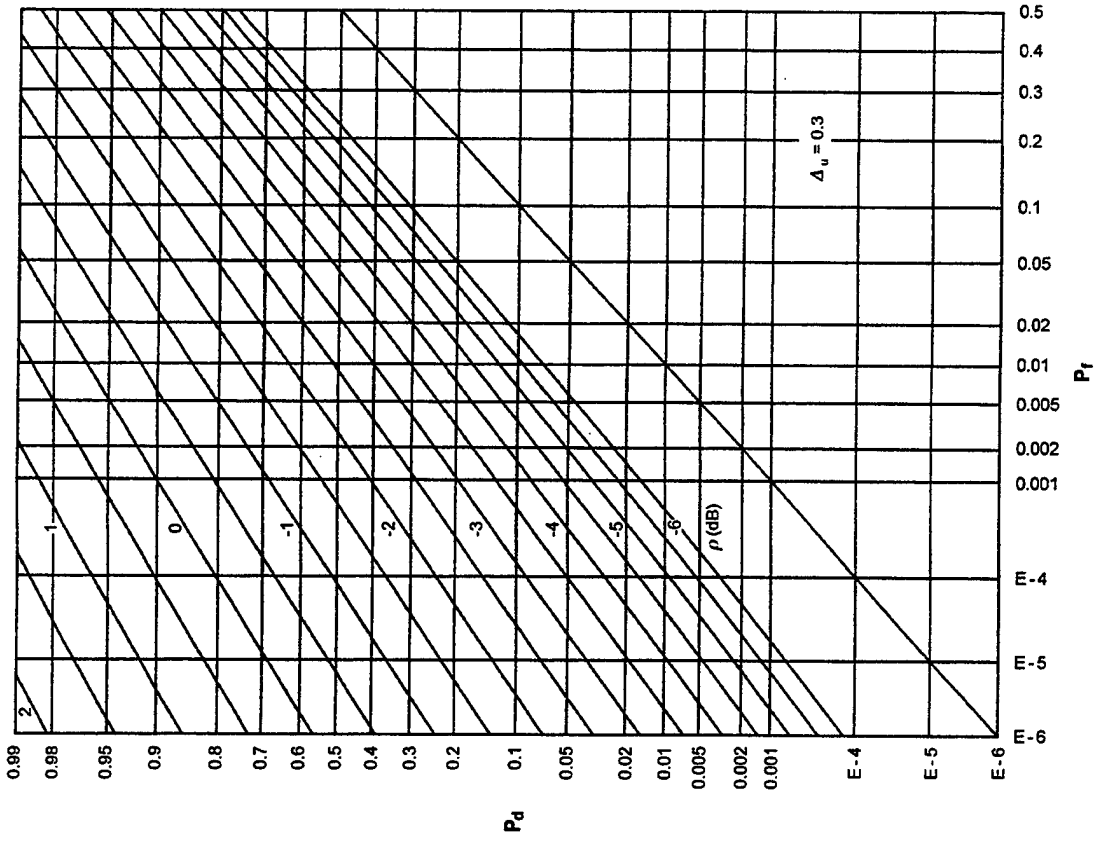

Figure F-13. ROCs for K = 16, N = 4, M = 4

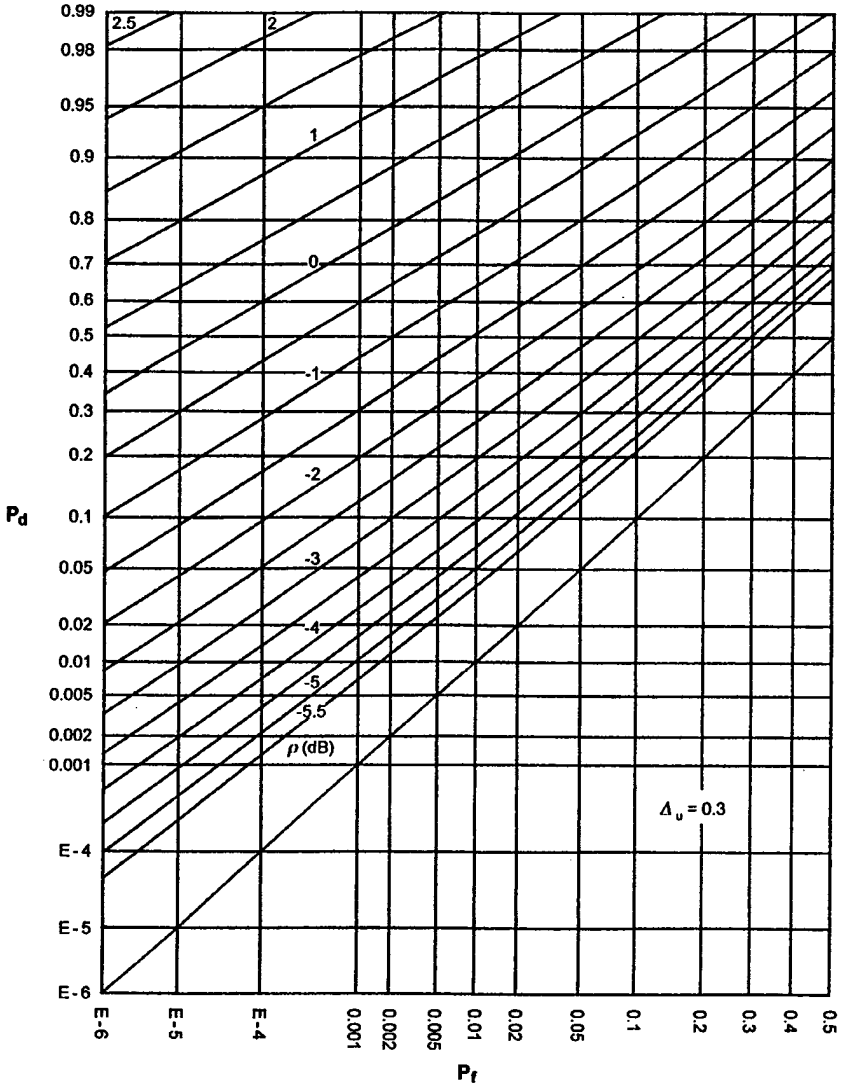

Figure F-15. ROCs for K = 16, N = 16, M = 4

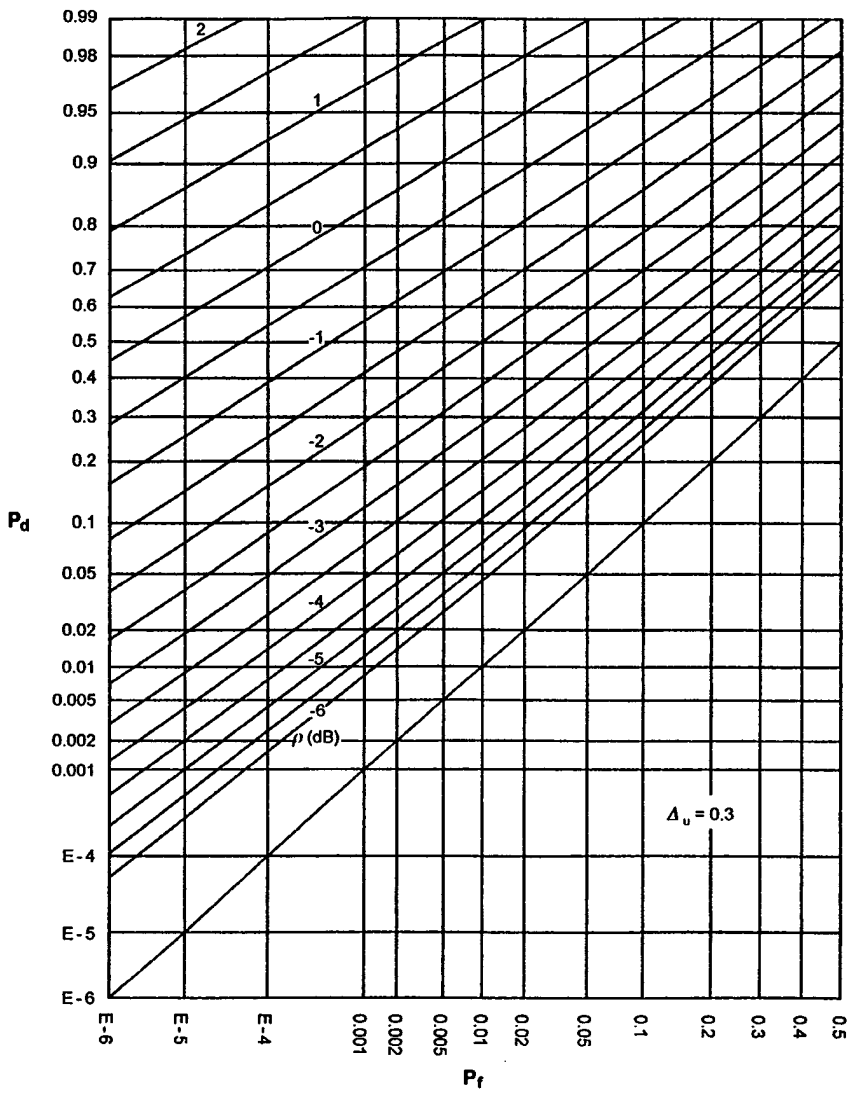

Figure F-16. ROCs for K = 16, N = 32, M = 4

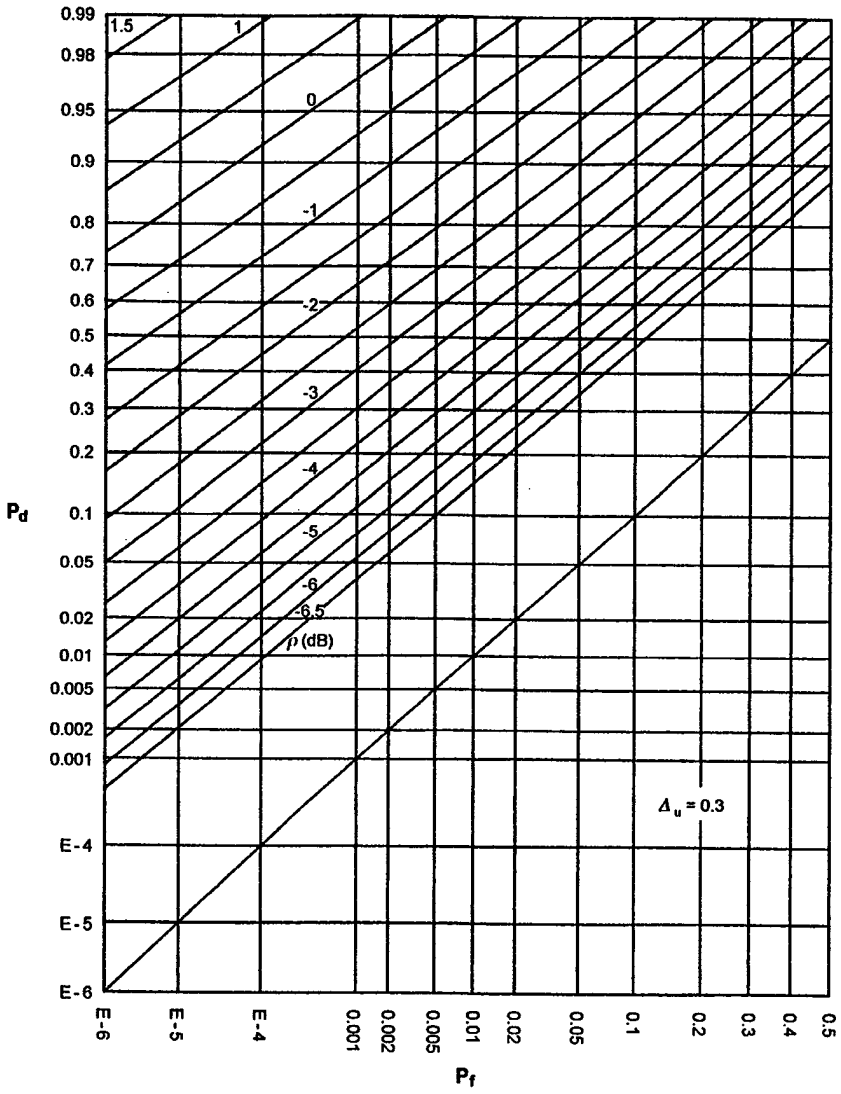

Figure F-17. ROCs for K = 8, N = 2, M = 8

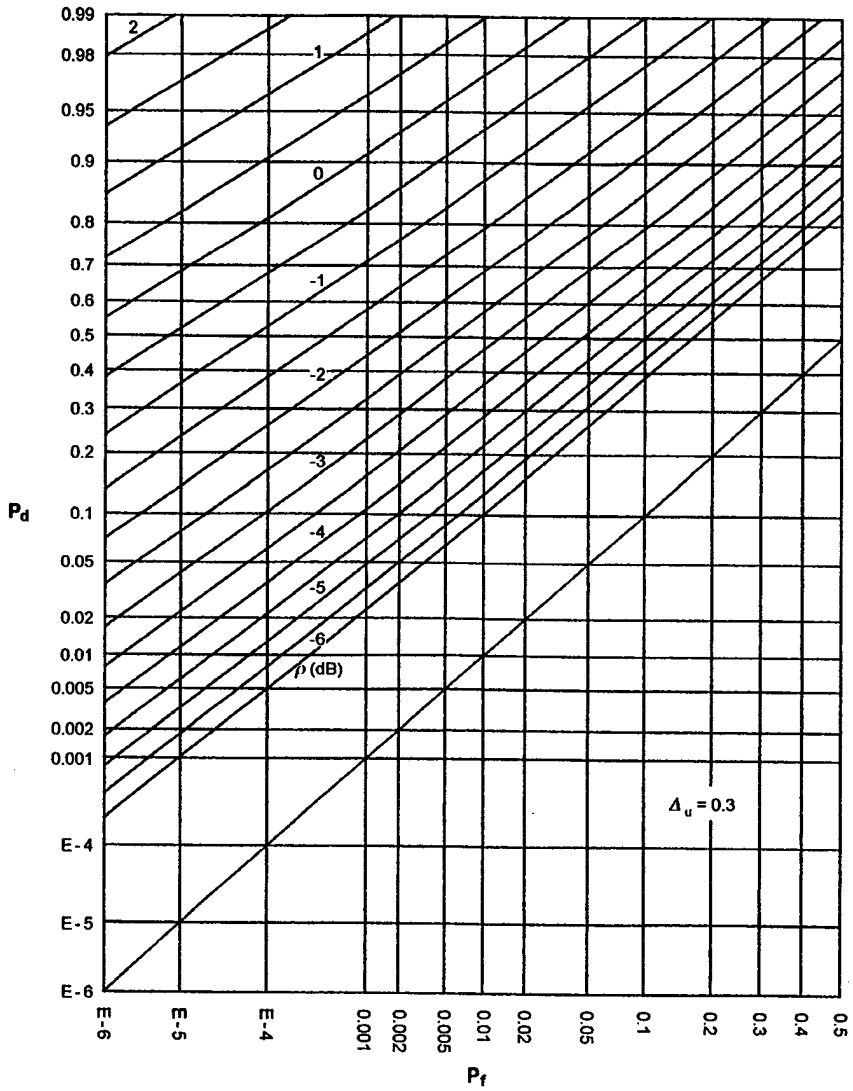

Figure F-18. ROCs for K = 8, N = 4, M = 8

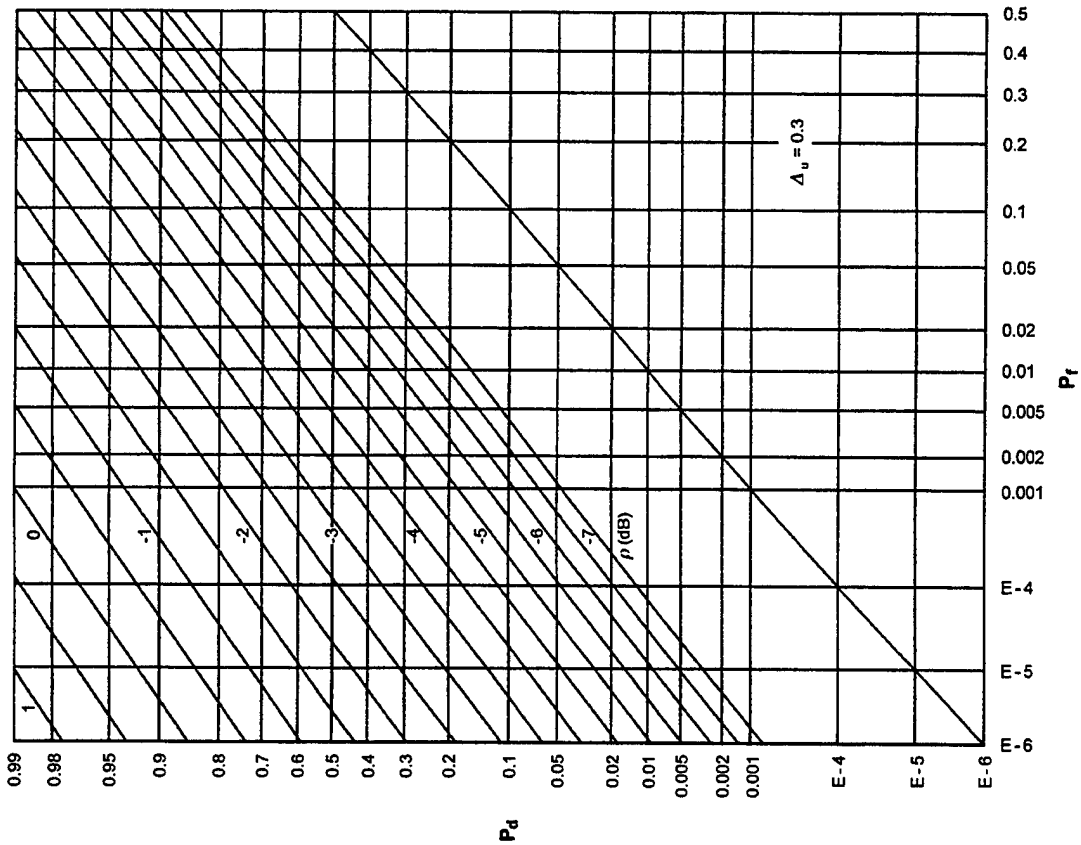

Figure F-20. ROCs for K = 8, N = 16, M = 8

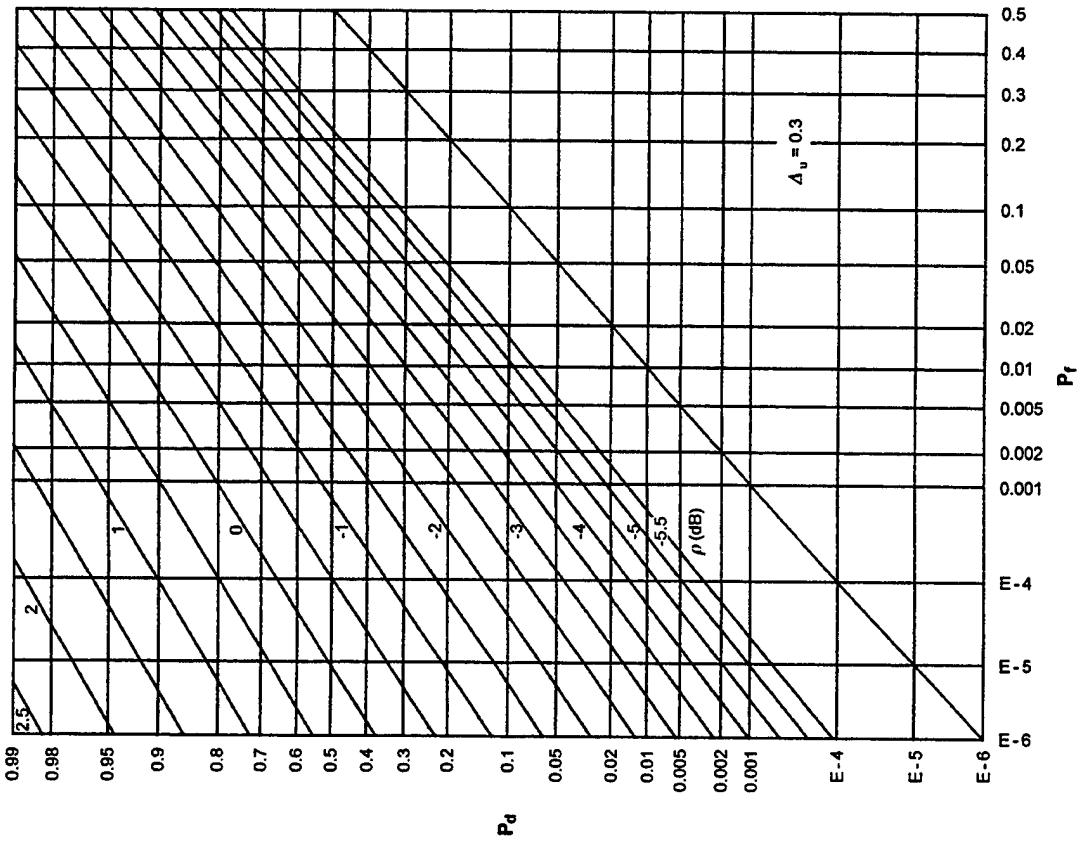

Figure F-19. ROCs for K = 8, N = 8, M = 8

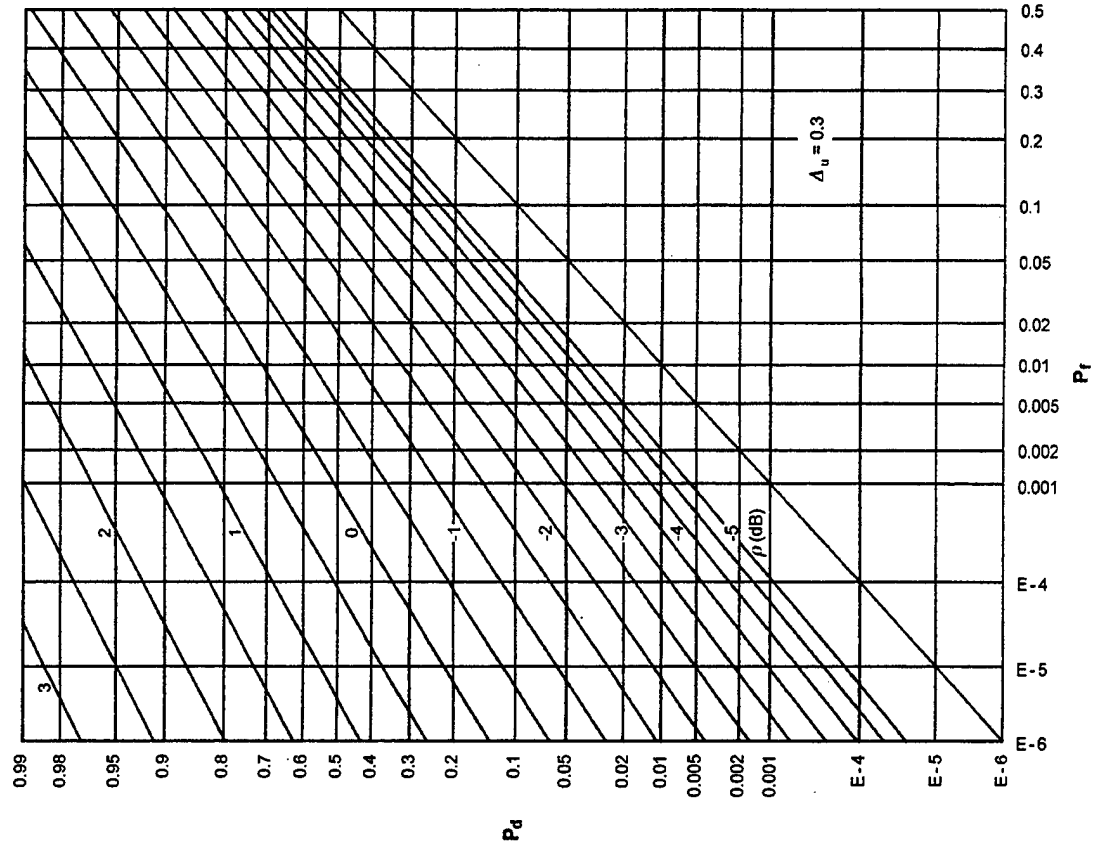

Figure F-22. ROCs for K = 4, N = 2, M = 16

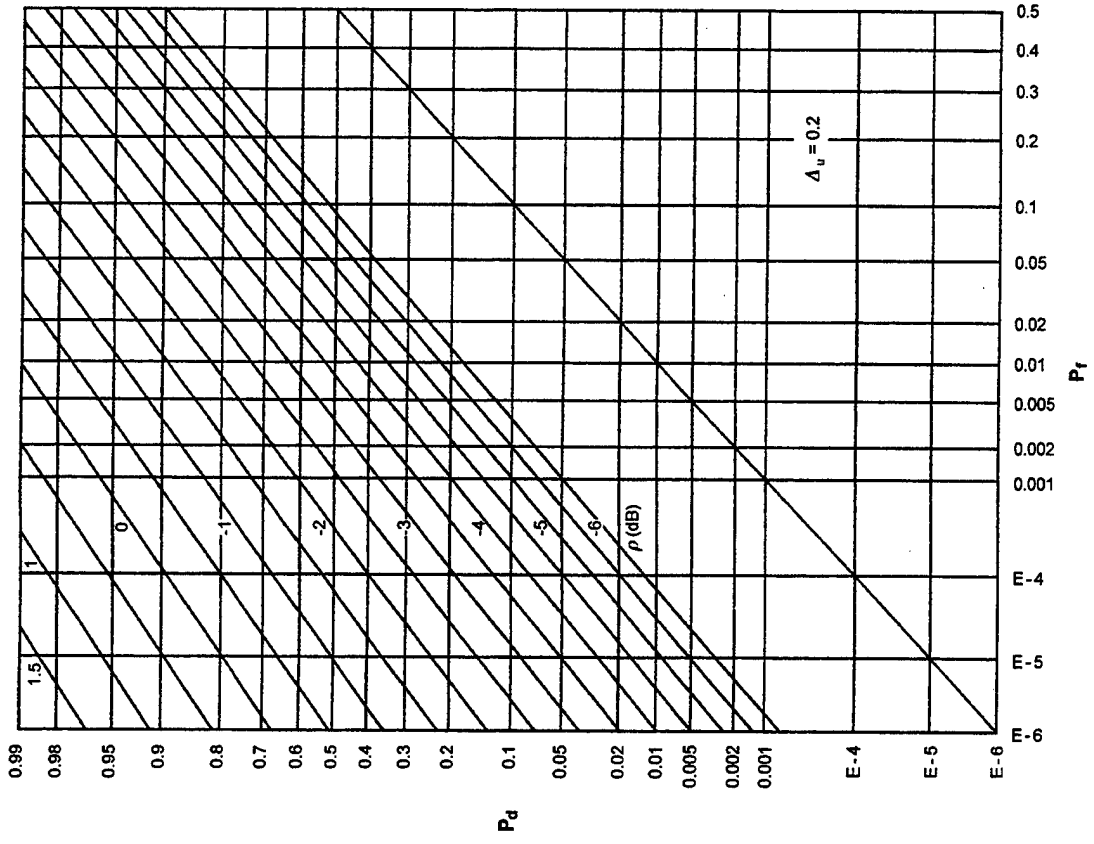

Figure F-21. ROCs for K = 8, N = 32, M = 8

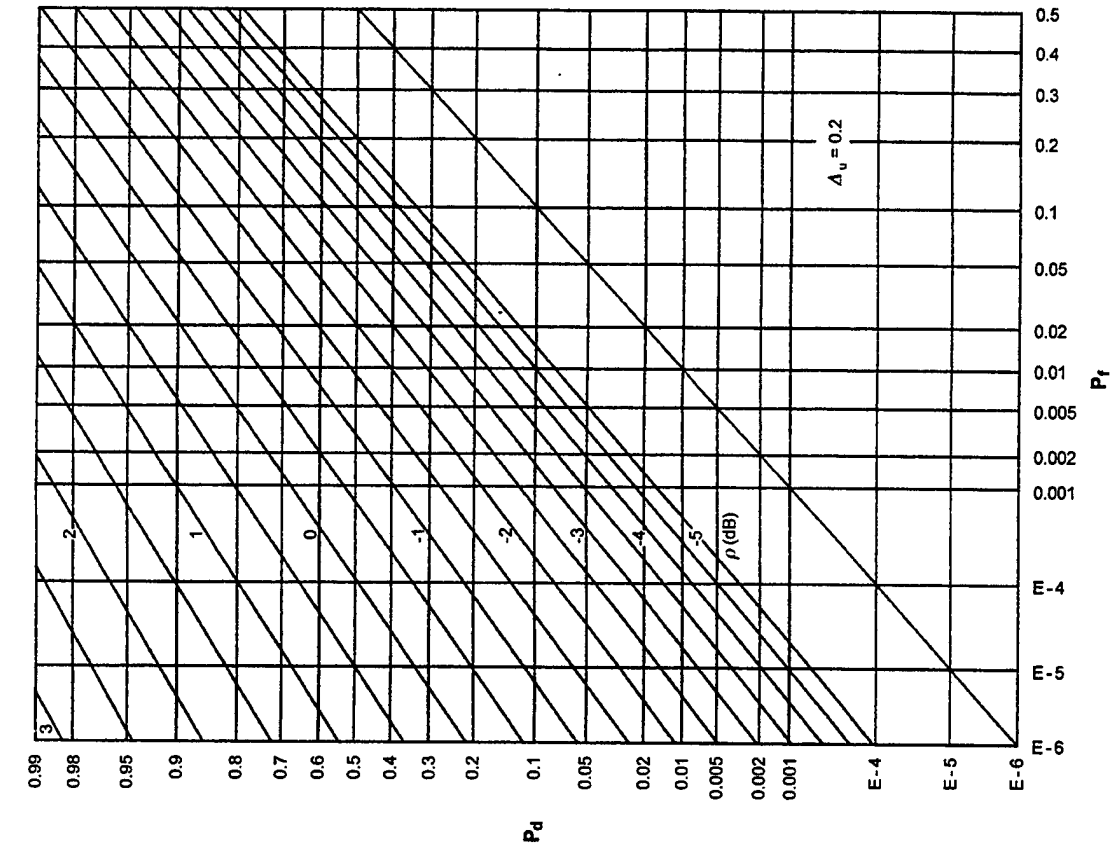

Figure F-24. ROCs for K = 4, N = 8, M = 16

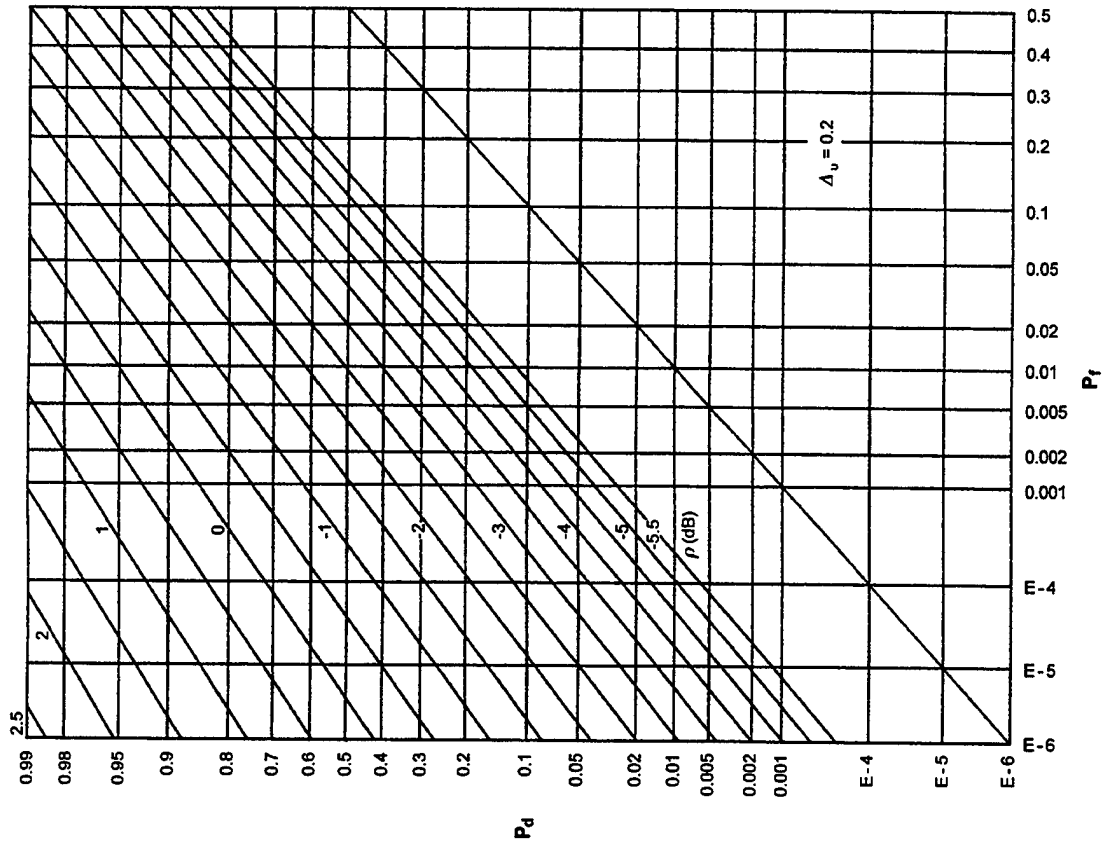

Figure F-23. ROCs for K = 4, N = 4, M = 16

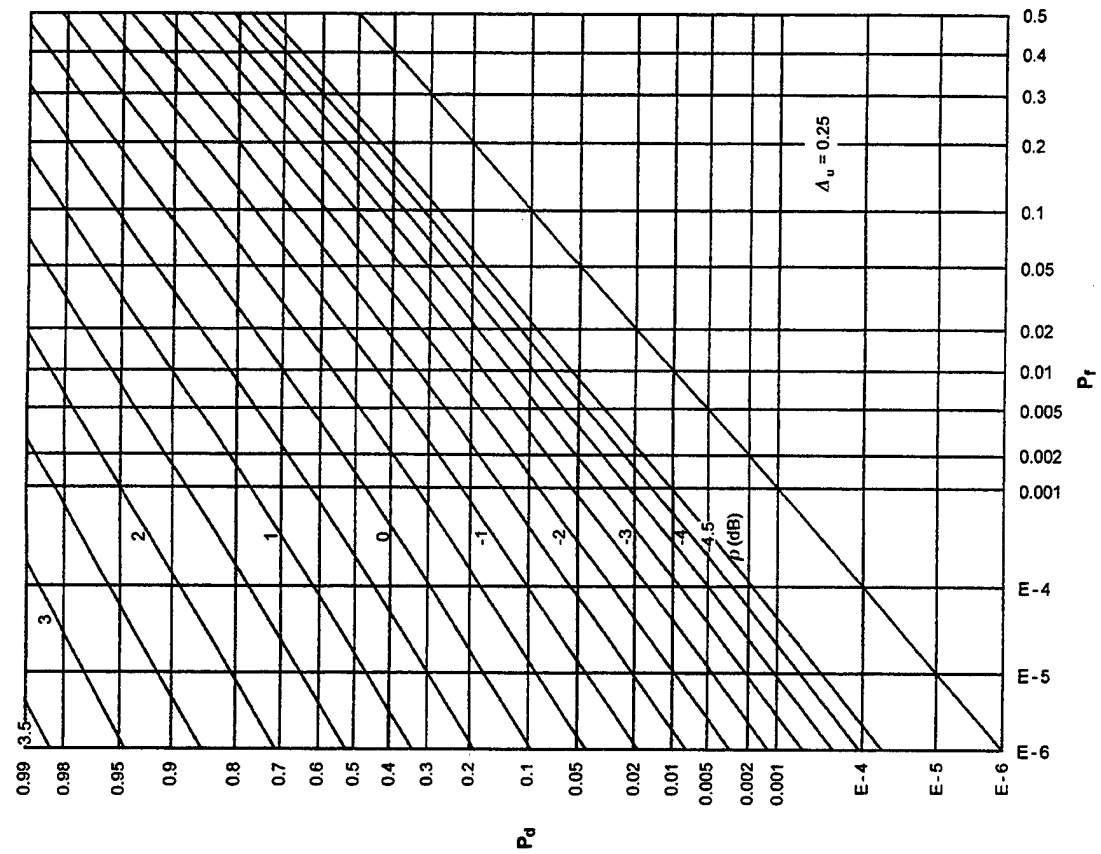

Figure F-26. ROCs for K = 4, N = 32, M = 16

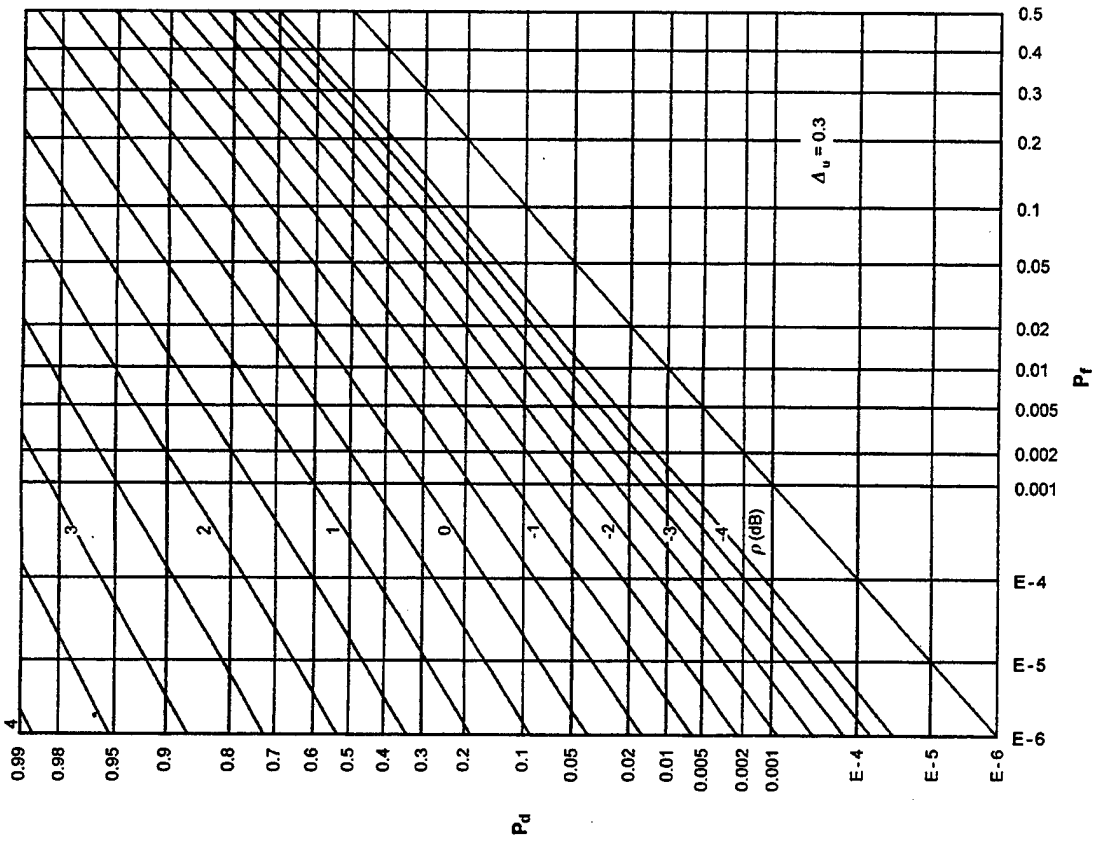

Figure F-25. ROCs for K = 4, N = 16, M = 16

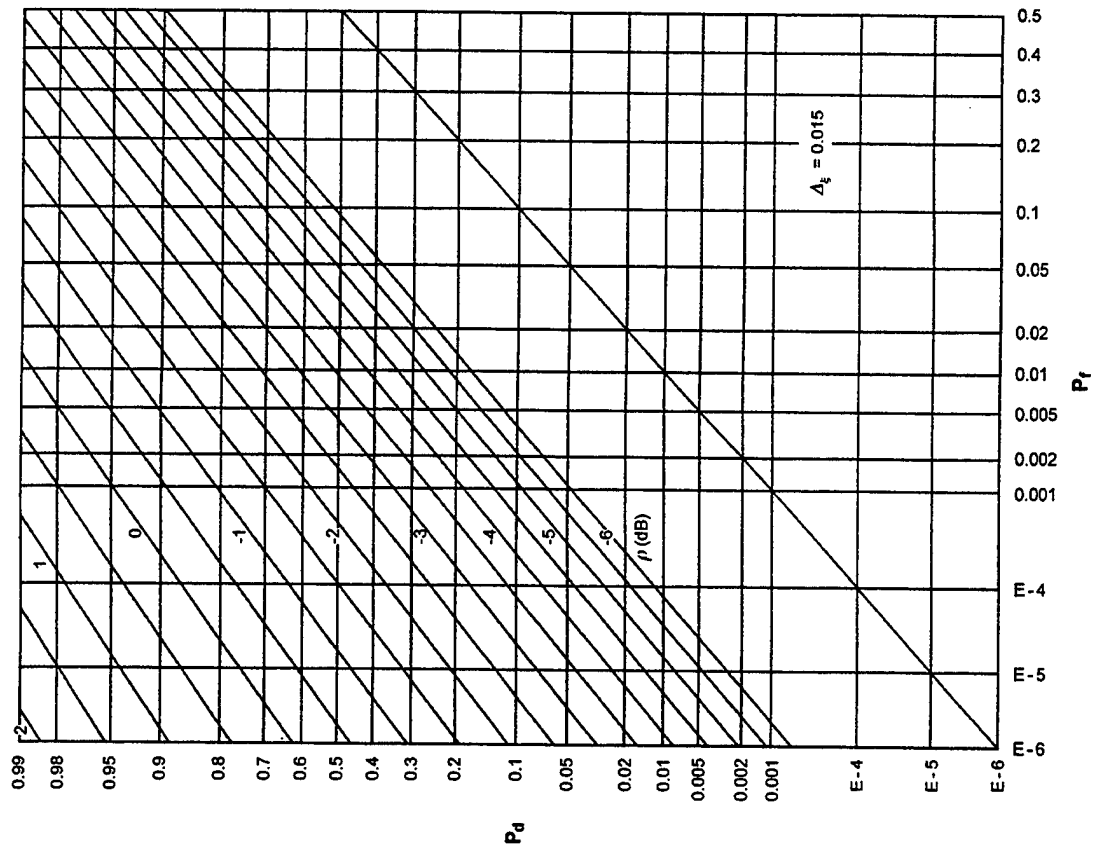

Figure F-27. ROCs for K = 2, N = 2, M = 32

Figure F-28. ROCs for K = 2, N = 4, M = 32

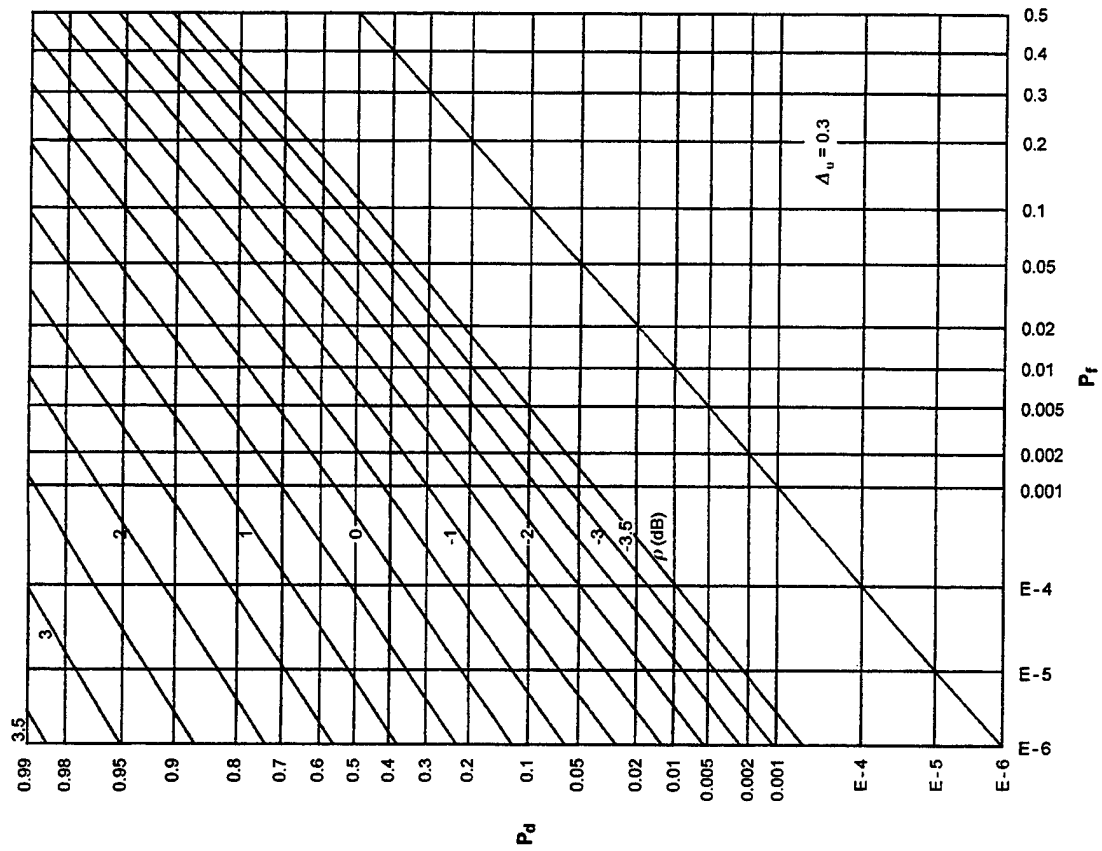

Figure F-30. ROCs for K = 2, N = 16, M = 32

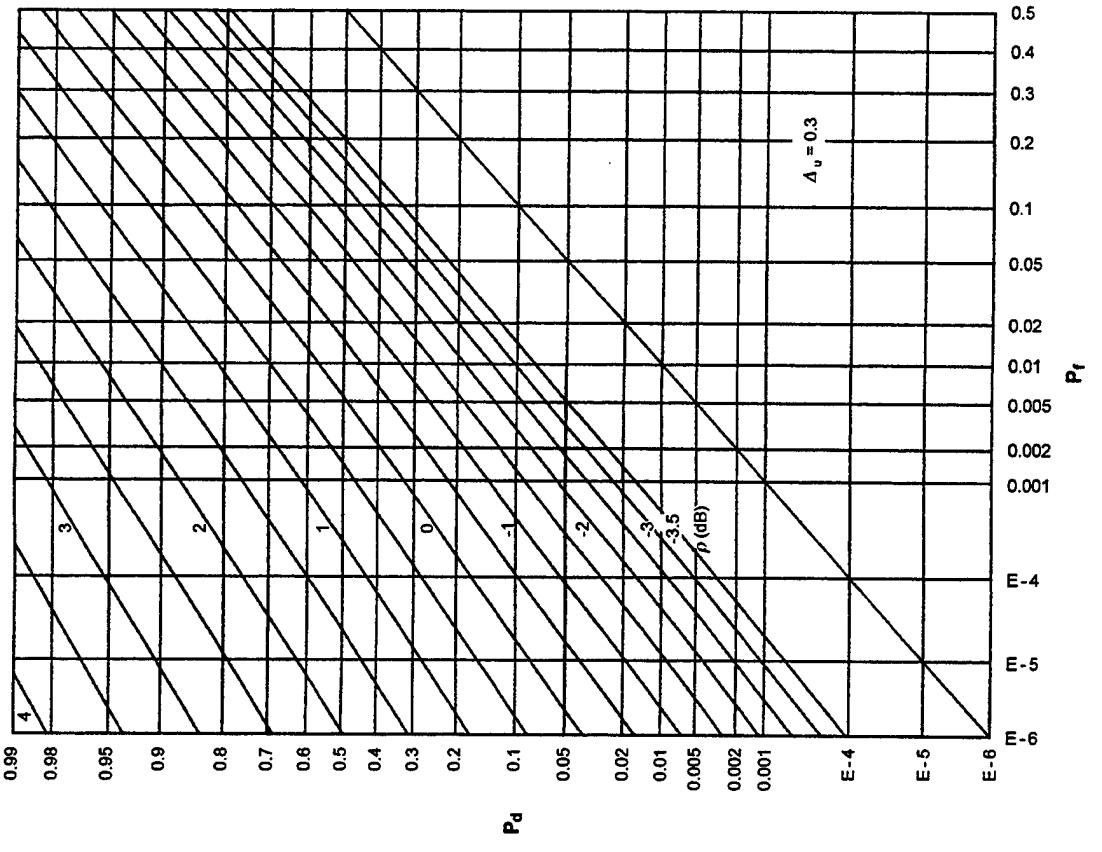

Figure F-29. ROCs for K = 2, N = 8, M = 32

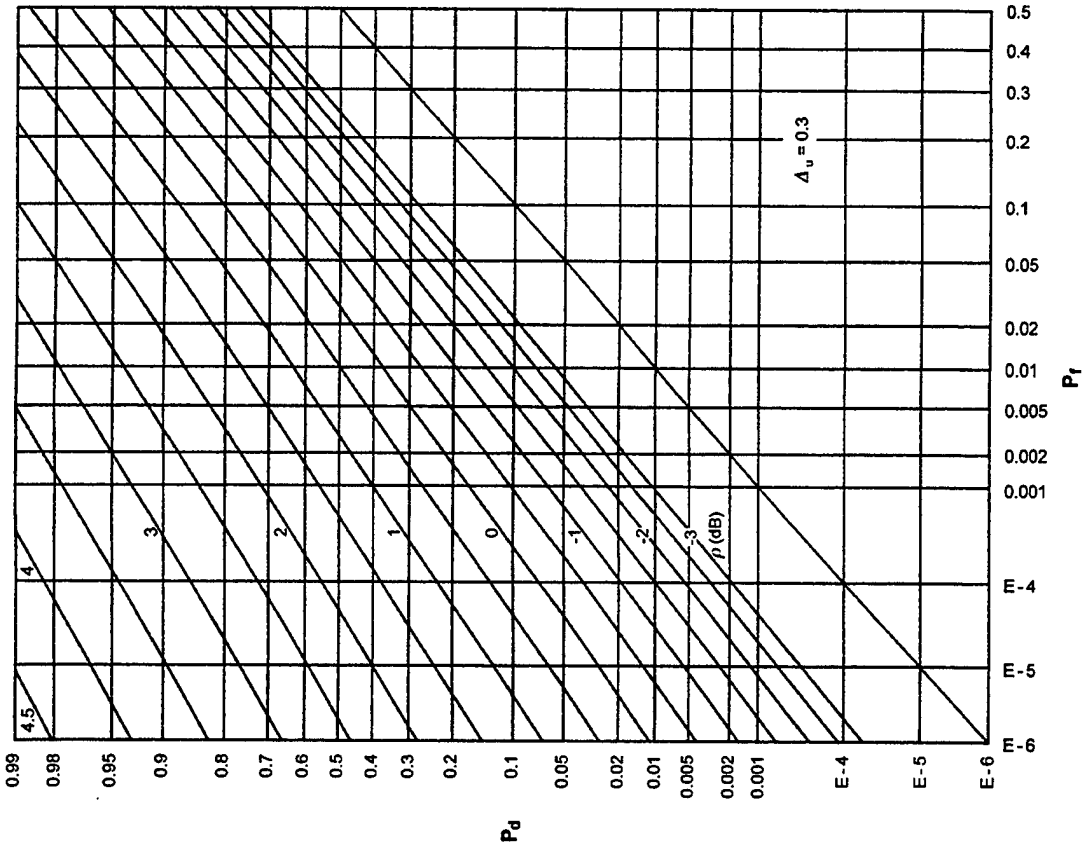

Figure F-32. ROCs for K = 1, N = 2, M = 64

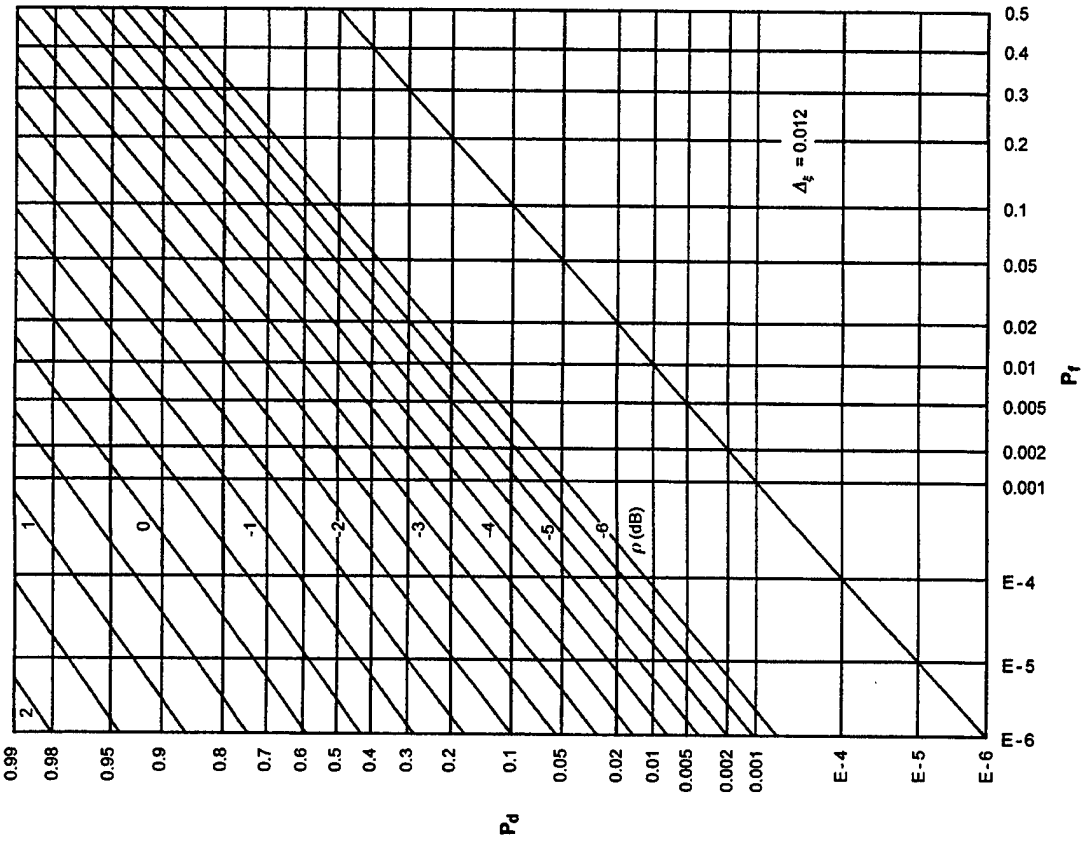

Figure F-31. ROCs for K = 2, N = 32, M = 32

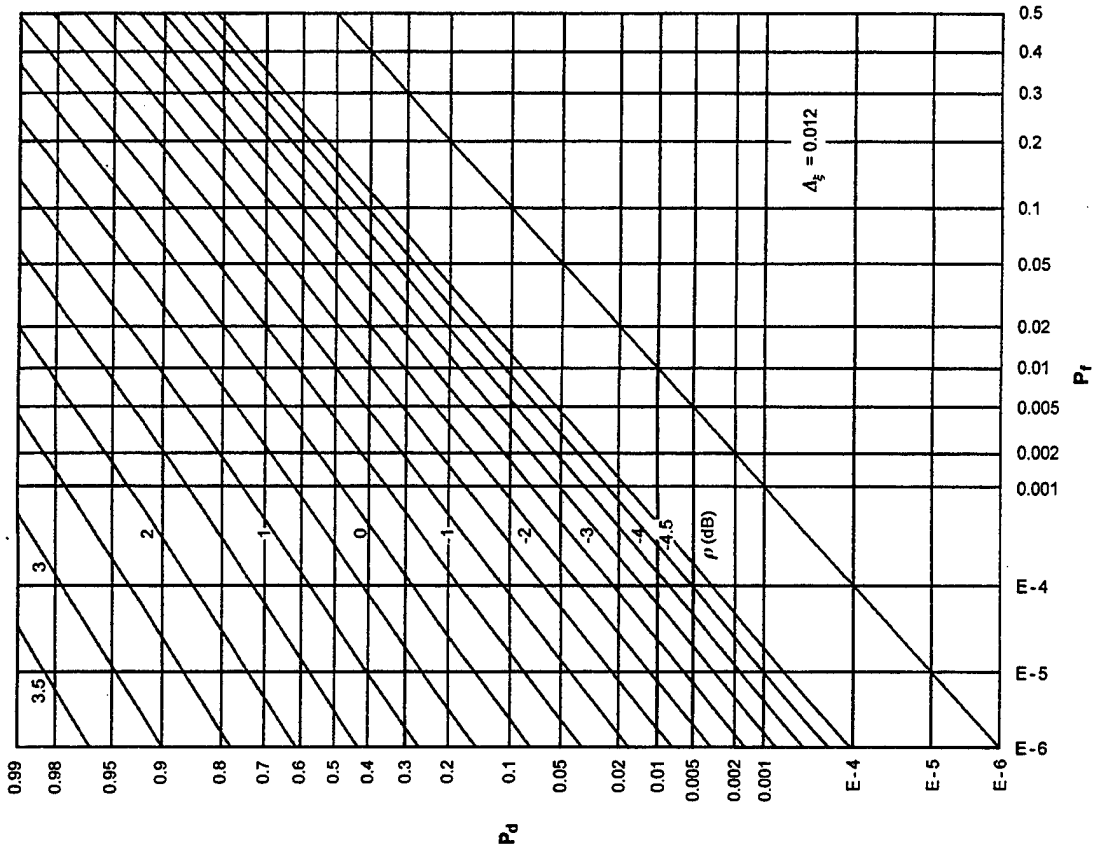

Figure F-34. ROCs for K = 1, N = 8, M = 64

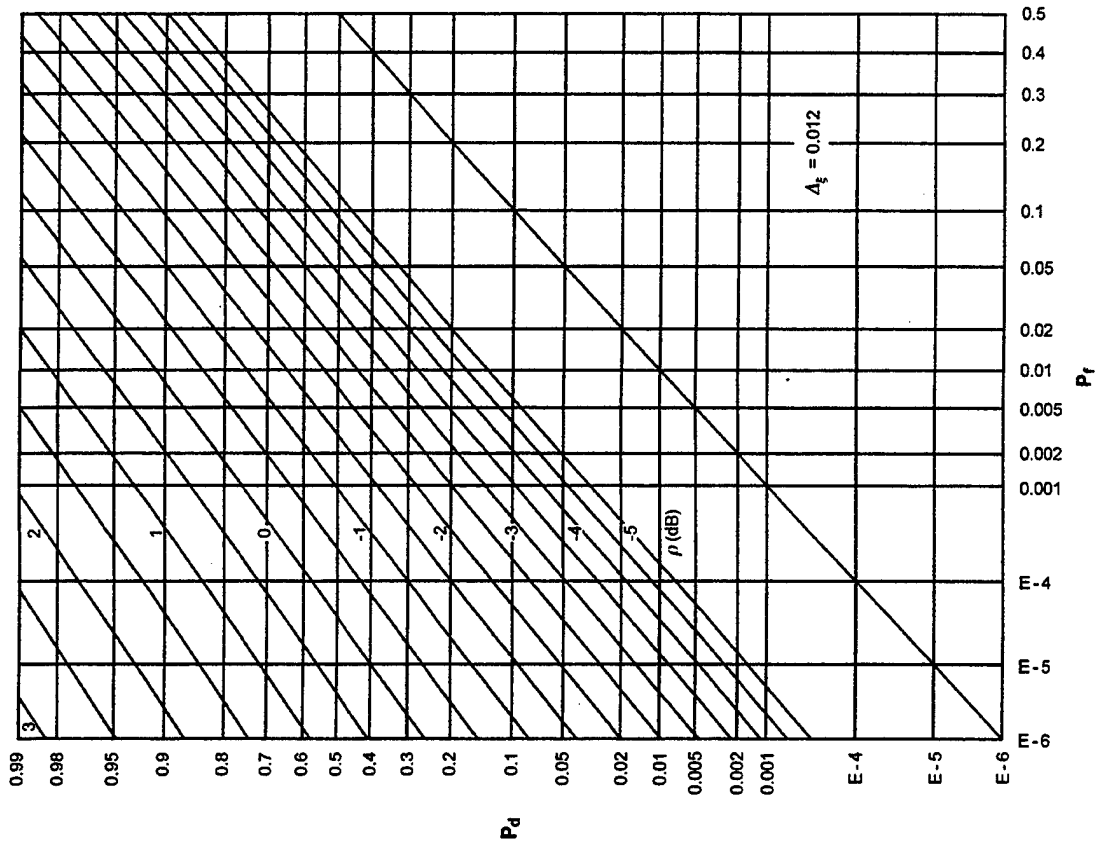

Figure F-33. ROCs for K = 1, N = 4, M = 64

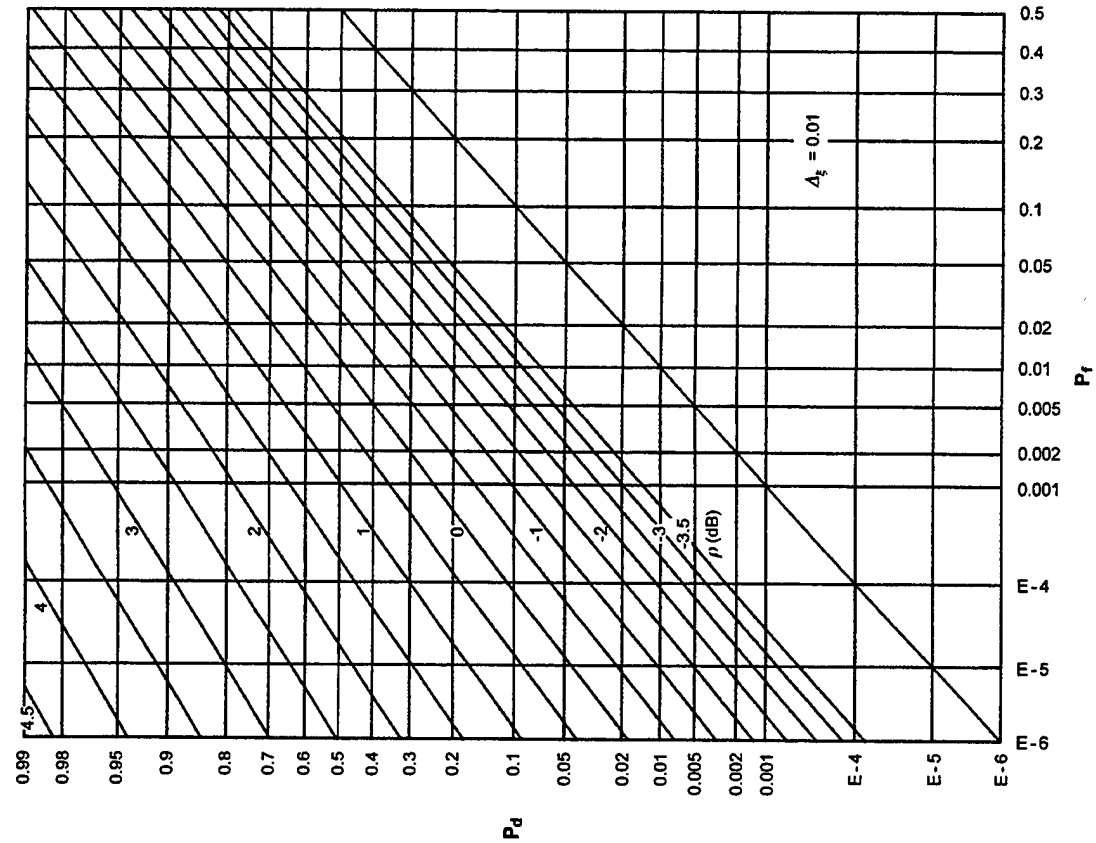

Figure F-36. ROCs for K = 1, N = 32, M = 64

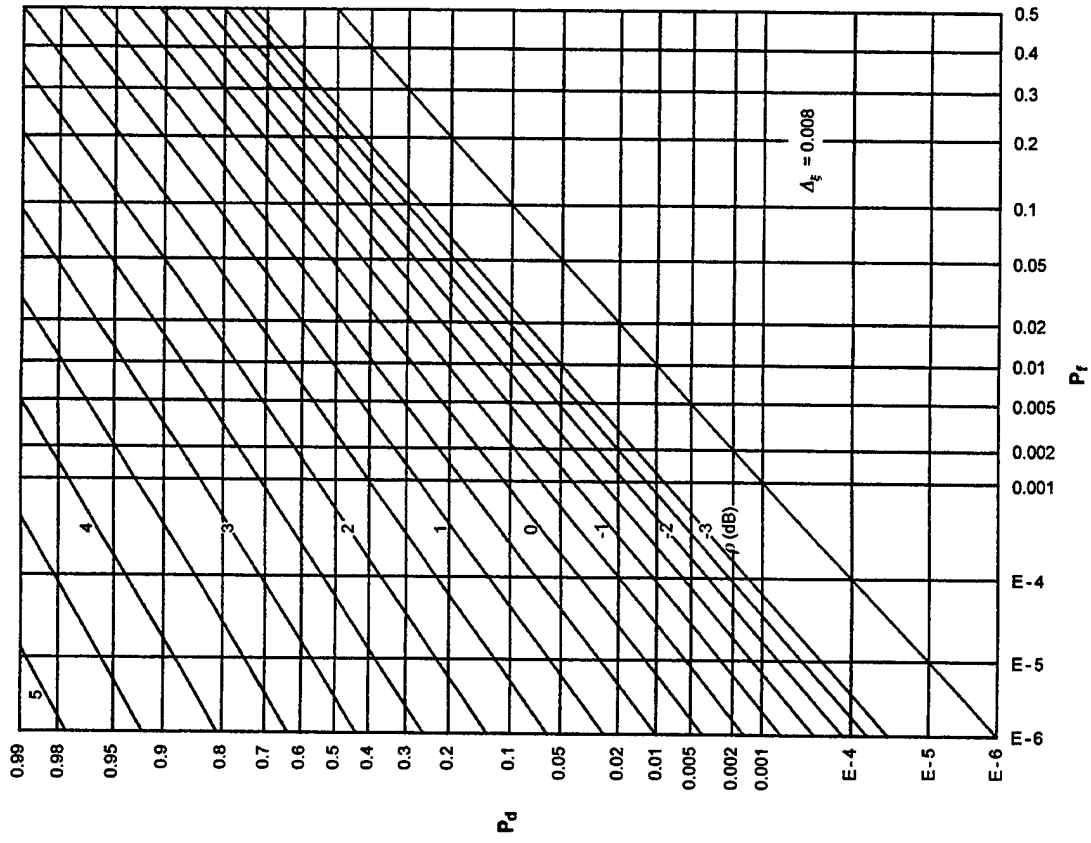

Figure F-35. ROCs for K = 1, N = 16, M = 64

APPENDIX G - ROCS FOR KM = 256, RANDOM GAUSSIAN SIGNAL

This appendix contains the ROCs for or-ing with pre- and post-averaging when the time-bandwidth product KM is fixed at 256; the possible combinations (from table 1) are repeated here:

K	M	N
256	1	1,2,4,8,16,32
128	2	
64	4	
32	8	
16	16	
8	32	
4	64	
2	128	
1	256	

For N = 1, only the product KM matters; the first plot in this appendix covers this special case, under the labeling K = 256, N = 1, M = 1. The other 5 values of N, along with the 9 possible combinations of K and M, yield 45 additional ROCs, for a total of 46 ROCs in this appendix.

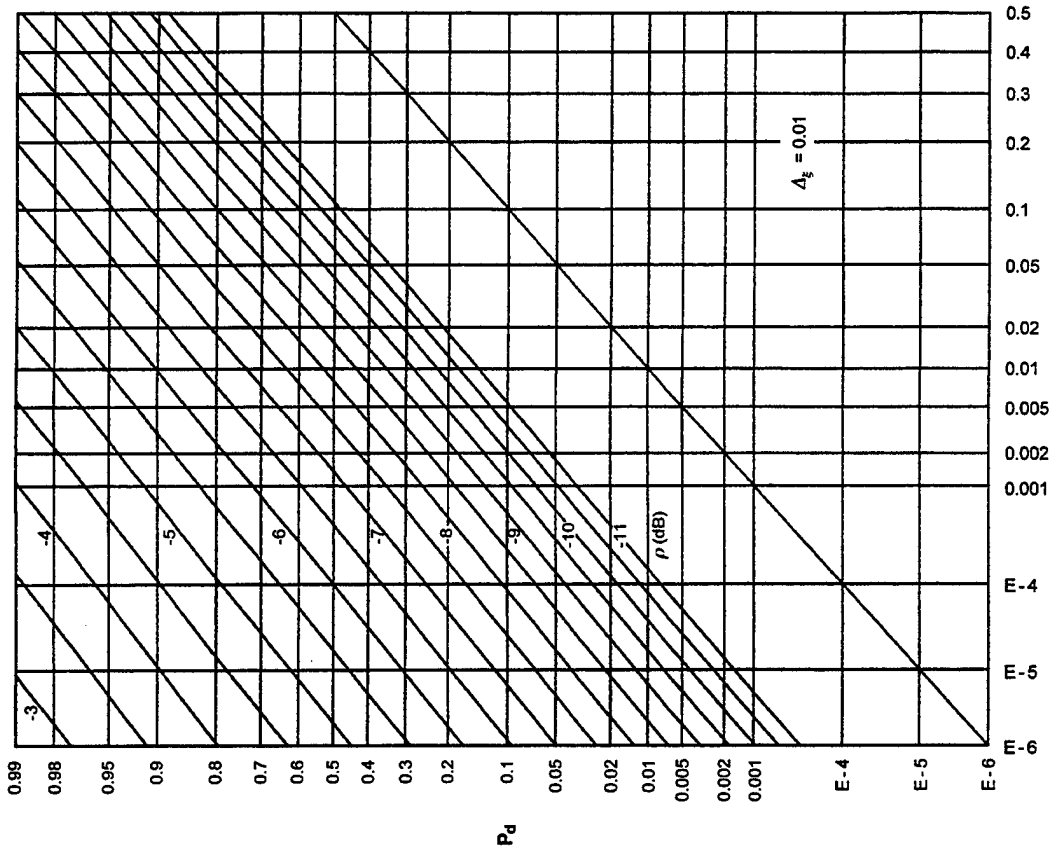

Figure G-2. ROCs for K = 256, N = 2, M = 1

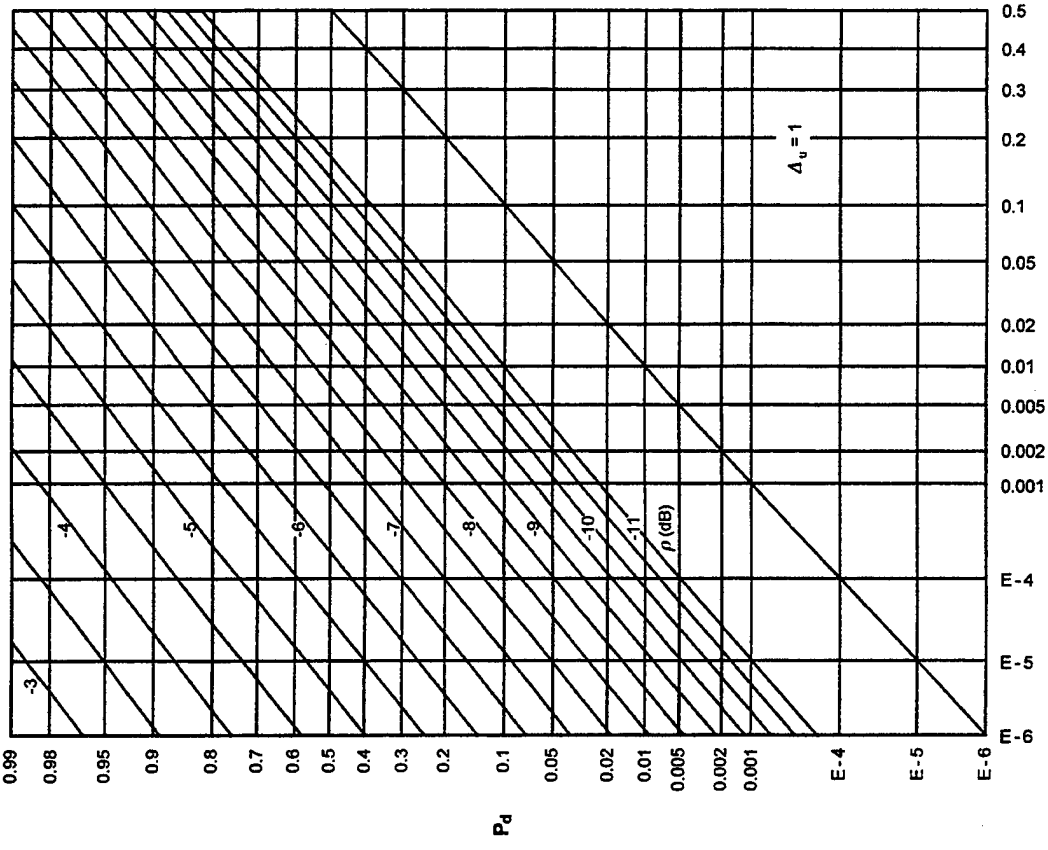

Figure G-1. ROCs for K = 256, N = 1, M = 1

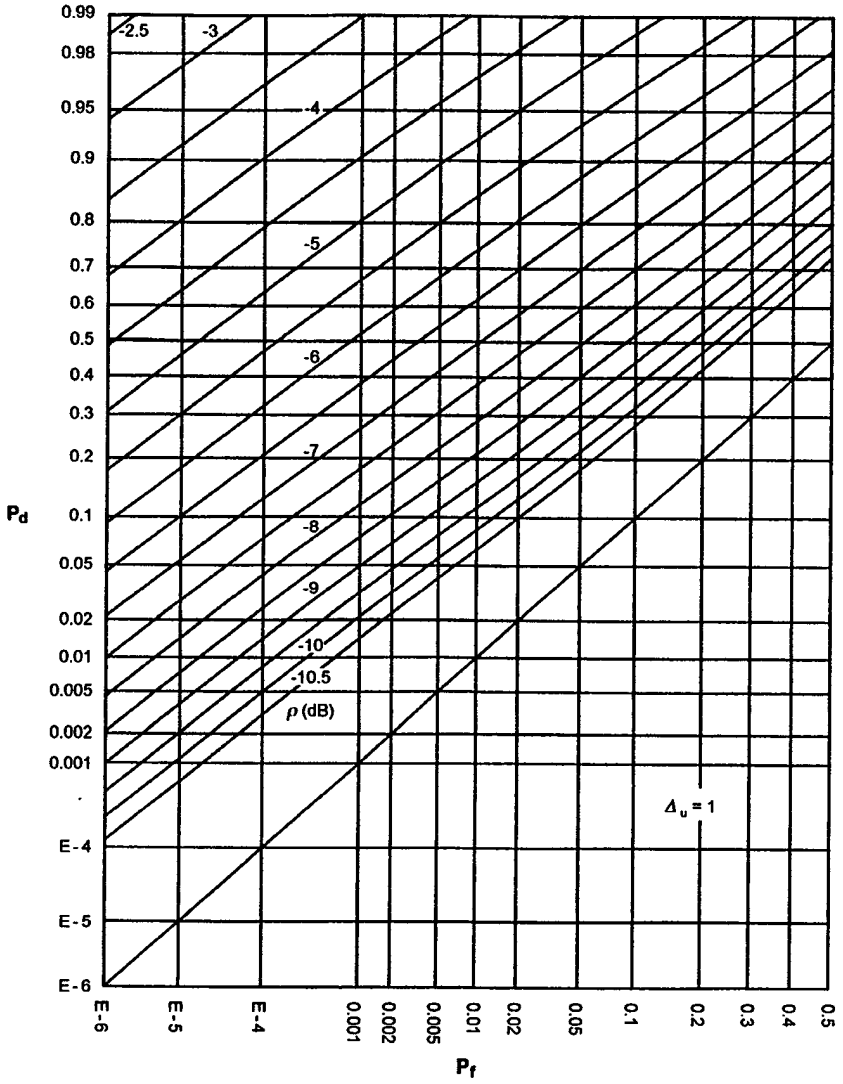

Figure G-3. ROCs for K = 256, N = 4, M = 1

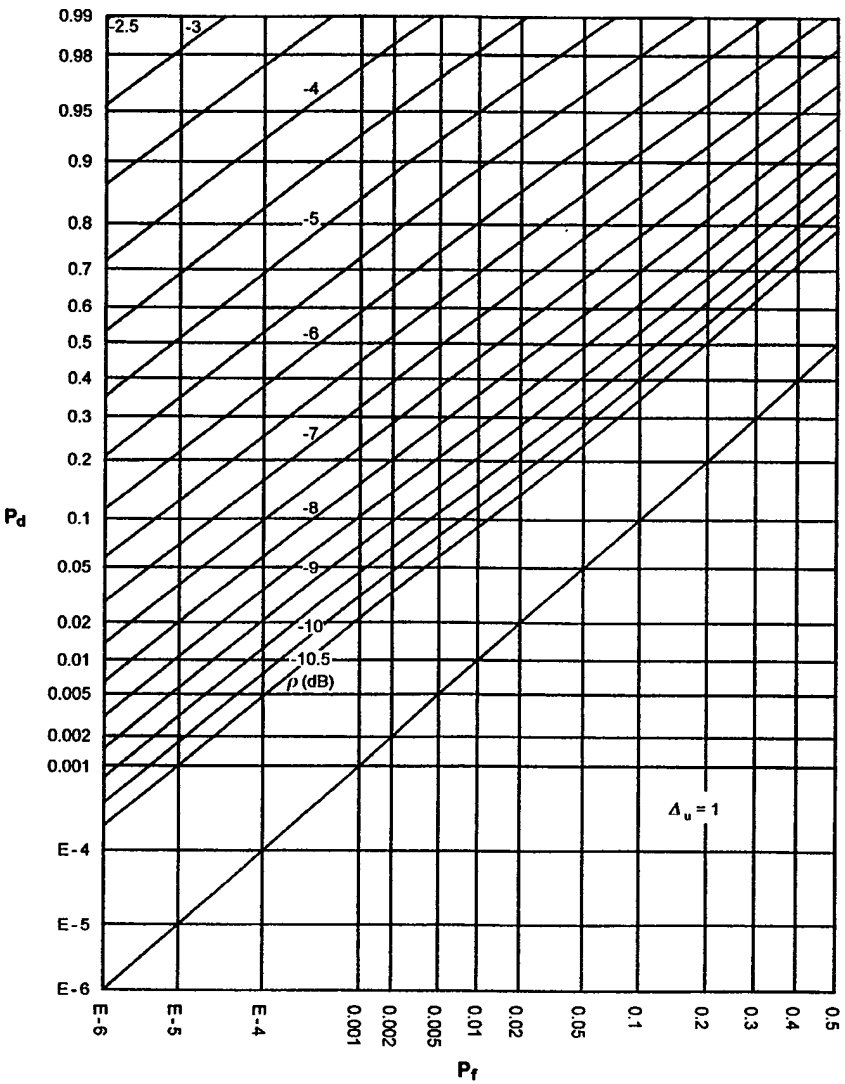

Figure G-4. ROCs for K = 256, N = 8, M = 1

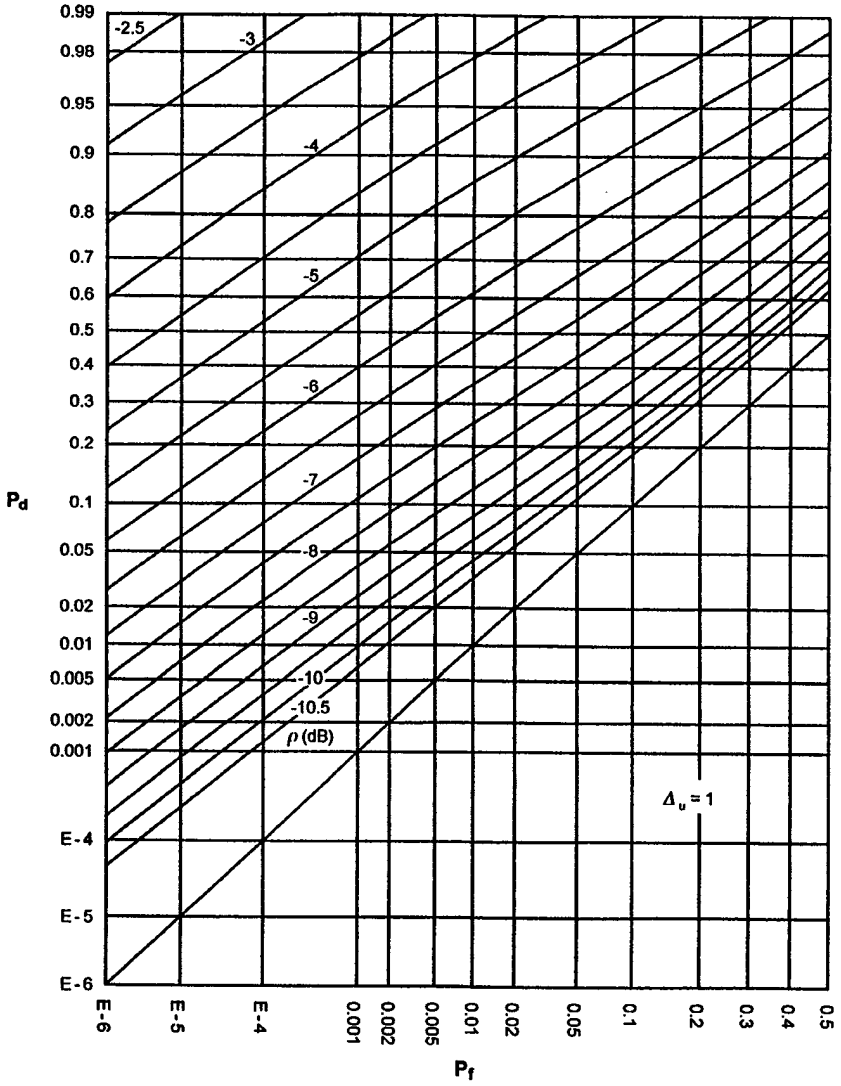

Figure G-5. ROCs for K = 256, N = 16, M = 1

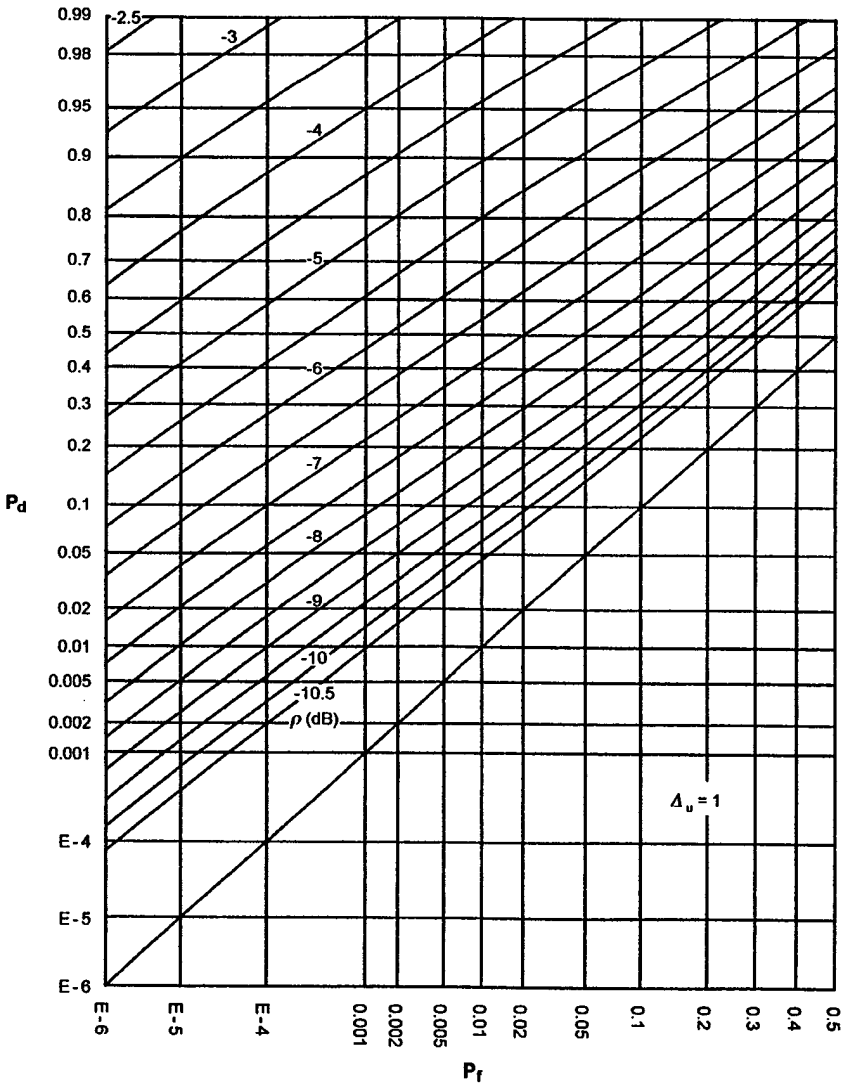

Figure G-6. ROCs for K = 256, N = 32, M = 1

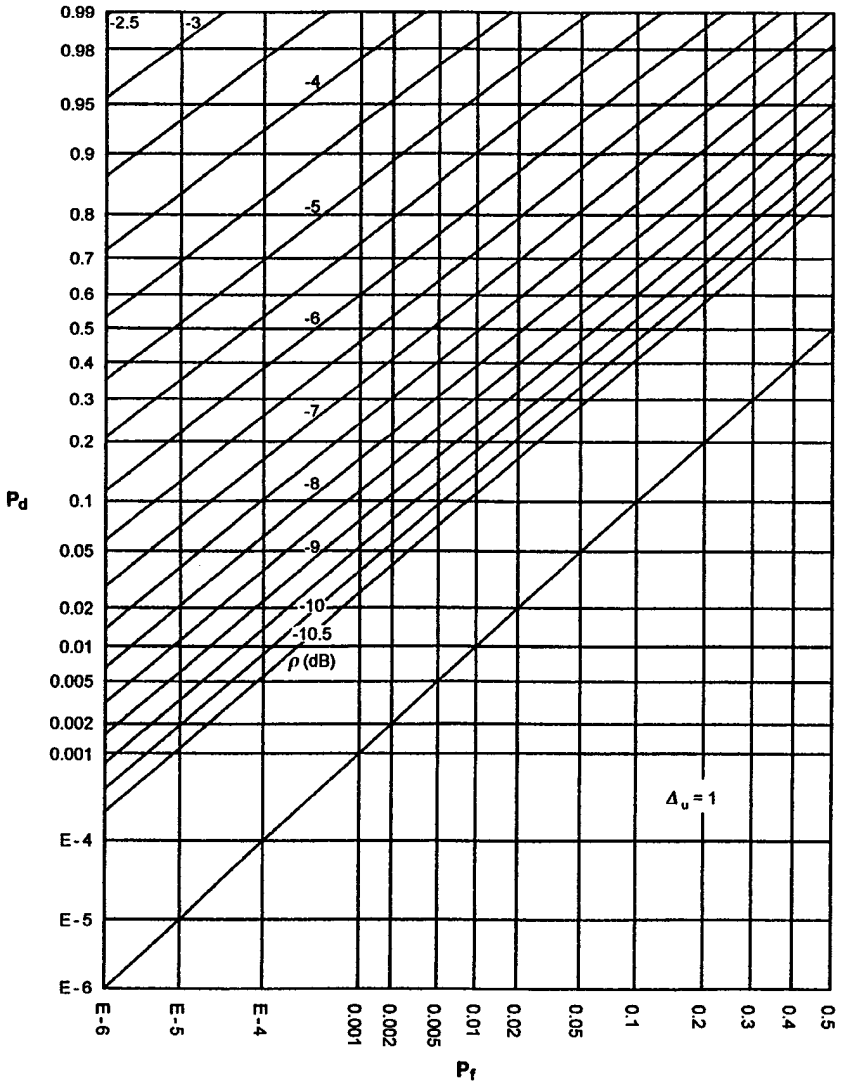

Figure G-7. ROCs for K = 128, N = 2, M = 2

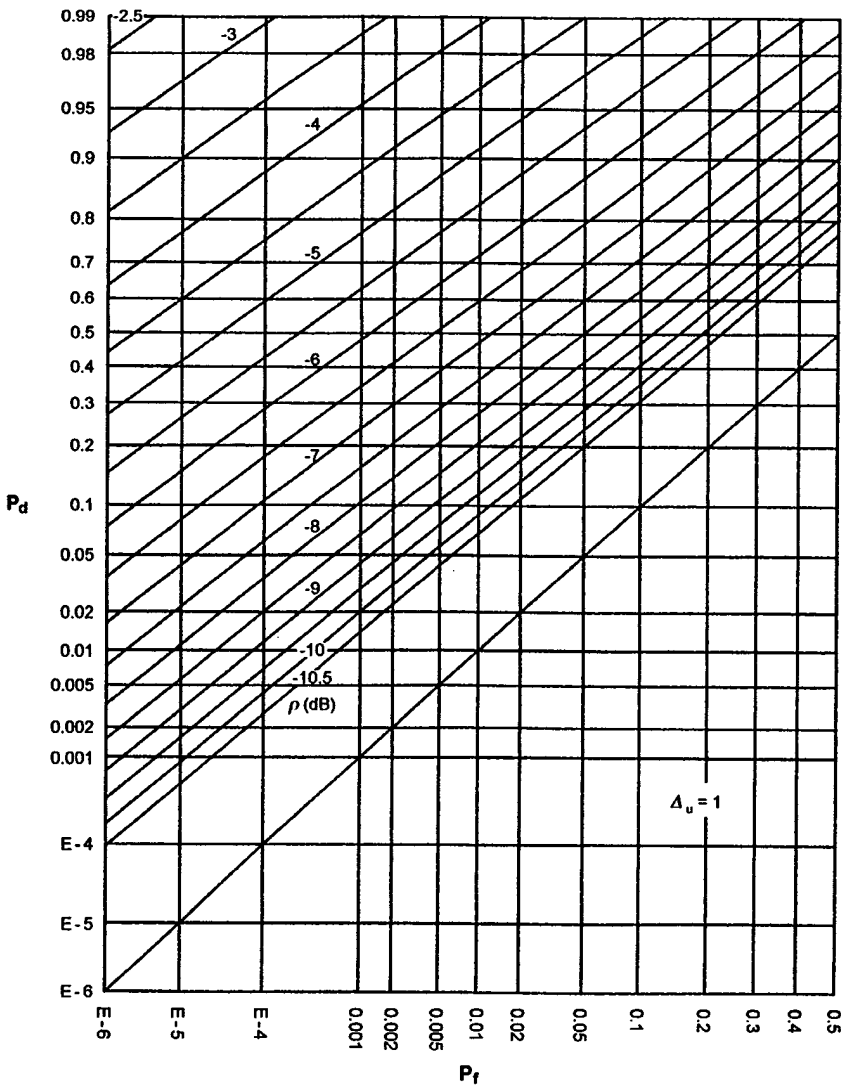

Figure G-8. ROCs for K = 128, N = 4, M = 2

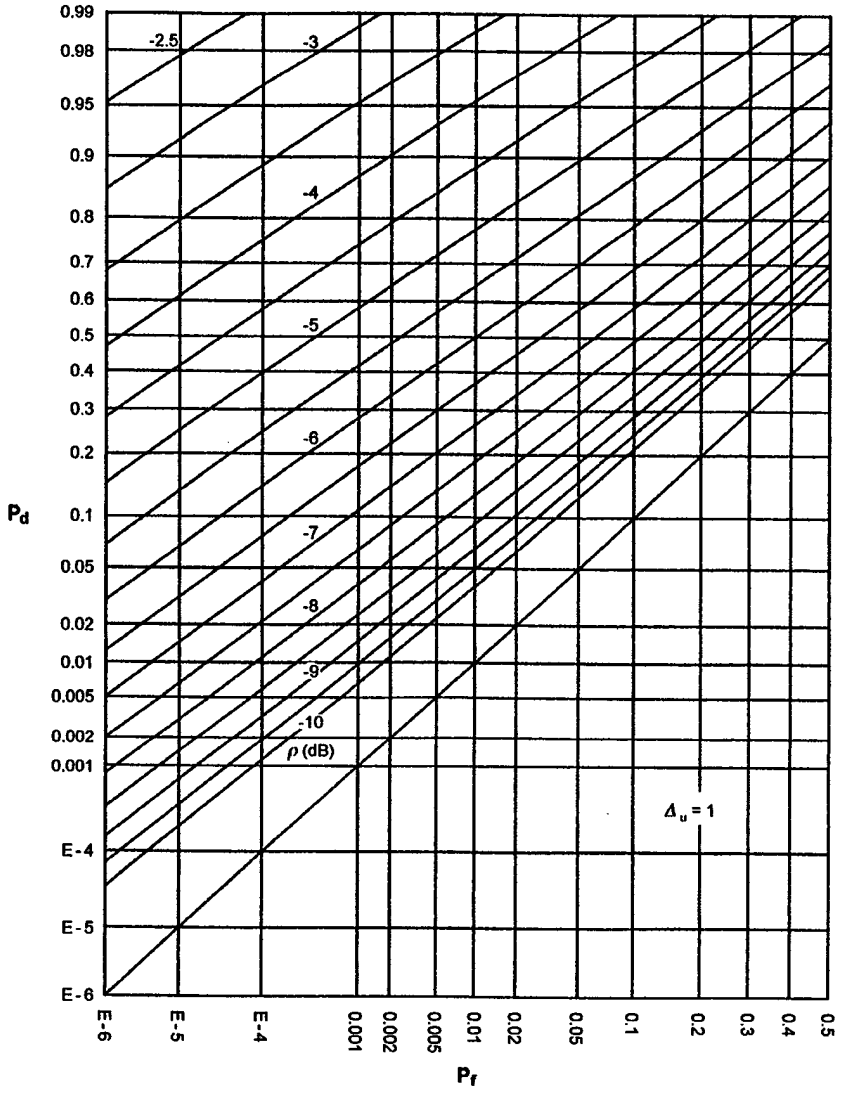

Figure G-9. ROCs for K = 128, N = 8, M = 2

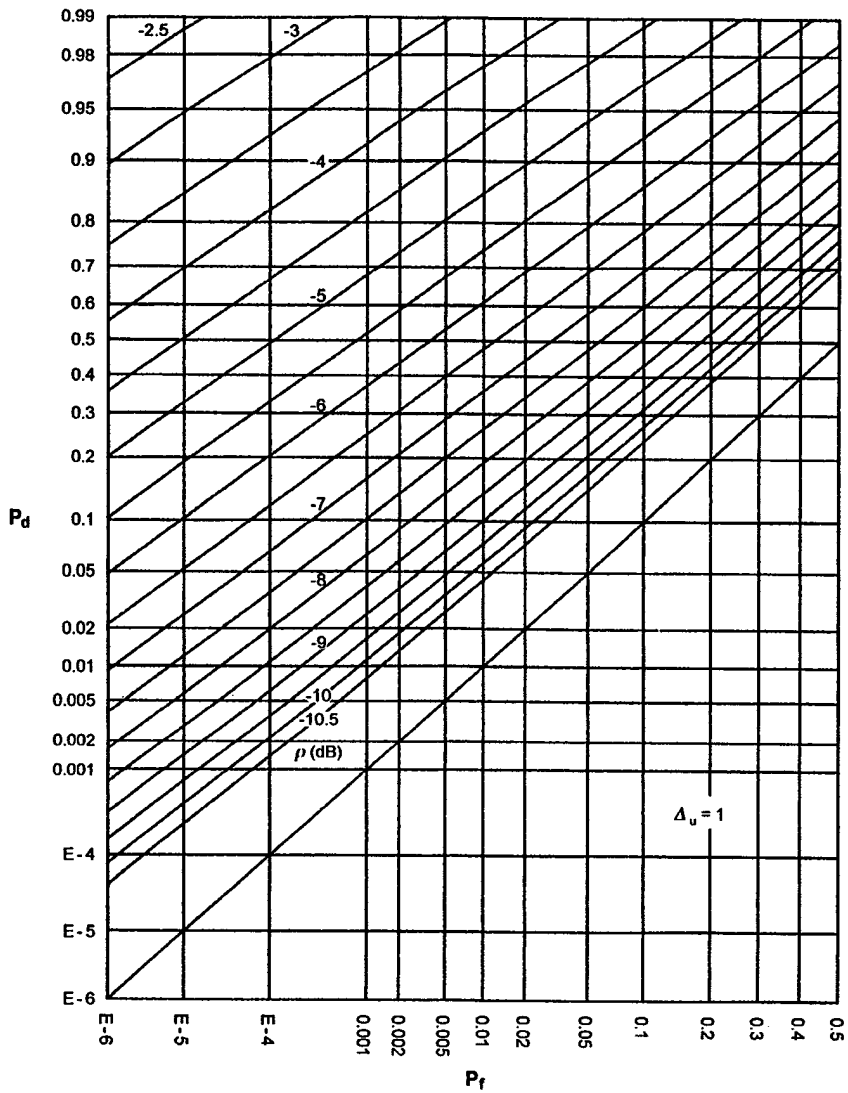

Figure G-10. ROCs for K = 128, N = 16, M = 2

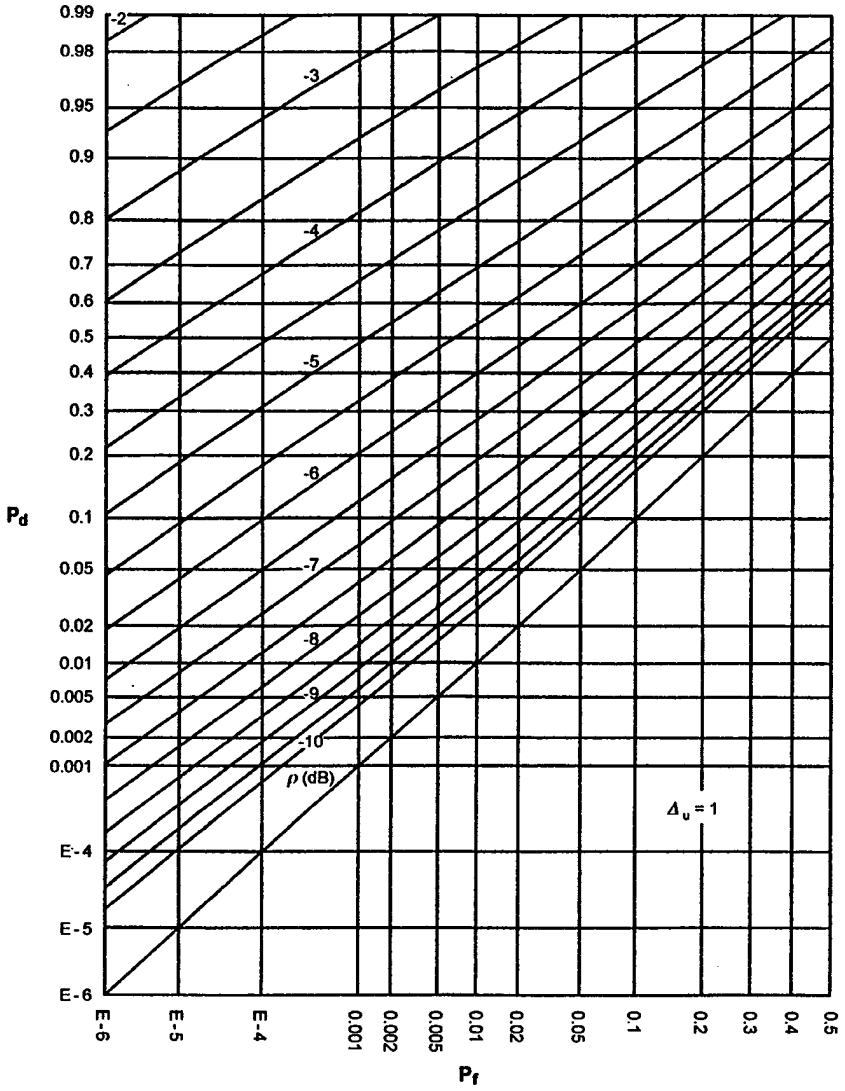

Figure G-11. ROCs for K = 128, N = 32, M = 2

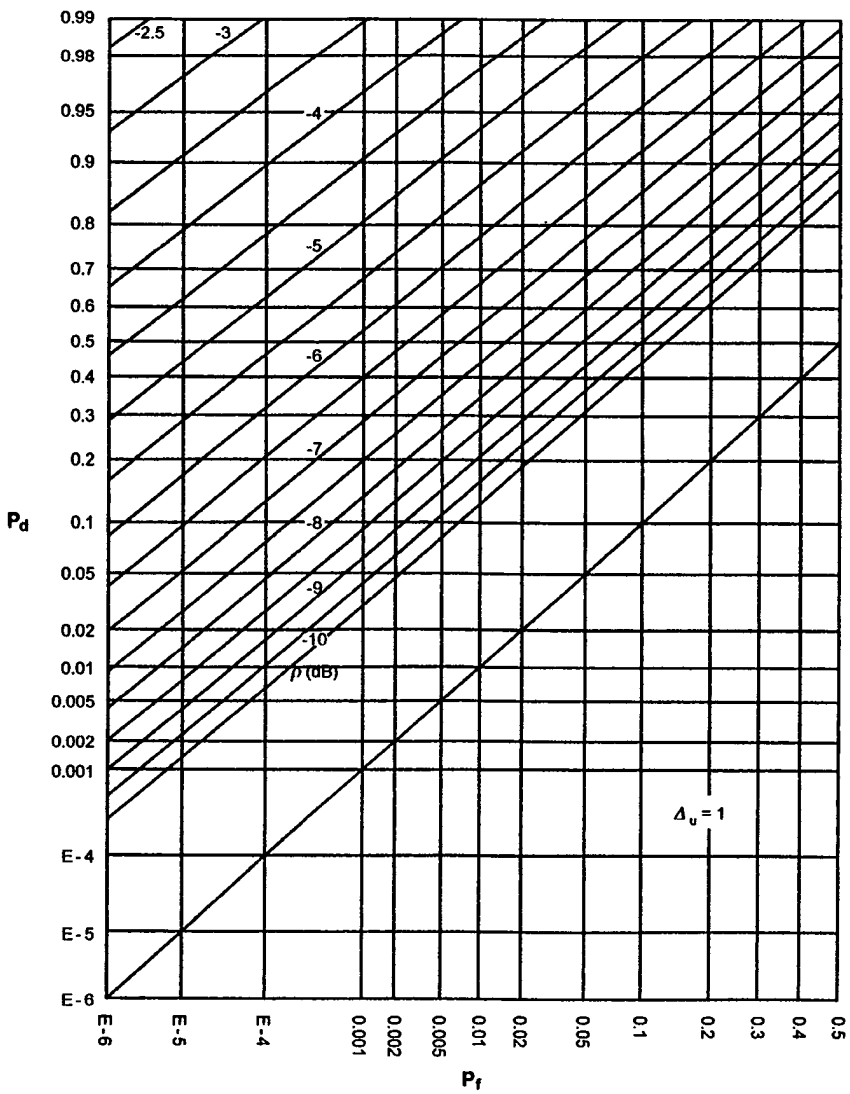

Figure G-12. ROCs for K = 64, N = 2, M = 4

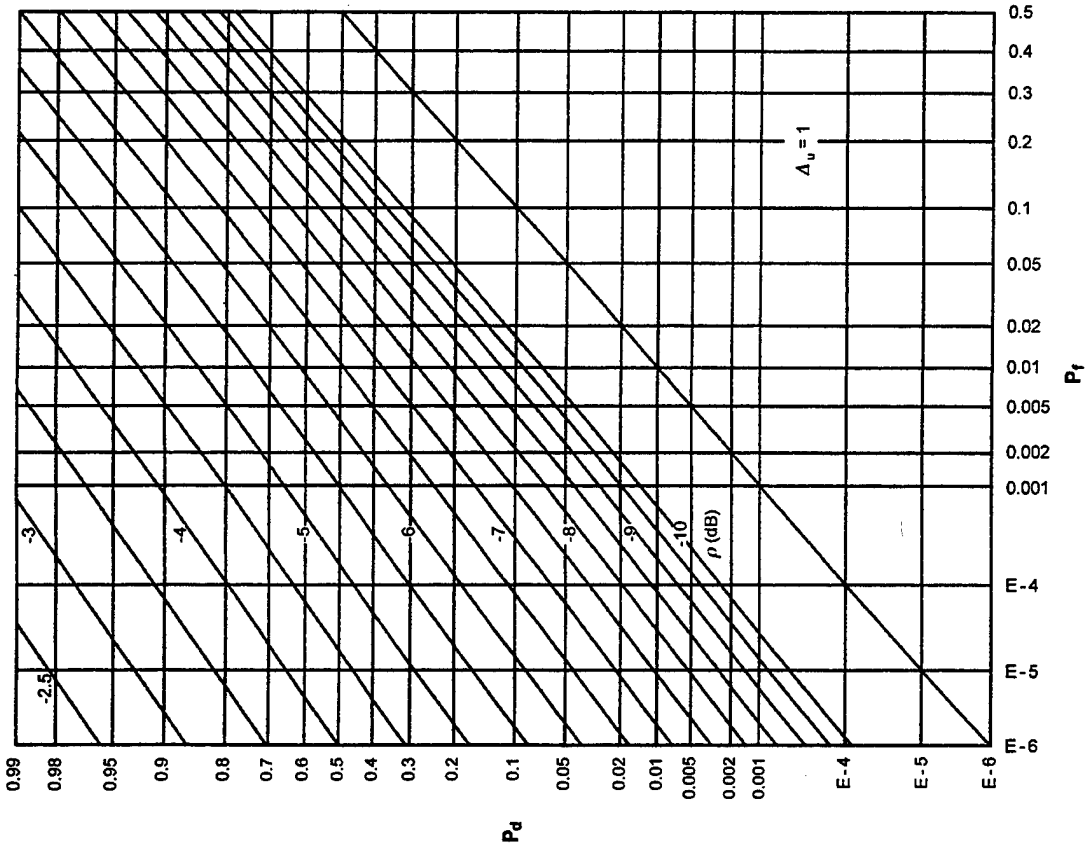

Figure G-14. ROCs for K = 64, N = 8, M = 4

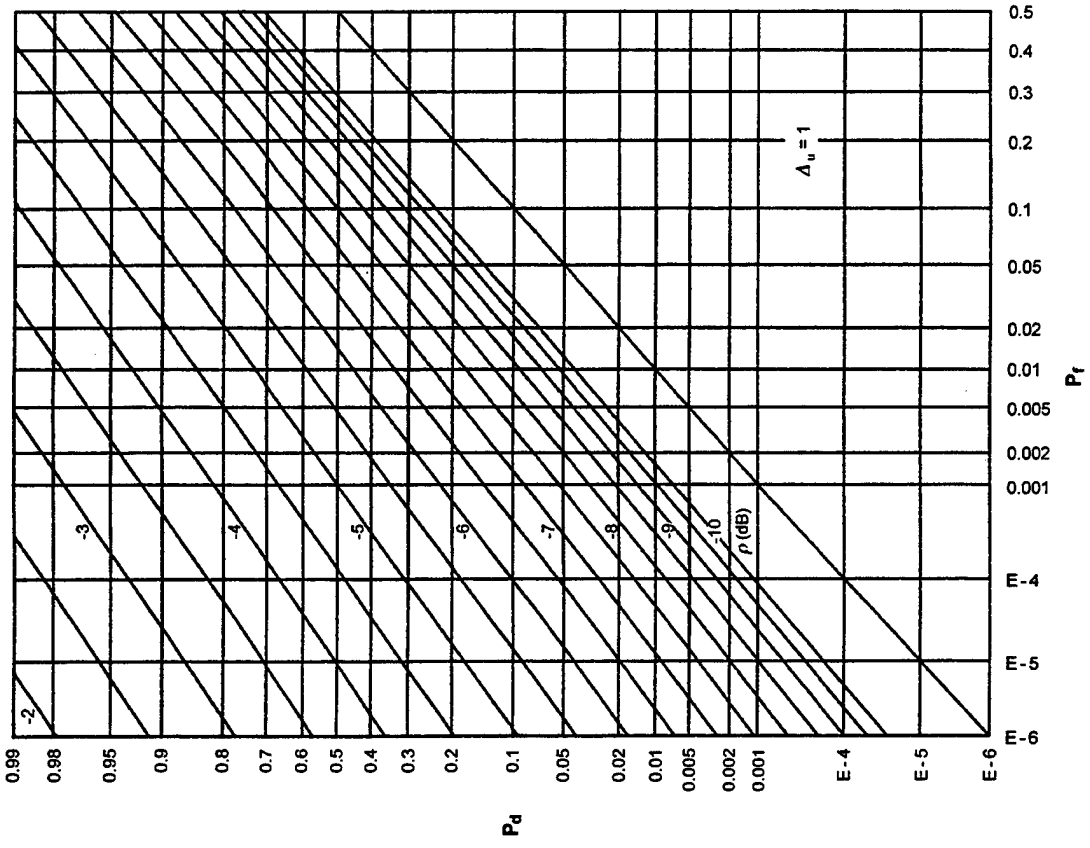

Figure G-13. ROCs for K = 64, N = 4, M = 4

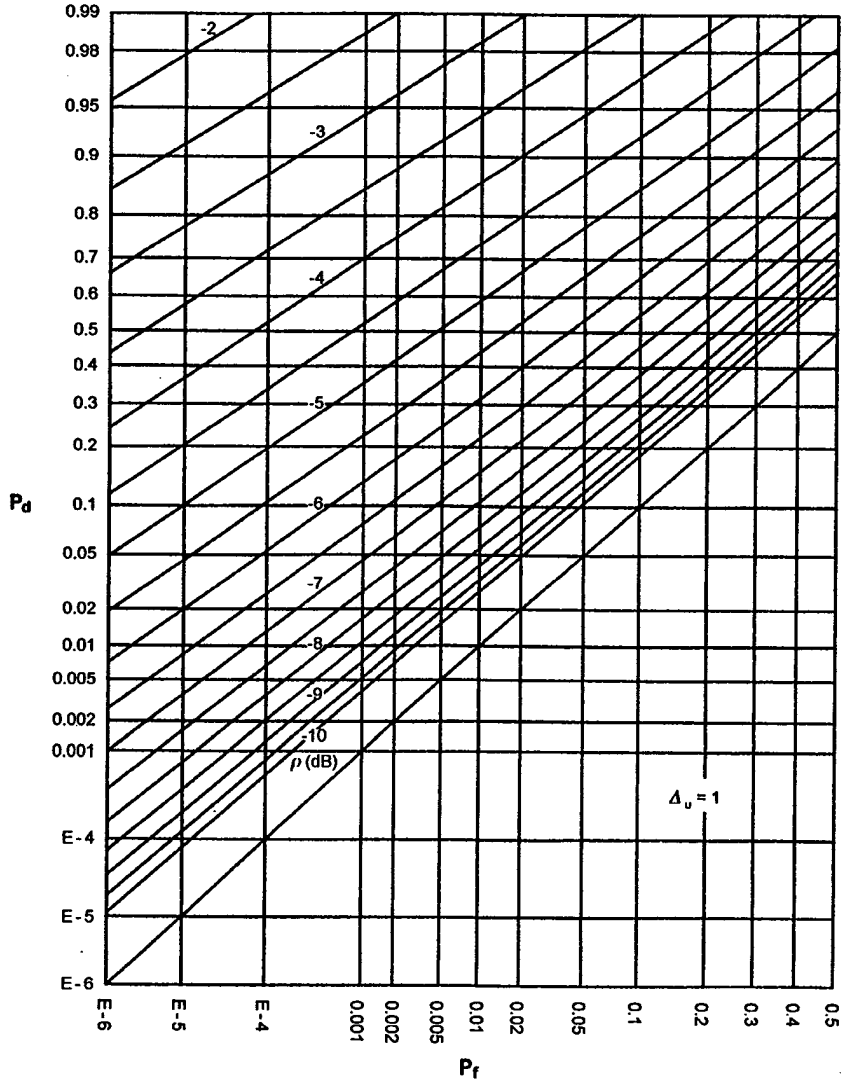

Figure G-15. ROCs for K = 64, N = 16, M = 4

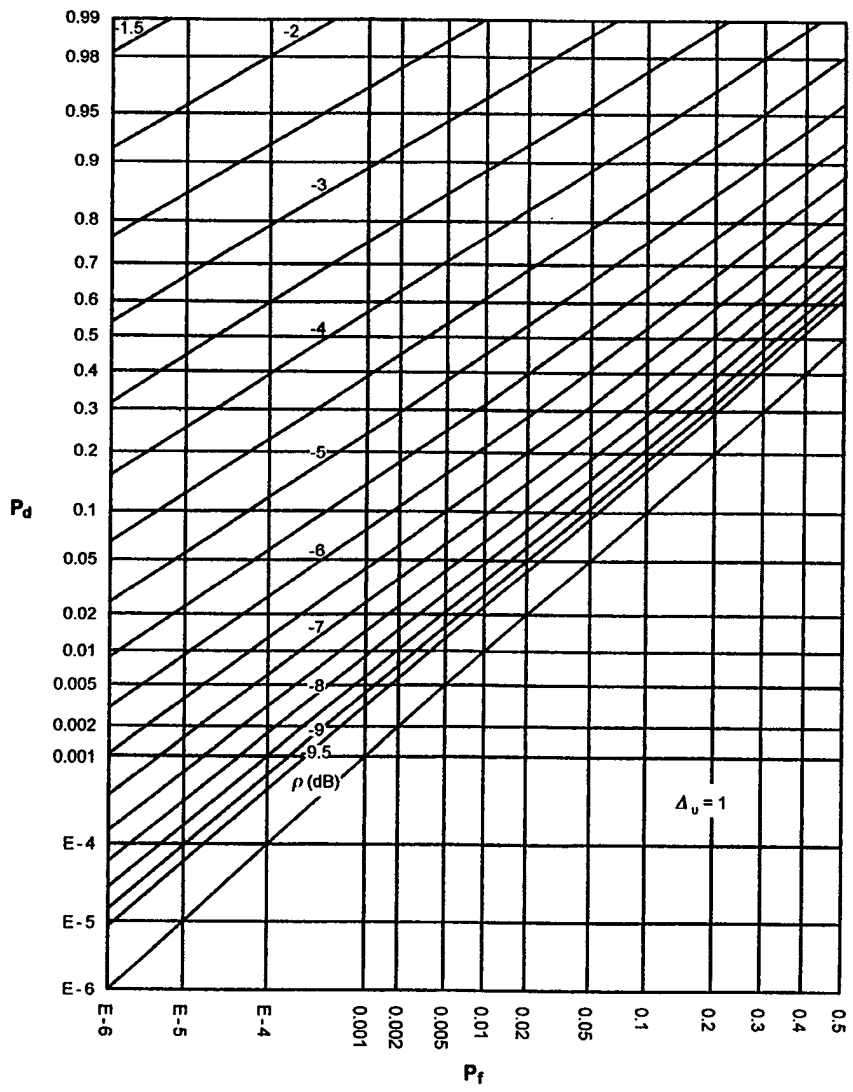

Figure G-16. ROCs for K = 64, N = 32, M = 4

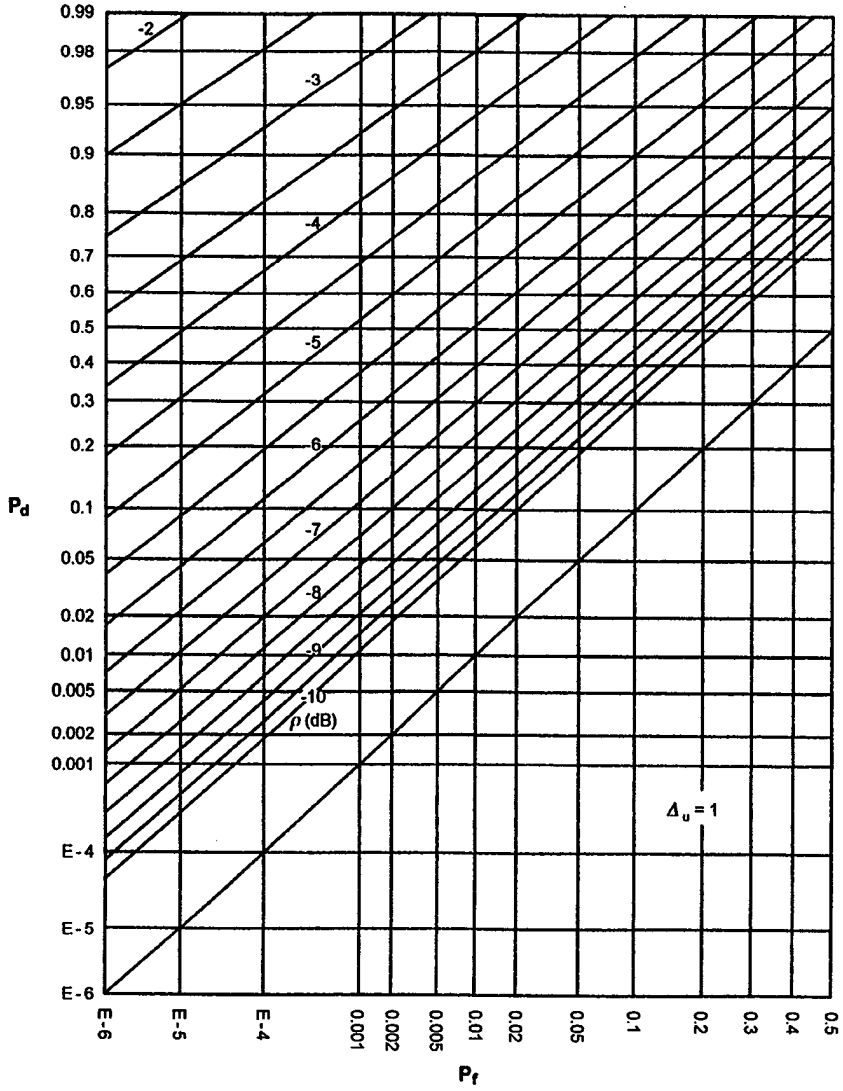

Figure G-17. ROCs for K = 32, N = 2, M = 8

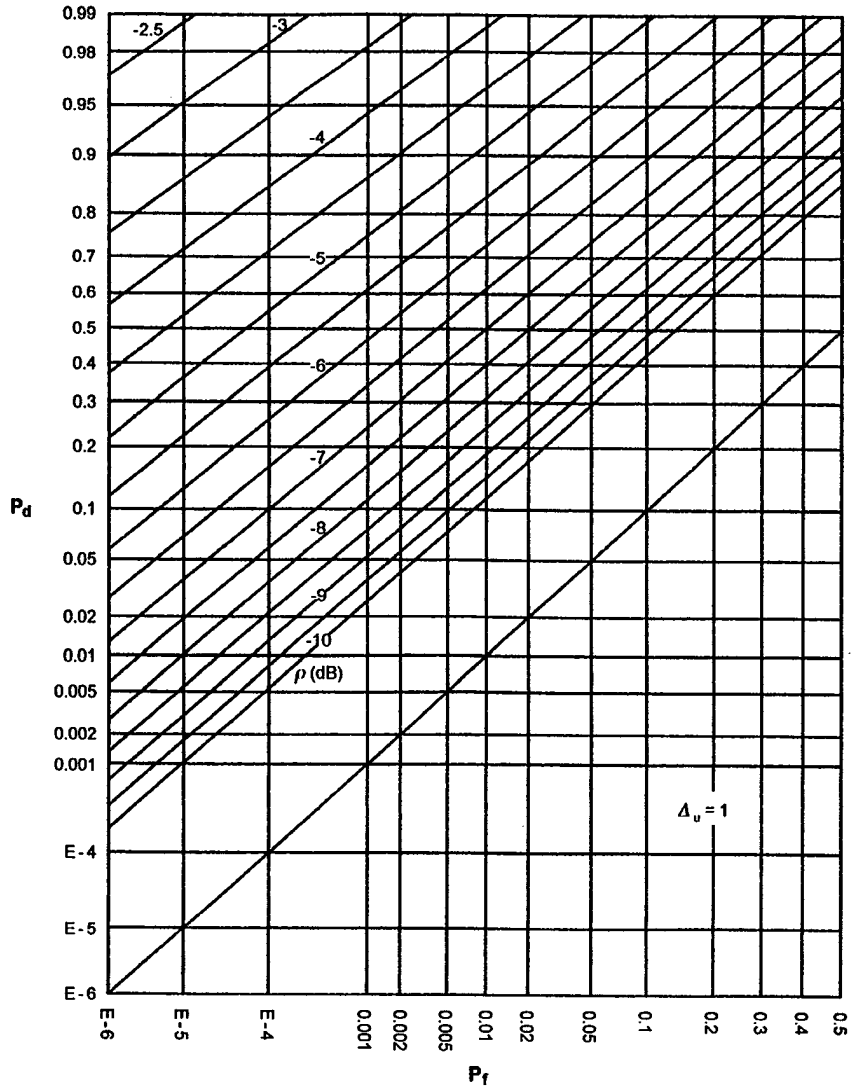

Figure G-18. ROCs for K = 32, N = 4, M = 8

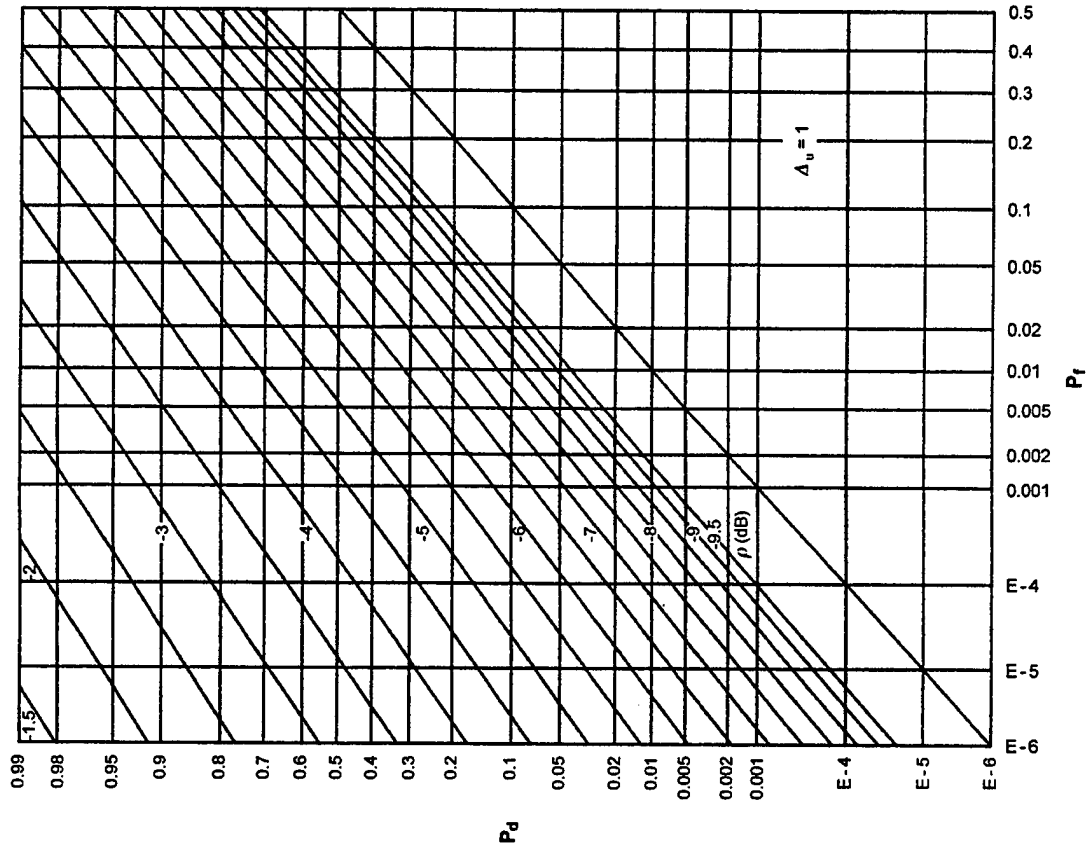

Figure G-20. ROCs for K = 32, N = 16, M = 8

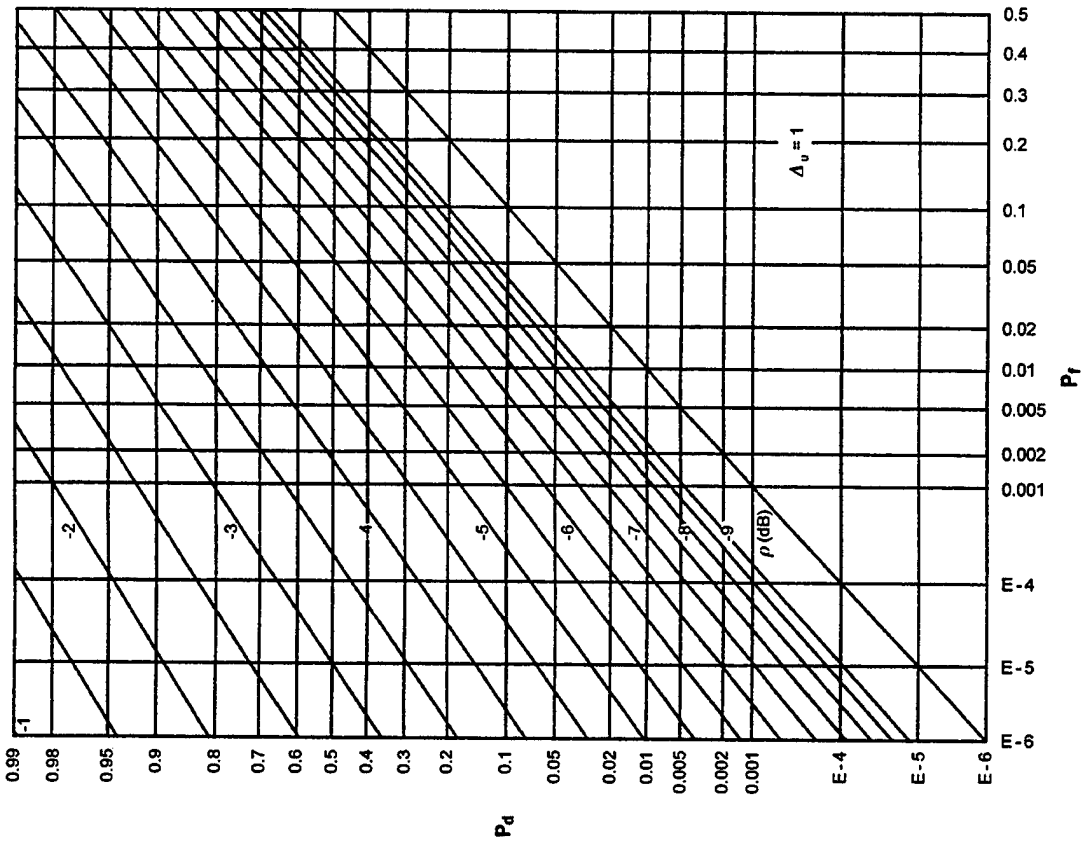

Figure G-19. ROCs for K = 32, N = 8, M = 8

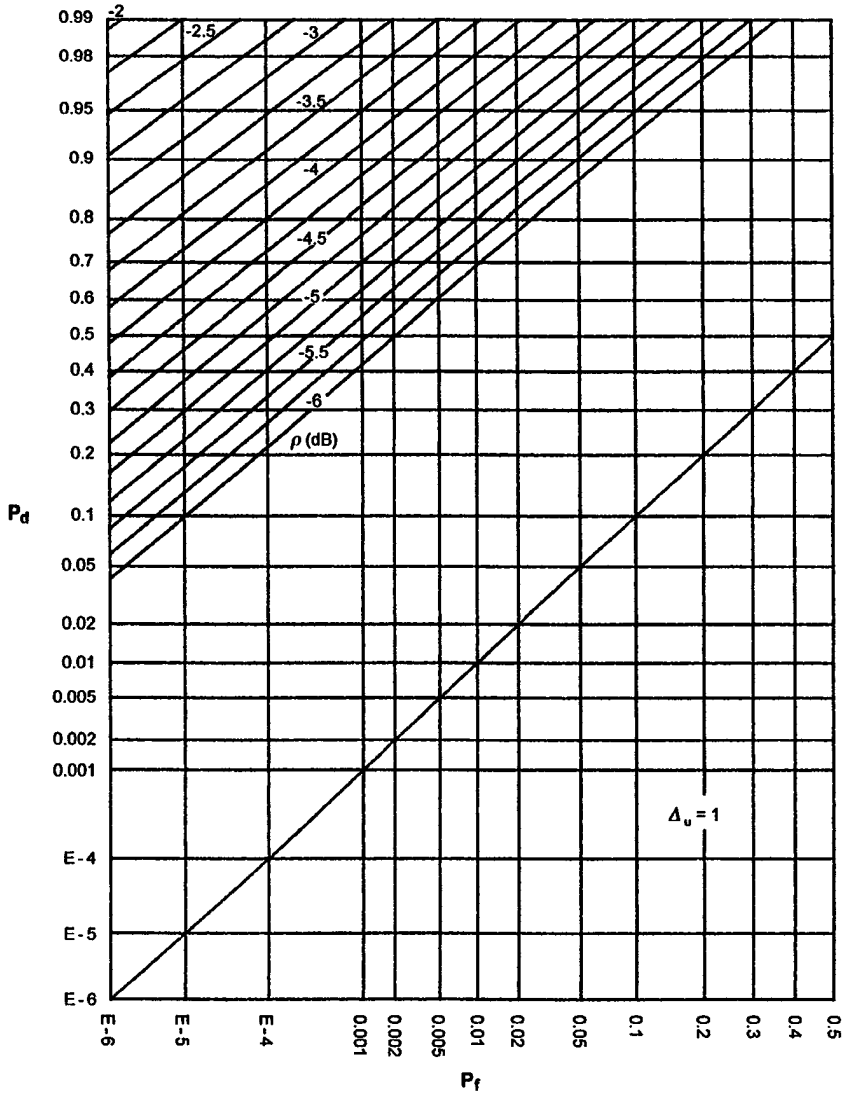

Figure G-21. ROCs for K = 32, N = 32, M = 8

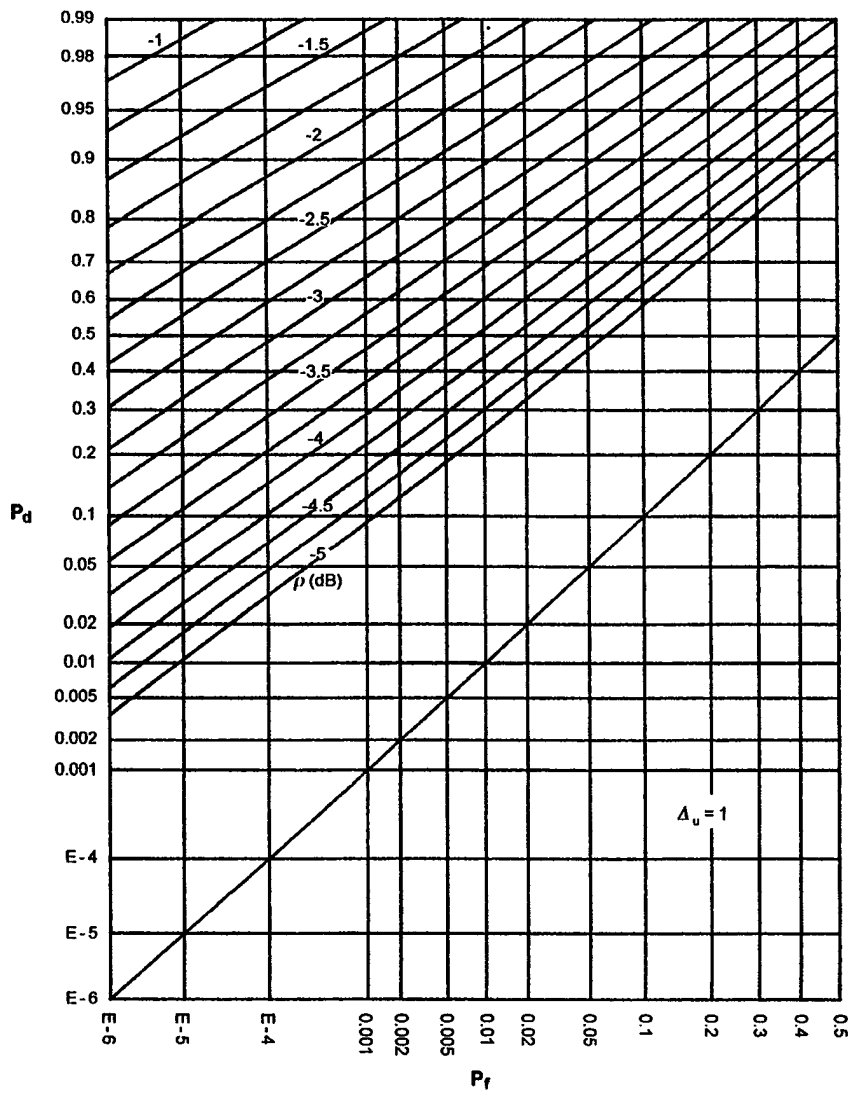

Figure G-22. ROCs for K = 16, N = 2, M = 16

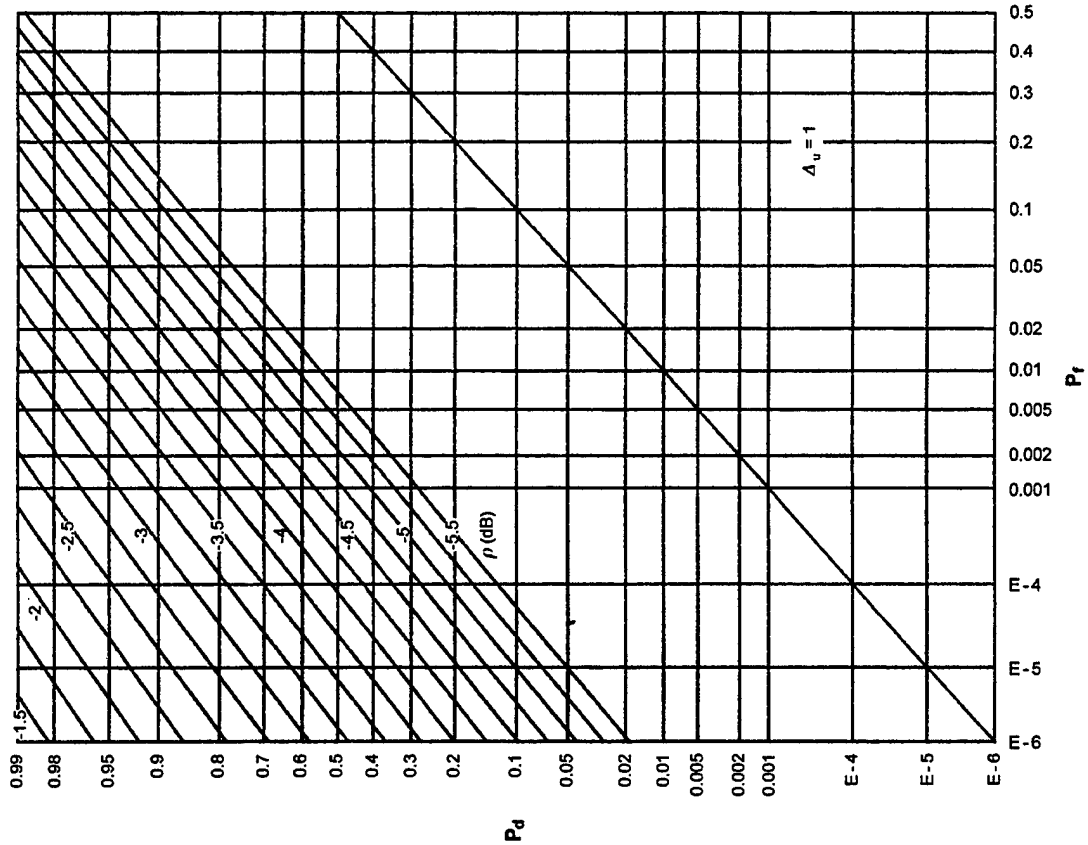

Figure G-24. ROCs for K = 16, N = 8, M = 16

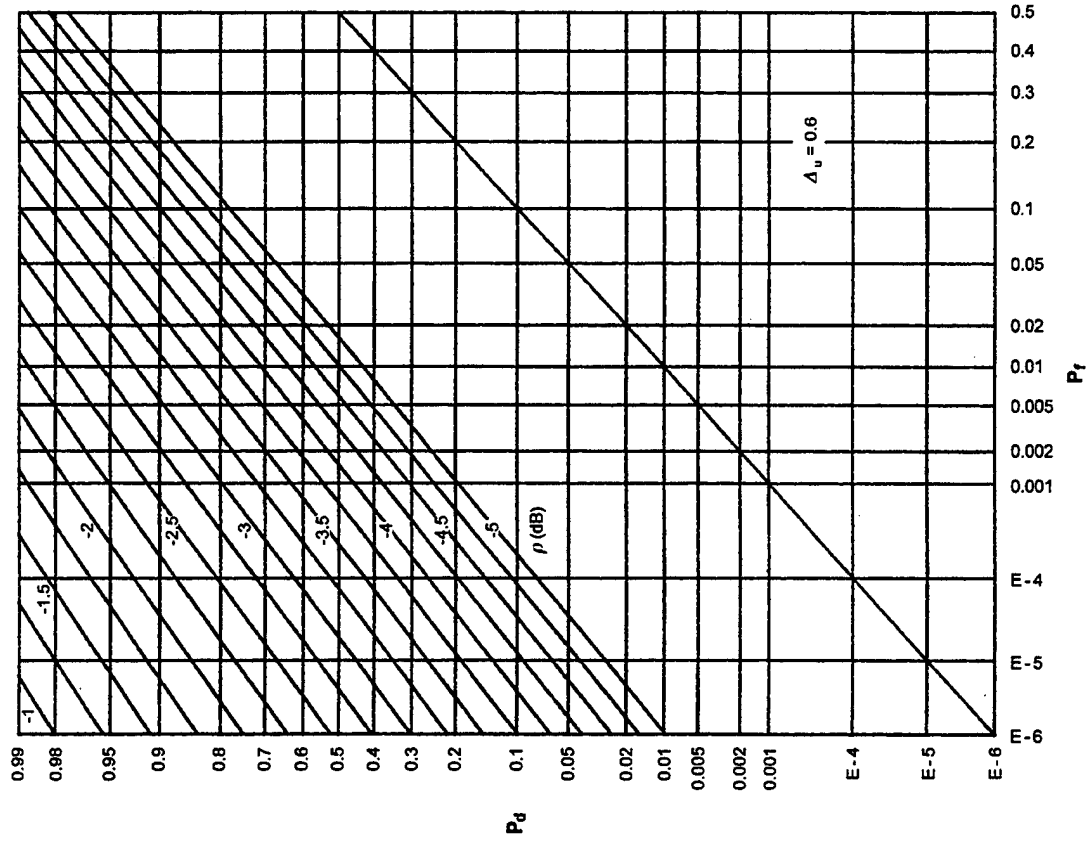

Figure G-23. ROCs for K = 16, N = 4, M = 16

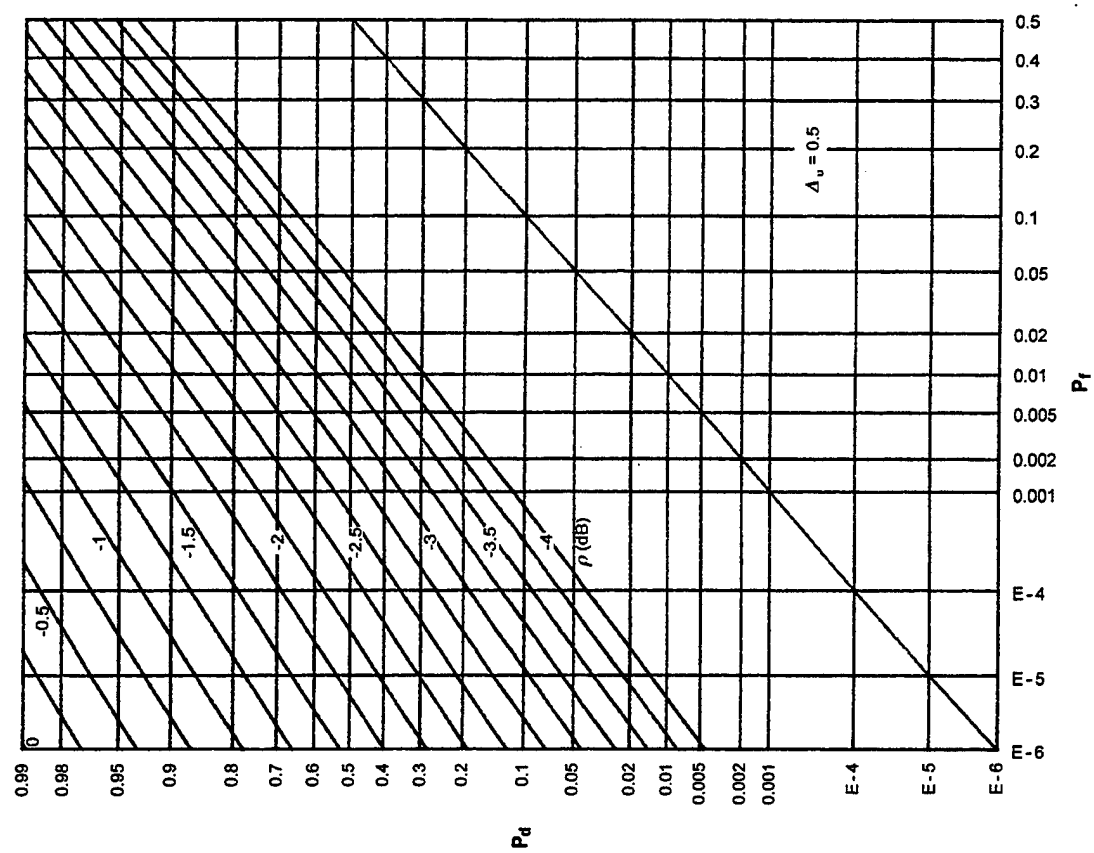

Figure G-26. ROCs for K = 16, N = 32, M = 16

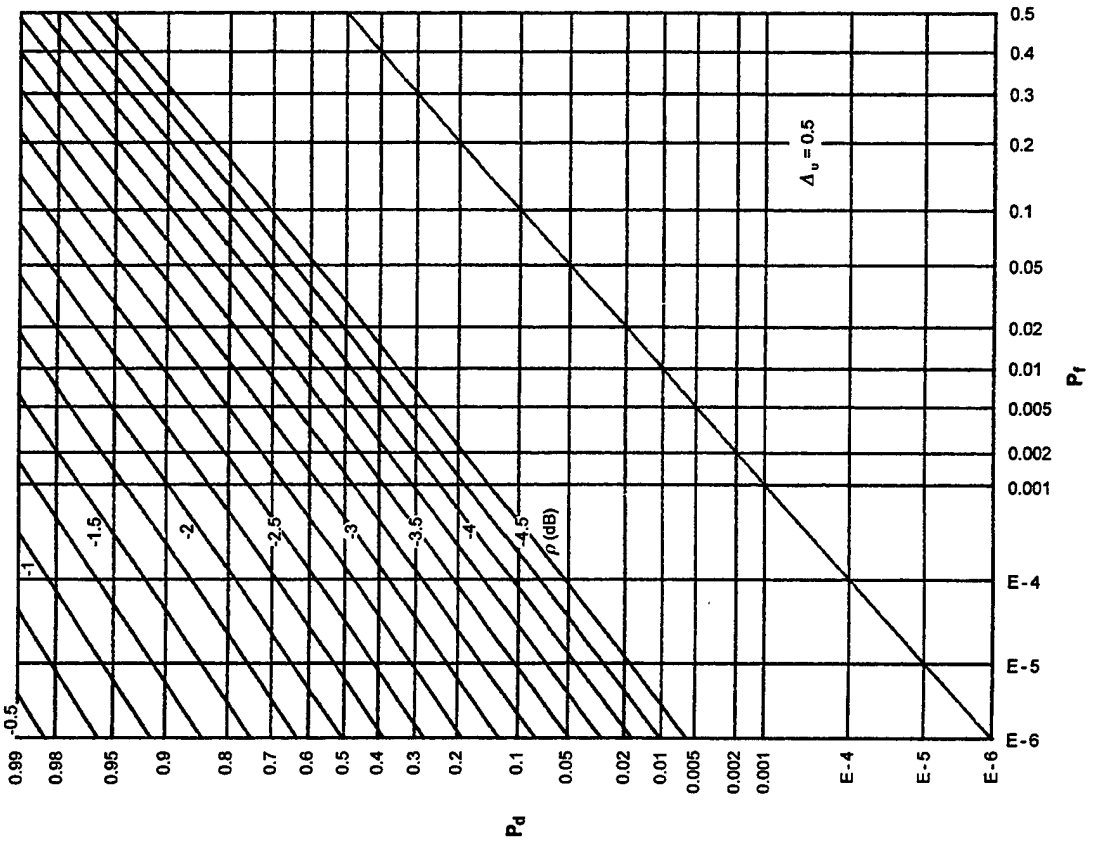

Figure G-25. ROCs for K = 16, N = 16, M = 16

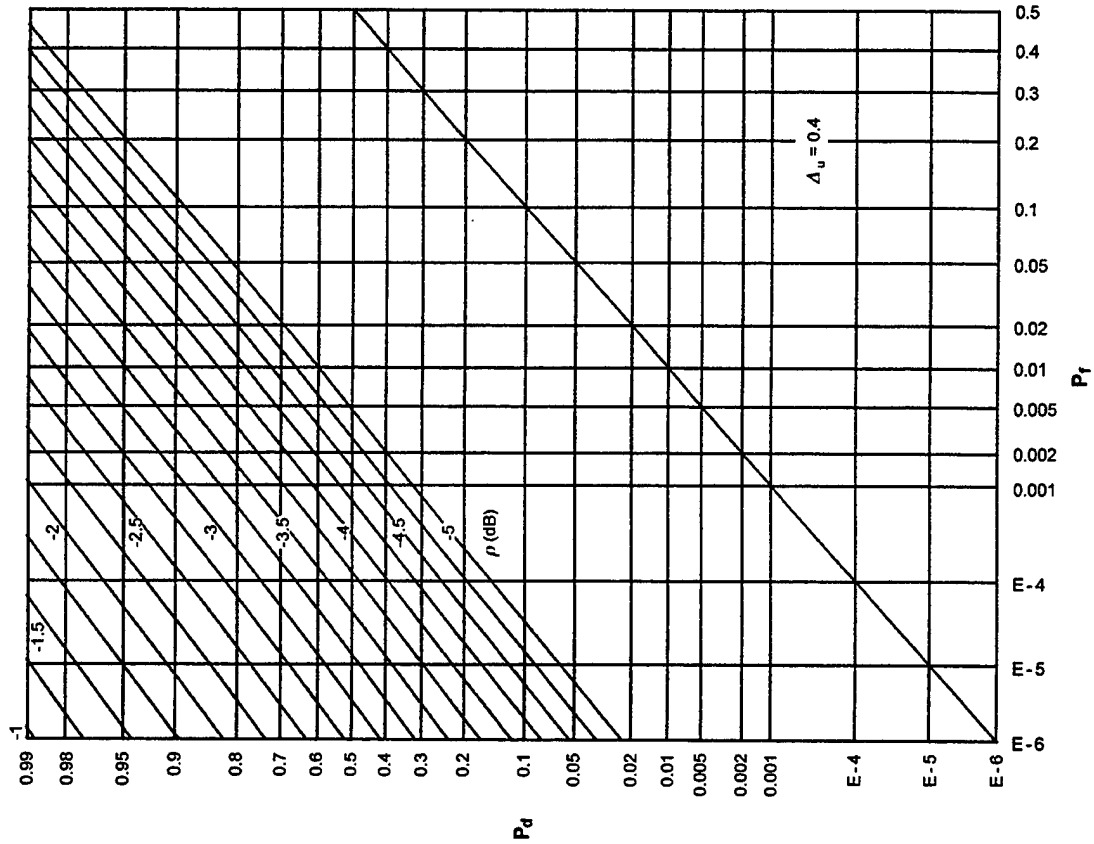

Figure G-28. ROCs for K = 8, N = 4, M = 32

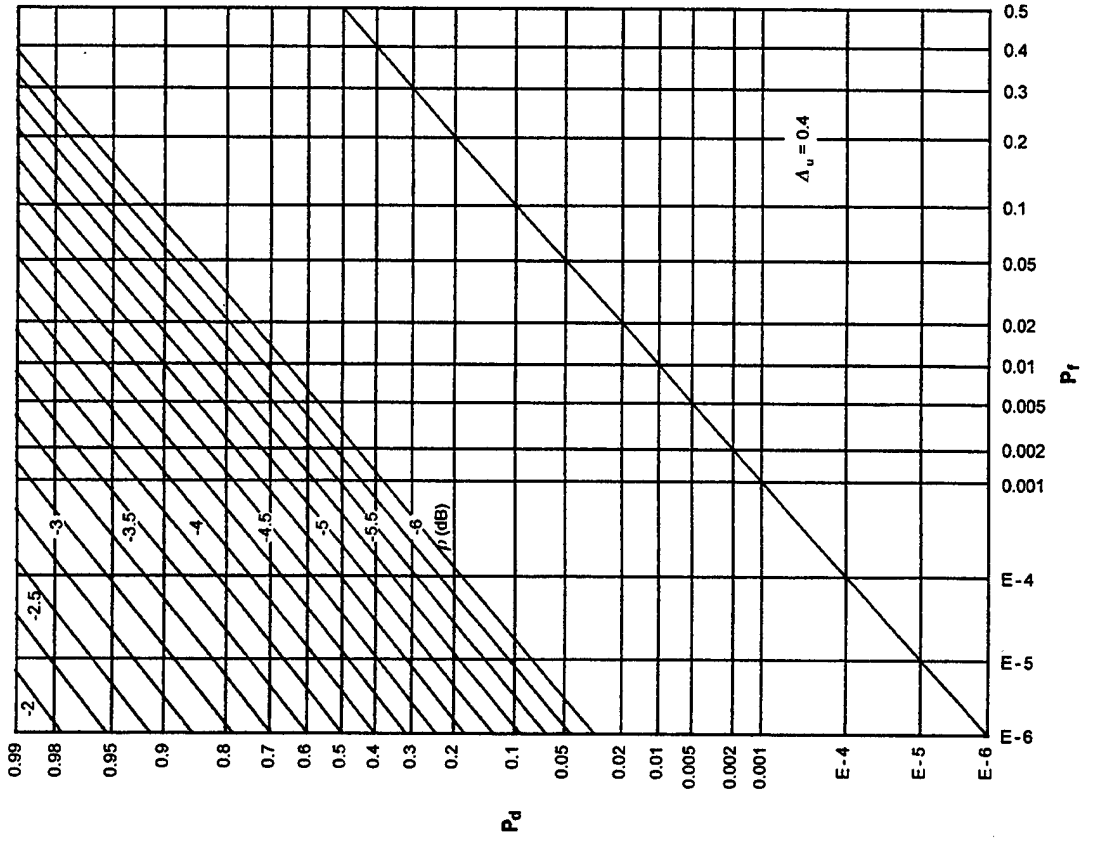

Figure G-27. ROCs for K = 8, N = 2, M = 32

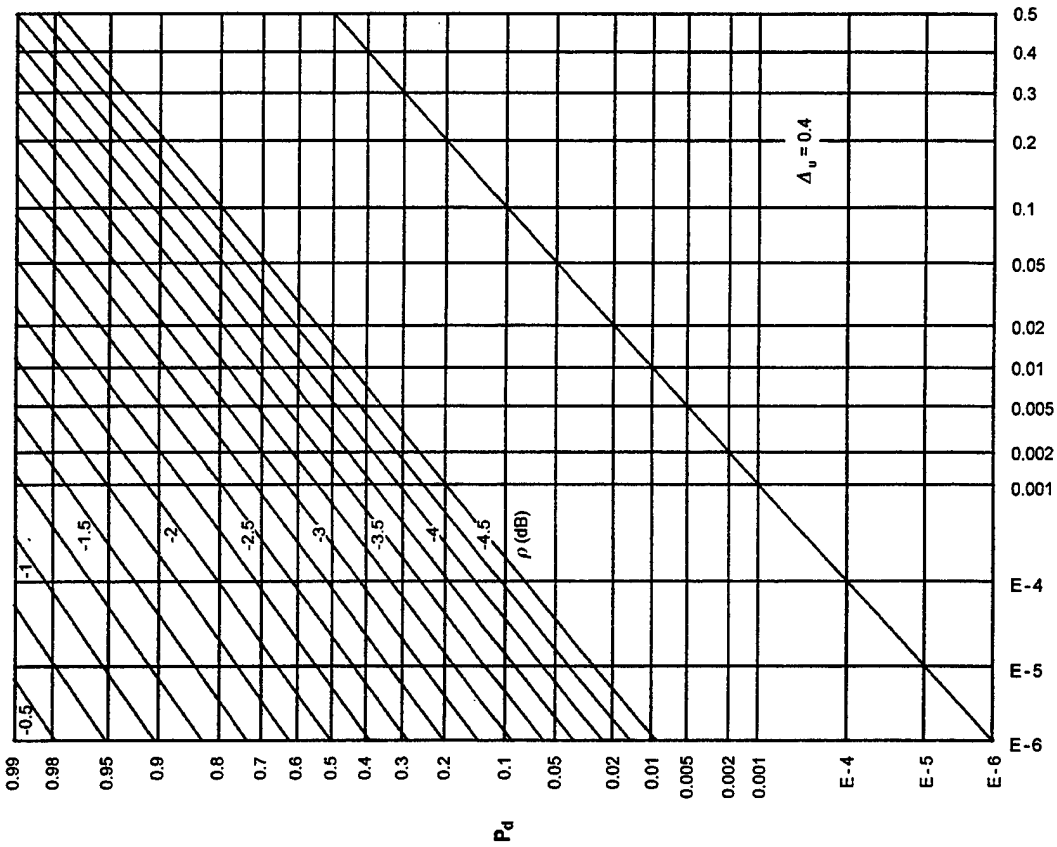

Figure G-30. ROCs for K = 8, N = 16, M = 32

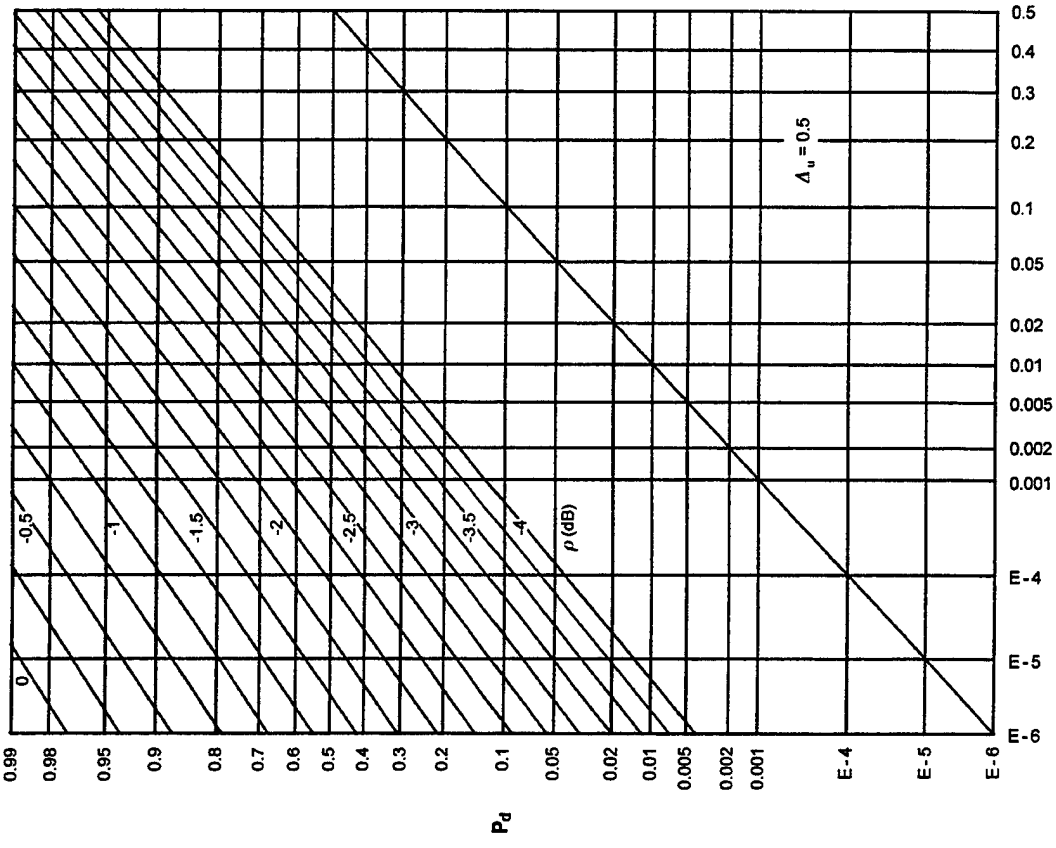

Figure G-29. ROCs for K = 8, N = 8, M = 32

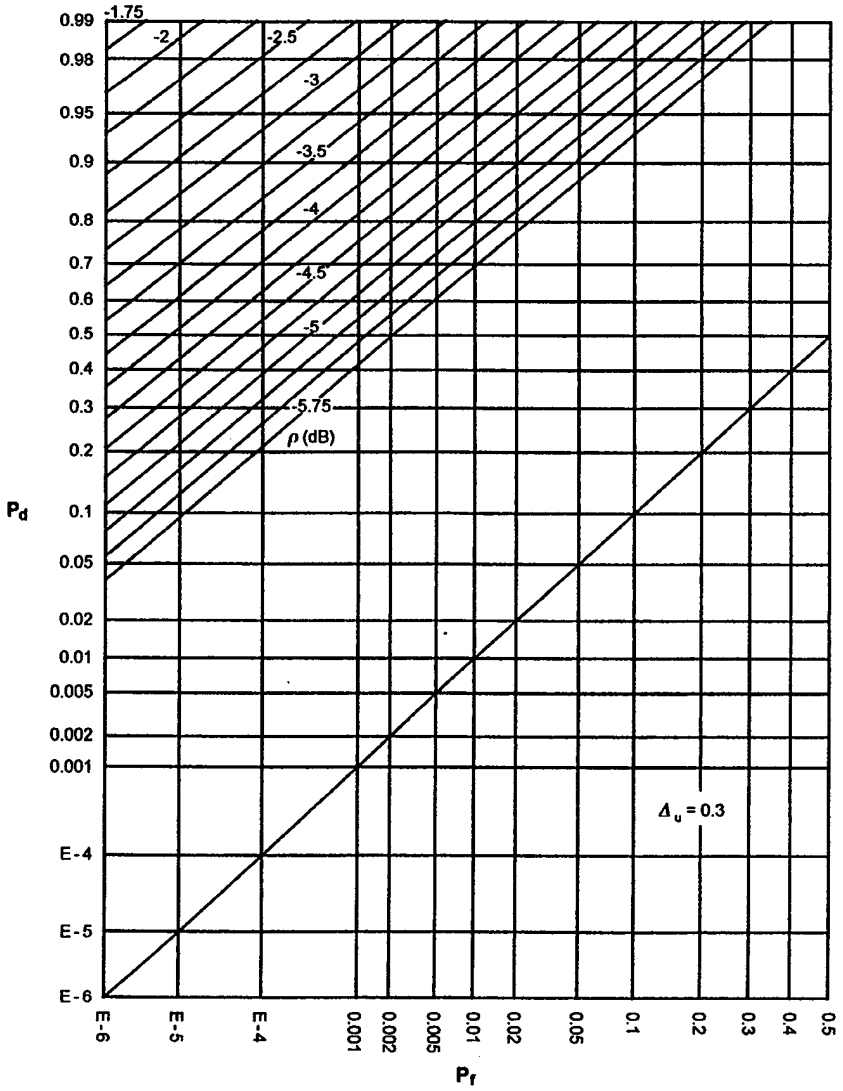

Figure G-31. ROCs for K = 8, N = 32, M = 32

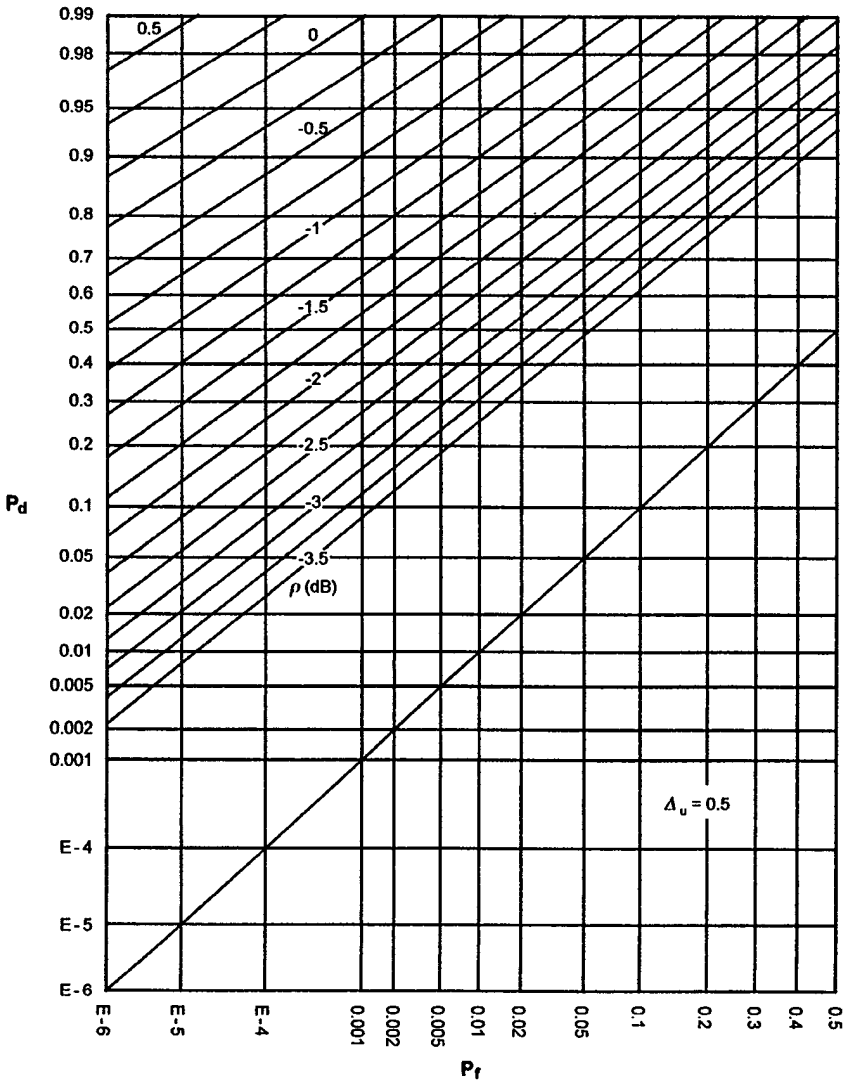

Figure G-32. ROCs for K = 4, N = 2, M = 64

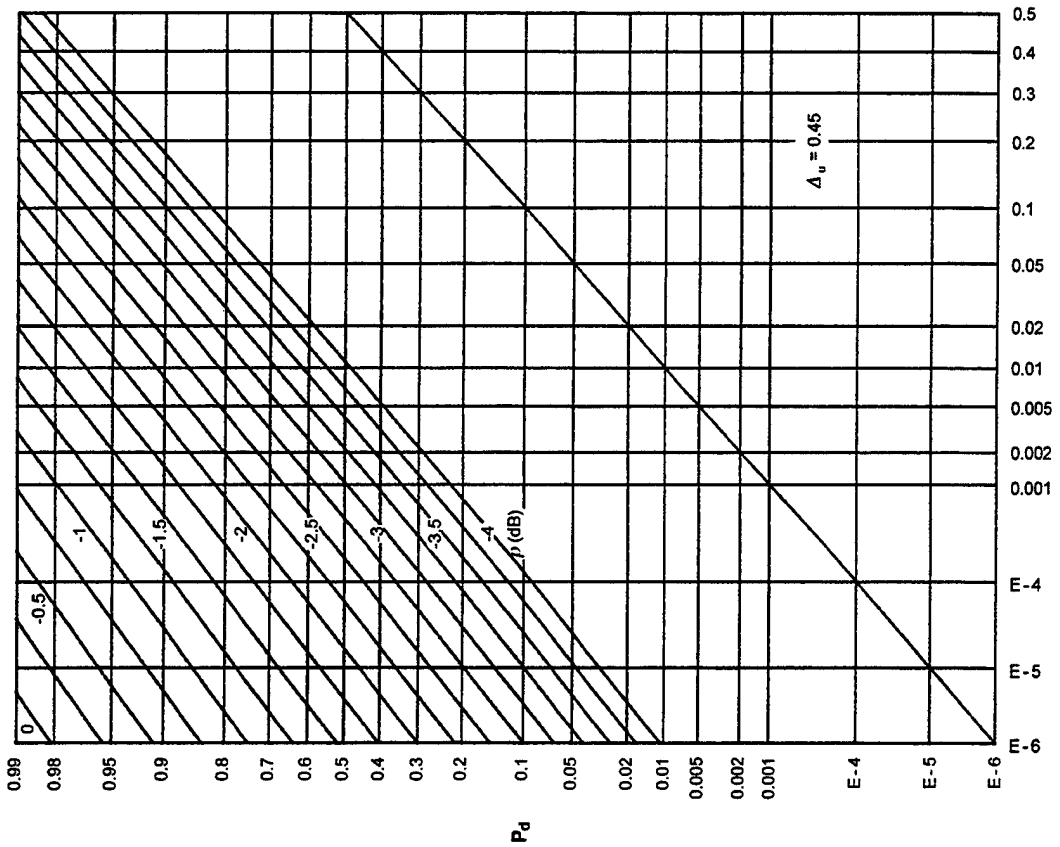

Figure G-34. ROCs for K = 4, N = 8, M = 64

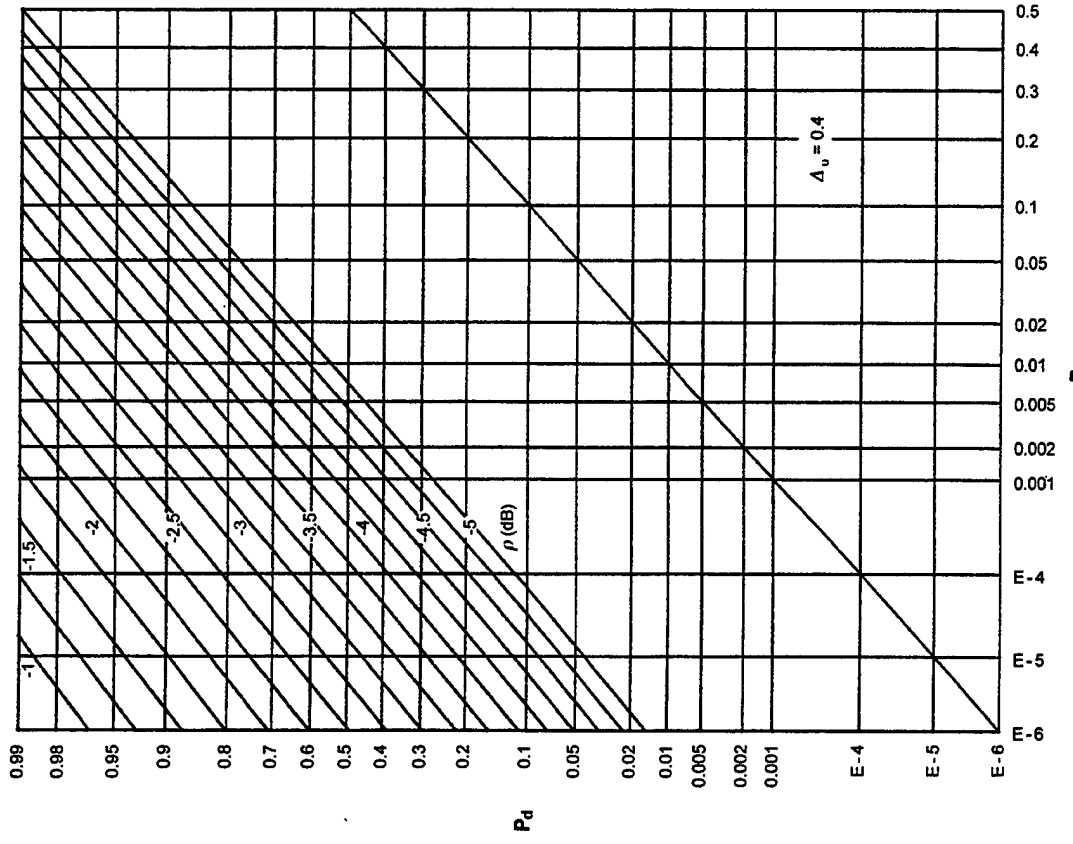

Figure G-33. ROCs for K = 4, N = 4, M = 64

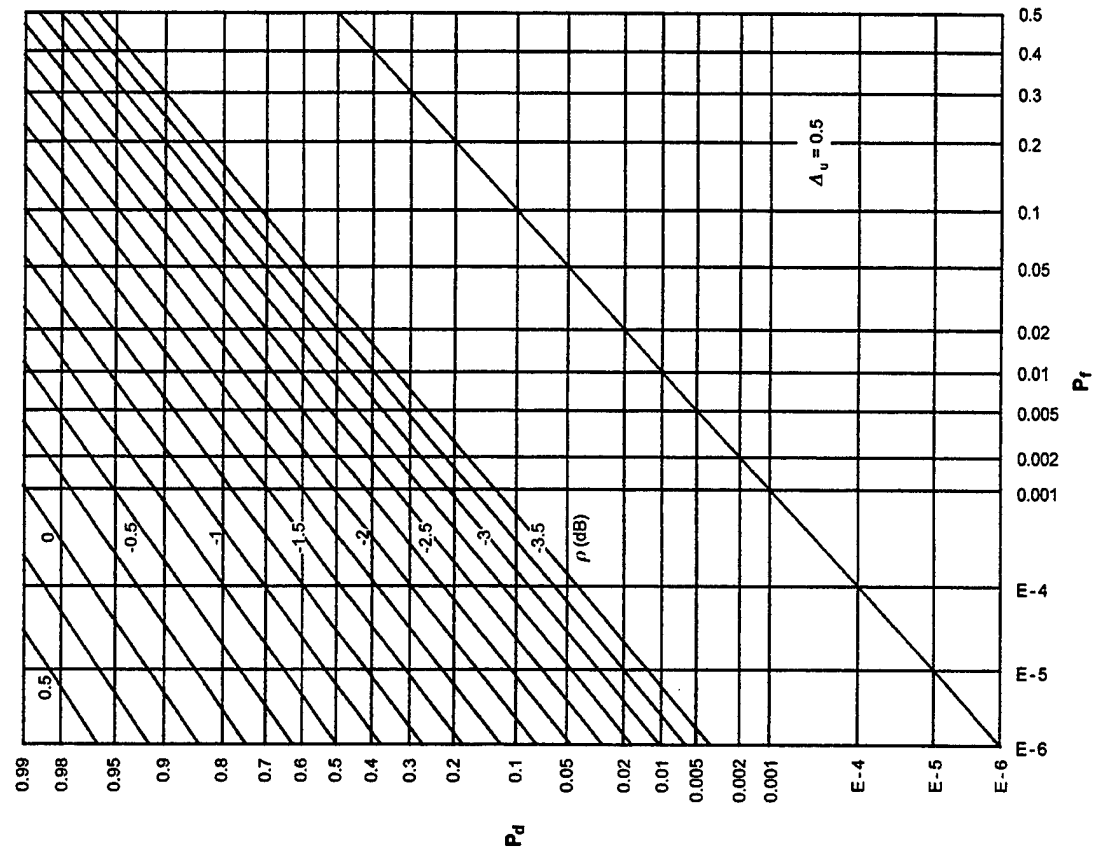

Figure G-36. ROCs for K = 4, N = 32, M = 64

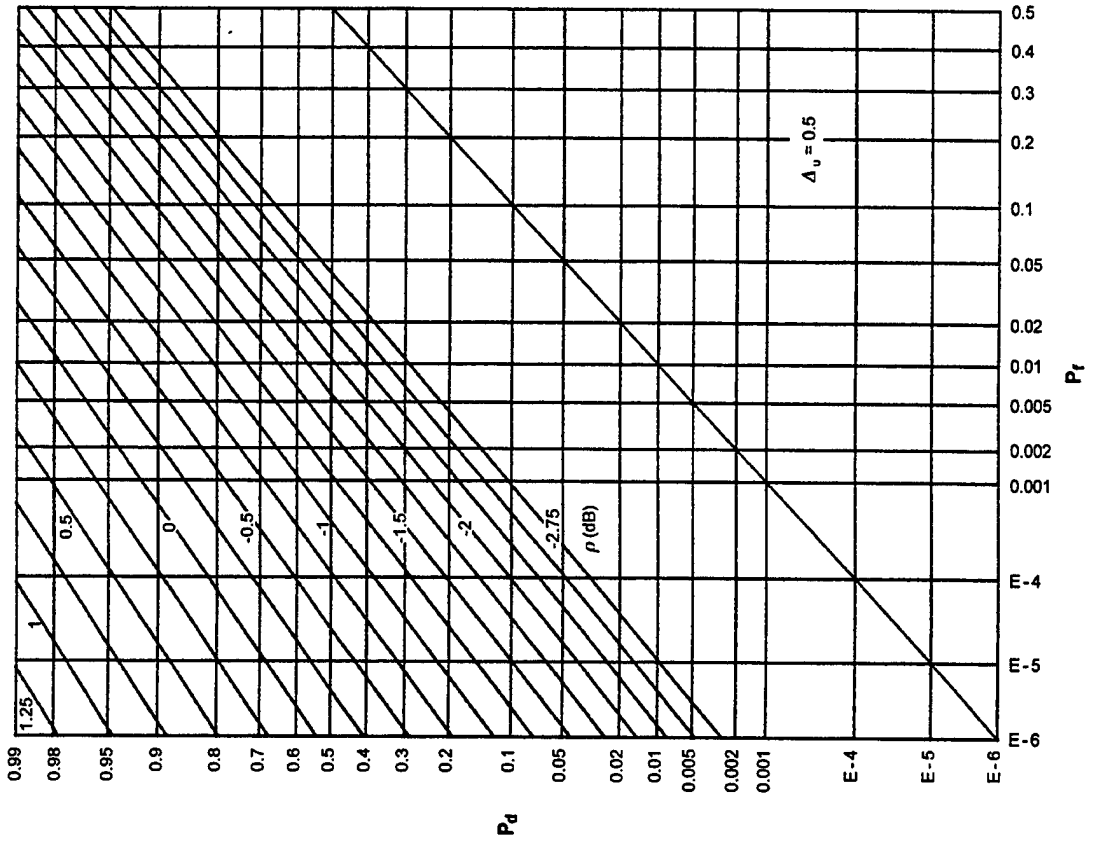

Figure G-35. ROCs for K = 4, N = 16, M = 64

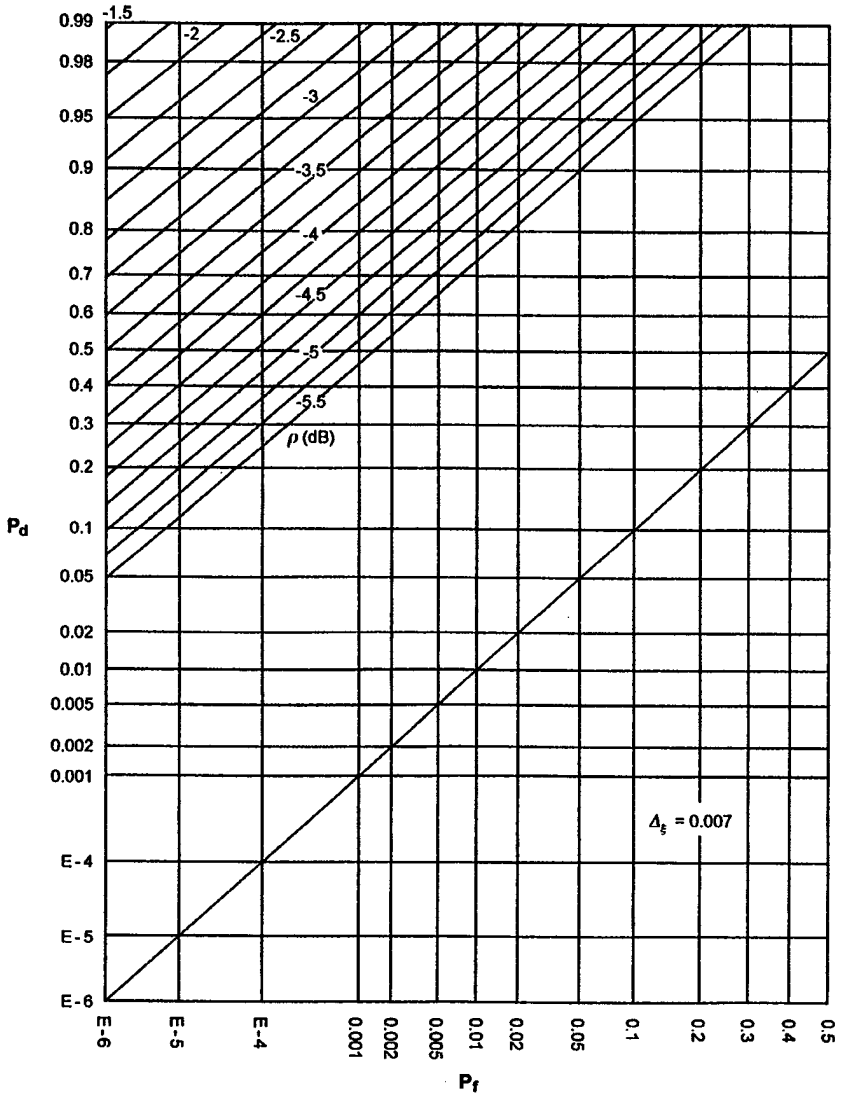

Figure G-37. ROCs for K = 2, N = 2, M = 128

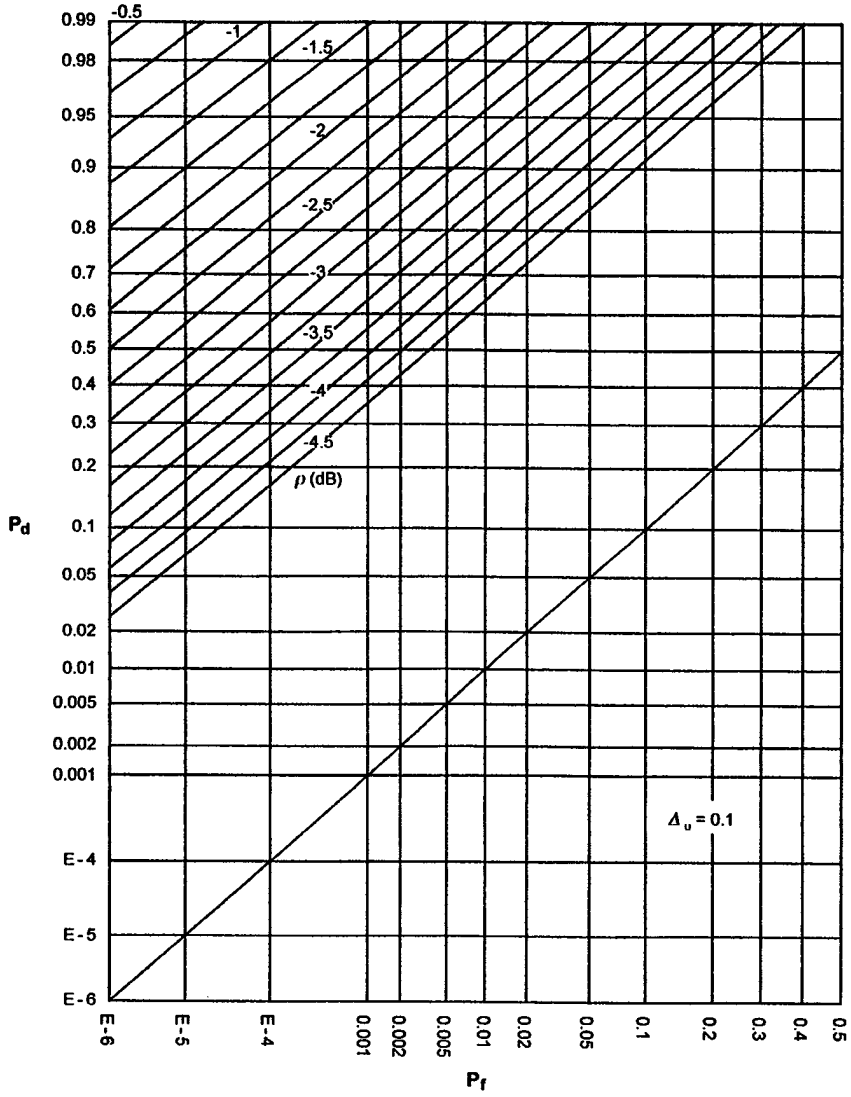

Figure G-38. ROCs for K = 2, N = 4, M = 128

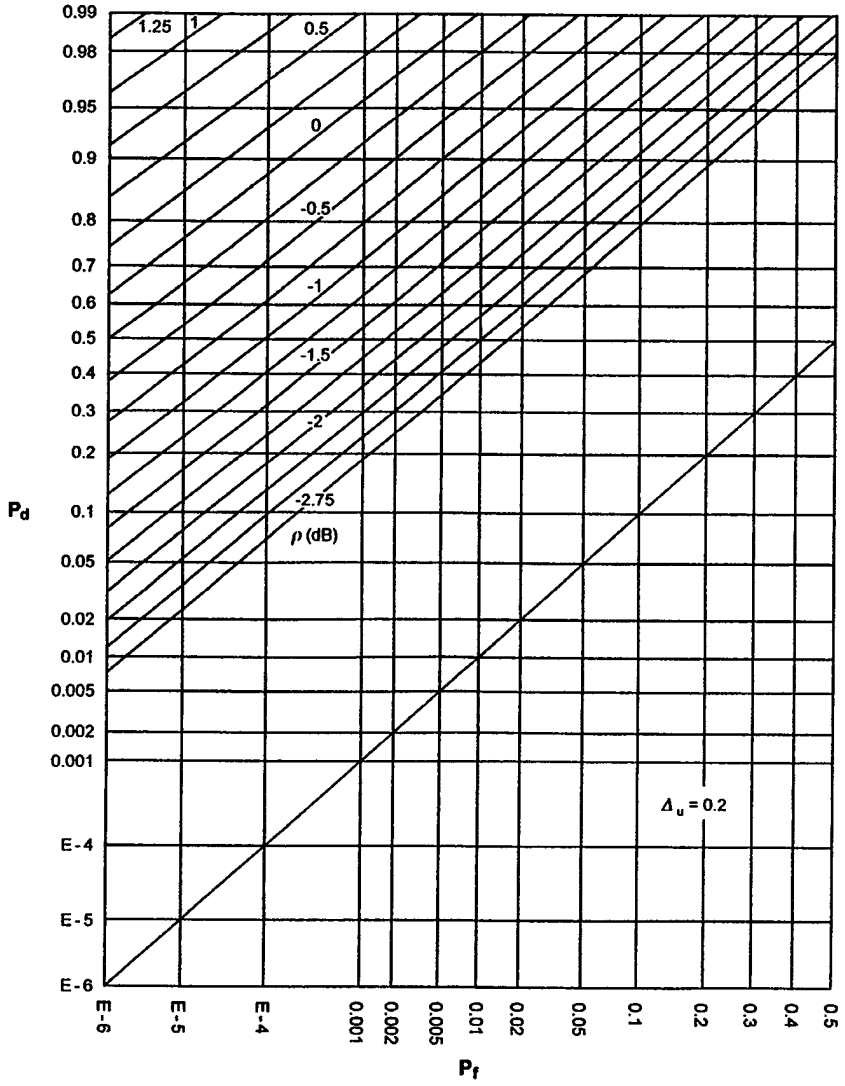

Figure G-39. ROCs for K = 2, N = 8, M = 128

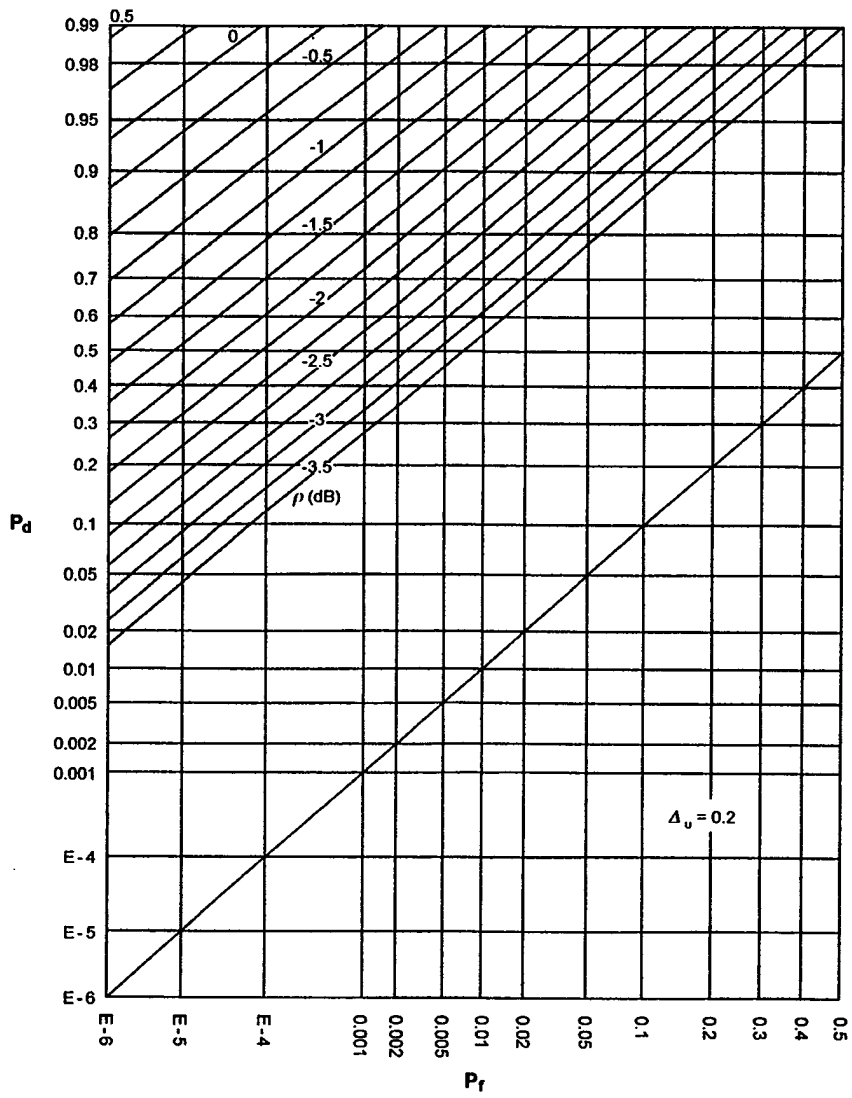

Figure G-40. ROCs for K = 2, N = 16, M = 128

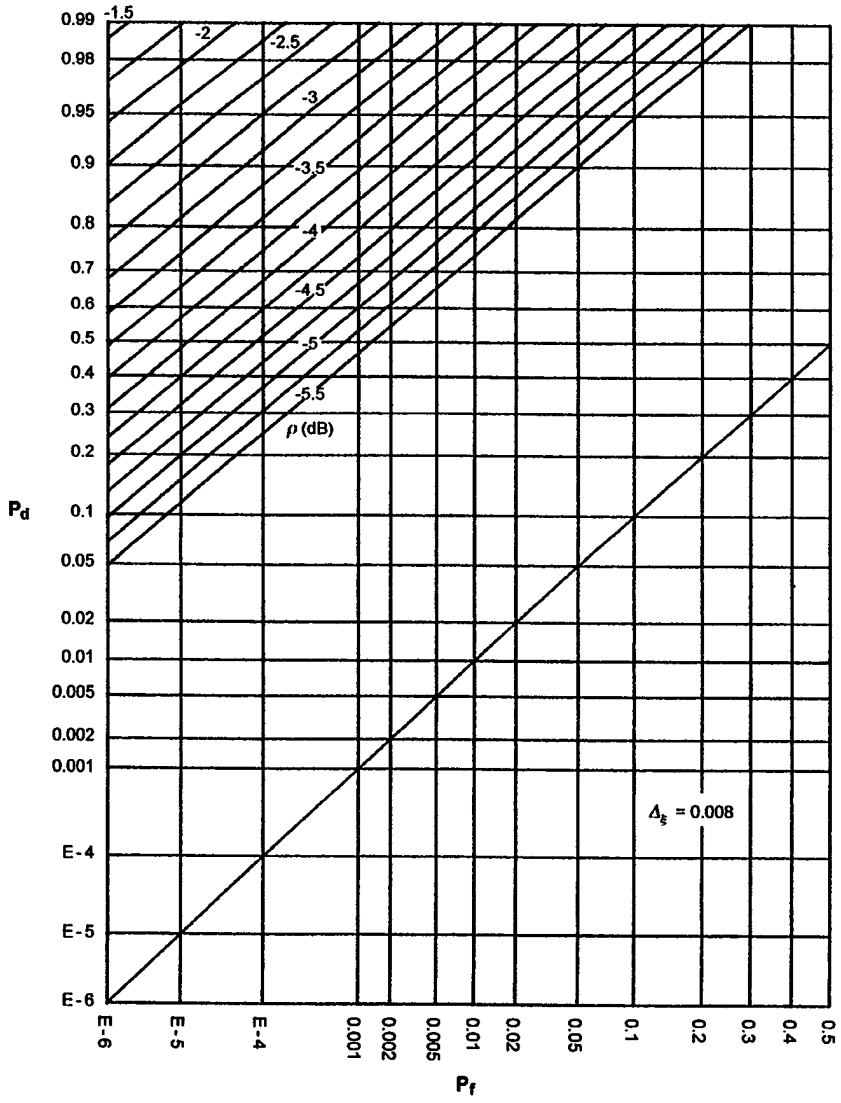

Figure G-41. ROCs for K = 2, N = 32, M = 128

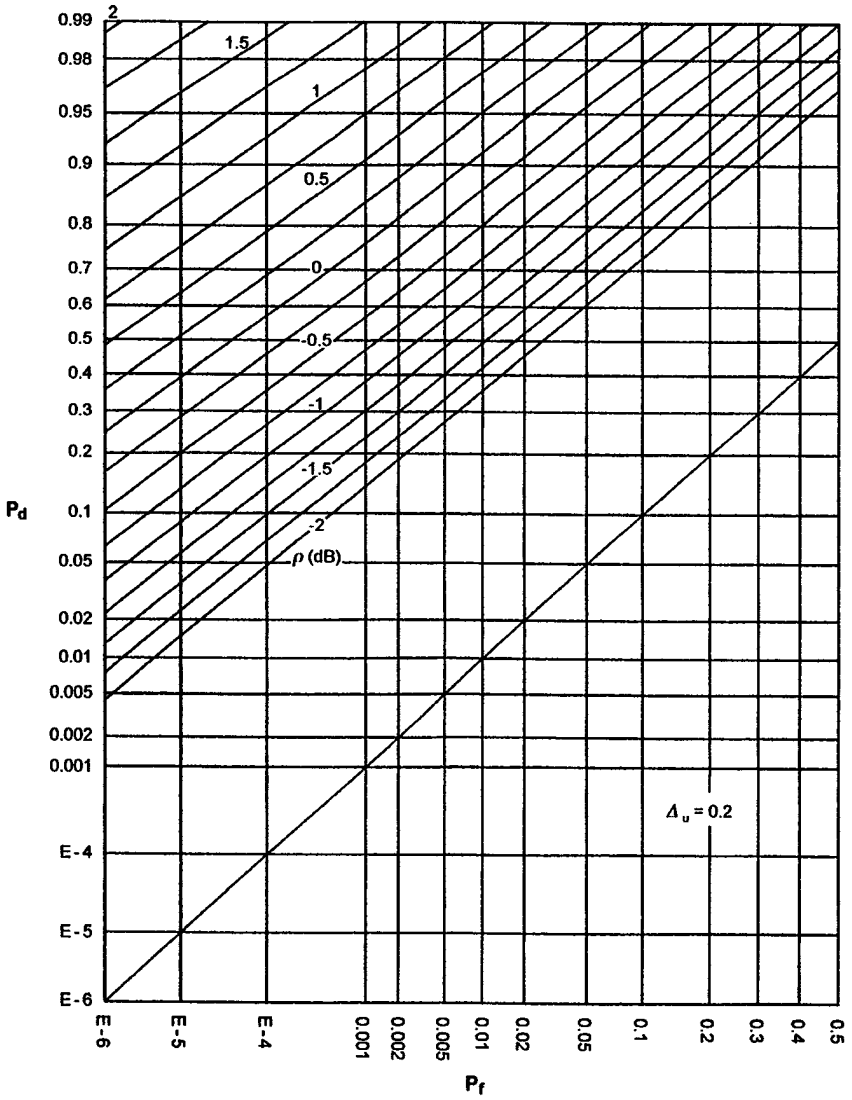

Figure G-42. ROCs for K = 1, N = 2, M = 256

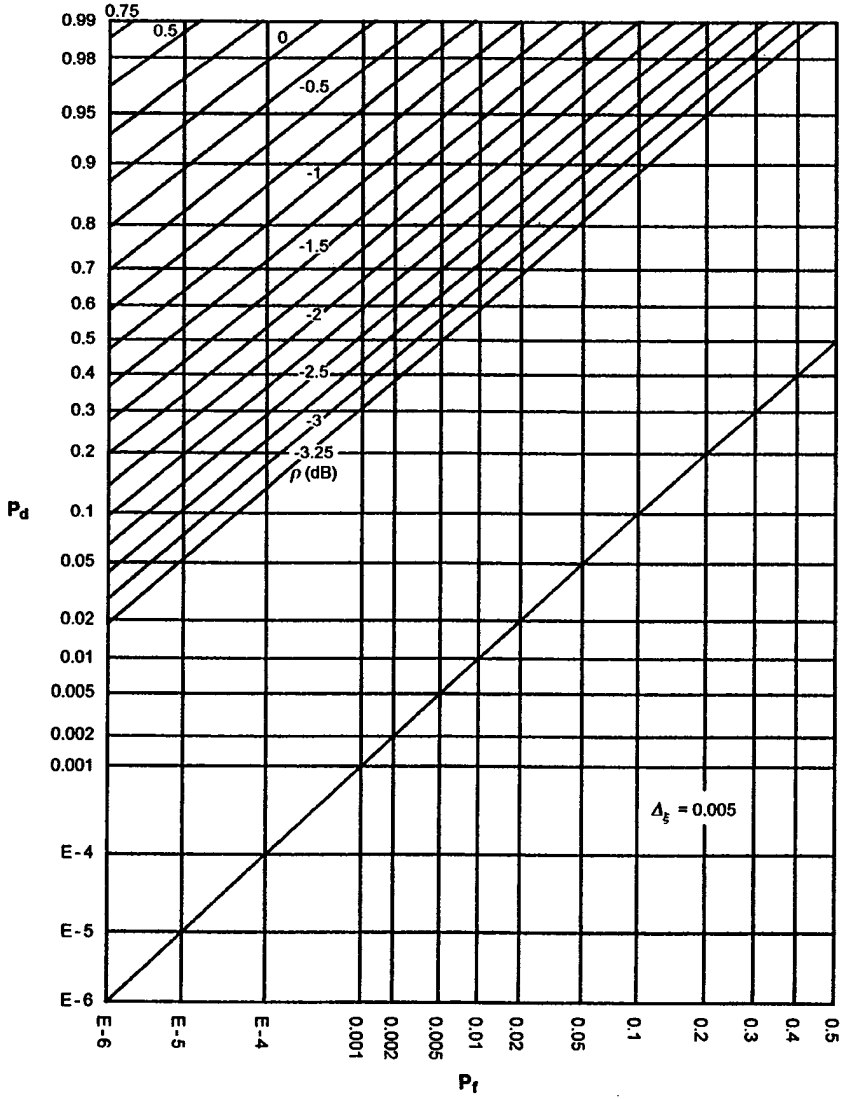

Figure G-43. ROCs for K = 1, N = 4, M = 256

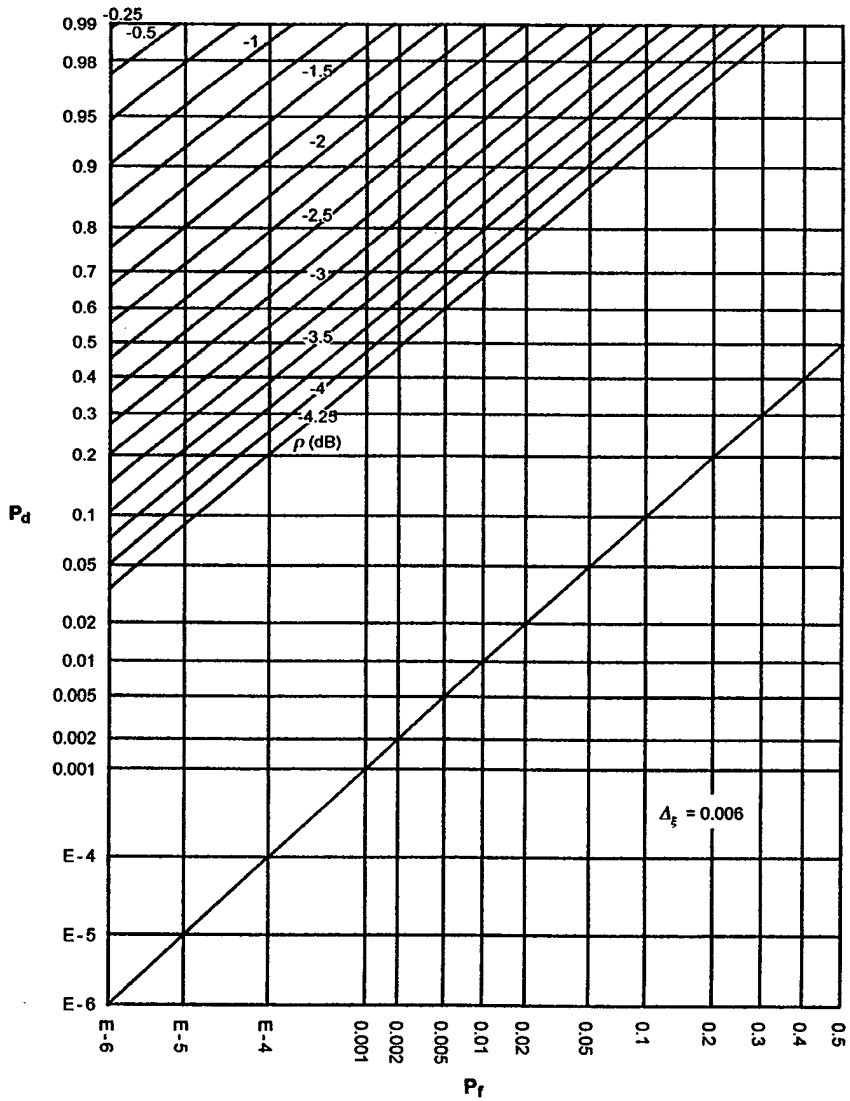

Figure G-44. ROCs for K = 1, N = 8, M = 256

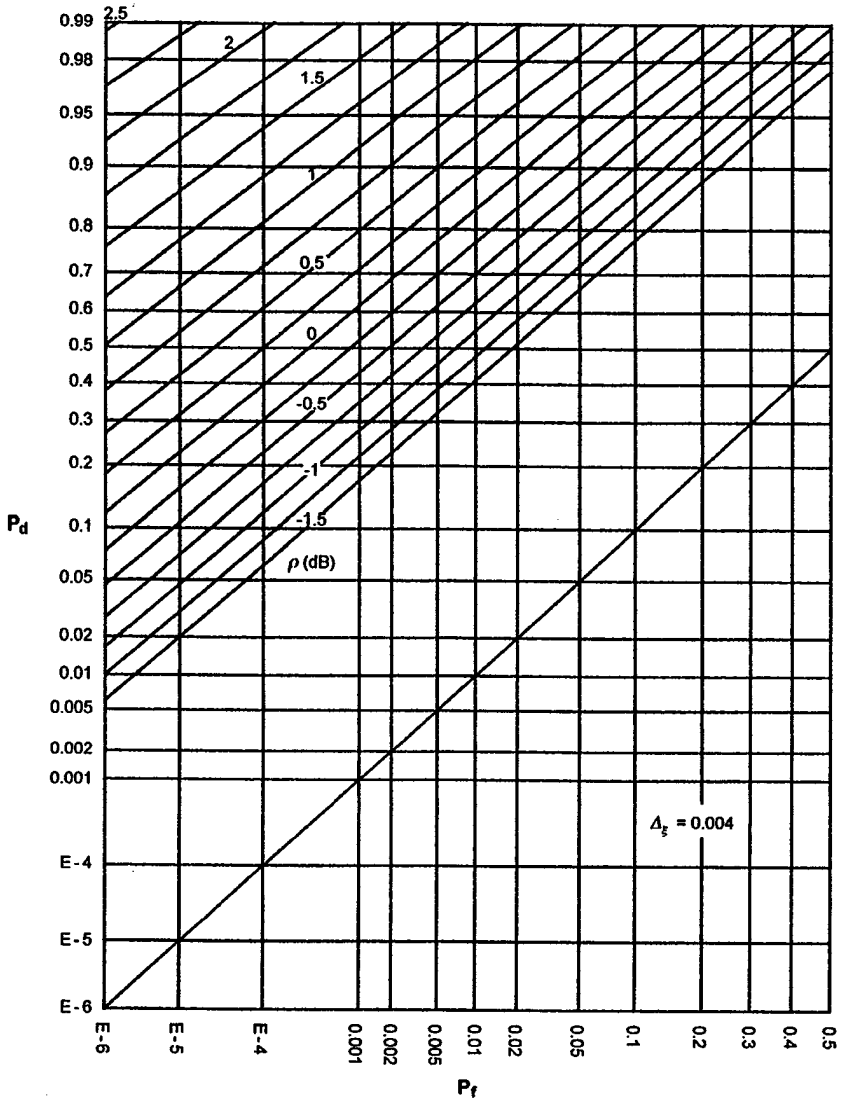

Figure G-45. ROCs for K = 1, N = 16, M = 256

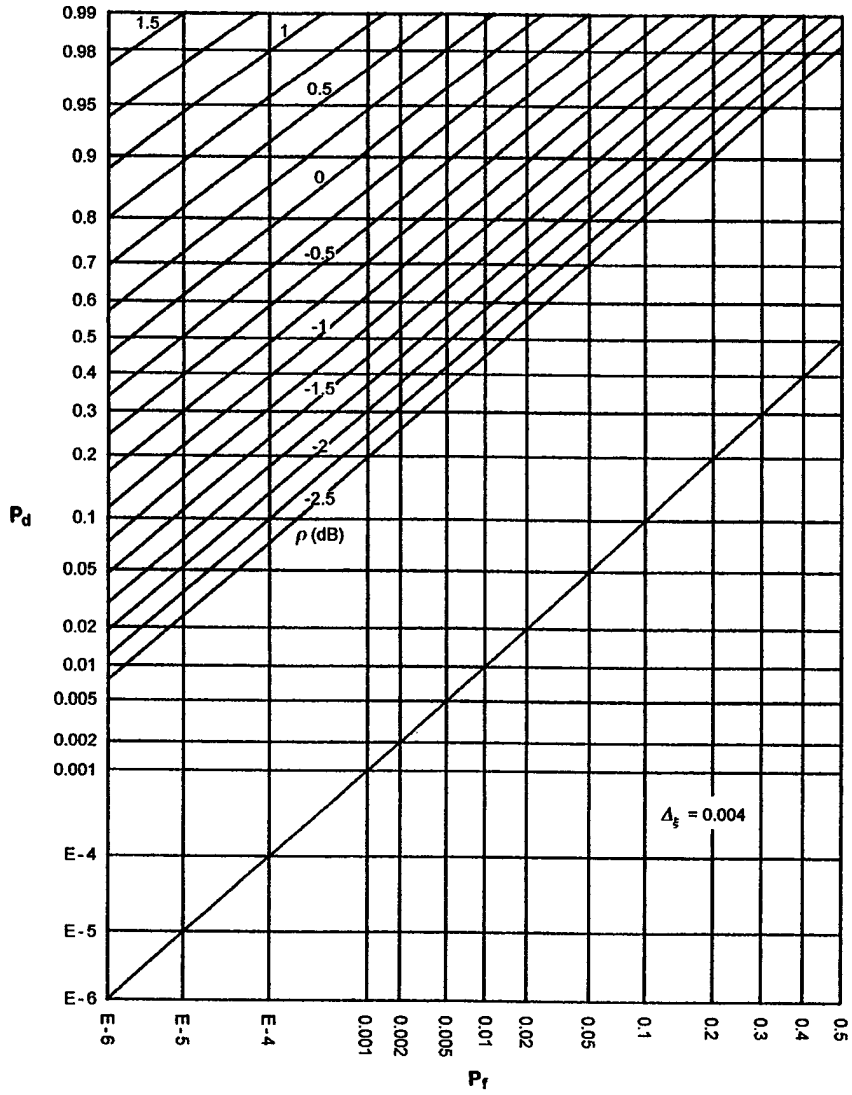

Figure G-46. ROCs for K = 1, N = 32, M = 256

APPENDIX H - STATISTICAL DEPENDENCE OF OR-ING OUTPUT v(t) AT SEPARATED TIME INSTANTS

The initial part of this appendix gives the results of a short simulation study of the covariance of the or-ing output v(t) at time separations less than K, while the second part details an analytic study of the conditional probability of the or-ing output v(t) at two separated time instants.

COVARIANCE OF OR-ING OUTPUT

The particular numerical case investigated here is K = 4, for which the pre-averager outputs are

$$y_n(t) = x_n(t) + x_n(t-1) + x_n(t-2) + x_n(t-3) \quad \text{for } 1 \le n \le N, \quad \text{(H-1)}$$

and the or-ing output is

$$v(t) = \max\{y_1(t),\ldots,y_N(t)\} \ . \quad \text{(H-2)}$$

The results of a simulation for hypothesis H_0, noise-only, using 50,000 independent trials, and using either exponential, flat, or Gaussian RVs for inputs $\{x_n(t)\}$, are listed in table H-1. For special case N = 1, no or-ing, there follows $v(t) = y_1(t)$, which is a sum of K independent inputs; then, v(t) has a simple triangular covariance function, going linearly to zero at delay I = K. This effect is confirmed by the N = 1 simulation results for the covariance coefficient in table H-1.

For larger N, where there is severe competition to get through the "greatest-of" device, there is more randomness between adjacent time values of v(t). This causes the covariance coefficients to decrease more rapidly with the time separation I. Then, it may be more costly to increase J above K/2 (roughly), at least for large N.

Under hypothesis H_1, as the input SNR increases, the one signal-bearing channel tends toward dominance of the greatest-of device; therefore, the covariance of v(t) should tend back towards the triangular shape as the input SNR increases. However, since the processor does not know whether H_0 or H_1 is prevalent, it may be operating on noise-only samples; this suggests keeping skip factor J smaller than K in order to lessen losses.

Table H-1. Estimated Covariance Coefficients for K = 4

N	I	0	1	2	3	4	
1		1	.750	.499	.250	.002	exponential
2		1	.719	.466	.231	.014	
4		1	.680	.418	.195	.007	
8		1	.643	.375	.166	.012	
1		1	.750	.501	.252	.003	flat
8		1	.536	.266	.097	-.005	
1		1	.749	.499	.248	-.002	Gaussian
8		1	.553	.278	.104	-.003	

CONDITIONAL PROBABILITY OF OR-ING OUTPUT

The following analysis makes no assumptions about the statistics of the inputs $\{x_n(t)\}$ except independence. However, the particular numerical example considered will presume zero-mean Gaussian noise; although not done here, the extension to signal-present is obvious. The parameters M and J are not relevant here, because post-averaging is not yet of concern at the or-ing output v(t).

The pre-averager outputs in the n-th channel at two separated time instants K and K+I are

$$y_n(K) = x_n(1) + \cdots + x_n(K) ,$$

$$y_n(K+I) = x_n(1+I) + \cdots + x_n(K+I) . \qquad \text{(H-3)}$$

The integer variable I lies in the range $0 \leq I \leq K$ for this analysis. Therefore, the covariance coefficient between pre-averager outputs $y_n(K)$ and $y_n(K+I)$ is $\rho_y(I) = 1 - I/K$.

The corresponding or-ing outputs are

$$v(K) = \max\{y_1(K), \ \ldots \ , y_N(K)\} =$$

$$= \max\{x_1(1) + \cdots + x_1(K), \ \ldots \ , x_N(1) + \cdots + x_N(K)\} \qquad \text{(H-4)}$$

and

$$v(K+I) = \max\{y_1(K+I), \ \ldots \ , y_N(K+I)\} =$$

$$= \max\{x_1(1+I) + \cdots + x_1(K+I), \ \ldots \ , x_N(1+I) + \cdots + x_N(K+I)\} \ . \quad \text{(H-5)}$$

At this point, define three disjoint subsequences

$$A_n = x_n(1) + \cdots + x_n(I) \ ,$$

$$B_n = x_n(I+1) + \cdots + x_n(K) \ ,$$

$$C_n = x_n(K+1) + \cdots + x_n(K+I) \ . \quad \text{(H-6)}$$

Since the inputs are independent and the sequences are disjoint, every RV $\{A_1, B_1, C_1, \ldots , A_N, B_N, C_N\}$ is independent of every other one.

Let p_K and c_K be the PDF and CDF, respectively, of pre-averager output $y_n(t)$ when it is composed of K terms, as in equation (H-3). Then, the joint cumulative probability of the two or-ing outputs (H-4) and (H-5) is

$$\Pr\{v(K) < \alpha, \ v(K+I) < \beta\} =$$

$$= \Pr\{A_1+B_1<\alpha, \ldots, A_N+B_N<\alpha, \ B_1+C_1<\beta, \ldots, B_N+C_N<\beta\} =$$

$$= [\Pr\{A_1+B_1<\alpha, \ B_1+C_1<\beta\}]^N = [\int du \ p_{K-I}(u) \ c_I(\alpha-u) \ c_I(\beta-u)]^N . \quad \text{(H-7)}$$

At the same time, the ordinary first-order CDF is

$$\Pr\{v(K)<\alpha\} = [c_K(\alpha)]^N \ . \quad \text{(H-8)}$$

Therefore, the conditional probability of interest is

$$\Pr\{v(K+I)<\beta \,|\, v(K)<\alpha\} = \left(\frac{\int du\ p_{K-I}(u)\ c_I(\alpha-u)\ c_I(\beta-u)}{c_K(\alpha)} \right)^N \equiv [Q(\alpha,\beta)]^N \tag{H-9}$$

This physically-meaningful measure of dependence needs only one integral evaluation once PDF p_K and CDF c_K are available. (By contrast, the covariance coefficient of v(t) requires much more numerical effort.) Notice that this conditional probability goes to zero as $N \to \infty$, that is, as the amount of or-ing increases, regardless of the value of separation $I > 0$. Thus, increased competition at the or-ing input leads to more independent or-ing outputs, even for $I = 1$, an adjacent time sample.

As checks on this result, for $I = 0$, then $A_n = 0$, $C_n = 0$, $p_0(u) = \delta(u)$, $c_0(u) = U(u)$, and there follows

$$Q(\alpha,\beta) = \frac{c_K(\min\{\alpha,\beta\})}{c_K(\alpha)} = \begin{Bmatrix} 1 & \text{for } \beta \geq \alpha \\ c_K(\beta)/c_K(\alpha) & \text{for } \beta \leq \alpha \end{Bmatrix} . \tag{H-10}$$

On the other hand, for $I = K$, there follows

$$p_{K-I}(u) = p_0(u) = \delta(u)\ , \quad Q(\alpha,\beta) = \frac{c_K(\alpha)\ c_K(\beta)}{c_K(\alpha)} = c_K(\beta)\ . \tag{H-11}$$

Both of these special cases are obviously correct.

As a numerical example, consider zero-mean unit-variance Gaussian noises $\{x_n(t)\}$. Then,

$$p_I(u) = \frac{1}{(2\pi I)^{\frac{1}{2}}} \exp\left(-\frac{u^2}{2I}\right) , \quad c_I(u) = \Phi\left(\frac{u}{\sqrt{I}}\right) ,$$

$$Q(\alpha,\beta) = \frac{1}{\Phi(\alpha/\sqrt{K})} \int dt\ \phi(t)\ \Phi\left(\frac{\alpha-(K-I)^{\frac{1}{2}}t}{\sqrt{I}}\right)\ \Phi\left(\frac{\beta-(K-I)^{\frac{1}{2}}t}{\sqrt{I}}\right) . \quad \text{(H-12)}$$

A couple of numerical examples of conditional probability (H-9) follow, which confirm the increased statistical dependence as separation I tends to zero.

$\alpha=1$, $\beta=1$, $K=4$:

I	1	2	3	4
$Q(\alpha,\beta)$	.854	.790	.738	.691

$\alpha=2$, $\beta=2$, $K=10$:

I	1	2	3	4	5	6	7	8	9	10
$Q(\alpha,\beta)$	.920	.887	.861	.838	.818	.800	.783	.767	.751	.736

APPENDIX I - MATLAB PROGRAM FOR EVALUATION OF ROCs FOR RANDOM GAUSSIAN SIGNAL

The parameters of interest are entered at the top of the program listed here. The sampling increment du is applied directly to the PDF of v(t) and controls the spacing of the aliasing lobes in the calculated CF of v(t). If the lobes are too close, yielding significant aliasing in the CF domain, the value of du must be decreased. The range of input SNR values to be investigated is governed by rmin and rinc.

For each input SNR value (isnr), the magnitude of the CF of v(t) is first plotted, so that the aliasing lobes can be viewed; if the lobes are too close, du must be decreased and the CF rerun. When satisfactory CF lobe spacing has been achieved, calculations continue with the corresponding EDF of w(t), which is plotted. If aliasing is a problem in this EDF domain, the size n of the FFT must be increased. Finally, when satisfactory values of du and n have been realized for all values of SNR of interest, the ROCs, namely, P_d versus P_f, are plotted for all the input SNR values considered.

To find the required input SNR necessary to achieve a specified P_f and P_d, these probability values must then be entered, along with the number of the ROC that is closest to the operating point of interest. Linear interpolation is conducted, and the required input SNR is printed out.

```
clear, clf                % NUWC TR 11,150
b=0;          % Additive bias to w
du=.1;        % Sampling increment in u
n=2^12;       % FFT size
kc=4;         % K, amount of pre-averaging
nc=1;         % N, amount of or-ing
mc=1;         % M, amount of post-averaging
rmin=-3;      % Minimum SNR (dB)
rinc=1;       % Increment in SNR (dB)
num=17;       % Number of ROCs
disp('b du n; kc nc mc:')
disp([b du n; kc nc mc])
xg=[1e-6 1e-5 1e-4 .001 .002 .005 .01 .02...
.05 .1 .2 .3 .4 .5];
yg=[1e-6 1e-5 1e-4 .001 .002 .005 .01 .02...
.05 .1 .2 .3 .4 .5 .6 .7 .8 .9 .95 .98 .99];
xg=phiinv(xg);
yg=phiinv(yg);
[Xg,Yg]=meshgrid(xg,yg);
Magcf=zeros(n,1);
EDF=zeros(n,1);
Pd=zeros(n,num+1);
n1=n-1; n2=n/2; kc1=kc-1; nc1=nc-1; n3=n2+1;
pn=pi/n; d2=du/2;
arg=pn.*(1:n2)';
sinc=sin(arg)./arg;
disp('          isnr   edf0 - 1')
for isnr=0:num
    rhodb=rmin+rinc*(isnr-1);
    rho=10^(.1*rhodb);
    if(isnr==0) rho=0; end
    as=1/(1+rho);
    X=zeros(n,1)+i*zeros(n,1);
    meanv=0; cdfk=0; k=-1;
    while(cdfk<.5 | area>1e-20)
        k=k+1; uk=du*k; u2=uk+d2;
        au=as*u2; p0=exp(-u2); e0=p0;
        p1=exp(-au); e1=p1;
        for j=1:kc1
            p0=p0*u2/j; e0=e0+p0;
            p1=p1*au/j; e1=e1+p1;
        end
        c0=max(1-e0,0); c1=max(1-e1,0);
```

```
        cdfo=cdfk; cdfk=c1*c0^nc1;
        area=cdfk-cdfo;
        j=mod(k,n);
        X(j+1)=X(j+1)+area;
        meanv=meanv+area*uk; % uk, not u2
    end
    X=fftgreen(X);
    Magcf=log10(X.*conj(X)+1e-50)*.5;
    plot(Magcf)
    axis([1 n+1 -16 0]); grid on
    pause(1)
    dxi=2*pi/(n*du);
    X(2:n3)=conj(X(2:n3))./sinc(1:n2);
    X(n2+2:n)=0;
    X=X.^mc;
    X(1:n3)=X(1:n3).*exp(i*b*dxi*(0:n2)');
    meanw=meanv*mc+b;
    X(1)=0;
    X(2:n3)=X(2:n3)./(1:n2)';
    X=fftgreen(X);
    a=.5+meanw/(n*du);
    edf0=a+imag(X(1))/pi;
    disp([isnr edf0-1])
    k=(1:n)';
    edf=a-(k-1)./n+imag(X(k))./pi;
    X=edf;
    EDF=log10(abs(edf)+1e-30);
    plot(EDF)
    axis([1 n+1 -18 0]); grid on
    pause(1)
    edf=real(X(k));
    edf=min(edf,1-1e-12);
    edf=max(edf,1e-12);
    Pd(:,isnr+1)=phiinv(edf);
end
beep
pause
clf
hold on
set(gcf,'PaperPosition',[.25 .25 8 10.5])
plot(xg,Yg,'k')
plot(Xg,yg,'k')
plot(xg,xg,'k') % zero SNR ROC
```

```
plot(Pd(:,1),Pd(:,[2:num+1]),'k')
axis([xg(1) xg(14) yg(1) yg(21)])
axis off
while 1
    T=input('pf pd isnr: ');
    if T(1)==0 break; end
    pft=phiinv(T(1));
    pdt=phiinv(T(2));
    isnr=T(3);
    for j=0:n1
        if(Pd(j+1,1)<pft) break; end
    end
    x1=Pd(j+1,1);
    x2=Pd(j,1);
    as=Pd(j+1,isnr+1);
    bs=Pd(j+1,isnr+2);
    cs=Pd(j,isnr+1);
    ss=(cs-as)/(x2-x1);
    a1=pdt-ss*pft;
    fs=(a1+ss*x1-as)/(bs-as);
    rc=rmin+rinc*(isnr-1+fs);
    disp([T fs rc])
end

%   function y=phiinv(x)  for  0 < x < 1
%   y=1.414213562373095*erfinv(2*x-1);
```

REFERENCES

1. A. H. Nuttall, "Signal-to-Noise Ratio Requirements for Greatest-Of Device Followed by Integrator," NUSC Technical Memorandum TC-13-75, Naval Underwater Systems Center, New London, CT, 24 July 1975.

2. A. H. Nuttall, "Input Deflection Requirements for Quantizers Followed by Greatest-Of Device and Integrator," NUSC Technical Memorandum 781174, Naval Underwater Systems Center, New London, CT, 24 August 1978.

3. A. H. Nuttall, "Detection Performance Characteristics for a System with Quantizers, Or-ing, and Accumulator," NUSC Technical Report 6815, Naval Underwater Systems Center, New London, CT, 1 October 1982.

4. A. H. Nuttall, "Detection Performance Characteristics for a System with Quantizers, Or-ing, and Accumulator," Journal of Acoustical Society of America, volume 73, number 5, pages 1631 - 1642, May 1983.

5. A. H. Nuttall, "Operating Characteristics of an Or-ing and Selection Processor with Pre- and Post-Averaging," NUSC Technical Report 6929, Naval Underwater Systems Center, New London, CT, 4 May 1983. (Also NUSC Technical Report 6929A, 7 January 1987.)

6. A. H. Nuttall, "Operating Characteristics for Indicator Or-ing of Incoherently-Combined Matched-Filter Outputs," NUSC Technical Report 8121, Naval Underwater Systems Center, New London, CT, 21 September 1987.

7. A. H. Nuttall, "Required Threshold Settings and Signal-to-Noise Ratios for Combined Normalization and Or-ing,"

NUSC Technical Report 8865, Naval Underwater Systems Center, New London, CT, 10 April 1991.

8. "A Common Methodology for the Calculation of Recognition Differentials," Volume 2, 15 August 1996, PMW 182, Space and Naval Warfare Systems Command, Arlington, VA. See Appendix O, "An Experiment in ORing Loss" by C. N. Pryor, 26 December 1995.

9. A. H. Nuttall, "Accurate Efficient Evaluation of Cumulative or Exceedance Probability Distributions Directly From Characteristic Functions," NUSC Technical Report 7023, Naval Underwater Systems Center, New London, CT, 1 October 1983.

10. **Handbook of Mathematical Functions**, U.S. Department of Commerce, National Bureau of Standards, Applied Mathematics Series, number 55, U.S. Government Printing Office, Washington, DC, June 1964.

11. I. S. Gradshteyn and I. M. Ryzhik, **Table of Integrals, Series, and Products**, Academic Press, Inc., New York, NY, 1980.

12. A. H. Nuttall, "Some Integrals Involving the Q_M-Function," NUSC Technical Report 4755, Naval Underwater Systems Center, New London, CT, 15 May 1974.

13. A. H. Nuttall, "Evaluation of Densities and Distributions via Hermite and Generalized Laguerre Series Employing High-Order Expansion Coefficients Determined Recursively via Moments or Cumulants," NUSC Technical Report 7377, Naval Underwater Systems Center, New London, CT, 28 February 1985.

INITIAL DISTRIBUTION LIST

Addressee	No. of Copies
Center for Naval Analyses, VA	1
Coast Guard Academy, CT	
J. Wolcin	1
Commander Submarine Force, U.S. Pacific Fleet, HI	
W. Mosa, CSP N72	1
Defense Technical Information Center	2
Griffiss Air Force Base, NY	
Documents Library	1
J. Michels	1
Hanscom Air Force Base, MA	
M. Rangaswamy	1
National Radio Astronomy Observatory, VA	
F. Schwab	1
National Security Agency, MD	
J. Maar	1
National Technical Information Service, VA	10
Naval Air Warfare Center, PA	
L. Allen	1
Naval Command Control and Ocean Surveillance Center, CA	
J. Alsup	1
W. Marsh	1
Naval Environmental Prediction Research Facility, CA	1
Naval Intelligence Command, DC	1
Naval Oceanographic and Atmospheric Research Laboratory, CA	
M. Pastore	1
Naval Oceanographic and Atmospheric Research Laboratory, MS	
B. Adams	1
R. Fiddler	1
E. Franchi	1
R. Wagstaff	1
Naval Oceanographic Office, MS	1
Naval Personnel Research and Development Center, CA	1
Naval Postgraduate School, CA	
Superintendent	1
C. Therrien	1
Naval Research Laboratory, DC	
W. Gabriel	1
D. Steiger	1
E. Wald	1
N. Yen	1
Naval Surface Warfare Center, FL	
E. Linsenmeyer	1
D. Skinner	1
Naval Surface Warfare Center, MD	
P. Prendergast	1
Naval Surface Warfare Center, VA	
J. Gray	1
Naval Technical Intelligence Center, DC	
Commanding Officer	1
D. Rothenberger	1
Naval Undersea Warfare Center, FL	
Officer in Charge	1

INITIAL DISTRIBUTION LIST (Cont'd)

Addressee	No. of Copies
Naval Weapons Center, CA	1
Office of the Chief of Naval Research, VA	
ONR 321 (D. Johnson)	1
ONR 321US (N. Harned)	1
ONR 322 (R. Tipper)	1
ONR 334 (P. Abraham)	1
Office of Naval Research	
ONR 31 (R. R. Junker)	1
ONR 311 (A. M. van Tilborg)	1
ONR 312 (M. N. Yoder)	1
ONR 313 (N. L. Gerr)	1
ONR 32 (S. E. Ramberg	1
ONR 321 (F. Herr)	1
ONR 322 (M. Briscoe)	1
ONR 33 (S. G. Lekoudis)	1
ONR 334 (A. J. Tucker)	1
ONR 342 (W. S. Vaughan)	1
ONR 343 (R. Cole)	1
ONR 362 (M. Sponder)	1
Program Executive Office, Undersea Warfare (ASTO), VA	
J. Thompson, A. Hommel, R. Zarnich	3
Space and Naval Warfare Systems Command, DC	
LCDR R. Holland	1
U.S. Air Force, Maxwell Air Force Base, AL	
Air University Library	1
U.S. Department of Commerce, CO	
A. Spaulding	1
Vandenberg Air Force Base, CA	
CAPT R. Leonard	1
Brown University, RI	
Documents Library	1
Catholic University of America, DC	
J. McCoy	1
Drexel University, PA	
S. Kesler	1
Duke University, NC	
J. Krolik	1
Harvard University, MA	
Gordon McKay Library	1
Johns Hopkins University, Applied Physics Laboratory, MD	
H. M. South	1
T. N. Stewart	1
Lawrence Livermore National Laboratory, CA	
L. Ng	1
Los Alamos National Laboratory, NM	1
Marine Biological Laboratory, MA	
Library	1
Massachusetts Institute of Technology, MA	
Barker Engineering Library	1
Massachusetts Institute of Technology, Lincoln Laboratory, MA	
V. Premus	1
J. Ward	1

INITIAL DISTRIBUTION LIST (Cont'd)

Addressee	No. of Copies
Northeastern University, MA	
C. Nikias	1
Pennsylvania State University, Applied Research Laboratory, PA	
R. Hettche	1
E. Liszka	1
F. Symons	1
Princeton University, NJ	
S. Schwartz	1
Rutgers University, NJ	
S. Orfanidis	1
San Diego State University, CA	
F. Harris	1
Sandia National Laboratory, NM	
J. Claasen	1
Scripps Institution of Oceanography, Marine Physical Laboratory, CA	
Director	1
Syracuse University, NY	
D. Weiner	1
United Engineering Center, NY	
Engineering Societies Library	1
University of Colorado, CO	
L. Scharf	1
University of Connecticut, CT	
Wilbur Cross Library	1
C. Knapp	1
P. Willett	1
University of Florida, FL	
D. Childers	1
University of Hartford	
Science and Engineering Library	1
University of Illinois, IL	
D. Jones	1
University of Illinois at Chicago, IL	
A. Nehorai	1
University of Massachusetts, MA	
C. Chen	1
University of Michigan, MI	
Communications and Signal Processing Laboratory	1
W. Williams	1
University of Minnesota, MN	
M. Kaveh	1
University of Rhode Island, RI	
Library	1
G. Boudreaux-Bartels	1
S. Kay	1
D. Tufts	1
University of Rochester, NY	
E. Titlebaum	1
University of Southern California, CA	
W. Lindsey	1
A. Polydoros	1

INITIAL DISTRIBUTION LIST (Cont'd)

Addressee	No. of Copies
University of Texas, TX	
Applied Research Laboratory	1
C. Penrod	1
University of Washington, WA	
Applied Physics Laboratory	1
D. Lytle	1
J. Ritcey	1
R. Spindel	1
Villanova University, PA	
M. Amin	1
Woods Hole Oceanographic Institution, MA	
Director	1
T. Stanton	1
Yale University, CT	
Kline Science Library	1
P. Schultheiss	1
Analysis and Technology, CT	
Library	1
Analysis and Technology, VA	
D. Clark	1
Atlantic Aerospace Electronics Corp.	
R. Stahl	1
Bell Communications Research, NJ	
D. Sunday	1
Berkeley Research, CA	
S. McDonald	1
Bolt, Beranek, and Newman, CT	
P. Cable	1
Bolt, Beranek, and Newman, MA	
H. Gish	1
DSR, Inc., VA	
M. Bozek-Kuzmicki	1
EDO Corporation, NY	
M. Blanchard	1
EG&G, VA	
D. Frohman	1
EG&G Services, CT	
J. Pratt	1
Engineering Technology Center	
D. Lerro	1
General Electric, MA	
R. Race	1
General Electric, NJ	
H. Urkowitz	1
Harris Scientific Services, NY	
B. Harris	1
Hughes Defense Communications, IN	
R. Kenefic	1
Hughes Aircraft, CA	
T. Posch	1
Kildare Corporation, CT	
R. Mellen	1

INITIAL DISTRIBUTION LIST (Cont'd)

Addressee	No. of Copies
Lincom Corporation, MA	
T. Schonhoff	1
Lockheed Martin, Undersea Systems, VA	
M. Flicker	1
Lockheed Martin, Ocean Sensor Systems, NY	
R. Schumacher	1
Marconi Aerospace Defense Systems, TX	
R. D. Wallace	1
MITRE Corporation, VA	
S. Pawlukiewicz	1
R. Bethel	1
Neural Technology, Inc., SC	
E. A. Tagliarini	1
Orincon Corporation, CA	
J. Young	1
Orincon Corporation, VA	
H. Cox	1
Philips Research Laboratory, Netherlands	
A. J. E. M. Janssen	1
Planning Systems, Inc., CA	
W. Marsh	1
Prometheus, RI	
M. Barrett	1
J. Byrnes	1
Raytheon, RI	
R. Conner	1
S. Reese	1
Schlumberger-Doll Research, CT	
R. Shenoy	1
Science Applications International Corporation, CA	
C. Katz	1
Science Applications International Corporation, VA	
P. Mikhalevsky	1
Toyon Research, CA	
M. Van Blaricum	1
Tracor, TX	
T. Leih	1
B. Jones	1
K. Scarbrough	1
TRW, VA	
R. Prager	1
G. Maher	1
Westinghouse Electric, MA	
R. Kennedy	1
Westinghouse Electric, Annapolis, MD	
H. Newman	1
Westinghouse Electric, Baltimore, MD	
R. Park	1
K. Harvel, Austin, TX	1